

Judul Artikel : Design and Synthesis of Conducting Polymer Bio-Based Polyurethane Produced from Palm Kernel Oil
Nama Jurnal : International Journal of Polymer Science
ISSN : 1687-9430
Tahun Terbit : 2022
Penerbit : Hindawi
No. Halaman : 1-13
Url Cek Plagiasi : http://repositor.almaata.ac.id/id/eprint/3175/1/P7_turnitin.pdf
Url Index : <https://www.scopus.com/sourceid/21100228096>
Url Jurnal : <https://doi.org/10.1155/2022/6815187>

Rekapitulasi Proses Publikasi

| No | Kegiatan | Tanggal |
|-----------|---------------------------------|------------------|
| 1 | Submit | 14 Juni 2021 |
| 2 | Hasil Reviu 1 dan Submit Revisi | 18 Juni 2021 |
| 3 | Hasil Reviu 2 dan Submit Revisi | 22 Juli 2021 |
| 4 | Hasil Reviu 3 dan Submit Revisi | 1 Oktober 2021 |
| 5 | Hasil Reviu 4 dan Submit Revisi | 2 Desember 2021 |
| 6 | Hasil Reviu 5 dan Submit Revisi | 2 Februari 2022 |
| 7 | Hasil Reviu 6 dan Submit Revisi | 13 Februari 2022 |
| 8 | Pemberitahuan Diterima | 22 Maret 2022 |

← BACK DASHBOARD / ARTICLE DETAILS  Updated on 2021-06-18 Version 1 ▾

Design and Synthesis of Conducting Polymer Based on Polyurethane produced from Palm Kernel Oil

VIEWING AN OLDER VERSION

ID 6815187

Muhammad Abdurrahman Munir ^{SA}¹,
Khairiah Haji Badri ^{CA}¹, Lee Yook Heng¹
[+ Show Affiliations](#)

Article Type

Research Article

Journal

International Journal of
Polymer Science

Rydz Joanna
Submitted on 2021-06-14 (2 years ago)

> Abstract

> Author Declaration

> Files 2

— Editorial Comments

Hasil Reviu 1 dan Submit Revisi: 18 Juni 2021

Peter Foot

18.06.2021

Decision

Revision requested

Message for Author

The topic of this manuscript is suitable for Int. J. Polym. Sci. but it must be revised before it can be sent for peer-review. The grammar and typing are very poor, and there are many incorrectly-used words. Reviewers would not properly understand the authors' meaning in many parts of the text. The authors should also emphasize the novel aspects of their research, since there is an abundance of published work on PUs made from vegetable oil derivatives.

[Hindawi](#) [Privacy Policy](#) [Terms of Service](#) Support: help@hindawi.com

Hindawi

Muhammad Abdurrahman Munir

Your Reply

Greetings, Dear Editor, Hope you are doing well. I have attached several documents such as the manuscript edited and the comments for reviewers. Best regards

File

Comments for Reviewers.docx 16 kB 

[+ Reviewer Reports](#)

[Hindawi](#) [Privacy Policy](#) [Terms of Service](#) Support: help@hindawi.com

Design and Synthesis of Conducting Polymer Based on Polyurethane produced from Palm Kernel Oil

Muhammad Abdurrahman Munir¹, Khairiah Haji Badri^{1,2*}, Lee Yook Heng¹

¹Department of Chemical Sciences, Faculty of Science and Technology, Universiti Kebangsaan Malaysia, Bangi, Malaysia

²Polymer Research Center, Universiti Kebangsaan Malaysia, Bangi, Malaysia

*Email: kaybadri@ukm.edu.my

Abstract

Polyurethane (PU) is a unique polymer that has versatile processing method and mechanical properties upon inclusion of selected additives. In this study, a freestanding bio-polyurethane film on screen – printed electrode (SPE) was prepared by solution casting technique, using acetone as solvent. It was a one-pot synthesis between major reactants namely, palm kernel oil-based polyol (PKOp) and 4,4-methylene diisocyanate. The PU undergone strong adhesion on SPE. The formation of urethane linkages (NHCO backbone) after polymerization was confirmed by the absence of N=C=O peak at 2241 cm⁻¹. The glass transition temperature (T_g) of the polyurethane was detected at 78.1°C. The conductivity of PU was determined using cyclic voltammetry (CV) and differential pulse voltammetry (DPV). The current of electrode was at 5.2 x 10⁻⁵ A.

Keywords: Polyurethane, polymerization, screen – printed electrode, voltammetry

1. Introduction

Polymers are molecules composed of many repeated sub-units referred to as monomers (Sengodu & Deshmukh 2015). Conducting polymers (CPs) are polymers that exhibit electrical behaviour (Alqarni et al. 2020). The conductivity of CPs was first observed in polyacetylene,

27 nevertheless owing to its instability led to the discovery of other forms of CPs such as
28 polyaniline (PANI), poly(o-toluidine) (PoT), polythiophene (PTh), polyfluorene (PF) and
29 polyurethane (PU). Furthermore, natural CPs have low conductivity and are often semi-
30 conductive. Therefore, it is essential to increase their conductivity mainly for use in
31 electrochemical sensor programs (Dzulkipli et al. 2021; Wang et al. 2018). Conducting
32 polymers (CPs) represent a sizeable range of useful organic substances. Their unique electrical,
33 chemical and physical properties; reasonable price; simple preparation; small dimensions and
34 large surface area have enabled researchers to discover a wide variety of uses such as sensors,
35 biochemical applications, solar cells and electrochromic devices (Alqarni et al. 2020). There
36 are many scientific documentations on the use of conductive polymers in various studies such
37 as polyaniline (Pan & Yu 2016), polypyrrole (Ladan et al. 2017) and polyurethane (Tran et al.
38 2020; Vieira et al. 2020; Guo et al. 2020; Fei et al. 2020).

39 The application of petroleum as polyol in order to produce polyurethane has been applied. The
40 coal and crude oil used as raw materials to produce it. Nevertheless, these materials become
41 very rare to find and the price is very expensive at the same time required sophisticated system
42 to produce it. These reasons have been considered and finding utilizing plants that can be used
43 as alternative polyols should be done immediately (Badri 2012). Furthermore, in order to avoid
44 the application of petroleum as raw material for polyol, vegetable oils become a better choice
45 as polyol in order to obtain a biodegradable polyol. Vegetable oils that generally used for
46 synthesis polyurethane are soybean oil, corn oil, sunflower seed oil, coconut oil, nuts oil, rape
47 seed, olive oil and palm oil (Badri 2012; Borowicz et al. 2019).

48 Biopolymer, a natural biodegradable polymer has attracted much attention in recent years.
49 Global environmental awareness and fossil fuel depletion urged researchers to work in the
50 biopolymer field (Priya et al. 2018). Polyurethane is one of the most common, versatile and
51 researched materials in the world. These materials combine the durability and toughness of

52 metals with the elasticity of rubber, making them suitable to replace metals, plastics and rubber
53 in several engineered products. They have been widely applied in biomedical applications,
54 building and construction applications, automotive, textiles and in several other industries due
55 to their superior properties in terms of hardness, elongation, strength and modulus (Zia et al.
56 2014; Romaskevicius et al. 2006).

57 The urethane group is the major repeating unit in PU and is produced from the reaction between
58 alcohol (-OH) and isocyanate (NCO); albeit polyurethanes also contain other groups such as
59 ethers, esters, urea and some aromatic compounds. Due to the wide variety of sources from
60 which PU can be synthesized, thus a wide range of specific applications can be generated.
61 They are grouped into several different classes based on the desired properties: rigid, flexible,
62 thermoplastic, waterborne, binders, coating, adhesives, sealants and elastomers (Akindoyo et
63 al. 2016).

64 Although, PU has low conductivity but it is lighter than other materials such as metals. The
65 hardness of PU also relies on the aromatic rings number in the polymer structure (Janpoung et
66 al, 2020; Su'ait et al. 2014), majorly contributed by the isocyanate derivatives. PU has also a
67 conjugate structure where electrons can move in the main chain that causing electricity
68 produced even the conductivity is low. The electrical conductivity of conjugated linear (π) can
69 be explained by the distance between the highest energy level containing electrons (HOMO)
70 called valence band and the lowest energy level not containing electrons (LUMO) called the
71 conduction band (Wang et al. 2017; Kotal et al. 2011).

72 The purpose of this work was to study the conductivity of polyurethane using cyclic
73 voltammetry (CV) and differential pulse voltammetry (DPV) attached onto screen printed
74 electrode (SPE). To the best of our knowledge, this is the first attempt to use a modified
75 polyurethane electrode. The electrochemistry of polyurethane mounted onto screen-printed

76 electrode (SPE) is discussed in detail. Polyurethane is possible to become an advanced frontier
77 material in chemically modified electrodes for bio sensing application.

78

79 **2. Experimental**

80 **2.1 Chemicals**

81 *Synthesis of polyurethana film:* Palm kernel oil (PKOp) supplied by UKM Technology Sdn
82 Bhd through MPOB/UKM station plant, Pekan Bangi Lama, Selangor and prepared using
83 Badri et al. (2000) method. 4, 4-diphenylmethane diisocyanate (MDI) was acquired from
84 Cosmopolyurethane (M) Sdn. Bhd., Klang, Malaysia. Solvents and analytical reagents were
85 benzene ($\geq 99.8\%$), toluene ($\geq 99.8\%$), hexane ($\geq 99\%$), acetone ($\geq 99\%$), tetrahydrofuran
86 (THF), dimethylformamide (DMF) ($\geq 99.8\%$), dimethylsulfoxide (DMSO) ($\geq 99.9\%$) and
87 polyethylene glycol (PED) with a molecular weight of 400 Da obtained from Sigma Aldrich
88 Sdn Bhd, Shah Alam.

89

90 **2.2 Apparatus**

91 Tensile testing was performed using a universal testing machine model Instron 5566 following
92 ASTM 638 (Standard Test Method for Tensile Properties of Plastics). The tensile properties of
93 the polyurethane film were measured at a velocity of 10 mm/min with a cell load of 5 kN.
94 The thermal properties were performed using thermogravimetry analysis (TGA) and
95 Differential Scanning Calorimetry (DSC) analysis. TGA was performed using a thermal
96 analyzer of Perkin Elmer Pyris model with heating rate of 10 °C/minute at a temperature range
97 of 30 to 800 °C under a nitrogen gas atmosphere. The DSC analysis was performed using a
98 thermal analyzer of Perkin Elmer Pyris model with heating rate of 10 °C /minute at a
99 temperature range of -100 to 200 °C under a nitrogen gas atmosphere. Approximately, 5-10
100 mg of PU was weighed. Sample was heated from 25 to 150 °C for one minute, then cooled

101 immediately from 150 -100 °C for another one minute and finally, reheated to 200 °C at a rate
102 of 10 °C /min. At this point, the polyurethane encounters changes from elastic properties to
103 brittle due to changes in the movement of the polymer chains. Therefore, the temperature in
104 the middle of the inclined regions is taken as the glass transition temperature (T_g). The melting
105 temperature (T_m) is identified as the maximum endothermic peak by taking the area below the
106 peak as the enthalpy point (ΔH_m).

107 The morphological analysis of PU film was performed by Field Emission Scanning Electron
108 Microscope (FESEM) model Gemini SEM microscope model 500-70-22. Before the analysis
109 was carried out, the polyurethane film was coated with a thin layer of gold to increase the
110 conductivity of the film. The coating method was carried out using a sputter - coater. The
111 observations were conducted at magnification of 200× and 5000 × with 10.00 kV (Electron
112 high tension - EHT).

113 The crosslinking of PU was determined using soxhlet extraction method. About 0.60 g of PU
114 sample was weighed and put in an extractor tube containing 250 ml of toluene, used as a
115 solvent. This flow of toluene was let to run for 24 hours. Mass of the PU was weighed before
116 and after the reflux process was carried out. Then, the sample was dried in the conventional
117 oven at 100 °C for 24 hours in order to get a constant mass. The percentage of crosslinking
118 content known as the gel content, can be calculated using Equation (1).

119

$$120 \quad \text{Gel content (\%)} = \frac{W_0 - W}{W} \times 100 \% \quad (1)$$

121 W_0 is mass of PU before the reflux process (g) and W is mass of PU after the reflux process
122 (g).

123

124 FTIR spectroscopic analysis was performed using a Perkin-Elmer Spectrum BX instrument
125 using the Diamond Attenuation Total Reflectance (DATR) method to confirm the

126 polyurethane, PKOp and MDI functional group. FTIR spectroscopic analysis was performed
127 at a wave number of 4000 to 600 cm^{-1} to identify the peaks of the major functional groups in
128 the formation of polymer such as amide group (-NH), urethane carbonyl group (-C = O) and
129 carbamate group (-CN).

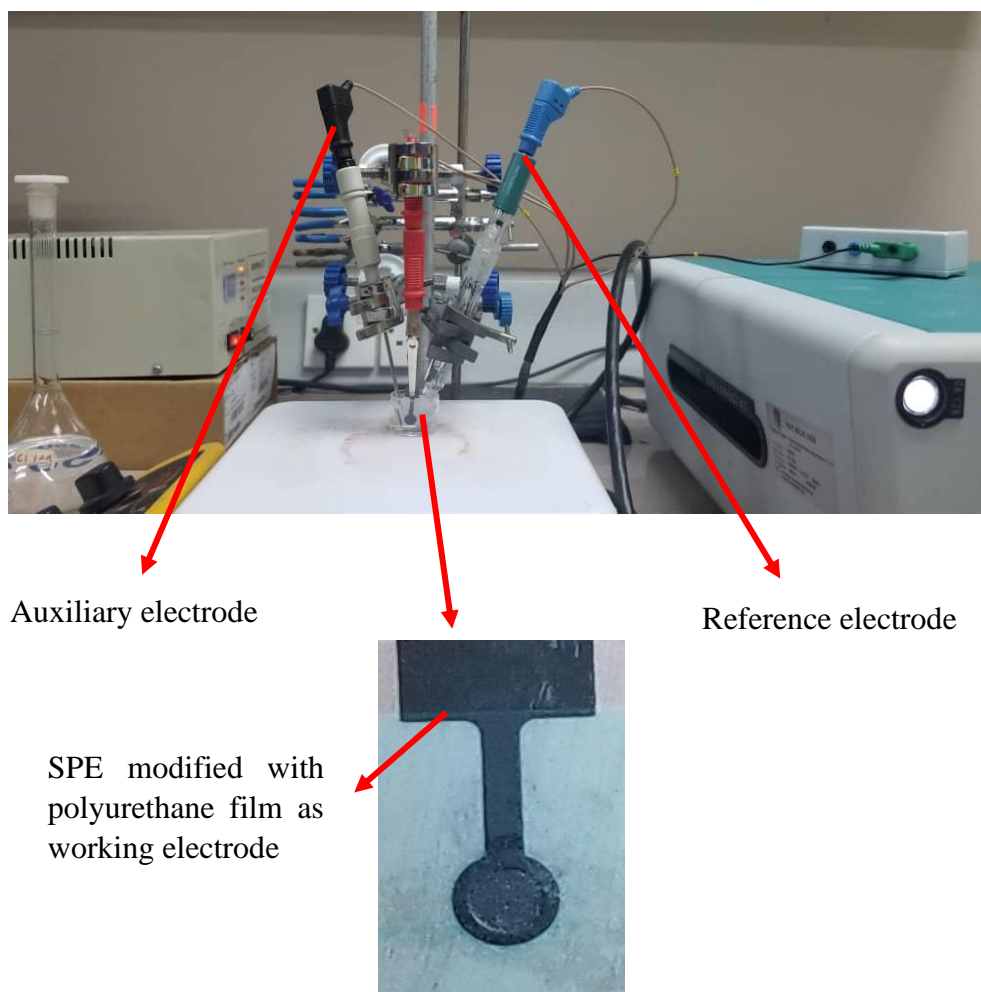
130

131 **2.3 Modification of Electrode**

132 Voltammetric tests were performed using Metrohm Autolab Software (**Figure 1**) analyzer
133 using cyclic voltammetry (CV) method or known as amperometric mode and differential pulse
134 voltammetry (DPV). All electrochemical experiments were carried out using screen printed
135 electrode (diameter 3 mm) modified using polyurethane film as working electrode, platinum
136 wire as auxiliary electrode and AG/AgCl electrode as reference electrode. All experiments
137 were conducted at temperature of $20 \pm 2^\circ\text{C}$.

138 PU casted onto the screen – printed electrode (SPE + PU) was analyzed using a single
139 voltammetric cycle between -1200 and +1500 mV (vs AG/AgCl) of ten cycles at a scanning rate
140 of 100 mV/s in 5 ml of KCl in order to study the activity of SPE and polyurethane film.
141 Approximately (0.1, 0.3 & 0.5) mg of palm – based prepolyurethane was dropped separately
142 onto the surface of the SPE and dried at room temperature. The modified palm-based
143 polyurethane electrodes were then rinsed with deionized water to remove physically adsorbed
144 impurities and residues of unreacted material on the electrode surface. All electrochemical
145 materials and calibration measurements were carried out in a 5 mL glass beaker with a
146 configuration of three electrodes inside it. Platinum wire and AG/AgCl electrodes were used
147 as auxiliary and reference electrodes, while screen printed electrode that had been modified
148 with polyurethane was applied as a working electrode.

149



150 **Figure 1.** Potentiostat instrument to study the conductivity of SPE modified with
 151 polyurethane film using cyclic voltametry (CV) and differential pulse voltammetry (DPV)

152

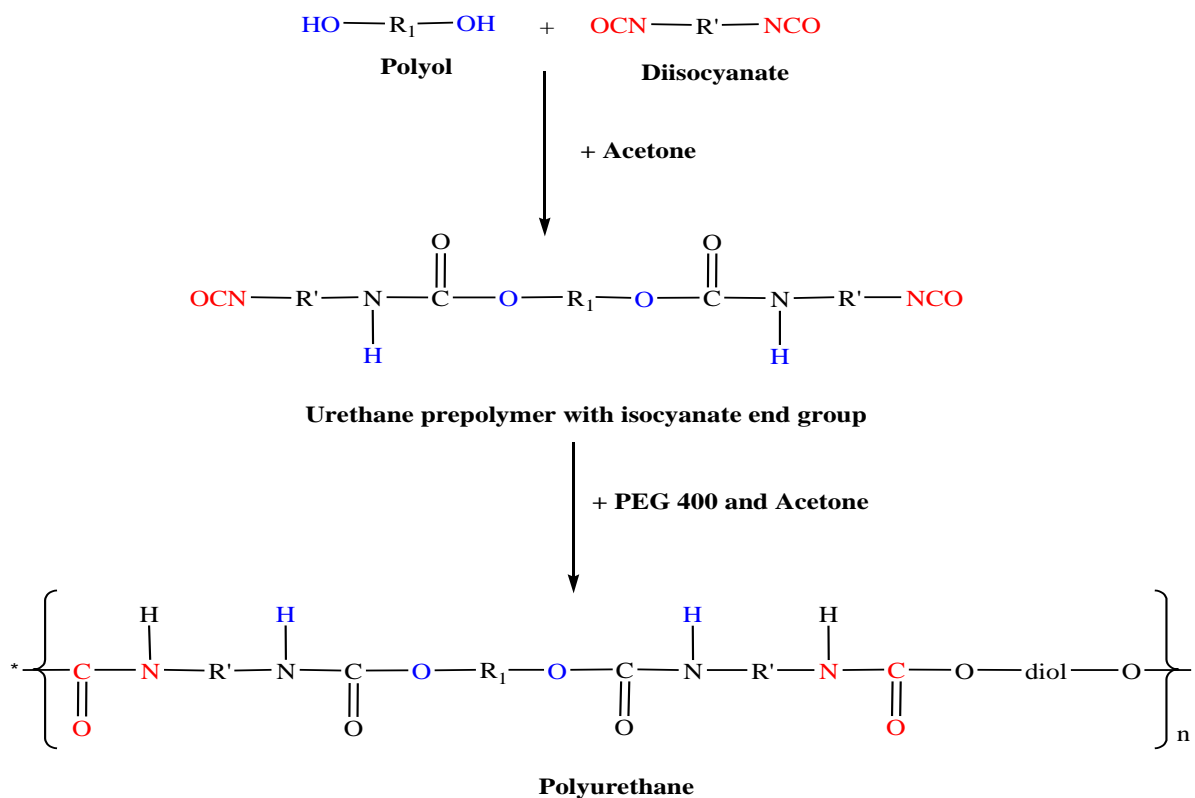
153 3. Results and Discussion

154 The synthesis of PU films was carried out using pre - polymerization method which involves
 155 the formation of urethane polymer at an early stage. The reaction took place between palm
 156 kernel oil – based polyol (PKOp) and diisocyanate (MDI). The structural chain was extended
 157 with the aid of polyethylene glycol (PED) to form flexible and elastic polyurethane film. In
 158 order to form the urethane prepolymer, one of the isocyanate groups (NCO) reacts with one
 159 hydroxyl group (OH) of polyol while the other isocyanate group attacks another hydroxyl
 160 group in the polyol (Wong & Badri 2012) as shown in **Figure 2.**

161

162 a. FTIR analysis

163 **Figure 3** shows the FTIR spectrum for polyurethane, exhibiting the important functional group
164 peaks. According to study researched by Wong & Badri 2012, PKO-p reacts with MDI to form
165 urethane prepolymers. The NCO group on MDI reacts with OH group on polyol whether
166 PKOp or PEG. It can be seen there are no important peaks of MDI in the FTIR spectrums.
167 This is further verified by the absence of peak at the 2400 cm^{-1} belongs to MDI (-NCO groups).
168 This could also confirm that the NCO group on MDI had completely reacted with PKO-p to
169 form the urethane -NHC (O) backbone. The presence of amides (-NH), carbonyl urethane
170 group (-C = O), carbamate group (C-NH) and -C-O-C confirmed the formation of urethane
171 chains. In this study, the peak of carbonyl urethane (C = O) detected at 1727 cm^{-1} indicated
172 that the carbonyl urethane group was bonded without hydrogen owing to the hydrogen reacted
173 with the carbonyl urethane group.



174

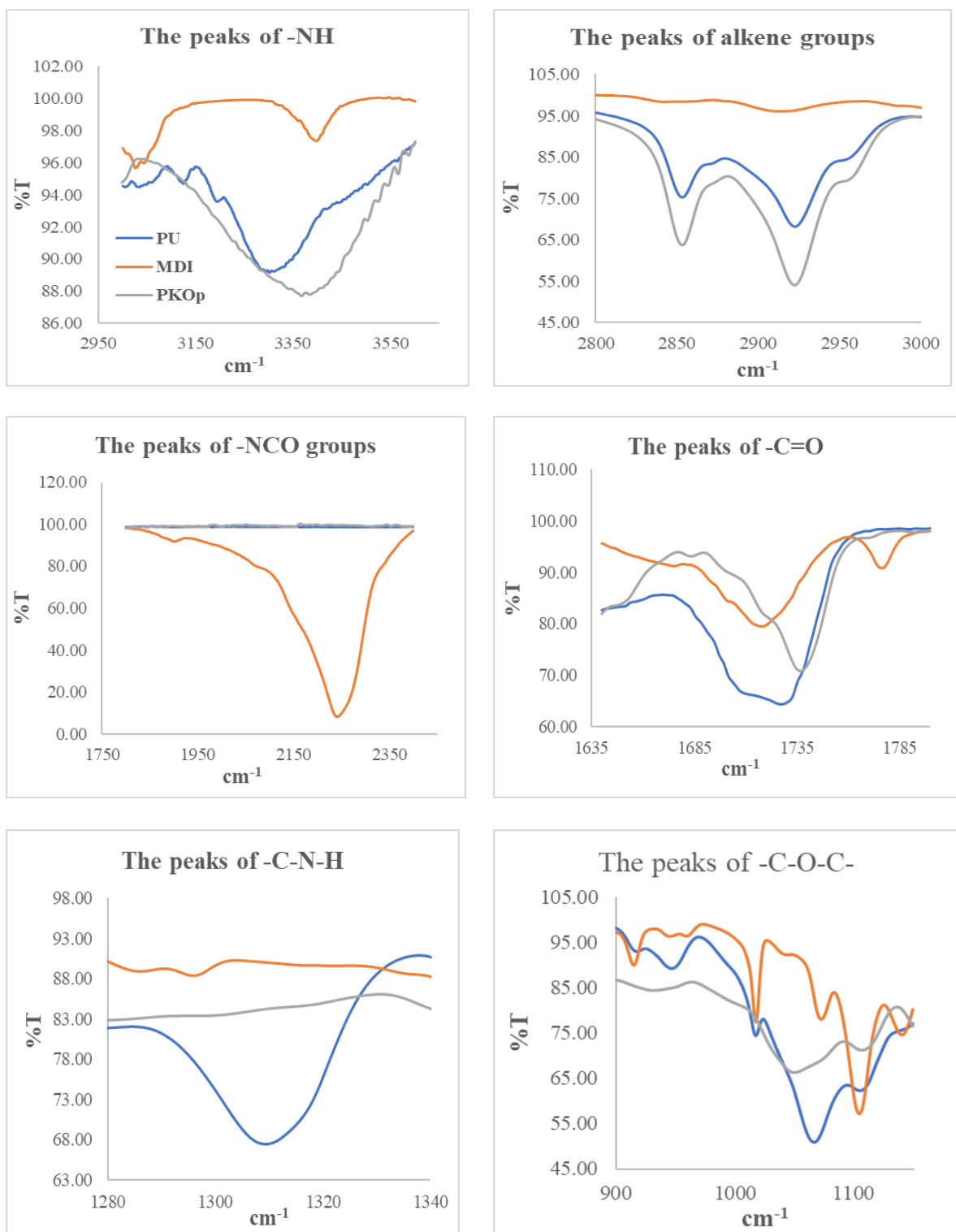
175 **Figure 2.** The chemical route of producing polyurethane via pre-polymerization method

176

(Wong & Badri 2012).

177 The reaction of polyurethane has been studied by Hamuzan & Badri (2016) where the urethane
178 carbonyl group was detected at $1730 - 1735 \text{ cm}^{-1}$ while the MDI carbonyl was detected at 2400
179 cm^{-1} . The absence of peaks at $2250 - 2270 \text{ cm}^{-1}$ indicates the absence of NCO groups. It shows
180 that the polymerization reaction occurs entirely between NCO groups in MDI with hydroxyl
181 groups on polyols and PEG (Mishra et al. 2012). The absence of peaks at 1690 cm^{-1}
182 representing urea (C = O) in this study indicated, there is no urea formation as a byproduct
183 (Clemitson 2008) of the polymerization reaction that possibly occur due to the excessive water.
184 For the amine (NH) group, hydrogen-bond to NH and oxygen to form ether and hydrogen bond
185 to NH and oxygen to form carbonyl on urethane can be detected at the peak of 3301 cm^{-1} and
186 in the wave number at range $3326 - 3428 \text{ cm}^{-1}$. This has also been studied and detected by
187 Lampman et. al. (2010) and Mutsuhisa et al. (2007). In this study, the hydrogen bond formed
188 by C = O acts as a proton acceptor whereas NH acts as a proton donor. The urethane group in
189 the hard segment (MDI) has electrostatic forces on the oxygen, hydrogen and nitrogen atoms
190 and these charged atoms form dipoles that attract other opposite atoms. These properties make
191 isocyanates are highly reactive and having different properties (Leykin et al. 2016).

192 MDI was one of the isocyanate used in this study, has an aromatic group and more
193 reactive compared to aliphatic group isocyanates such as hexamethylene diisocyanate (HDI)
194 or isoporona diisocyanate (IPDI). Isocyanates have two groups of isocyanates on each
195 molecule. Diphenylmethane diisocyanate is an exception owing to its structure consists of two,
196 three, four or more isocyanate groups (Nohra et al. 2013). The use of PEG 400 in this study as
197 a chain extender for polyurethane increases the chain mobility of polyurethane at an optimal
198 amount. The properties of polyurethane are contributed by hard and soft copolymer segments
199 of both polyol monomers and MDI. This makes the hard segment of urethane serves as a
200 crosslinking site between the soft segments of the polyol (Leykin et al. 2016).



201 **Figure 3.** FTIR spectrums of several important peaks between polyurethane, PKO-p and MDI

202

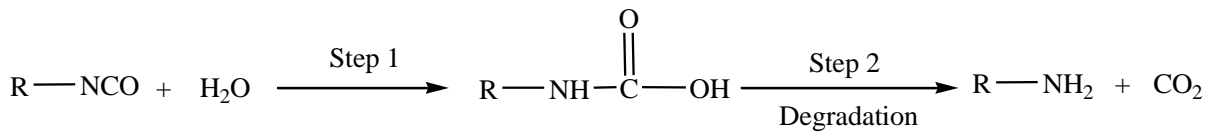
203 The mechanism of the pre – polymerization in urethane chains formation is a

204 nucleophilic substitution reaction as studied by Yong et al. (2009). However, this study found

205 amines as nucleophiles. Amine attacks carbonyl on isocyanate in MDI in order to form two
206 resonance structures of intermediate complexes A and B. Intermediate complex B has a greater
207 tendency to react with polyols due to stronger carbonyl (C = O) bonds than C = N bonds on
208 intermediate complexes A. Thus, intermediate complex B is more stable than intermediate
209 complex A, as suggested by previous researchers who have conducted by Wong and Badri
210 (2012). Moreover, nitrogen was more electropositive than oxygen, therefore, -CN bonds were
211 more attracted to cations (H⁺) than -CO. The combination between long polymer chain and
212 low cross linking content gives the polymer an elastic properties whereas short chain and high
213 cross linking producing hard and rigid polymers. Cross linking in polymers consist of three -
214 dimensional networks with high molecular weight. In some aspects, polyurethane can be a
215 macromolecule, a giant molecule. Polyurethanes are usually thermoset polymers (Petrovic
216 2008).

217 Moreover, reaction between MDI and PEG as a chain extender where oxygen on the
218 nucleophile PEG attacks the NCO group in the MDI to form two intermediate complexes A
219 and B can occur. Nevertheless, nucleophilic substitution reactions have a greater tendency to
220 occur in PKOp compared to PEG because the presence of nitrogen atoms is more
221 electropositive than oxygen atoms in PEG. Amine has a higher probability of to react compared
222 to hydroxyl (Herrington & Hock 1997). Amine with high alkalinity reacts with carbon atoms
223 on MDI as proposed by Wong and Badri (2012). PKOp contains long carbon chains that can
224 easily stabilize alkyl ions when intermediate complexes are formed. Therefore, polyol is more
225 reactive than PEG to react with MDI. However, the addition of PEG will increase the length
226 of the polyurethane chain and prevent side effects such as the formation of urea by -products
227 of the NCO group reaction in urethane pre - polymer and water molecules from the
228 environment. If the NCO group reacts with the excess water in the environment, the formation

229 of urea and carbon dioxide gas will also occur excessively (**Figure 4**). This reaction can cause
230 a polyurethane foam not polyurethane film as we studied the film.



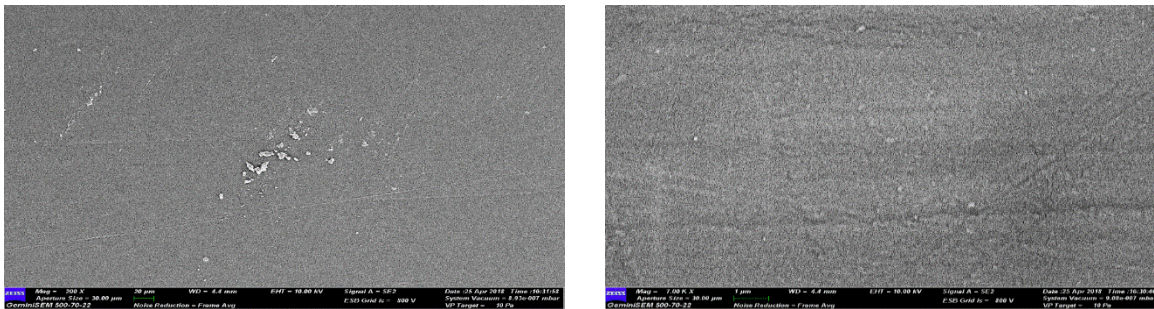
232 **Figure 4.** The reaction between NCO group and water producing carbon dioxide

233

234 b. Morphological analysis

235 The Field Emission Scanning Electron Microscope (FESEM) micrograph in **Figure 5** shows
236 the formation of a uniform polymer film contributed by the polymerization method applied.
237 The magnification used for this surface analysis ranged from 200 to 5000 ×. The
238 polymerization method can also avoid the failure of the reaction in PU polymerization.
239 Furthermore, no trace of separation was detected by FESEM. This has also been justified by
240 the wavelengths obtained by the FTIR spectrums above.

241



242 **Figure 5.** The micrograph of polyurethane films analysed by FESEM at (a) 200 × and (b)
243 5000× magnifications.

244

245 c. The crosslinking analysis

246 Soxhlet analysis was applied to determine the degree of crosslinking between the hard
247 segments and the soft segments in the polyurethane. The urethane group on the hard segment
248 along the polyurethane chain is polar (Cuve & Pascault 1991). Therefore, during the testing, it
249 was very difficult to dissolve in toluene, as the testing reagent. The degree of the crosslinking

250 is determined by the percentage of the gel content. The analysis result obtained from the
 251 Soxhlet testing indicating a 99.3 % gel content. This is significant in getting a stable polymer
 252 at higher working temperature (Rogulska et al. 2007).

$$\text{Gel content (\%)} = \frac{(0.6 - 0.301) \text{ g}}{0.301 \text{ g}} \times 100\% = 99.33\%$$

253
 254
 255 d. The thermal analysis

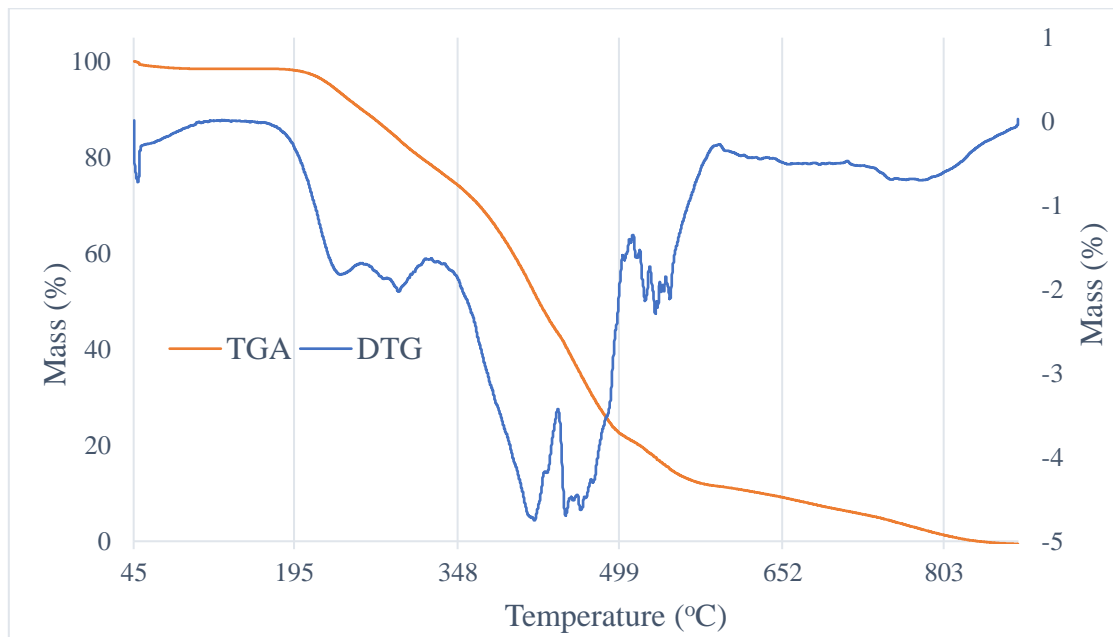
256 **Figure 6** shows the TGA and DTG thermograms of polyurethane. The percentage weight loss
 257 (%) is listed in **Table 1**. Generally, only a small amount of weight was observed. It is shown
 258 in **Figure 6** in the region of 45 – 180°C. This is due to the presence of condensation on moisture
 259 and solvent residues.

260 **Table1** Weight loss percentage of (wt%) polyurethane film

| Sample | % Weight loss (wt%) | | | | Total of weight loss (%) | Residue after 550°C (%) |
|--------------|--------------------------|----------------------------------|----------------------------------|----------------------------------|--------------------------------|----------------------------|
| | T _{max} , °C | T _{d1} , 200 – 290°C | T _{d2} , 350 – 500°C | T _{d3} , 500 – 550°C | | |
| Polyurethane | 240 | 8.04 | 39.29 | 34.37 | 81.7 | 18.3 |

261 The bio polyurethane is thermally stable up to 240 °C before it undergone thermal degradation.
 262
 263 The first stage of thermal degradation (T_{d1}) on polyurethane films was shown in the region of
 264 200 – 290°C as shown in **Figure 6**. The T_{d1} is associated with degradation of the hard segments
 265 of the urethane bond, forming alcohol or degradation of the polyol chains and releasing of
 266 isocyanates (Berta et al. 2006), primary and secondary amines as well as carbon dioxide
 267 (Corcuera et al. 2011; Pan & Webster 2012). Meanwhile, the second thermal degradation stage
 268 (T_{d2}) of polyurethane films experienced a weight loss of 39.29 %. This endotherm of T_{d2} is
 269 related to dimerization of isocyanates to form carbodiimides and release CO₂. The formed

270 carbodiimide reacts with alcohol to form urea. For the third stage of thermal degradation (T_{d3})
271 is related to the degradation on urea (Berta et al. 2006) and the soft segment on polyurethane.

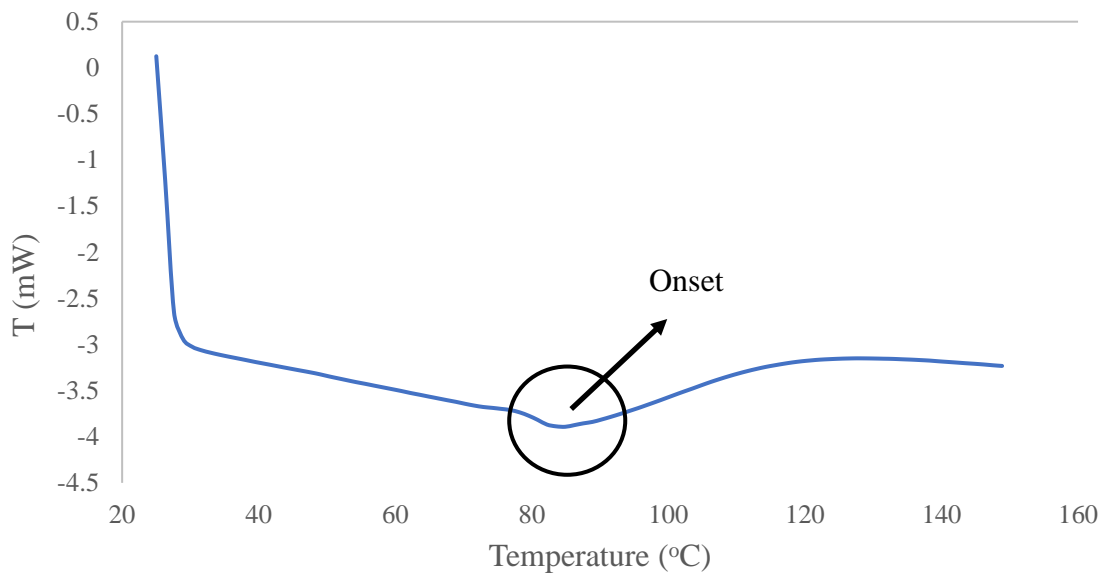


272
273
274

Figure 6. DTG and TGA thermogram of polyurethane film

275 Generally, DSC analysis exhibited thermal transitions as well as the initial
276 crystallisation and melting temperatures of the polyurethane (Khairuddin et al. 2018). It serves
277 to analyse changes in thermal behaviour due to changes occurring in the chemical chain
278 structure based on the glass transition temperature (T_g) of the sample obtained from the DSC
279 thermogram (**Figure 7**). DSC analysis on polyurethane films was performed in the temperature
280 at range 100 °C to 200 °C using nitrogen gas as blanket as proposed by Furtwengler et al.
281 (2017). The glass transition temperature (T_g) on polyurethane was above room temperature, at
282 78.1 °C indicated the state of glass on polyurethane. The presence of MDI contributes to the
283 formation of hard segments in polyurethanes. During polymerization, this hard segment
284 restricts the mobility of the polymer chain (Ren et al. 2013) owing to steric effect on benzene
285 ring in hard segment. The endothermic peak of acetone used as the solvent in this study was
286 supposedly be at 56°C. However, it was detected in the DSC thermogram nor the TGA
287 thermogram, which indicates that acetone was removed from the polyurethane during the

288 synthesis process, owing to its volatility nature. The presence of acetone in the synthesis was
289 to lower the reaction kinetics.



290
291
292

Figure 7. DSC thermogram of polyurethane film

293
294

e. The solubility and mechanical properties of the polyurethane film

295 The chemical resistivity of a polymer will be the determinant in performing as conductor. Thus,
296 its solubility in various solvents was determined by dissolving the polymer in selected solvents
297 such as hexane, benzene, acetone, tetrahydrofuran (THF), dimethylformamide (DMF) and
298 dimethylformamide (DMSO). On the other hand, the mechanical properties of polyurethane
299 were determined based on the standard testing following ASTM D 638 (Standard Test Method
300 for Tensile Properties of Plastics) . The results from the polyurethane film solubility and tensile
301 test are shown in **Table 2**. Polyurethane films were insoluble with benzene, hexane and acetone
302 and are only slightly soluble in tetrahydrofuran (THF), dimethylformamide (DMF) and
303 dimethylformamide (DMSO) solutions. While the tensile strength of a PU film indicated how
304 much elongation load the film was capable of withstanding the material before breaking.

305 The tensile stress, strain and modulus of polyurethane film also indicated that polyurethane has
 306 good mechanical properties that are capable of being a supporting substrate for the next stage
 307 of study. In the production of polyurethane, the properties of polyurethane are easily influenced
 308 by the content of MDI and polyol used. The length of the chain and its flexibility are contributed
 309 by the polyol which makes it elastic. High crosslinking content can also produce hard and rigid
 310 polymers. MDI is a major component in the formation of hard segments in polyurethane. It is
 311 this hard segment that determines the rigidity of the PU. Therefore, high isocyanate content
 312 results in higher rigidity on PU (Petrovic et al. 2002). Thus, the polymer has a higher resistance
 313 to deformation and more stress can be applied to the PU.

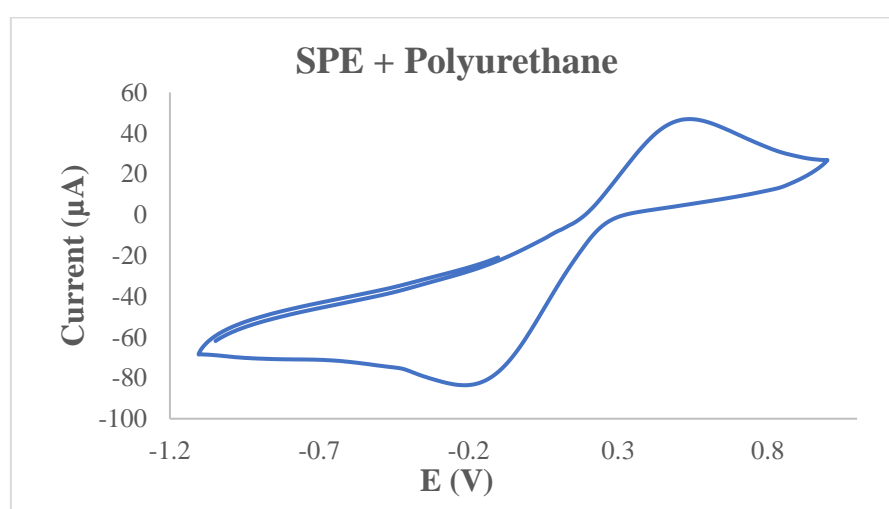
314 **Table 2** The solubility and mechanical properties of the polyurethane film

315

| Parameters | Polyurethane film |
|----------------------------|----------------------|
| Solubility | Benzene Insoluble |
| | Hexane Insoluble |
| | Acetone Insoluble |
| | THF Less soluble |
| | DMF Less soluble |
| | DMSO Less soluble |
| Stress (MPa) | 8.53 |
| Elongation percentage (%) | 43.34 |
| Strain modulus (100) (MPa) | 222.10 |

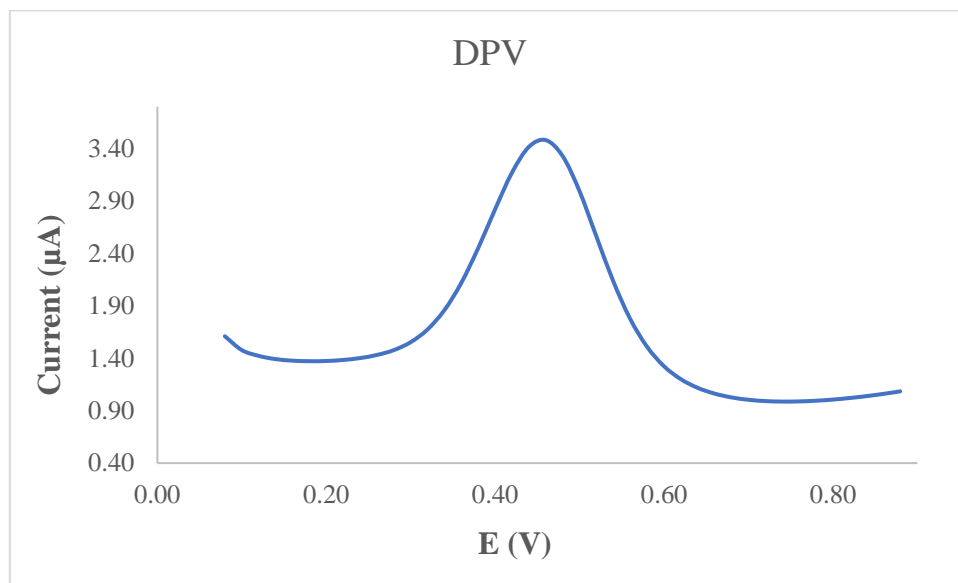
316
 317 f. Conductivity of the polyurethane as polymeric film on SPE
 318
 319 Polyurethane film deposited onto the screen printed electrode by casting method as shown in
 320 **Figure 1**. After that, the modified electrode was analysed using cyclic voltammetry (CV) and

321 differential pulse voltammetry (DPV) in order to study the behaviour of modified electrode.
322 The modified electrode was tested in a 0.1 mmol/L KCl solution containing 5 mmol/L (K_3Fe
323 $(CN)_6$). The use of potassium ferricyanide is intended to increase the sensitivity of the KCl
324 solution. The conductivity of the modified electrode was studied. The electrode was analyzed
325 by cyclic voltammetry method with a potential range of -1.00 to +1.00 with a scan rate of 0.05
326 V/s. The voltamogram at electrode have shown a specific redox reactions. Furthermore, the
327 conductivity of the modified electrode is lower due to the use of polyurethane. This occurs due
328 to PU is a natural polymer produced from the polyol of palm kernel oil. The electrochemical
329 signal at the electrode is low if there is a decrease in electrochemical conductivity (El - Raheem
330 et al. 2020). It can be concluded that polyurethane is a bio – polymer with a low conductivity
331 value. The current of modified electrode was found at 5.3×10^{-5} A or 53 μ A.
332 According to **Figure 8**, it can be concluded that the anodic peak present in the modified
333 electrode was at +0.5 V, it also represented the oxidation process of the modified electrode. The
334 first oxidation scan on both electrodes ranged from -0.2 to +1.0 V, which showed a significant
335 anodic peak at a potential of +0.5 V.



336
337 **Figure 8.** The voltamogram of SPE – PU modified electrode after analysed using cyclic
338 voltammetry (CV) technique
339

340 **Figure 9** also presents the DPV voltammogram of modified electrode. DPV is a measurement
 341 based on the difference in potential pulses that produce an electric current. Scanning the
 342 capability pulses to the working electrode will produce different currents. Optimal peak
 343 currents will be produced to the reduction capacity of the redox material. The peak current
 344 produced is proportional to the concentration of the redox substance and can be detected up to
 345 concentration below 10^{-8} M. DPV conducted to obtain the current value that more accurate than
 346 CV (Lee et al. 2018).



347
 348 **Figure 9.** The voltammogram of SPE – PU modified electrode after analyzed using
 349 differential pulse voltammetry (DPV) technique

350
 351 This study used a redox pair ($K_3Fe(CN)_6$) as a test device (probe). The currents generated by
 352 SPE-PU and proved by CV and DPV have shown conductivity on polyurethane films. This
 353 suggests that polyurethane films can conduct electron transfer. The electrochemical area on the
 354 modified electrode can be calculated using the formula from Randles-Sevcik (Butwong et al.
 355 2019), where the electrochemical area for SPE-PU is considered to be A, using Equation 2:

356
 357 **Current of SPE-PU , $I_p = 2.65 \times 10^5 n^{3/2} A v^{1/2} CD^{1/2}$** (2)

358 Where, $n - 1$ is the amount of electron transfer involved, while C is the solvent concentration
359 used (mmol/L) and the value of D is the diffusion constant of 5 mmol/L at $(K_3Fe(CN)_6)$
360 dissolved using 0.1 mmol/L KCl. The estimated surface area of the electrode (**Figure 1**) was
361 0.2 cm^2 where the length and width of the electrode used during the study was $0.44 \text{ cm} \times 0.44$
362 cm while the surface area of the modified electrode was 0.25 cm^2 with the length and width of
363 the electrode estimated at $0.5 \text{ cm} \times 0.5 \text{ cm}$, and causing the modified electrode has a larger
364 surface. The corresponding surface concentration (τ) (mol/cm^2) is calculated using Equation 3.

$$365 \quad I_p = (n^2 F^2 / 4RT) A \tau v \quad (3)$$

366 I_p is the peak current (A), while A is the surface area of the electrode (cm^2), the value of v is
367 the applied scan rate (mV/s) and F is the Faraday constant (96,584 C/mol), R is the constant
368 ideal gas (8.314 J/mol K) and T is the temperature used during the experiment being conducted
369 (298 K) (Koita et al. 2014).

370

371 **4. Conclusion**

372 Polyurethane film was prepared by pre-polymerization between palm kernel oil-based polyol
373 (PKO-p) with MDI. The presence of PEG 400 as the chain extender formed freestanding
374 flexible film. Acetone was used as the solvent to lower the reaction kinetics since the pre-
375 polymerization was carried out at room temperature. The formation of urethane links (NHCO
376 – backbone) after polymerization was confirmed by the absence of $N=C=O$ peak at 2241 cm^{-1}
377 and the presence of N-H peak at 3300 cm^{-1} , carbonyl (C=O) at 1710 cm^{-1} , carbamate (C-N) at
378 1600 cm^{-1} , ether (C-O-C) at 1065 cm^{-1} , benzene ring (C = C) at 1535 cm^{-1} in the bio
379 polyurethane chain structure. Soxhlet analysis for the determination of crosslinking on
380 polyurethane films has yielded a high percentage of 99.33 %. This is contributed by the hard
381 segments formed from the reaction between isocyanates and hydroxyl groups causing
382 elongation of polymer chains. FESEM analysis exhibited absence of phase separation and

383 smooth surface. Meanwhile, the current of modified electrode was found at 5.2×10^{-5} A. This
384 bio polyurethane film can be used as a conducting bio – polymer and it is very useful for other
385 studies such as electrochemical sensor purpose.

386

387 **5. Patents**

388 There are no patents resulting from the work reported in this manuscript.

389 **6. Author contributions**

390 Munir. M.A. and Badri. K.H. performed the measurements, Badri. K.H. and Heng. L.Y. were
391 involved in planning and supervised the work, Munir. M.A and Badri. K.H. processed the
392 experimental data, performed the analysis, drafted the manuscript, designed the figures, and
393 performed the calculations. Munir. M.A. and Badri. K.H. prepared and characterized the
394 samples through FTIR spectroscopy, TGA and DSC analyses as well as the conductivity.
395 Munir. M.A. and Badri. K.H. conducted the interpretation of results and write up of the
396 manuscript. All authors discussed the results and commented on the manuscript.

397

398 **7. Funding**

399 This research was funded by Universiti Kebangsaan Malaysia, through its internal grant
400 number GGP-2019-021. The APC was funded by Faculty of Science and Technology,
401 Universiti Kebangsaan Malaysia.

402

403 **8. Acknowledgement**

404 The authors would like to thank Universiti Kebangsaan Malaysia for the partial sponsorship of
405 the honorarium given to the first author through the research grant number GGP-2019-021. We
406 would like to also, thank Department of Chemical Sciences, Universiti Kebangsaan Malaysia
407 for the laboratory facilities and CRIM, UKM for the analysis infrastructure.

408

409 **9. Conflict of Interest**

410 The authors declare no conflict of interest.

411

412 **10. References**

413 Akindoyo, J. O., Beg, M.D.H., Ghazali, S., Islam, M.R., Jeyaratnam, N. & Yuvaraj, A.R.

414 (2016). Polyurethane types, synthesis and applications – a review. *RSC Advances*. **6**:

415 114453 – 114482.

416 Alqarni, S. A., Hussein, M. A., Ganash, A. A. & Khan, A. (2020). Composite material – based

417 conducting polymers for electrochemical sensor applications: a mini review.

418 *BioNanoScience*. **10**: 351 – 364.

419 Badri, K.H. (2012) Biobased polyurethane from palm kernel oil-based polyol. In Polyurethane;

420 Zafar, F., Sharmin, E., Eds. InTechOpen: Rijeka, Croatia. pp. 447–470.

421 Badri, K.H., Ahmad, S.H. & Zakaria, S. 2000. Production of a high-functionality RBD palm

422 kernel oil – based polyester polyol. *Journal of Applied Polymer Science* 81(2): 384 –

423 389.

424 Berta, M., Lindsay, C., Pans, G., & Camino, G. (2006). Effect of chemical structure on

425 combustion and thermal behaviour of polyurethane elastomer layered silicate

426 nanocomposites. *Polymer Degradation and Stability*. **91**: 1179-1191.

427 Borowicz, M., Sadowska, J. P., Lubczak, J. & Czuprynski, B. (2019). Biodegradable, flame –

428 retardant, and bio – based rigid polyurethane/polyisocyanurate foams for thermal

429 insulation application. *Polymers*. **11**: 1816 – 1839.

430 Butwong, N., Khajonklin, J., Thongbor, A. & Luong, J.H.T. (2019). Electrochemical sensing

431 of histamine using a glassy carbon electrode modified with multiwalled carbon nanotubes

432 decorated with Ag – Ag₂O nanoparticles. *Microchimica Acta*. **186 (11)**: 1 – 10.

433 Clemitson, I. (2008). Castable Polyurethane Elastomers. Taylor & Francis Group, New York.
434 doi:10.1201/9781420065770.

435 Corcuera, M.A., Rueda, L., Saralegui, A., Martin, M.D., Fernandez-d'Arlas, B., Mondragon,
436 I. & Eceiza, A. (2011). Effect of diisocyanate structure on the properties and
437 microstructure of polyurethanes based on polyols derived from renewable resources.
438 *Journal of Applied Polymer Science*. **122**: 3677-3685.

439 Cuve, L. & Pascault, J.P. (1991). Synthesis and properties of polyurethanes based on
440 polyolefine: Rigid polyurethanes and amorphous segmented polyurethanes prepared in
441 polar solvents under homogeneous conditions. *Polymer*. **32** (2): 343- 352.

442 Dzulkipli, M. Z., Karim, J., Ahmad, A., Dzulkurnain, N. A., Su'ait, M S., Fujita, M. Y., Khoon,
443 L. T. & Hassan, N. H. (2021). The influences of 1-butyl-3-methylimidazolium
444 tetrafluoroborate on electrochemical, thermal and structural studies as ionic liquid gel
445 polymer electrolyte. *Polymers*. 13 (8): 1277 – 1294.

446 El-Raheem, H.A., Hassan, R.Y.A., Khaled, R., Farghali, A. & El-Sherbiny, I.M. (2020).
447 Polyurethane – doped platinum nanoparticles modified carbon paste electrode for the
448 sensitive and selective voltammetric determination of free copper ions in biological
449 samples. *Microchemical Journal*. **155**: 104765.

450 Fei, T., Li, Y., Liu, B. & Xia, C. (2019). Flexible polyurethane/boron nitride composites with
451 enhanced thermal conductivity. *High Performance Polymers*. **32** (3): 1 – 10.

452 Furtwengler, P., Perrin R., Redl, A. & Averous, L. (2017). Synthesis and characterization of
453 polyurethane foams derived of fully renewable polyesters polyols from sorbitol.
454 *European Polymer Journal*. **97**: 319 – 327.

455 Guo, S., Zhang, C., Yang, M., Zhou, Y., Bi, C., Lv, Q. & Ma, N. (2020). A facile and sensitive
456 electrochemical sensor for non – enzymatic glucose detection based on three –

457 dimensional flexible polyurethane sponge decorated with nickel hydroxide. *Analytica*
458 *Chimica Acta*. **1109**: 130 – 139.

459 Hamuzan, H.A. & Badri, K.H. (2016). The role of isocyanates in determining the viscoelastic
460 properties of polyurethane. AIP Conference Proceedings. 1784, Issue 1.

461 Herrington, R. & Hock, K. (1997). Flexible polyurethane foams. 2nd Edition. Dow Chemical
462 Company. Midlan.

463 Janpoung, P., Pattanauwat, P. & Potiyaraj, P. (2020). Improvement of electrical conductivity
464 of polyurethane/polypyrrole blends by graphene. *Key Engineering Materials*. **831**: 122 –
465 126.

466 Khairuddin, F.H., Yusof, N. I. M., Badri, K., Ceylan, H., Tawil, S. N. M. (2018). Thermal,
467 chemical and imaging analysis of polyurethane/cecabase modified bitumen. *IOP Conf.*
468 *Series: Materials Science and Engineering*. 512: 012032.

469 Koita, D., Tzedakis, T., Kane, C., Diaw, M., Sock, O. & Lavedan, P. (2014). Study of the
470 histamine electrochemical oxidation catalyzed by nickel sulfate. *Electroanalysis*. **26 (10)**:
471 2224 – 2236.

472 Kotal, M., Srivastava, S.K. & Paramanik, B. (2011). Enhancements in conductivity and thermal
473 stabilities of polyurethane/polypyrrole nanoblends. *The Journal of Physical Chemistry*
474 *C*. **115 (5)**: 1496 – 1505.

475 Ladan, M., Basirun, W.J., Kazi, S.N., Rahman, F.A. (2017). Corrosion protection of AISI 1018
476 steel using Co – doped TiO₂/polypyrrole nanocomposites in 3.5% NaCl solution.
477 *Materials Chemistry and Physics*. **192**: 361 – 373.

478 Lampman, G.M., Pavia, D.L., Kriz, G.S. & Vyvyan, J.R. (2010). Spectroscopy. 4th Edition.
479 Brooks/Cole Cengage Learning, Belmont, USA.

480 Lee, K.J., Elgrishi, N., Kandemir, B. & Dempsey, J.L. 2018. Electrochemical and spectroscopic
481 methods for evaluating molecular electrocatalysts. *Nature Reviews Chemistry* 1(5): 1 -
482 14.

483 Leykin, A., Shapovalov, L. & Figovsky, O. (2016). Non – isocyanate polyurethanes –
484 Yesterday, today and tomorrow. *Alternative Energy and Ecology*. **191** (3 – 4): 95 – 108.

485 Mishra, K., Narayan, R., Raju, K.V.S.N. & Aminabhavi, T.M. (2012). Hyperbranched
486 polyurethane (HBPU)-urea and HBPU-imide coatings: Effect of chain extender and
487 NCO/OH ratio on their properties. *Progress in Organic Coatings*. **74**: 134 – 141.

488 Mutsuhisa F., Ken, K. & Shohei, N. (2007). Microphase separated structure and mechanical
489 properties of norbornane diisocyanate – based polyurethane. *Polymer*. **48** (4): 997 – 1004.

490 Nohra, B., Candy, L., Blancos, J.F., Guerin, C., Raoul, Y. & Mouloungui, Z. (2013). From
491 petrochemical polyurethanes to biobased polyhydroxyurethanes. *Macromolecules*. **46**
492 (10): 3771 – 3792.

493 Pan, T. & Yu, Q. (2016). Anti – corrosion methods and materials comprehensive evaluation of
494 anti – corrosion capacity of electroactive polyaniline for steels. *Anti – Corrosion Methods
495 and Materials*. **63**: 360 – 368.

496 Pan, X. & Webster, D.C. (2012). New biobased high functionality polyols and their use in
497 polyurethane coatings. *ChemSusChem*. **5**: 419-429.

498 Petrovic, Z.S. (2008). Polyurethanes from vegetable oils. *Polymer Reviews*. **48** (1): 109 – 155.

499 Priya, S. S., Karthika, M., Selvasekarapandian, S. & Manjuladevi, R. (2018). Preparation and
500 characterization of polymer electrolyte based on biopolymer I-carrageenan with
501 magnesium nitrate. *Solid State Ionics*. **327**: 136 – 149.

502 Ren, D. & Frazier, C.E. (2013). Structure–property behaviour of moisture-cure polyurethane
503 wood adhesives: Influence of hard segment content. *Adhesion and Adhesives*. **45**: 118-
504 124.

505 Rogulska, S.K., Kultys, A. & Podkoscielny, W. (2007). Studies on thermoplastic polyurethanes
506 based on new diphenylethane – derivative diols. II. Synthesis and characterization of
507 segmented polyurethanes from HDI and MDI. *European Polymer Journal*. **43**: 1402 –
508 1414.

509 Romaskevicius, T., Budriene, S., Pielichowski, K. & Pielichowski, J. (2006). Application of
510 polyurethane – based materials for immobilization of enzymes and cells: a review.
511 *Chemija*. **17**: 74 – 89.

512 Sengodu, P. & Deshmukh, A. D. (2015). Conducting polymers and their inorganic composites
513 for advanced Li-ion batteries: a review. *RSC Advances*. **5**: 42109 – 42130.

514 Su'ait, M. S., Ahmad, A., Badri, K. H., Mohamed, N. S., Rahman, M. Y. A., Ricardi, C. L. A.
515 & Scardi, P. The potential of polyurethane bio – based solid polymer electrolyte for
516 photoelectrochemical cell application. *International Journal of Hydrogen Energy*. 39 (6):
517 3005 – 3017.

518 Tran, V.H., Kim, J.D., Kim, J.H., Kim, S.K., Lee, J.M. (2020). Influence of cellulose
519 nanocrystal on the cryogenic mechanical behaviour and thermal conductivity of
520 polyurethane composite. *Journal of Polymers and The Environment*. **28**: 1169 – 1179.

521 Viera, I.R.S., Costa, L.D.F.D.O., Miranda, G.D.S., Nardehcia, S., Monteiro, M.S.D. S.D.B.,
522 Junior, E.R. & Delpech, M.C. (2020). Waterborne poly (urethane – urea)s
523 nanocomposites reinforced with clay, reduced graphene oxide and respective hybrids:
524 Synthesis, stability and structural characterization. *Journal of Polymers and The
525 Environment*. **28**: 74 – 90.

526 Wang, B., Wang, L., Li, X., Liu, Y., Zhang, Z., Hedrick, E., Safe, S., Qiu, J., Lu, G. & Wang,
527 S. (2018). Template – free fabrication of vertically – aligned polymer nanowire array on
528 the flat – end tip for quantifying the single living cancer cells and nanosurface interaction.
529 *a Manufacturing Letters*. **16**: 27 – 31.

- 530 Wang, J., Xiao, L., Du, X., Wang, J. & Ma, H. (2017). Polypyrrole composites with carbon
531 materials for supercapacitors. *Chemical Papers*. **71** (2): 293 – 316.
- 532 Wong, C.S. & Badri, K.H. (2012). Chemical analyses of palm kernel oil – based polyurethane
533 prepolymer. *Materials Sciences and Applications*. **3**: 78 – 86.
- 534 Yong, Z., Bo, Z.M., Bo, W., Lin, J.Z. & Jun, N. (2009). Synthesis and properties of novel
535 polyurethane acrylate containing 3-(2-Hydroxyethyl) isocyanurate segment. *Progress in*
536 *Organic Coatings*. **67**: 264 – 268
- 537 Zia, K. M., Anjum, S., Zuber, M., Mujahid, M. & Jamil, T. (2014). Synthesis and molecular
538 characterization of chitosan based polyurethane elastomers using aromatic diisocyanate.
539 *International of Journal of Biological Macromolecules*. **66**: 26 – 32.
- 540
- 541
- 542

Hasil Reviu 2 dan Submit Revisi: 22 Juli 2021

Peter Foot

Decision

Major Revision Requested

Message for Author

This manuscript is interesting and has sufficient merits to be considered further for publication after due amendments to address the reviewers' comments. The English is quite understandable, but it requires revision to improve the clarity sufficiently for publication.

— Response to Revision Request

Muhammad Abdurrahman Munir

22.07.2021

Your Reply

Dear Editor, Thank you for your comments to this manuscript. Here I attached the revised manuscript and I have highlighted several sentences as to response your comments before. Kind Regards.

File

Manuscript - Munir.docx 909 kB 

+ Reviewer Reports

1 **Design and Synthesis of Conducting Polymer Based on Polyurethane** 2 **produced from Palm Kernel Oil**

3 Muhammad Abdurrahman Munir^{1,2*}, Khairiah Haji Badri^{1,3}, Lee Yook Heng¹

4 ¹Department of Chemical Sciences, Faculty of Science and Technology, Universiti
5 Kebangsaan Malaysia, Bangi, Malaysia

6 ²Department of Pharmacy, Faculty of Health Science, Universitas Alma Ata, Daerah
7 Istimewa Yogyakarta, Indonesia

8 ³Polymer Research Center, Universiti Kebangsaan Malaysia, Bangi, Malaysia

9 *Email: muhammad@almaata.ac.id

11 **Abstract**

12 Polyurethane (PU) is a unique polymer that has versatile processing method and mechanical
13 properties upon inclusion of selected additives. In this study, a freestanding bio-polyurethane
14 film on screen – printed electrode (SPE) was prepared by solution casting technique, using
15 acetone as solvent. It was a one-pot synthesis between major reactants namely, palm kernel
16 oil-based polyol (PKOp) and 4,4-methylene diisocyanate. The PU undergone strong adhesion
17 on SPE. The formation of urethane linkages (NHCO backbone) after polymerization was
18 confirmed by the absence of N=C=O peak at 2241 cm⁻¹. The glass transition temperature (T_g)
19 of the polyurethane was detected at 78.1°C. The conductivity of PU was determined using
20 cyclic voltammetry (CV) and differential pulse voltammetry (DPV). The current of electrode
21 was at 5.2 x 10⁻⁵ A.

22 **Keywords:** Polyurethane, polymerization, screen – printed electrode, voltammetry

26 **1. Introduction**

27 Polymers are molecules composed of many repeated sub-units referred to as monomers
28 (Sengodu & Deshmukh 2015). Conducting polymers (CPs) are polymers that exhibit
29 electrical behaviour (Alqarni et al. 2020). The conductivity of CPs was first observed in
30 polyacetylene, nevertheless owing to its instability led to the discovery of other forms of CPs
31 such as polyaniline (PANI), poly (o-toluidine) (PoT), polythiophene (PTh), polyfluorene (PF)
32 and polyurethane (PU). Furthermore, natural CPs have low conductivity and are often semi-
33 conductive. Therefore, it is essential to increase their conductivity mainly for use in
34 electrochemical sensor programs (Dzulkipli et al. 2021; Wang et al. 2018). Conducting
35 polymers (CPs) represent a sizeable range of useful organic substances. Their unique
36 electrical, chemical and physical properties; reasonable price; simple preparation; small
37 dimensions and large surface area have enabled researchers to discover a wide variety of uses
38 such as sensors, biochemical applications, solar cells and electrochromic devices (Alqarni et
39 al. 2020; Ghosh et al. 2018). There are scientific documentations on the use of conductive
40 polymers in various studies such as polyaniline (Pan & Yu 2016), polypyrrole (Ladan et al.
41 2017) and polyurethane (Tran et al. 2020; Vieira et al. 2020; Guo et al. 2020; Fei et al. 2020).
42 The application of petroleum as polyol in order to produce polyurethane has been applied.
43 The coal and crude oil used as raw materials to produce it. Nevertheless, these materials
44 become very rare to find and the price is very expensive at the same time required
45 sophisticated system to produce it. These reasons have been considered and finding utilizing
46 plants that can be used as alternative polyols should be done immediately (Badri 2012).
47 Furthermore, in order to avoid the application of petroleum as raw material for polyol,
48 vegetable oils become a better choice as polyol in order to obtain a biodegradable polyol.
49 Vegetable oils that generally used for synthesis polyurethane are soybean oil, corn oil,

50 sunflower seed oil, coconut oil, nuts oil, rape seed, olive oil and palm oil (Badri 2012;
51 Borowicz et al. 2019).

52 It is very straightforward for vegetable oils to react with specific group in order to form PU
53 such as epoxy, hydroxyl, carboxyl and acrylate owing to the existence of (-C=C-) in
54 vegetable oils. Thus, it has provided appealing profits to vegetables oils compared to
55 petroleum considered the toxicity, price and harm the environment (Mustapha et al. 2019;
56 Mohd Noor et al. 2020). Palm oil becomes the chosen in this study to produce PU owing to it
57 is largely cultivated in South Asia particularly in Malaysia and Indonesia. It has several
58 profits compared to other vegetables oils such as the easiest materials obtained, the lowest
59 cost of all the common vegetable oils and recognized as the plantation that has low
60 environmental impact and removing CO₂ from atmosphere as netsequester (Tajau et al. 2021;
61 Septevani et al. 2015).

62 Biopolymer, a natural biodegradable polymer has attracted much attention in recent years.
63 Global environmental awareness and fossil fuel depletion urged researchers to work in the
64 biopolymer field (Priya et al. 2018). Polyurethane is one of the most common, versatile and
65 researched materials in the world. These materials combine the durability and toughness of
66 metals with the elasticity of rubber, making them suitable to replace metals, plastics and
67 rubber in several engineered products. They have been widely applied in biomedical
68 applications, building and construction applications, automotive, textiles and in several other
69 industries due to their superior properties in terms of hardness, elongation, strength and
70 modulus (Zia et al. 2014; Romaskevicius et al. 2006). Polyurethanes also considered to be one
71 of the most useful materials with many profits such as, possess low conductivity, low density,
72 absorption capability and dimensional stability. They are clearly a great research subject
73 owing to their mechanical, physical and chemical properties (Badan & Majka 2017).

74 The urethane group is the major repeating unit in PUs and is produced from the reaction
75 between alcohol (-OH) and isocyanate (NCO); albeit polyurethanes also contain other groups
76 such as ethers, esters, urea and some aromatic compounds. Due to the wide variety of sources
77 from which PUs can be synthesized, thus a wide range of specific applications can be
78 generated. They are grouped into several different classes based on the desired properties:
79 rigid, flexible, thermoplastic, waterborne, binders, coating, adhesives, sealants and elastomers
80 (Akindoyo et al. 2016).

81 Although, PU has low conductivity but it is lighter than other materials such as metals. The
82 hardness of PU also relies on the aromatic rings number in the polymer structure (Janpoung
83 et al, 2020; Su'ait et al. 2014), majorly contributed by the isocyanate derivatives. PU has also
84 a conjugate structure where electrons can move in the main chain that causing electricity
85 produced even the conductivity is low. The electrical conductivity of conjugated linear (π)
86 can be explained by the distance between the highest energy level containing electrons
87 (HOMO) called valence band and the lowest energy level not containing electrons (LUMO)
88 called the conduction band (Wang et al. 2017; Kotal et al. 2011).

89 Nowadays, screen – printed electrodes (SPEs) modified with conducting polymer have been
90 developed for various electrochemical sensing. SPE becomes the best solution owing to its
91 frugal manufacture, tiny size, able to produce in large – scale and can be applied for on – site
92 detection (Nakthong et al. 2020). Conducting polymers (CPs) become an alternative to
93 modify the screen – printed electrodes due to their electrical conductivity, able to capture
94 analyte by chemical/physical adsorption, large surface area and making CPs are very
95 appealing material from electrochemical perspectives (Baig et al. 2019). Such advantages of
96 SPE encourage us to construct a new electrode for electrochemical sensing, and no research
97 reported on direct electrochemical oxidation of histamine using screen printed electrode

98 modified by polyurethane. Therefore, this research is the first to develop a new electrode
99 using (screen printed polyurethane electrode) SPPE without any conducting materials.

100 The purpose of this work was to synthesis, characterize and study the conductivity of
101 polyurethane using cyclic voltammetry (CV) and differential pulse voltammetry (DPV)
102 attached onto screen printed electrode (SPE). To the best of our knowledge, this is the first
103 attempt to use a modified polyurethane electrode. The electrochemistry of polyurethane
104 mounted onto screen-printed electrode (SPE) is discussed in detail. Polyurethane is possible
105 to become an advanced frontier material in chemically modified electrodes for bio sensing
106 application.

107

108 **2. Experimental**

109 **2.1 Chemicals**

110 *Synthesis of polyurethana film:* Palm kernel oil (PKOp) supplied by UKM Technology Sdn
111 Bhd through MPOB/UKM station plant, Pekan Bangi Lama, Selangor and prepared using
112 Badri et al. (2000) method. 4, 4-diphenylmethane diisocyanate (MDI) was acquired from
113 Cosmopolyurethane (M) Sdn. Bhd., Klang, Malaysia. Solvents and analytical reagents were
114 benzene ($\geq 99.8\%$), toluene ($\geq 99.8\%$), hexane ($\geq 99\%$), acetone ($\geq 99\%$), tetrahydrofuran
115 (THF), dimethylformamide (DMF) ($\geq 99.8\%$), dimethylsulfoxide (DMSO) ($\geq 99.9\%$) and
116 polyethylene glycol (PED) with a molecular weight of 400 Da obtained from Sigma Aldrich
117 Sdn Bhd, Shah Alam.

118

119 **2.2 Apparatus**

120 Tensile testing was performed using a universal testing machine model Instron 5566
121 following ASTM 638 (Standard Test Method for Tensile Properties of Plastics). The tensile

122 properties of the polyurethane film were measured at a velocity of 10 mm/min with a cell
123 load of 5 kN.

124 The thermal properties were performed using thermogravimetry analysis (TGA) and
125 differential scanning calorimetry (DSC) analysis. TGA was performed using a thermal
126 analyzer of Perkin Elmer Pyris model with heating rate of 10 °C/minute at a temperature
127 range of 30 to 800 °C under a nitrogen gas atmosphere. The DSC analysis was performed
128 using a thermal analyzer of Perkin Elmer Pyris model with heating rate of 10 °C /minute at a
129 temperature range of -100 to 200 °C under a nitrogen gas atmosphere. Approximately, 5-10
130 mg of PU was weighed. Sample was heated from 25 to 150 °C for one minute, then cooled
131 immediately from 150 -100 °C for another one minute and finally, reheated to 200 °C at a
132 rate of 10 °C /min. At this point, the polyurethane encounters changes from elastic properties
133 to brittle due to changes in the movement of the polymer chains. Therefore, the temperature
134 in the middle of the inclined regions is taken as the glass transition temperature (T_g). The
135 melting temperature (T_m) is identified as the maximum endothermic peak by taking the area
136 below the peak as the enthalpy point (ΔH_m).

137 The morphological analysis of PU film was performed by Field Emission Scanning Electron
138 Microscope (FESEM) model Gemini SEM microscope model 500-70-22. Before the analysis
139 was carried out, the polyurethane film was coated with a thin layer of gold to increase the
140 conductivity of the film. The coating method was carried out using a sputter - coater. The
141 observations were conducted at magnification of 200× and 5000 × with 10.00 kV (Electron
142 high tension - EHT).

143 The crosslinking of PU was determined using soxhlet extraction method. About 0.60 g of PU
144 sample was weighed and put in an extractor tube containing 250 ml of toluene, used as a
145 solvent. This flow of toluene was let to run for 24 hours. Mass of the PU was weighed before
146 and after the reflux process was carried out. Then, the sample was dried in the conventional

147 oven at 100 °C for 24 hours in order to get a constant mass. The percentage of crosslinking
148 content known as the gel content, can be calculated using Equation (1).

$$149 \quad \text{Gel content (\%)} = \frac{W_0 - W}{W} \times 100 \% \quad (1)$$

150 W_0 is mass of PU before the reflux process (g) and W is mass of PU after the reflux process
151 (g).

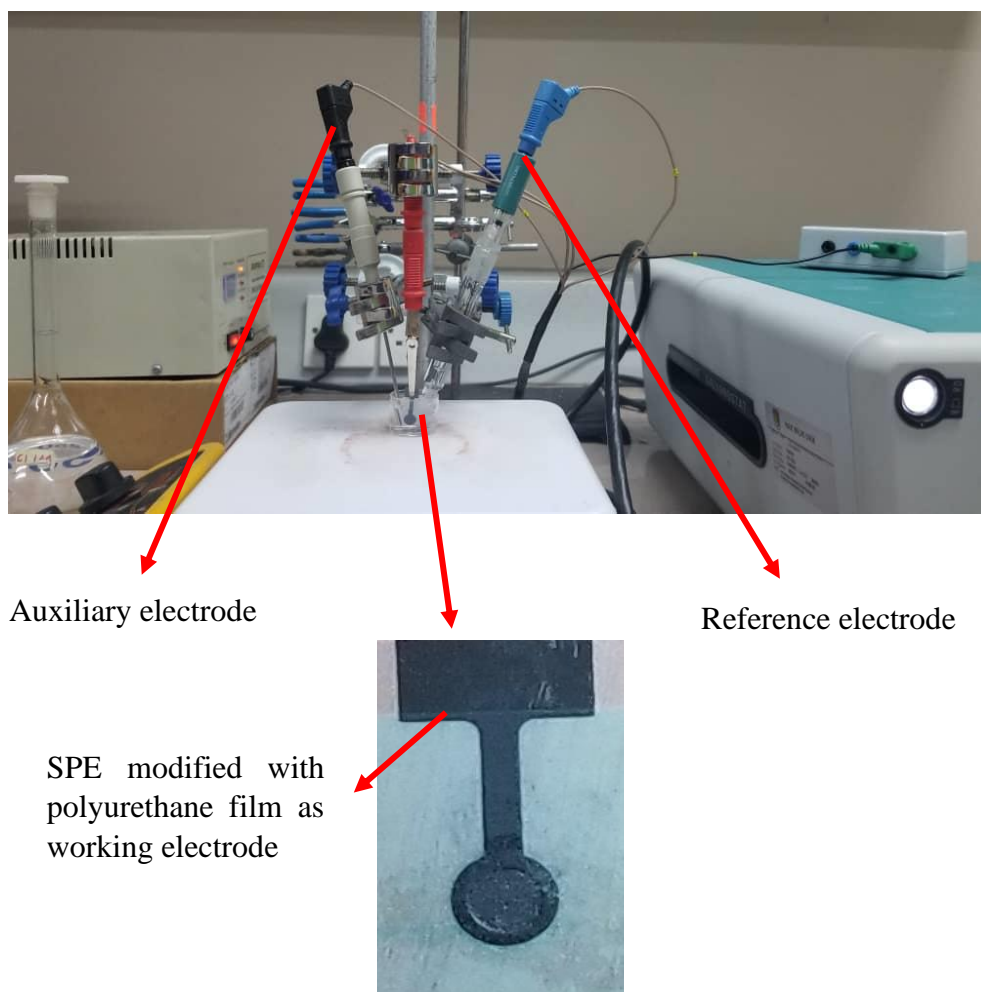
152

153 FTIR spectroscopic analysis was performed using a Perkin-Elmer Spectrum BX instrument
154 using the Diamond Attenuation Total Reflectance (DATR) method to confirm the
155 polyurethane, PKOp and MDI functional group. FTIR spectroscopic analysis was performed
156 at a wave number of 4000 to 600 cm^{-1} to identify the peaks of the major functional groups in
157 the formation of polymer such as amide group (-NH), urethane carbonyl group (-C = O) and
158 carbamate group (-CN).

159

160 **2.3 Modification of Electrode**

161 Voltammetric tests were performed using Metrohm Autolab Software (**Figure 1**) analyzer
162 using cyclic voltammetry (CV) method or known as amperometric mode and differential
163 pulse voltammetry (DPV). All electrochemical experiments were carried out using screen
164 printed electrode (diameter 3 mm) modified using polyurethane film as working electrode,
165 platinum wire as auxiliary electrode and Ag/AgCl electrode as reference electrode. All
166 experiments were conducted at temperature of $20 \pm 2^\circ\text{C}$.



167 **Figure 1.** Potentiostat instrument to study the conductivity of SPE modified with
 168 polyurethane film using cyclic voltametry (CV) and differential pulse voltammetry (DPV)
 169
 170 PU casted onto the screen – printed electrode (SPE + PU) was analyzed using a single
 171 voltammetric cycle between -1200 and +1500 mV (vs Ag/AgCl) of ten cycles at a scanning
 172 rate of 100 mV/s in 5 ml of KCl in order to study the activity of SPE and polyurethane film.
 173 Approximately (0.1, 0.3 & 0.5) mg of palm – based prepolyurethane was dropped separately
 174 onto the surface of the SPE and dried at room temperature. The modified palm-based
 175 polyurethane electrodes were then rinsed with deionized water to remove physically adsorbed
 176 impurities and residues of unreacted material on the electrode surface. All electrochemical
 177 materials and calibration measurements were carried out in a 5 mL glass beaker with a
 178 configuration of three electrodes inside it. Platinum wire and silver/silver chloride (Ag/AgCl)

179 electrodes were used as auxiliary and reference electrodes, while screen printed electrode that
180 had been modified with polyurethane was applied as a working electrode.

181

182 3. Results and Discussion

183 The synthesis of PU films was carried out using pre - polymerization method which involves
184 the formation of urethane polymer at an early stage. The reaction took place between palm
185 kernel oil – based polyol (PKOp) and diisocyanate (MDI). **Table 1** presents the PKO-p
186 properties used in this study. The structural chain was extended with the aid of polyethylene
187 glycol (PEG) to form flexible and elastic polyurethane film. In order to form the urethane
188 prepolymer, one of the isocyanate groups (NCO) reacts with one hydroxyl group (OH) of
189 polyol while the other isocyanate group attacks another hydroxyl group in the polyol (Wong
190 & Badri 2012) as shown in **Figure 2**.

191

192 **Table 1** Characteristics of PKO-p (Badri et al. (2000)).

| Property | Values |
|------------------------------|-----------|
| Viscosity at 25°C (cps) | 1313.3 |
| Specific gravity (g/mL) | 1.114 |
| Moisture content (%) | 0.09 |
| pH value | 10 – 11 |
| The hydroxyl number mg KOH/g | 450 - 470 |

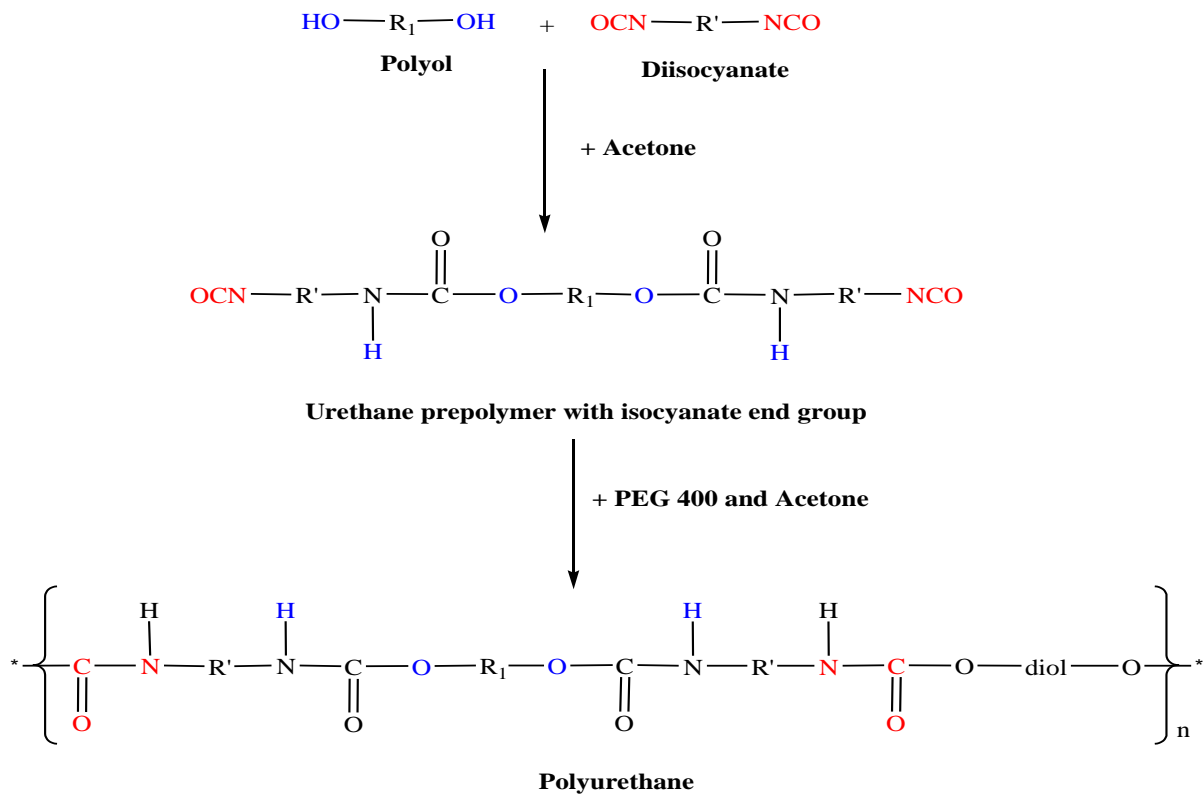
193

194 a. FTIR analysis

195 **Figure 3** shows the FTIR spectrum for polyurethane, exhibiting the important functional
196 group peaks. According to study researched by Wong & Badri 2012, PKO-p reacts with MDI
197 to form urethane prepolymers. The NCO group on MDI reacts with OH group on polyol

198 whether PKOp or PEG. It can be seen there are no important peaks of MDI in the FTIR
199 spectrums. This is further verified by the absence of peak at the 2400 cm^{-1} belongs to MDI (-
200 NCO groups). This could also confirm that the NCO group on MDI had completely reacted
201 with PKO-p to form the urethane -NHC (O) backbone. The presence of amides (-NH),
202 carbonyl urethane group (-C = O), carbamate group (C-NH) and -C-O-C confirmed the
203 formation of urethane chains. In this study, the peak of carbonyl urethane (C = O) detected at
204 1727 cm^{-1} indicated that the carbonyl urethane group was bonded without hydrogen owing to
205 the hydrogen reacted with the carbonyl urethane group.

206 The reaction of polyurethane has been studied by Hamuzan & Badri (2016) where the
207 urethane carbonyl group was detected at $1730 - 1735\text{ cm}^{-1}$ while the MDI carbonyl was
208 detected at 2400 cm^{-1} . The absence of peaks at $2250 - 2270\text{ cm}^{-1}$ indicates the absence of
209 NCO groups. It shows that the polymerization reaction occurs entirely between NCO groups
210 in MDI with hydroxyl groups on polyols and PEG (Mishra et al. 2012). The absence of peaks
211 at 1690 cm^{-1} representing urea (C = O) in this study indicated, there is no urea formation as a
212 byproduct (Clemitson 2008) of the polymerization reaction that possibly occur due to the
213 excessive water. For the amine (NH) group, hydrogen-bond to NH and oxygen to form ether
214 and hydrogen bond to NH and oxygen to form carbonyl on urethane can be detected at the
215 peak of 3301 cm^{-1} and in the wave number at range $3326 - 3428\text{ cm}^{-1}$. This has also been
216 studied and detected by Lampman et. al. (2010) and Mutsuhisa et al. (2007). In this study, the
217 hydrogen bond formed by C = O acts as a proton acceptor whereas NH acts as a proton
218 donor. The urethane group in the hard segment (MDI) has electrostatic forces on the oxygen,
219 hydrogen and nitrogen atoms and these charged atoms form dipoles that attract other opposite
220 atoms. These properties make isocyanates are highly reactive and having different properties
221 (Leykin et al. 2016).



222

223 **Figure 2.** The chemical route of producing polyurethane via pre-polymerization method

224 (Wong & Badri 2012).

225

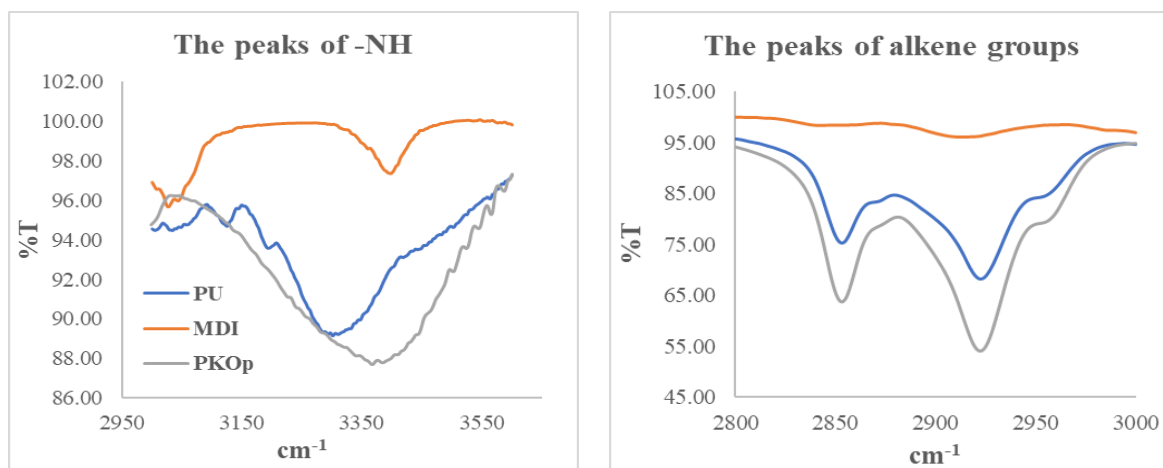
226 MDI was one of the isocyanate used in this study, has an aromatic group and more
 227 reactive compared to aliphatic group isocyanates such as hexamethylene diisocyanate (HDI)
 228 or isophorone diisocyanate (IPDI). Isocyanates have two groups of isocyanates on each
 229 molecule. Diphenylmethane diisocyanate is an exception owing to its structure consists of two,
 230 three, four or more isocyanate groups (Nohra et al. 2013). The use of PEG 400 in this study
 231 as a chain extender for polyurethane increases the chain mobility of polyurethane at an
 232 optimal amount. The properties of polyurethane are contributed by hard and soft copolymer
 233 segments of both polyol monomers and MDI. This makes the hard segment of urethane
 234 serves as a crosslinking site between the soft segments of the polyol (Leykin et al. 2016).

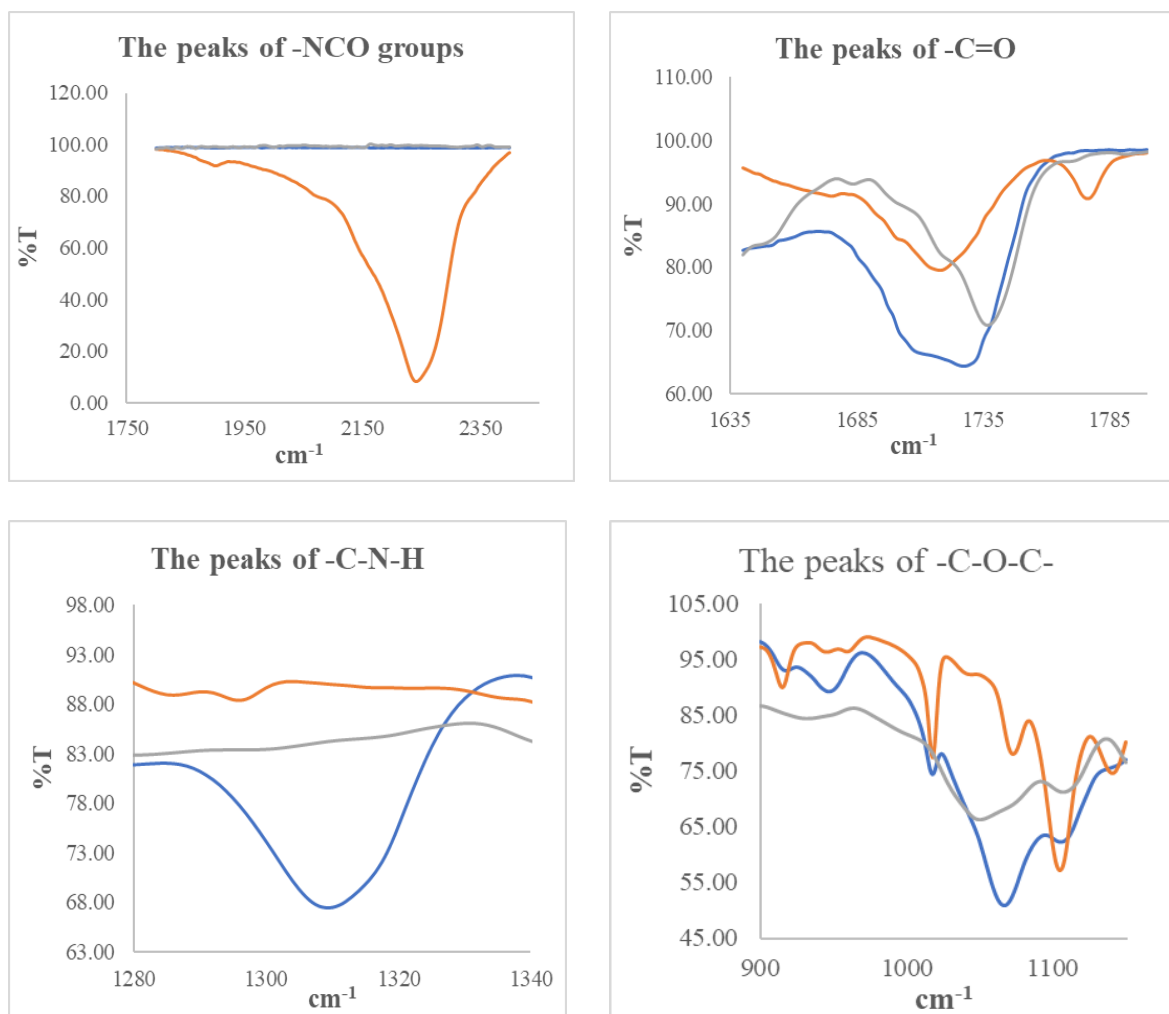
235 The mechanism of the pre – polymerization in urethane chains formation is a
 236 nucleophilic substitution reaction as studied by Yong et al. (2009). However, this study found

237 amines as nucleophiles. Amine attacks carbonyl on isocyanate in MDI in order to form two
238 resonance structures of intermediate complexes A and B. Intermediate complex B has a
239 greater tendency to react with polyols due to stronger carbonyl (C = O) bonds than C = N
240 bonds on intermediate complexes A. Thus, intermediate complex B is more stable than
241 intermediate complex A, as suggested by previous researchers who have conducted by Wong
242 and Badri (2012).

243 Moreover, nitrogen was more electropositive than oxygen, therefore, -CN bonds were
244 more attracted to cations (H⁺) than -CO. The combination between long polymer chain and
245 low cross linking content gives the polymer an elastic properties whereas short chain and
246 high cross linking producing hard and rigid polymers. Cross linking in polymers consist of
247 three - dimensional networks with high molecular weight. In some aspects, polyurethane can
248 be a macromolecule, a giant molecule (Petrovic 2008).

249



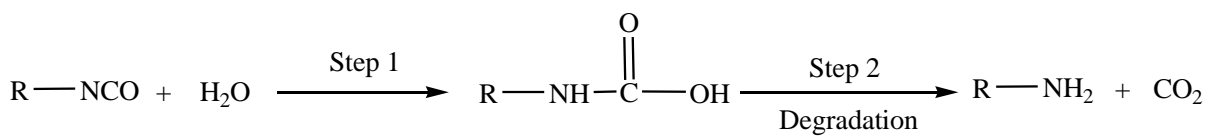


250 **Figure 3.** FTIR spectrums of several important peaks between polyurethane, PKO-p and
 251 MDI

252

253 However, reaction between MDI and PEG as a chain extender where oxygen on the
 254 nucleophile PEG attacks the NCO group in the MDI to form two intermediate complexes A
 255 and B can occur. Nevertheless, nucleophilic substitution reactions have a greater tendency to
 256 occur in PKOp compared to PEG because the presence of nitrogen atoms is more
 257 electropositive than oxygen atoms in PEG. Amine has a higher probability of to react
 258 compared to hydroxyl (Herrington & Hock 1997). Amine with high alkalinity reacts with
 259 carbon atoms on MDI as proposed by Wong and Badri (2012). PKOp contains long carbon
 260 chains that can easily stabilize alkyl ions when intermediate complexes are formed.

261 Therefore, polyol is more reactive than PEG to react with MDI. However, the addition of
 262 PEG will increase the length of the polyurethane chain and prevent side effects such as the
 263 formation of urea by -products of the NCO group reaction in urethane pre - polymer and
 264 water molecules from the environment. If the NCO group reacts with the excess water in the
 265 environment, the formation of urea and carbon dioxide gas will also occur excessively
 266 (**Figure 4**). This reaction can cause a polyurethane foam not polyurethane film as we studied
 267 the film.



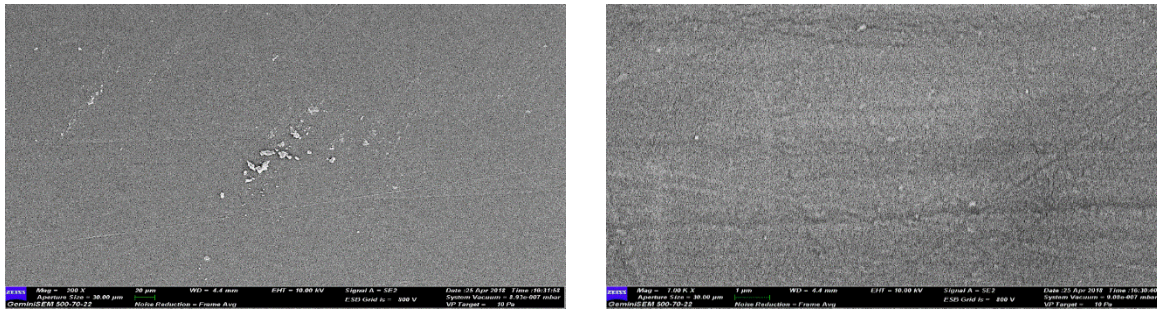
268
 269 **Figure 4.** The reaction between NCO group and water producing carbon dioxide

270
 271 Furthermore, the application of PEG can influence the conductivity of PU where
 272 Porcarelli et al. (2017) have reported the application of PEG using several molecular weights.
 273 PEG 1500 decreased the conductivity of PU in consequence of the semicrystalline phase of
 274 PEG 1500 that acted as a poor ion conducting phase for PU. It is also well known that PEG
 275 with molecular weight more than 1000 g·mol⁻¹ tends to crystallize with deleterious effects on
 276 room temperature ionic conductivity (Porcarelli et al. 2017).

277
 278 b. Morphological analysis

279 The Field Emission Scanning Electron Microscope (FESEM) micrograph in **Figure 5** shows
 280 the formation of a uniform polymer film contributed by the polymerization method applied.
 281 The magnification used for this surface analysis ranged from 200 to 5000 ×. The
 282 polymerization method can also avoid the failure of the reaction in PU polymerization.
 283 Furthermore, no trace of separation was detected by FESEM. This has also been justified by
 284 the wavelengths obtained by the FTIR spectrums above.

285



286 **Figure 5.** The micrograph of polyurethane films analysed by FESEM at (a) 200 × and
 287 5000× magnifications.

288
 289 c. The crosslinking analysis

290 Soxhlet analysis was applied to determine the degree of crosslinking between the hard
 291 segments and the soft segments in the polyurethane. The urethane group on the hard segment
 292 along the polyurethane chain is polar (Cuve & Pascault 1991). Therefore, during the testing,
 293 it was very difficult to dissolve in toluene, as the testing reagent. The degree of the
 294 crosslinking is determined by the percentage of the gel content. The analysis result obtained
 295 from the Soxhlet testing indicating a 99.3 % gel content. This is significant in getting a stable
 296 polymer at higher working temperature (Rogulska et al. 2007).

297

$$\text{Gel content (\%)} = \frac{(0.6 - 0.301) \text{ g}}{0.301 \text{ g}} \times 100\% = 99.33\%$$

298

299 d. The thermal analysis

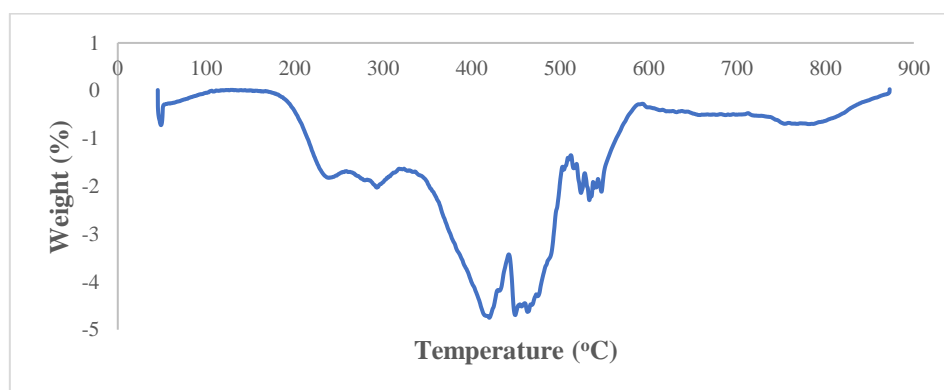
300 Thermogravimetric analysis (TGA) can be used to observe the material mass based on
 301 temperature shift. It can also examine and estimate the thermal stability and materials
 302 properties such as the alteration weight owing to absorption or desorption, decomposition,
 303 reduction and oxidation. The material composition of polymer is specified by analysing the
 304 temperatures and the heights of the individual mass steps (Alamawi et al. 2019). **Figure 6**
 305 shows the TGA and DTG thermograms of polyurethane. The percentage weight loss (%) is

306 listed in **Table 2**. Generally, only a small amount of weight was observed. It is shown in
 307 **Figure 6** in the region of 45 – 180°C. This is due to the presence of condensation on moisture
 308 and solvent residues.

309 **Table2** Weight loss percentage of (wt%) polyurethane film

| Sample | % Weight loss (wt%) | | | | Total of weight loss (%) | Residue after 550°C (%) |
|--------------|-----------------------|-------------------------------|-------------------------------|-------------------------------|--------------------------|-------------------------|
| | T _{max} , °C | T _{d1} , 200 – 290°C | T _{d2} , 350 – 500°C | T _{d3} , 500 – 550°C | | |
| Polyurethane | 240 | 8.04 | 39.29 | 34.37 | 81.7 | 18.3 |

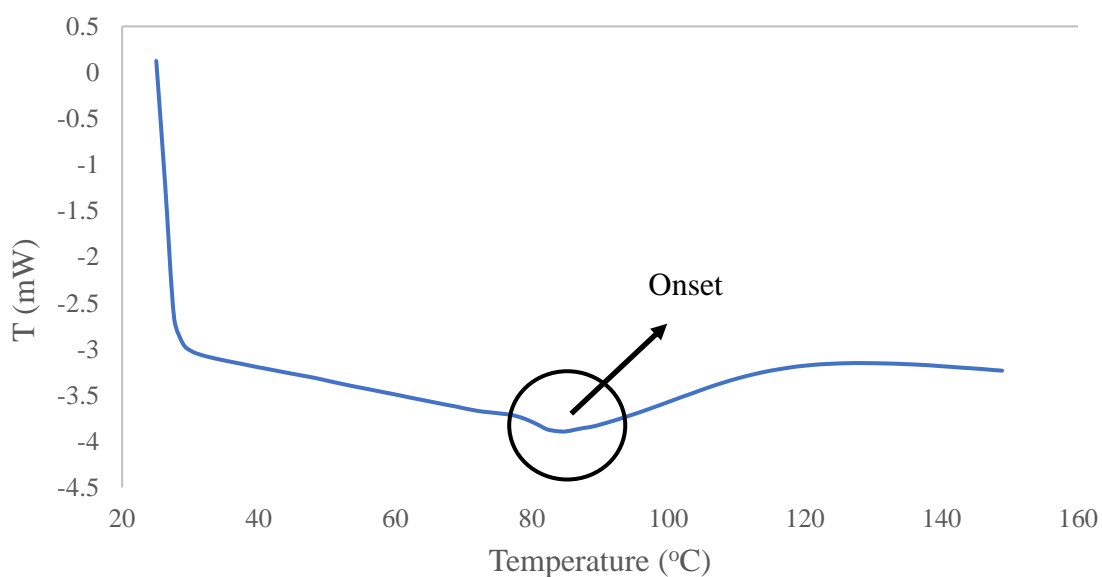
310 The bio polyurethane is thermally stable up to 240 °C before it undergone thermal
 311 degradation (Agrawal et al. 2017). The first stage of thermal degradation (T_{d1}) on
 312 polyurethane films was shown in the region of 200 – 290 °C as shown in **Figure 6**. The T_{d1} is
 313 associated with degradation of the hard segments of the urethane bond, forming alcohol or
 314 degradation of the polyol chains and releasing of isocyanates (Berta et al. 2006), primary and
 315 secondary amines as well as carbon dioxide (Corcuera et al. 2011; Pan & Webster 2012).
 316 Meanwhile, the second thermal degradation stage (T_{d2}) of polyurethane films experienced a
 317 weight loss of 39.29 %. This endotherm of T_{d2} is related to dimerization of isocyanates to
 318 form carbodiimides and release CO₂. The formed carbodiimide reacts with alcohol to form
 319 urea. For the third stage of thermal degradation (T_{d3}) is related to the degradation on urea
 320 (Berta et al. 2006) and the soft segment on polyurethane.



322 **Figure 6.** DTG thermogram of polyurethane film
 323

324 Generally, DSC analysis exhibited thermal transitions as well as the initial
325 crystallisation and melting temperatures of the polyurethane (Khairuddin et al. 2018). It
326 serves to analyse changes in thermal behaviour due to changes occurring in the chemical
327 chain structure based on the glass transition temperature (T_g) of the sample obtained from the
328 DSC thermogram (**Figure 7**). DSC analysis on polyurethane films was performed in the
329 temperature at range 100 °C to 200 °C using nitrogen gas as blanket as proposed by
330 Furtwengler et al. (2017). The glass transition temperature (T_g) on polyurethane was above
331 room temperature, at 78.1 °C indicated the state of glass on polyurethane. The presence of
332 MDI contributes to the formation of hard segments in polyurethanes. Porcarelli et al. (2017)
333 stated that possess a low glass transition (T_g) may contribute to PU conductivity.

334 During polymerization, this hard segment restricts the mobility of the polymer chain
335 (Ren et al. 2013) owing to steric effect on benzene ring in hard segment. The endothermic
336 peak of acetone used as the solvent in this study was supposedly be at 56°C. However, it was
337 detected in the DSC thermogram nor the TGA thermogram, which indicates that acetone was
338 removed from the polyurethane during the synthesis process, owing to its volatility nature.
339 The presence of acetone in the synthesis was to lower the reaction kinetics.



340
341

Figure 7. DSC thermogram of polyurethane film

342 e. The solubility and mechanical properties of the polyurethane film
 343 The chemical resistivity of a polymer will be the determinant in performing as conductor.
 344 Thus, its solubility in various solvents was determined by dissolving the polymer in selected
 345 solvents such as hexane, benzene, acetone, tetrahydrofuran (THF), dimethylformamide
 346 (DMF) and dimethylformamide (DMSO). On the other hand, the mechanical properties of
 347 polyurethane were determined based on the standard testing following ASTM D 638
 348 (Standard Test Method for Tensile Properties of Plastics). The results from the polyurethane
 349 film solubility and tensile test are shown in **Table 3**. Polyurethane films were insoluble with
 350 benzene, hexane and acetone and are only slightly soluble in tetrahydrofuran (THF),
 351 dimethylformamide (DMF) and dimethylformamide (DMSO) solutions. While the tensile
 352 strength of a PU film indicated how much elongation load the film was capable of
 353 withstanding the material before breaking.

354 **Table 3** The solubility and mechanical properties of the polyurethane film

| Parameters | Polyurethane film | |
|----------------------------|-------------------|--------------|
| Solubility | Benzene | Insoluble |
| | Hexane | Insoluble |
| | Acetone | Insoluble |
| | THF | Less soluble |
| | DMF | Less soluble |
| | DMSO | Less soluble |
| Stress (MPa) | 8.53 | |
| Elongation percentage (%) | 43.34 | |
| Strain modulus (100) (MPa) | 222.10 | |

356

357 The tensile stress, strain and modulus of polyurethane film also indicated that polyurethane
358 has good mechanical properties that are capable of being a supporting substrate for the next
359 stage of study. In the production of polyurethane, the properties of polyurethane are easily
360 influenced by the content of MDI and polyol used. The length of the chain and its flexibility
361 are contributed by the polyol which makes it elastic. High crosslinking content can also
362 produce hard and rigid polymers. MDI is a major component in the formation of hard
363 segments in polyurethane. It is this hard segment that determines the rigidity of the PU.
364 Therefore, high isocyanate content results in higher rigidity on PU (Petrovic et al. 2002).
365 Thus, the polymer has a higher resistance to deformation and more stress can be applied to
366 the PU.

367

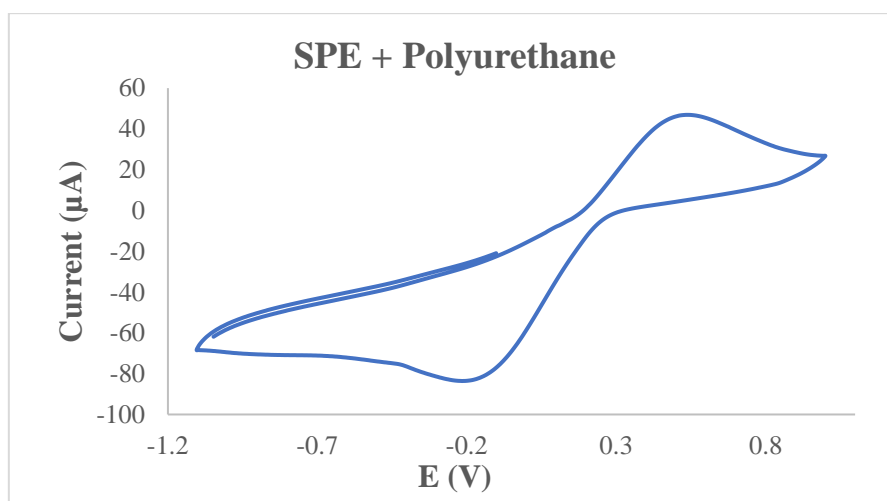
368 f. Conductivity of the polyurethane as polymeric film on SPE

369 Polyurethane film deposited onto the screen printed electrode by casting method as shown in
370 **Figure 1**. After that, the modified electrode was analysed using cyclic voltammetry (CV) and
371 differential pulse voltammetry (DPV) in order to study the behaviour of modified electrode.
372 The modified electrode was tested in a 0.1 mmol/L KCl solution containing 5 mmol/L (K_3Fe
373 $(CN)_6$). The use of potassium ferricyanide is intended to increase the sensitivity of the KCl
374 solution. The conductivity of the modified electrode was studied. The electrode was analyzed
375 by cyclic voltametry method with a potential range of -1.00 to +1.00 with a scan rate of 0.05
376 V/s. The voltamogram at electrode have shown a specific redox reactions. Furthermore, the
377 conductivity of the modified electrode is lower due to the use of polyurethane. This occurs
378 due to PU is a natural polymer produced from the polyol of palm kernel oil. The
379 electrochemical signal at the electrode is low if there is a decrease in electrochemical
380 conductivity (El - Raheem et al. 2020). It can be concluded that polyurethane is a bio –
381 polymer with a low conductivity value. The current of modified electrode was found at 5.3 x

382 10^{-5} A or 53 μA . Nevertheless, the electroconductivity of PU in this study shows better
383 conductivity several times compared to Bahrami et al. (2019) that reported the conductivity
384 of PU as 1.26×10^{-6} A, whereas Li et al. (2019) reported the PU conductivity in their study
385 was even very low, namely 10^{-14} A. The conductivity of PU owing to the benzene ring in
386 hard segment (MDI) could exhibit the conductivity by inducing electron delocalization along
387 the polyurethane chain (Wong et al. 2014). The conductivity of PU can also caused by PEG.
388 The application of PEG as polyol has been studied by Porcarelli et al. (2017), that reported
389 that conductivity of PU based on PEG – polyol was 9.2×10^{-8} .

390 According to **Figure 8**, it can be concluded that the anodic peak present in the modified
391 electrode was at +0.5 V, it also represented the oxidation process of the modified electrode.
392 The first oxidation scan on both electrodes ranged from -0.2 to +1.0 V, which showed a
393 significant anodic peak at a potential of +0.5 V.

394



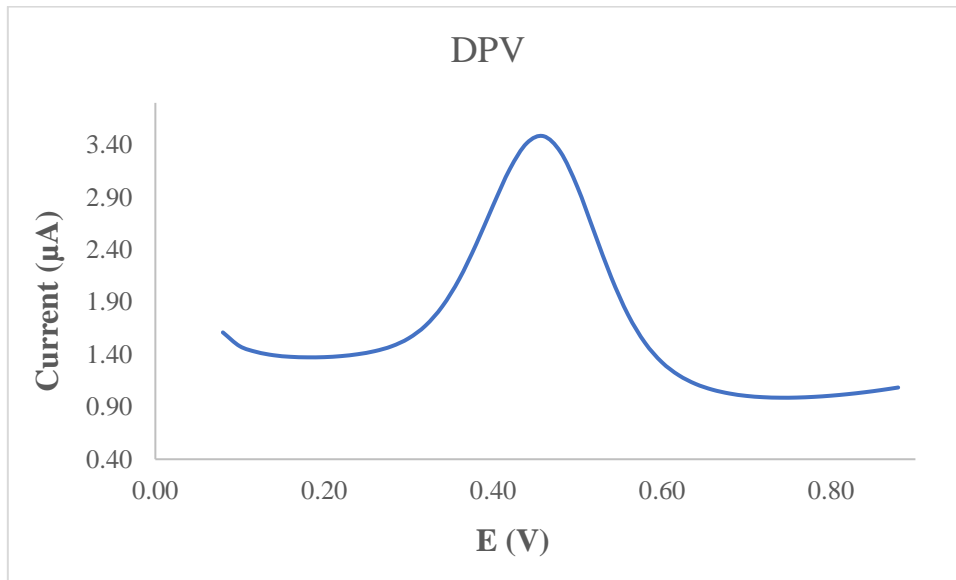
395

396 **Figure 8.** The voltamogram of SPE – PU modified electrode after analysed using cyclic
397 voltammetry (CV) technique

398

399 **Figure 9** also presents the DPV voltammogram of modified electrode. DPV is a measurement
400 based on the difference in potential pulses that produce an electric current. Scanning the
401 capability pulses to the working electrode will produce different currents. Optimal peak

402 currents will be produced to the reduction capacity of the redox material. The peak current
 403 produced is proportional to the concentration of the redox substance and can be detected up
 404 to concentration below 10^{-8} M. DPV conducted to obtain the current value that more accurate
 405 than CV (Lee et al. 2018).



406
 407 **Figure 9.** The voltammogram of SPE – PU modified electrode after analyzed using
 408 differential pulse voltammetry (DPV) technique
 409

410 This study used a redox pair ($K_3Fe(CN)_6$) as a test device (probe). The currents generated by
 411 SPE-PU and proved by CV and DPV have shown conductivity on polyurethane films. This
 412 suggests that polyurethane films can conduct electron transfer. The electrochemical area on
 413 the modified electrode can be calculated using the formula from Randles-Sevcik (Butwong et
 414 al. 2019), where the electrochemical area for SPE-PU is considered to be A, using Equation
 415 2:

$$416 \quad \text{Current of SPE-PU, } I_p = 2.65 \times 10^5 n^{3/2} A v^{1/2} C D^{1/2} \quad (2)$$

417 Where, n – 1 is the amount of electron transfer involved, while C is the solvent concentration
 418 used (mmol/L) and the value of D is the diffusion constant of 5 mmol/L at ($K_3Fe(CN)_6$)
 419 dissolved using 0.1 mmol/L KCl. The estimated surface area of the electrode (**Figure 1**) was
 420 0.2 cm^2 where the length and width of the electrode used during the study was $0.44 \text{ cm} \times 0.44$

421 cm while the surface area of the modified electrode was 0.25 cm² with the length and width
422 of the electrode estimated at 0.5 cm × 0.5 cm, and causing the modified electrode has a larger
423 surface. The corresponding surface concentration (τ) (mol/cm²) is calculated using Equation
424 3.

$$425 \quad I_p = (n^2 F^2 / 4RT) A \tau v \quad (3)$$

426 I_p is the peak current (A), while A is the surface area of the electrode (cm²), the value of v is
427 the applied scan rate (mV/s) and F is the Faraday constant (96,584 C/mol), R is the constant
428 ideal gas (8.314 J/mol K) and T is the temperature used during the experiment being
429 conducted (298 K) (Koita et al. 2014). The development of conducting polymer from palm
430 oil – based biomaterials seems to be one of the potential future applications of palm oil
431 products, as this novel material has the potential to contribute positively to the analytical
432 industry. Likewise, other palm oil-based products, such as refined-bleached-deodorised
433 (RBD) palm oil, palm oil, and palm stearin are abundantly available in Malaysia. They are
434 known to be economical, sustainable, and environmentally biodegradable. These palm oil-
435 based products are promising prospects for manufacturing biomaterials that become
436 alternative products to other polymers from synthetic/chemical-based (Tajao et al. 2021).
437 Several studies have been reported the application of PU to produce elastic conductive fibres
438 and films owing to it is highly elastic, scratch resistant and adhesive (Tadese et al. 2019), thus
439 it is easy for PU to adhere on the screen printed electrode in order to modify the electrode.
440 PU is also being used as a composite material to make elastic conducting composite films
441 (Khatoon & Ahmad 2017).

442

443 4. Conclusion

444 Polyurethane film was prepared by pre-polymerization between palm kernel oil-based polyol
445 (PKO-p) with MDI. The presence of PEG 400 as the chain extender formed freestanding

446 flexible film. Acetone was used as the solvent to lower the reaction kinetics since the pre-
447 polymerization was carried out at room temperature. The formation of urethane links (NHCO
448 – backbone) after polymerization was confirmed by the absence of N=C=O peak at 2241 cm⁻¹
449 and the presence of N-H peak at 3300 cm⁻¹, carbonyl (C=O) at 1710 cm⁻¹, carbamate (C-N) at
450 1600 cm⁻¹, ether (C-O-C) at 1065 cm⁻¹, benzene ring (C = C) at 1535 cm⁻¹ in the bio
451 polyurethane chain structure. Soxhlet analysis for the determination of crosslinking on
452 polyurethane films has yielded a high percentage of 99.33 %. This is contributed by the hard
453 segments formed from the reaction between isocyanates and hydroxyl groups causing
454 elongation of polymer chains. FESEM analysis exhibited absence of phase separation and
455 smooth surface. Meanwhile, the current of modified electrode was found at 5.2×10^{-5} A. This
456 bio polyurethane film can be used as a conducting bio – polymer and it is very useful for
457 other studies such as electrochemical sensor purpose. **Furthermore, advanced technologies are**
458 **promising and the future of bio – based polyols looks very bright.**

459

460 **5. Acknowledgement**

461 The authors would like to thank Universitas Alma Ata for the sponsorship given to the first
462 author. We would like to also, thank Department of Chemical Sciences, Universiti
463 Kebangsaan Malaysia for the laboratory facilities and CRIM, UKM for the analysis
464 infrastructure.

465

466 **6. Conflict of Interest**

467 The authors declare no conflict of interest.

468

469

470

471 **7. References**

- 472 Agrawal, A., Kaur, R., Walia, R. S. (2017). PU foam derived from renewable sources:
473 Perspective on properties enhancement: An overview. *European Polymer Journal*. 95:
474 255 – 274.
- 475 Akindoyo, J. O., Beg, M.D.H., Ghazali, S., Islam, M.R., Jeyaratnam, N. & Yuvaraj, A.R.
476 (2016). Polyurethane types, synthesis and applications – a review. *RSC Advances*. 6:
477 114453 – 114482.
- 478 Alamawi, M. Y., Khairuddin, F. H., Yusoff, N. I. M., Badri, K., Ceylan, H. (2019).
479 Investigation on physical, thermal and chemical properties of palm kernel oil polyol bio
480 – based binder as a replacement for bituminous binder. *Construction and Building*
481 *Materials*. 204: 122 – 131.
- 482 Alqarni, S. A., Hussein, M. A., Ganash, A. A. & Khan, A. (2020). Composite material –
483 based conducting polymers for electrochemical sensor applications: a mini review.
484 *BioNanoScience*. 10: 351 – 364.
- 485 Badan, A., Majka, T. M. (2017). The influence of vegetable – oil based polyols on physico –
486 mechanical and thermal properties of polyurethane foams. *Proceedings*. 1 – 7.
- 487 Badri, K.H. (2012) Biobased polyurethane from palm kernel oil-based polyol. In
488 Polyurethane; Zafar, F., Sharmin, E., Eds. InTechOpen: Rijeka, Croatia. pp. 447–470.
- 489 Badri, K.H., Ahmad, S.H. & Zakaria, S. 2000. Production of a high-functionality RBD palm
490 kernel oil – based polyester polyol. *Journal of Applied Polymer Science* 81(2): 384 –
491 389.
- 492 Baig, N., Sajid, M. and Saleh, T. A. 2019. Recent trends in nanomaterial – modified
493 electrodes for electroanalytical applications. *Trends in Analytical Chemistry*. 111: 47 –
494 61.

495 Berta, M., Lindsay, C., Pans, G., & Camino, G. (2006). Effect of chemical structure on
496 combustion and thermal behaviour of polyurethane elastomer layered silicate
497 nanocomposites. *Polymer Degradation and Stability*. **91**: 1179-1191.

498 Borowicz, M., Sadowska, J. P., Lubczak, J. & Czuprynski, B. (2019). Biodegradable, flame –
499 retardant, and bio – based rigid polyurethane/polyisocyanurate foams for thermal
500 insulation application. *Polymers*. 11: 1816 – 1839.

501 Butwong, N., Khajonklin, J., Thongbor, A. & Luong, J.H.T. (2019). Electrochemical sensing
502 of histamine using a glassy carbon electrode modified with multiwalled carbon
503 nanotubes decorated with Ag – Ag₂O nanoparticles. *Microchimica Acta*. **186 (11)**: 1 –
504 10.

505 Clemitson, I. (2008). Castable Polyurethane Elastomers. Taylor & Francis Group, New York.
506 doi:10.1201/9781420065770.

507 Corcuera, M.A., Rueda, L., Saralegui, A., Martin, M.D., Fernandez-d’Arlas, B., Mondragon,
508 I. & Eceiza, A. (2011). Effect of diisocyanate structure on the properties and
509 microstructure of polyurethanes based on polyols derived from renewable resources.
510 *Journal of Applied Polymer Science*. **122**: 3677-3685.

511 Cuve, L. & Pascault, J.P. (1991). Synthesis and properties of polyurethanes based on
512 polyolefine: Rigid polyurethanes and amorphous segmented polyurethanes prepared in
513 polar solvents under homogeneous conditions. *Polymer*. **32 (2)**: 343- 352.

514 Dzulkipli, M. Z., Karim, J., Ahmad, A., Dzulkurnain, N. A., Su’ait, M S., Fujita, M. Y.,
515 Khoon, L. T. & Hassan, N. H. (2021). The influences of 1-butyl-3-methylimidazolium
516 tetrafluoroborate on electrochemical, thermal and structural studies as ionic liquid gel
517 polymer electrolyte. *Polymers*. 13 (8): 1277 – 1294.

518 El-Raheem, H.A., Hassan, R.Y.A., Khaled, R., Farghali, A. & El-Sherbiny, I.M. (2020).
519 Polyurethane – doped platinum nanoparticles modified carbon paste electrode for the

520 sensitive and selective voltammetric determination of free copper ions in biological
521 samples. *Microchemical Journal*. **155**: 104765.

522 Fei, T., Li, Y., Liu, B. & Xia, C. (2019). Flexible polyurethane/boron nitride composites with
523 enhanced thermal conductivity. *High Performance Polymers*. **32** (3): 1 – 10.

524 Furtwengler, P., Perrin R., Redl, A. & Averous, L. (2017). Synthesis and characterization of
525 polyurethane foams derived of fully renewable polyesters polyols from sorbitol.
526 *European Polymer Journal*. **97**: 319 – 327.

527 Ghosh, S., Ganguly, S., Remanan, S., Mondal, S., Jana, S., Maji, P. K., Singha, N., Das, N.
528 C. (2018). Ultra – light weight, water durable and flexible highly electrical conductive
529 polyurethane foam for superior electromagnetic interference shielding materials.
530 *Journal of Materials Science: Materials in Electronics*. **29**: 10177 – 10189.

531 Guo, S., Zhang, C., Yang, M., Zhou, Y., Bi, C., Lv, Q. & Ma, N. (2020). A facile and
532 sensitive electrochemical sensor for non – enzymatic glucose detection based on three –
533 dimensional flexible polyurethane sponge decorated with nickel hydroxide. *Analytica
534 Chimica Acta*. **1109**: 130 – 139.

535 Hamuzan, H.A. & Badri, K.H. (2016). The role of isocyanates in determining the viscoelastic
536 properties of polyurethane. AIP Conference Proceedings. 1784, Issue 1.

537 Herrington, R. & Hock, K. (1997). Flexible polyurethane foams. 2nd Edition. Dow Chemical
538 Company. Midlan.

539 Janpoung, P., Pattanauwat, P. & Potiyaraj, P. (2020). Improvement of electrical conductivity
540 of polyurethane/polypyrrole blends by graphene. *Key Engineering Materials*. **831**: 122
541 – 126.

542 Khairuddin, F.H., Yusof, N. I. M., Badri, K., Ceylan, H., Tawil, S. N. M. (2018). Thermal,
543 chemical and imaging analysis of polyurethane/cecabase modified bitumen. *IOP Conf.
544 Series: Materials Science and Engineering*. **512**: 012032.

545 Khatoon, H., Ahmad, S. (2017). A review on conducting polymer reinforced polyurethane
546 composites. *Journal of Industrial and Engineering Chemistry*. 53: 1 – 22.

547 Koita, D., Tzedakis, T., Kane, C., Diaw, M., Sock, O. & Lavedan, P. (2014). Study of the
548 histamine electrochemical oxidation catalyzed by nickel sulfate. *Electroanalysis*. **26**
549 (10): 2224 – 2236.

550 Kotal, M., Srivastava, S.K. & Paramanik, B. (2011). Enhancements in conductivity and
551 thermal stabilities of polyurethane/polypyrrole nanoblends. *The Journal of Physical*
552 *Chemistry C*. **115** (5): 1496 – 1505.

553 Ladan, M., Basirun, W.J., Kazi, S.N., Rahman, F.A. (2017). Corrosion protection of AISI
554 1018 steel using Co – doped TiO₂/polypyrrole nanocomposites in 3.5% NaCl solution.
555 *Materials Chemistry and Physics*. **192**: 361 – 373.

556 Lampman, G.M., Pavia, D.L., Kriz, G.S. & Vyvyan, J.R. (2010). Spectroscopy. 4th Edition.
557 Brooks/Cole Cengage Learning, Belmont, USA.

558 Lee, K.J., Elgrishi, N., Kandemir, B. & Dempsey, J.L. 2018. Electrochemical and
559 spectroscopic methods for evaluating molecular electrocatalysts. *Nature Reviews*
560 *Chemistry* 1(5): 1 - 14.

561 Leykin, A., Shapovalov, L. & Figovsky, O. (2016). Non – isocyanate polyurethanes –
562 Yesterday, today and tomorrow. *Alternative Energy and Ecology*. **191** (3 – 4): 95 – 108.

563 Li, H., Yuan, D., Li, P., He, C. (2019). High conductive and mechanical robust carbon
564 nanotubes/waterborne polyurethane composite films for efficient electromagnetic
565 interference shielding. *Composites Part A*. 121: 411 – 417.

566 Nakthong, P., Kondo, T., Chailapakul, O., Siangproh, W. (2020). Development of an
567 unmodified screen – printed graphene electrode for nonenzymatic histamine detection.
568 *Analytical Methods*. 12: 5407 – 5414.

569 Mishra, K., Narayan, R., Raju, K.V.S.N. & Aminabhavi, T.M. (2012). Hyperbranched
570 polyurethane (HBPU)-urea and HBPU-imide coatings: Effect of chain extender and
571 NCO/OH ratio on their properties. *Progress in Organic Coatings*. **74**: 134 – 141.

572 Mohd Noor, M. A., Tuan Ismail, T. N. M., Ghazali, R. (2020). Bio – based content of
573 oligomers derived from palm oil: Sample combustion and liquid scintillation counting
574 technique. *Malaysia Journal of Analytical Science*. **24**: 906 – 917.

575 Mutsuhisa F., Ken, K. & Shohei, N. (2007). Microphase separated structure and mechanical
576 properties of norbornane diisocyanate – based polyurethane. *Polymer*. **48** (4): 997 –
577 1004.

578 Mustapha, R., Rahmat, A. R., Abdul Majid, R., Mustapha, S. N. H. (2019). Vegetable oil –
579 based epoxy resins and their composites with bio – based hardener: A short review.
580 *Polymer- Plastic Technology and Materials*. **58**: 1311 – 1326.

581 Nohra, B., Candy, L., Blancos, J.F., Guerin, C., Raoul, Y. & Mouloungui, Z. (2013). From
582 petrochemical polyurethanes to biobased polyhydroxyurethanes. *Macromolecules*. **46**
583 (10): 3771 – 3792.

584 Pan, T. & Yu, Q. (2016). Anti – corrosion methods and materials comprehensive evaluation
585 of anti – corrosion capacity of electroactive polyaniline for steels. *Anti – Corrosion*
586 *Methods and Materials*. **63**: 360 – 368.

587 Pan, X. & Webster, D.C. (2012). New biobased high functionality polyols and their use in
588 polyurethane coatings. *ChemSusChem*. **5**: 419-429.

589 Petrovic, Z.S. (2008). Polyurethanes from vegetable oils. *Polymer Reviews*. **48** (1): 109 –
590 155.

591 Porcarelli, L., Manojkumar, K., Sardon, H., Llorente, O., Shaplov, A. S., Vijayakrishna, K.,
592 Gerbaldi, C., Mecerreyes, D. (2017). Single ion conducting polymer electrolytes based
593 on versatile polyurethanes. *Electrochimica Acta*. **241**: 526 – 534.

594 Priya, S. S., Karthika, M., Selvasekarapandian, S. & Manjuladevi, R. (2018). Preparation and
595 characterization of polymer electrolyte based on biopolymer I-carrageenan with
596 magnesium nitrate. *Solid State Ionics*. **327**: 136 – 149.

597 Ren, D. & Frazier, C.E. (2013). Structure–property behaviour of moisture-cure polyurethane
598 wood adhesives: Influence of hard segment content. *Adhesion and Adhesives*. **45**: 118-
599 124.

600 Rogulska, S.K., Kultys, A. & Podkoscielny, W. (2007). Studies on thermoplastic
601 polyurethanes based on new diphenylethane – derivative diols. II. Synthesis and
602 characterization of segmented polyurethanes from HDI and MDI. *European Polymer*
603 *Journal*. **43**: 1402 – 1414.

604 Romaskevicius, T., Budriene, S., Pielichowski, K. & Pielichowski, J. (2006). Application of
605 polyurethane – based materials for immobilization of enzymes and cells: a review.
606 *Chemija*. **17**: 74 – 89.

607 Sengodu, P. & Deshmukh, A. D. (2015). Conducting polymers and their inorganic
608 composites for advanced Li-ion batteries: a review. *RSC Advances*. **5**: 42109 – 42130.

609 Septevani, A. A., Evans, D. A. C., Chaleat, C., Martin, D. J., Annamalai, P. K. (2015). A
610 systematic study substituting polyether polyol with palm kernel oil based polyester
611 polyol in rigid polyurethane foam. *Industrial Corrosion and Products*. **66**: 16 – 26.

612 Su'ait, M. S., Ahmad, A., Badri, K. H., Mohamed, N. S., Rahman, M. Y. A., Ricardi, C. L.
613 A. & Scardi, P. The potential of polyurethane bio – based solid polymer electrolyte for
614 photoelectrochemical cell application. *International Journal of Hydrogen Energy*. **39**
615 (6): 3005 – 3017.

616 Tadesse, M. G., Mengistie, D. A., Chen, Y., Wang, L., Loghin, C., Nierstrasz, V. (2019).
617 Electrically conductive highly elastic polyamide/lycra fabric treated with PEDOT: PSS
618 and polyurethane. *Journal of Materials Science*. **54**: 9591 – 9602.

619 Tajau, R., R, Rosiah, Alias, M. S., Mudri, N. H., Halim, K. A. A., Harun, M. H., Isa, N. M.,
620 Ismail, R. C., Faisal, S. M., Talib, M., Zin, M. R. M., Yusoff, I. I., Zaman, N. K., Illias,
621 I. A. (2021). Emergence of polymeric material utilising sustainable radiation curable
622 palm oil – based products for advanced technology applications. *Polymers*. 13: 1865 –
623 1886.

624 Tran, V.H., Kim, J.D., Kim, J.H., Kim, S.K., Lee, J.M. (2020). Influence of cellulose
625 nanocrystal on the cryogenic mechanical behaviour and thermal conductivity of
626 polyurethane composite. *Journal of Polymers and The Environment*. **28**: 1169 – 1179.

627 Viera, I.R.S., Costa, L.D.F.D.O., Miranda, G.D.S., Nardehcia, S., Monteiro, M.S.D. S.D.B.,
628 Junior, E.R. & Delpech, M.C. (2020). Waterborne poly (urethane – urea)s
629 nanocomposites reinforced with clay, reduced graphene oxide and respective hybrids:
630 Synthesis, stability and structural characterization. *Journal of Polymers and The
631 Environment*. **28**: 74 – 90.

632 Wang, B., Wang, L., Li, X., Liu, Y., Zhang, Z., Hedrick, E., Safe, S., Qiu, J., Lu, G. & Wang,
633 S. (2018). Template – free fabrication of vertically – aligned polymer nanowire array
634 on the flat – end tip for quantifying the single living cancer cells and nanosurface
635 interaction. a *Manufacturing Letters*. **16**: 27 – 31.

636 Wang, J., Xiao, L., Du, X., Wang, J. & Ma, H. (2017). Polypyrrole composites with carbon
637 materials for supercapacitors. *Chemical Papers*. **71 (2)**: 293 – 316.

638 Wong, C.S. & Badri, K.H. (2012). Chemical analyses of palm kernel oil – based
639 polyurethane prepolymer. *Materials Sciences and Applications*. **3**: 78 – 86.

640 Wong, C. S., Badri, K., Ataollahi, N., Law, K., Su'ait, M. S., Hassan, N. I. (2014). Synthesis
641 of new bio – based solid polymer electrolyte polyurethane – LiClO₄ via
642 prepolymerization method: Effect of NCO/OH ratio on their chemical, thermal
643 properties and ionic conductivity. *World Academy of Science, Engineering and*

644 *Technology, International Journal of Chemical, Molecular, Nuclear, Materials and*
645 *Metallurgical Engineering. 8: 1243 – 1250.*

646 Yong, Z., Bo, Z.M., Bo, W., Lin, J.Z. & Jun, N. (2009). Synthesis and properties of novel
647 polyurethane acrylate containing 3-(2-Hydroxyethyl) isocyanurate segment. *Progress*
648 *in Organic Coatings. 67: 264 – 268*

649 Zia, K. M., Anjum, S., Zuber, M., Mujahid, M. & Jamil, T. (2014). Synthesis and molecular
650 characterization of chitosan based polyurethane elastomers using aromatic diisocyanate.
651 *International of Journal of Biological Macromolecules. 66: 26 – 32.*

652

653

654

Hasil Reviu 3 dan Submit Revisi: 1 Oktober 2021

Hindawi

Peter Foot

Decision

Major Revision Requested

Message for Author

* The synthetic chemistry and general polymer characterization are fine.
* I am satisfied with the revisions made by the authors, but I agree with the following comments of Reviewer #3:

1. The reported electrical properties are misleading and incorrect. A current of 53 microamps signifies nothing on its own, and it cannot be used as the basis of a comparison of the authors' polymer with other polymers. The mentions of "conductivity" in the following sentences should be corrected or preferably the sentences should be deleted completely:

Lines 432-435: "Nevertheless, the electroconductivity of PU in this study shows better conductivity several times compared to Bahrami et al. (2019) that reported the conductivity of PU as 1.26×10^{-6} A, whereas Li et al. (2019) reported the PU conductivity in their study was even very low, namely 10-14 A. "

and in lines 438-440: "The application of PEG as polyol has been studied by Porcarelli et al. (2017), that reported that the conductivity of PU based on PEG – polyol was 9.2×10^{-8} ." (This sentence doesn't even mention the units of the reported conductivity.)

2. The English is still poor and hard to follow in some places. This includes missing verbs, e.g. line 420 "Polyurethane film deposited" should be "Polyurethane film was deposited"; orthographic errors e.g. lines 123-125 "SPE becomes the best solution owing to its frugal manufacture, tiny size, able to produce on large-scale and can be applied for on-site detection".

Typographic errors should be corrected e.g. line 89: change Pus to PUs; and lines 138-139 "Polyurethane is possible to become an advanced frontier material is chemically modified electrodes.."

As noted by the reviewer, in line 299 "spectrums" is an incorrect word, which should change to "spectra".

Also repetitious or awkward sentences should be rewritten or deleted, e.g. line 53 "The application of petroleum as polyol in order to produce polyurethane has been applied." or lines 56-57 "These reasons have been considered and finding utilizing plants that can be used as alternative polyols should be done immediately."

The sentence in lines 37-38 must be deleted; readers of IJPS don't need to be told what a polymer is!

The authors are strongly advised to seek the help of a fluent English speaker when they revise their manuscript, or to use a professional scientific editing service.

— Response to Revision Request

Peter Foot**Decision**

Major Revision Requested

Message for Author

* The synthetic chemistry and general polymer characterization are fine.

* I am satisfied with the revisions made by the authors, but I agree with the following comments of Reviewer #3:

1. The reported electrical properties are misleading and incorrect. A current of 53 microamps signifies nothing on its own, and it cannot be used as the basis of a comparison of the authors' polymer with other polymers. The mentions of "conductivity" in the following sentences should be corrected or preferably the sentences should be deleted completely:

Lines 432-435: "Nevertheless, the electroconductivity of PU in this study shows better conductivity several times compared to Bahrami et al. (2019) that reported the conductivity of PU as 1.26×10^{-6} A, whereas Li et al. (2019) reported the PU conductivity in their study was even very low, namely 10-14 A. "

and in lines 438-440: "The application of PEG as polyol has been studied by Porcarelli et al. (2017), that reported that the conductivity of PU based on PEG – polyol was 9.2×10^{-8} ." (This sentence doesn't even mention the units of the reported conductivity.)

2. The English is still poor and hard to follow in some places. This includes missing verbs, e.g. line 420 "Polyurethane film deposited" should be "Polyurethane film was deposited"; orthographic errors e.g. lines 123-125 "SPE becomes the best solution owing to its frugal manufacture, tiny size, able to produce on large-scale and can be applied for on-site detection".

Typographic errors should be corrected e.g. line 89: change Pus to PUs; and lines 138-139 "Polyurethane is possible to become an advanced frontier material is chemically modified electrodes.."

As noted by the reviewer, in line 299 "spectrums" is an incorrect word, which should change to "spectra".

Also repetitious or awkward sentences should be rewritten or deleted, e.g. line 53 "The application of petroleum as polyol in order to produce polyurethane has been applied." or lines 56-57 "These reasons have been considered and finding utilizing plants that can be used as alternative polyols should be done immediately."

The sentence in lines 37-38 must be deleted; readers of IJPS don't need to be told what a polymer is!

The authors are strongly advised to seek the help of a fluent English speaker when they revise their manuscript, or to use a professional scientific editing service.

— Response to Revision Request

1 **Design and Synthesis of Conducting Polymer Based on Polyurethane**
2 **produced from Palm Kernel Oil**

3
4 Muhammad Abdurrahman Munir^{1*}, Khairiah Haji Badri^{2,3}, Lee Yook Heng², Ahlam
5 Inayatullah⁴, Ari Susiana Wulandari¹, Emelda¹, Eliza Dwinta¹, Rachmad Bagus Yahya
6 Supriyono¹

7
8 ¹Department of Pharmacy, Faculty of Health Science, Universitas Alma Ata, Daerah
9 Istimewa Yogyakarta, 55183, Indonesia

10 ²Department of Chemical Sciences, Faculty of Science and Technology, Universiti
11 Kebangsaan Malaysia, Bangi, 43600, Malaysia

12 ³Polymer Research Center, Universiti Kebangsaan Malaysia, Bangi, 43600, Malaysia

13 ⁴Faculty of Science and Technology, Universiti Sains Islam Malaysia, Nilai, 71800, Malaysia

14 *Email: muhammad@almaata.ac.id

15
16 **Abstract**

17 Polyurethane (PU) is a unique polymer that has versatile processing methods and mechanical
18 properties upon inclusion of selected additives. In this study, a freestanding bio-polyurethane
19 film on screen-printed electrode (SPE) was prepared by the solution casting technique, using
20 acetone as solvent. It was a one-pot synthesis between major reactants namely, palm kernel oil-
21 based polyol (PKOp) and 4,4-methylene diisocyanate. The PU has strong adhesion on SPE
22 surface. The synthesized polyurethane was characterized using thermogravimetry analysis
23 (TGA), differential scanning calorimetry (DSC), Fourier – transform infrared spectroscopy
24 (FTIR), surface area analysis by field emission scanning electron microscope (FESEM) and

25 cyclic voltammetry (CV). Cyclic voltammetry was employed to study electro-catalytic
26 properties of SPE-Polyurethane towards oxidation of PU. Remarkably, SPE-PU exhibited
27 improved anodic peak current as compared to SPE itself using the differential pulse
28 voltammetry (DPV) method. Furthermore, the formation of urethane linkages (NHCO
29 backbone) after polymerization was analysed using FTIR and confirmed by the absence of
30 N=C=O peak at 2241 cm^{-1} . The glass transition temperature (T_g) of the polyurethane was
31 detected at 78.1°C .

32

33 **Keywords:** Polyurethane, polymerization, screen-printed electrode, voltammetry

34

35

36 1. Introduction

37 Polymers are molecules composed of many repeated sub-units referred to as monomers
38 (Sengodu & Deshmukh 2015). Conducting polymers (CPs) are polymers that exhibit electrical
39 behavior (Alqarni et al. 2020). The conductivity of CPs was first observed in polyacetylene,
40 nevertheless owing to its instability led to the discovery of other forms of CPs such as
41 polyaniline (PANI), poly (o-toluidine) (PoT), polythiophene (PTh), polyfluorene (PF) and
42 polyurethane (PU). Furthermore, natural CPs have low conductivity and are often semi-
43 conductive. Therefore, it is essential to increase their conductivity mainly for use in
44 electrochemical sensor programs (Dzulkipli et al. 2021; Wang et al. 2018). Conducting
45 polymers (CPs) represent a sizeable range of useful organic substances. Their unique electrical,
46 chemical and physical properties; reasonable price; simple preparation; small dimensions and
47 large surface area have enabled researchers to discover a wide variety of uses such as sensors,
48 biochemical applications, solar cells and electrochromic devices (Alqarni et al. 2020; Ghosh et
49 al. 2018). There are scientific documentation on the use of conductive polymers in various

50 studies such as polyaniline (Pan & Yu 2016), polypyrrole (Ladan et al. 2017) and polyurethane
51 (Tran et al. 2020; Vieira et al. 2020; Guo et al. 2020; Fei et al. 2020).

52

53 The application of petroleum as polyol in order to produce polyurethane has been applied. Coal
54 and crude oil were used as raw materials to produce it. Nevertheless, these materials have
55 become very rare to find and the price is very expensive at the same time required a
56 sophisticated system to produce it. These reasons have been considered and finding utilizing
57 plants that can be used as alternative polyols should be done immediately (Badri 2012).
58 Furthermore, in order to avoid the application of petroleum as raw material for a polyol,
59 vegetable oils become a better choice as polyol in order to obtain a biodegradable polyol.
60 Vegetable oils that are generally used for synthesis polyurethane are soybean oil, corn oil,
61 sunflower seed oil, coconut oil, nuts oil, rapeseed, olive oil and palm oil (Badri 2012; Borowicz
62 et al. 2019).

63

64 It is very straightforward for vegetable oils to react with a specific group in order to form PU
65 such as epoxy, hydroxyl, carboxyl and acrylate owing to the existence of (-C=C-) in vegetable
66 oils. Thus, it has provided appealing profits to vegetable oils compared to petroleum considered
67 the toxicity, price and harm to the environment (Mustapha et al. 2019; Mohd Noor et al. 2020).
68 Palm oil becomes the chosen in this study to produce PU owing to it is largely cultivated in
69 South Asia particularly in Malaysia and Indonesia. It has several profits compared to other
70 vegetable oils such as the easiest materials obtained, the lowest cost of all the common
71 vegetable oils and recognized as the plantation that has a low environmental impact and
72 removing CO₂ from the atmosphere as net sequester (Tajau et al. 2021; Septevani et al. 2015).
73 Biopolymer, a natural biodegradable polymer has attracted much attention in recent years.
74 Global environmental awareness and fossil fuel depletion urged researchers to work in the

75 biopolymer field (Priya et al. 2018). Polyurethane is one of the most common, versatile and
76 researched materials in the world. These materials combine the durability and toughness of
77 metals with the elasticity of rubber, making them suitable to replace metals, plastics and rubber
78 in several engineered products. They have been widely applied in biomedical applications,
79 building and construction applications, automotive, textiles and in several other industries due
80 to their superior properties in terms of hardness, elongation, strength and modulus (Zia et al.
81 2014; Romaskevicius et al. 2006). Polyurethanes are also considered to be one of the most useful
82 materials with many profits such as, possess low conductivity, low density, absorption
83 capability and dimensional stability. They are clearly a great research subject owing to their
84 mechanical, physical and chemical properties (Badan & Majka 2017).

85

86 The urethane group is the major repeating unit in PUs and is produced from the reaction
87 between alcohol (-OH) and isocyanate (NCO); albeit polyurethanes also contain other groups
88 such as ethers, esters, urea and some aromatic compounds. Due to the wide variety of sources
89 from which PUs can be synthesized, thus a wide range of specific applications can be generated.
90 They are grouped into several different classes based on the desired properties: rigid, flexible,
91 thermoplastic, waterborne, binders, coating, adhesives, sealants and elastomers (Akindoyo et
92 al. 2016).

93

94 Although, PU has low conductivity, it is lighter than other materials such as metals. The
95 hardness of PU also relies on the number of the aromatic rings in the polymer structure
96 (Janpoung et al, 2020; Su'ait et al. 2014), majorly contributed by the isocyanate derivatives.
97 PU has also a conjugate structure where electrons can move in the main chain that causing
98 electricity produced even the conductivity is low. The electrical conductivity of conjugated
99 linear (π) can be explained by the distance between the highest energy level containing

100 electrons (HOMO) called valence band and the lowest energy level not containing electrons
101 (LUMO) called the conduction band (Wang et al. 2017; Kotal et al. 2011).

102

103 In the recent past, several conventional methods have been developed such as capillary
104 electrophoresis, liquid and gas chromatography coupled with several detectors. Nevertheless,
105 although chromatographic and spectrometric approaches are well developed for qualitative and
106 quantitative analyses of analytes, several limitations emerged such as complicated
107 instrumentation, expensive, tedious sample preparations and requiring large amounts of
108 expensive solvents that will harm the users and environment (Kilele et al. 2020). Therefore, is
109 is imperative to obtain and develop an alternative material that can be used to analyse a specific
110 analyte. Electrochemical methods are extremely promising methods in the determination of an
111 analyte in samples owing to the high selectivities, sensitivities, inexpensive, requirements of
112 small amounts of solvents and can be operated by people who have no background in analytical
113 chemistry. In addition, the sample preparation such as separation and extraction steps are not
114 needed owing to the selectivity of this instrument where no obvious interference on the current
115 response recorded (Chokkareddy et al. 2020). Few works have been reported on the
116 electrochemical methods for the determination of analyte using electrode combined with
117 several electrode modifiers such as carbon nanotube, gold and graphene (Chokkareddy et al.
118 2020; Kilele et al. 2021). Nevertheless, the materials are costly and the modification procedures
119 are not straightforward. Thus, an electrochemical approach using inexpensive and easily
120 available materials as electrode modifiers should be developed (Degefu et al. 2014).

121

122 Nowadays, screen-printed electrodes (SPEs) modified with conducting polymer have been
123 developed for various electrochemical sensing. SPE becomes the best solution owing to its
124 frugal manufacture, tiny size, able to produce on large-scale and can be applied for on-site

125 detection (Nakthong et al. 2020). Conducting polymers (CPs) become an alternative to
126 modifying the screen-printed electrodes due to their electrical conductivity, able to capture
127 analyte by chemical/physical adsorption, large surface area and making CPs are very appealing
128 materials from electrochemical perspectives (Baig et al. 2019). Such advantages of SPE
129 encourage us to construct a new electrode for electrochemical sensing, and no research reported
130 on the direct electrochemical oxidation of histamine using screen-printed electrode modified
131 by polyurethane. Therefore, this research is the first to develop a new electrode using (screen
132 printed polyurethane electrode) SPPE without any conducting materials.

133

134 The purpose of this work was to synthesize, characterize and study the conductivity of
135 polyurethane using cyclic voltammetry (CV) and differential pulse voltammetry (DPV)
136 attached to screen-printed electrode (SPE). To the best of our knowledge, this is the first
137 attempt to use a modified polyurethane electrode. The electrochemistry of polyurethane
138 mounted onto screen-printed electrode (SPE) is discussed in detail. Polyurethane is possible to
139 become an advanced frontier material is chemically modified electrodes for bio/chemical
140 sensing application.

141

142 **2. Experimental**

143 **2.1 Chemicals**

144 ***Synthesis of polyurethane film:*** Palm kernel oil (PKOp) supplied by UKM Technology Sdn
145 Bhd through MPOB/UKM station plant, Pekan Bangi Lama, Selangor and prepared using
146 Badri et al. (2000) method. 4, 4-diphenylmethane diisocyanate (MDI) was acquired from
147 Cosmopolyurethane (M) Sdn. Bhd., Klang, Malaysia. Solvents and analytical reagents were
148 benzene ($\geq 99.8\%$), toluene ($\geq 99.8\%$), hexane ($\geq 99\%$), acetone ($\geq 99\%$), tetrahydrofuran
149 (THF), dimethylformamide (DMF) ($\geq 99.8\%$), dimethylsulfoxide (DMSO) ($\geq 99.9\%$) and

150 polyethylene glycol (PED) with a molecular weight of 400 Da obtained from Sigma Aldrich
151 Sdn Bhd, Shah Alam.

152

153 **2.2 Apparatus**

154 Tensile testing was performed using a universal testing machine model Instron 5566 following
155 ASTM 638 (Standard Test Method for Tensile Properties of Plastics). The tensile properties of
156 the polyurethane film were measured at a velocity of 10 mm/min with a cell load of 5 kN.

157 The thermal properties were performed using thermogravimetry analysis (TGA) and
158 differential scanning calorimetry (DSC) analysis. TGA was performed using a thermal analyzer
159 of Perkin Elmer Pyris model with a heating rate of 10 °C/minute at a temperature range of 30
160 to 800 °C under a nitrogen gas atmosphere. The DSC analysis was performed using a thermal
161 analyzer of Perkin Elmer Pyris model with a heating rate of 10 °C /minute at a temperature
162 range of -100 to 200 °C under a nitrogen gas atmosphere. Approximately, 5-10 mg of PU was
163 weighed. The sample was heated from 25 to 150 °C for one minute, then cooled immediately
164 from 150 -100 °C for another one minute and finally, reheated to 200 °C at a rate of 10 °C /min.
165 At this point, the polyurethane encounters changes from elastic properties to brittle due to
166 changes in the movement of the polymer chains. Therefore, the temperature in the middle of
167 the inclined regions is taken as the glass transition temperature (T_g). The melting temperature
168 (T_m) is identified as the maximum endothermic peak by taking the area below the peak as the
169 enthalpy point (ΔH_m).

170

171 The morphological analysis of PU film was performed by Field Emission Scanning Electron
172 Microscope (FESEM) model Gemini SEM microscope model 500-70-22. Before the analysis
173 was carried out, the polyurethane film was coated with a thin layer of gold to increase the
174 conductivity of the film. The coating method was carried out using a sputter-coater. The

175 observations were conducted at a magnification of 200× and 5000 × with 10.00 kV (Electron
176 high tension - EHT).

177

178 The crosslinking of PU was determined using the soxhlet extraction method. About 0.60 g of
179 PU sample was weighed and put in an extractor tube containing 250 ml of toluene, used as a
180 solvent. This flow of toluene was let running for 24 hours. Mass of the PU was weighed before
181 and after the reflux process was carried out. Then, the sample was dried in the conventional
182 oven at 100 °C for 24 hours in order to get a constant mass. The percentage of crosslinking
183 content known as the gel content can be calculated using Equation (1).

$$184 \quad \text{Gel content (\%)} = \frac{W_0 - W}{W} \times 100 \% \quad (1)$$

185 W_0 is the mass of PU before the reflux process (g) and W is the mass of PU after the reflux
186 process (g).

187

188 FTIR spectroscopic analysis was performed using a Perkin-Elmer Spectrum BX instrument
189 using the Diamond Attenuation Total Reflectance (DATR) method to confirm the
190 polyurethane, PKOp and MDI functional group. FTIR spectroscopic analysis was performed
191 at a wave number of 4000 to 600 cm^{-1} to identify the peaks of the major functional groups in
192 the formation of the polymer such as amide group (-NH), urethane carbonyl group (-C = O)
193 and carbamate group (-CN).

194

195 **2.3 Synthesis of Polyurethane**

196 Palm kernel oil (PKO)p and polyethylene glycol (PEG) 400 (100:40 g/g) were combined and
197 dissolved by acetone 30% in order to form a polyol prepolymer solution. The mixture was
198 mixed using centrifuge with 100 rpm for 5 min to acquire a homogenized solution. Whereas,
199 diisocyanate prepolymer was obtained by mixing 4,4'-diphenyl-methane diisocyanate (MDI)
200 (100 g) to acetone 30%, afterward the mixture was mixed using centrifuge for 1 min to obtain

201 a homogenized solution. Then, 10 g of diisocyanate solution was poured into a container that
202 containing 10 g of a polyol prepolymer solution slowly in order to avoid an exothermic reaction
203 occur. The mixture was mixed for 30 sec until a homogenized solution acquired. Lastly, the
204 polyurethane solution was poured on the electrode surface by using casting method and dried
205 at ambient temperature for 12 hours.

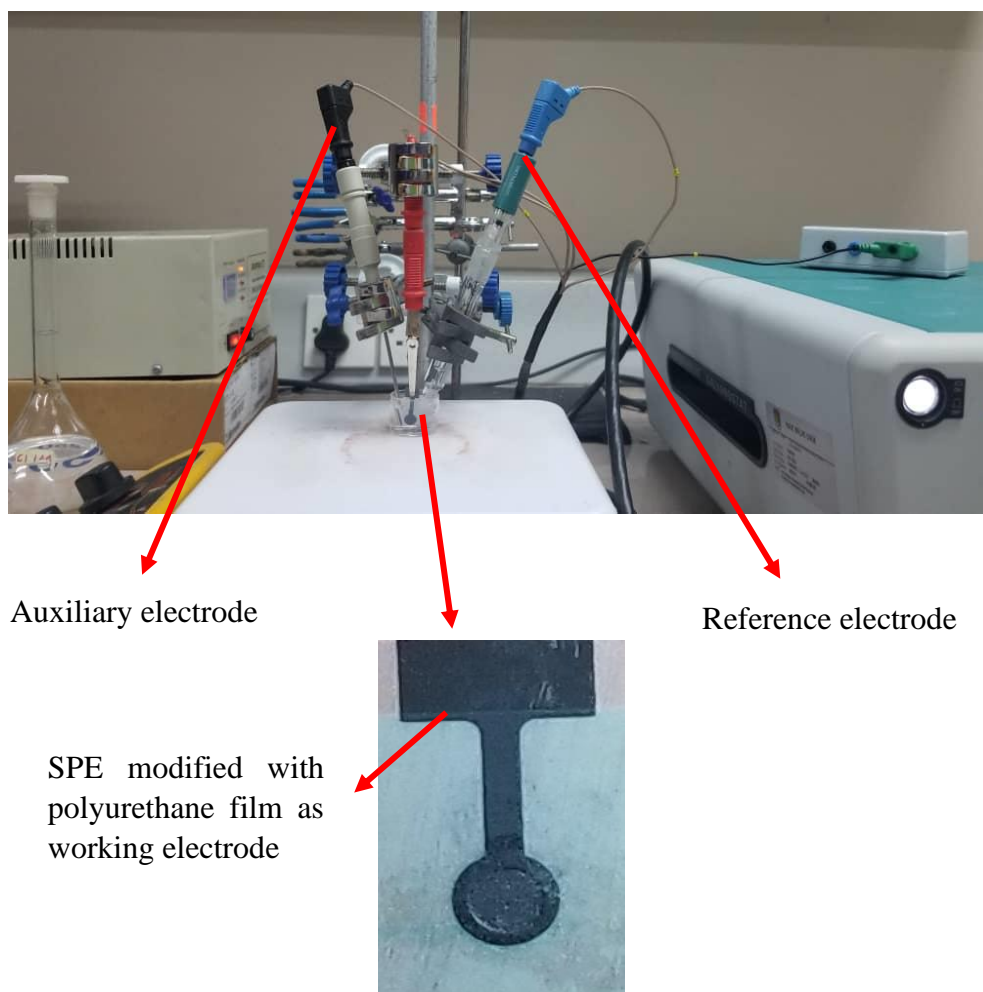
206

207 **2.4 Modification of Electrode**

208 Voltammetric tests were performed using Metrohm Autolab Software (**Figure 1**) analyzer
209 using cyclic voltammetry (CV) method or known as amperometric mode and differential pulse
210 voltammetry (DPV). All electrochemical experiments were carried out using screen-printed
211 electrode (diameter 3 mm) modified using polyurethane film as working electrode, platinum
212 wire as auxiliary electrode and Ag/AgCl electrode as a reference electrode. All experiments
213 were conducted at a temperature of $20 \pm 2^\circ\text{C}$.

214

215 The PU was cast onto the screen – printed electrode (SPE + PU) and analyzed using a single
216 voltammetric cycle between -1200 and +1500 mV (vs Ag/AgCl) of ten cycles at a scanning
217 rate of 100 mV/s in 5 ml of KCl in order to study the activity of SPE and polyurethane film.
218 Approximately (0.1, 0.3 & 0.5) mg of palm-based prepolyurethane was dropped separately
219 onto the surface of the SPE and dried at room temperature. The modified palm-based
220 polyurethane electrodes were then rinsed with deionized water to remove physically adsorbed
221 impurities and residues of unreacted material on the electrode surface. All electrochemical
222 materials and calibration measurements were carried out in a 5 mL glass beaker with a
223 configuration of three electrodes inside it. Platinum wire and silver/silver chloride (Ag/AgCl)
224 electrodes were used as auxiliary and reference electrodes, while screen-printed electrode that
225 had been modified with polyurethane was applied as a working electrode.



226 **Figure 1.** Potentiostat instrument to study the conductivity of SPE modified with
 227 polyurethane film using cyclic voltammetry (CV) and differential pulse voltammetry (DPV)

228

229 3. Results and Discussion

230 The synthesis of PU films was carried out using pre-polymerization method which involves
 231 the formation of urethane polymer at an early stage. The reaction took place between palm
 232 kernel oil-based polyol (PKOp) and diisocyanate (MDI). **Table 1** presents the PKO-p
 233 properties used in this study. The structural chain was extended with the aid of polyethylene
 234 glycol (PEG) to form flexible and elastic polyurethane film. In order to form the urethane
 235 prepolymer, one of the isocyanate groups (NCO) reacts with one hydroxyl group (OH) of
 236 polyol while the other isocyanate group attacks another hydroxyl group in the polyol (Wong &
 237 Badri 2012) as shown in **Figure 2**.

238 **Table 1** The specification of PKO-p (Badri et al. (2000)).

| Property | Values |
|------------------------------|-----------|
| Viscosity at 25°C (cps) | 1313.3 |
| Specific gravity (g/mL) | 1.114 |
| Moisture content (%) | 0.09 |
| pH value | 10 – 11 |
| The hydroxyl number mg KOH/g | 450 - 470 |

239

240

241 a. FTIR analysis

242 **Figure 3** shows the FTIR spectrum for polyurethane, exhibiting the important functional group
 243 peaks. According to a study researched by Wong & Badri 2012, PKO-p reacts with MDI to
 244 form urethane prepolymers. The NCO group on MDI reacts with the OH group on polyol
 245 whether PKOp or PEG. It can be seen there are no important peaks of MDI in the FTIR
 246 spectrums. This is further verified by the absence of peak at the 2400 cm^{-1} belongs to MDI (-
 247 NCO groups). This could also confirm that the NCO group on MDI had completely reacted
 248 with PKO-p to form the urethane -NHC (O) backbone. The presence of amides (-NH),
 249 carbonyl urethane group (-C = O), carbamate group (C-NH) and -C-O-C confirmed the
 250 formation of urethane chains. In this study, the peak of carbonyl urethane (C = O) detected at
 251 1727 cm^{-1} indicated that the carbonyl urethane group was bonded without hydrogen owing to
 252 the hydrogen reacted with the carbonyl urethane group.

253

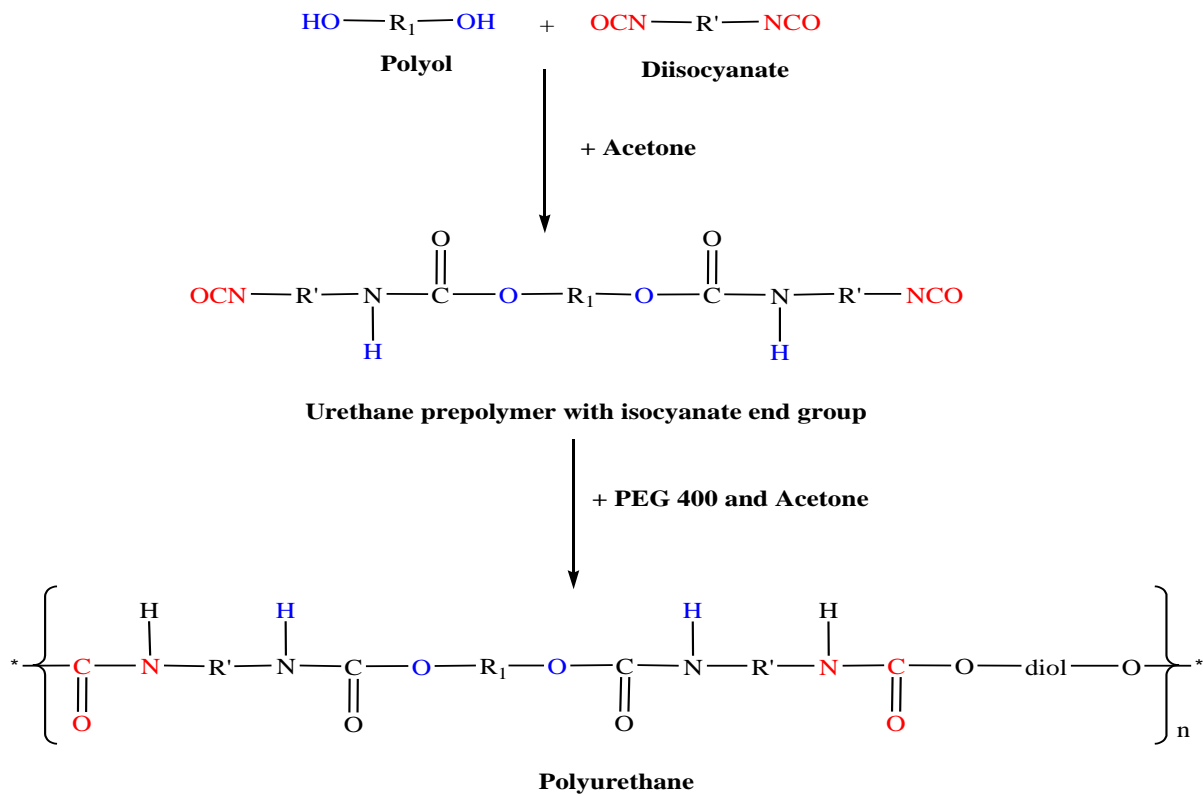
254 The reaction of polyurethane has been studied by Hamuzan & Badri (2016) where the urethane
 255 carbonyl group was detected at $1730 - 1735\text{ cm}^{-1}$ while the MDI carbonyl was detected at 2400
 256 cm^{-1} . The absence of peaks at $2250 - 2270\text{ cm}^{-1}$ indicates the absence of NCO groups. It shows

257 that the polymerization reaction occurs entirely between NCO groups in MDI with hydroxyl
258 groups on polyols and PEG (Mishra et al. 2012). The absence of peaks at 1690 cm^{-1}
259 representing urea ($\text{C} = \text{O}$) in this study indicated, there is no urea formation as a byproduct
260 (Clemitson 2008) of the polymerization reaction that possibly occurs due to the excessive
261 water. For the amine (NH) group, hydrogen-bond to NH and oxygen to form ether and
262 hydrogen bond to NH and oxygen to form carbonyl on urethane can be detected at the peak of
263 3301 cm^{-1} and in the wavenumber at range $3326 - 3428\text{ cm}^{-1}$. This has also been studied and
264 detected by Lampman et. al. (2010) and Mutsuhisa et al. (2007). In this study, the hydrogen
265 bond formed by $\text{C} = \text{O}$ acts as a proton acceptor whereas NH acts as a proton donor. The
266 urethane group in the hard segment (MDI) has electrostatic forces on the oxygen, hydrogen
267 and nitrogen atoms and these charged atoms form dipoles that attract other opposite atoms.
268 These properties make isocyanates are highly reactive and having different properties (Leykin
269 et al. 2016).

270

271 MDI was one of the isocyanates used in this study, has an aromatic group and is more
272 reactive compared to aliphatic group isocyanates such as hexamethylene diisocyanate (HDI)
273 or isophorone diisocyanate (IPDI). Isocyanates have two groups of isocyanates on each
274 molecule. Diphenylmethane diisocyanate is an exception owing to its structure consists of two,
275 three, four or more isocyanate groups (Nohra et al. 2013). The use of PEG 400 in this study as
276 a chain extender for polyurethane increases the chain mobility of polyurethane at an optimal
277 amount. The properties of a polyurethane are contributed by hard and soft copolymer segments
278 of both polyol monomers and MDI. This makes the hard segment of urethane serves as a
279 crosslinking site between the soft segments of the polyol (Leykin et al. 2016).

280



281

282 **Figure 2.** The chemical route of producing polyurethane via pre-polymerization method

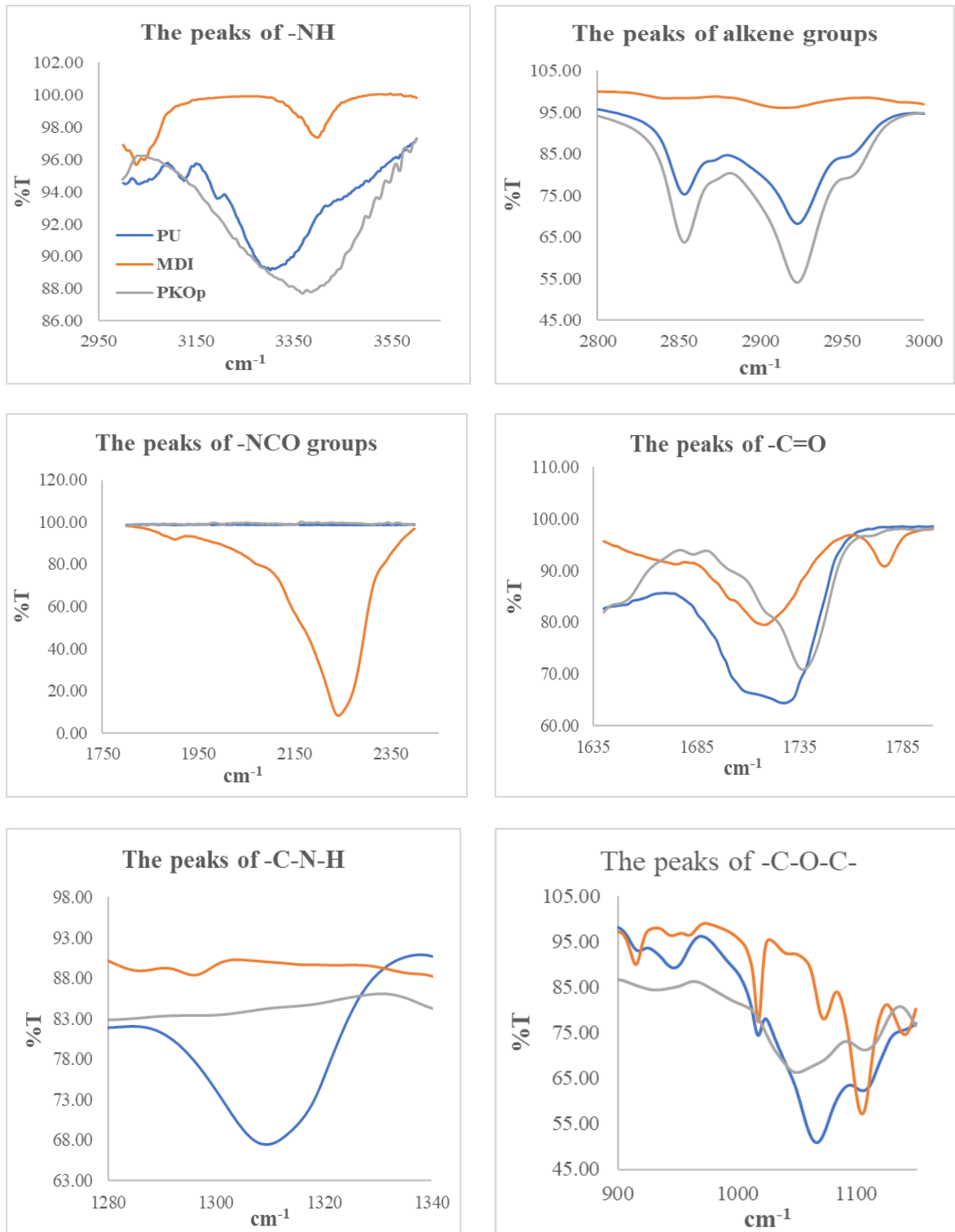
283 (Wong & Badri 2012).

284

285 The mechanism of the pre-polymerization in urethane chains formation is a
 286 nucleophilic substitution reaction as studied by Yong et al. (2009). However, this study found
 287 amines as nucleophiles. Amine attacks carbonyl on isocyanate in MDI in order to form two
 288 resonance structures of intermediate complexes A and B. Intermediate complex B has a greater
 289 tendency to react with polyols due to stronger carbonyl (C = O) bonds than C = N bonds on
 290 intermediate complexes A. Thus, intermediate complex B is more stable than intermediate
 291 complex A, as suggested by previous researchers who have conducted by Wong and Badri
 292 (2012). Moreover, nitrogen was more electropositive than oxygen, therefore, -CN bonds were
 293 more attracted to cations (H+) than -CO. The combination between long polymer chain and
 294 low cross-linking content gives the polymer elastic properties whereas short chain and high
 295 cross linking producing hard and rigid polymers. Cross-linking in polymers consists of three-

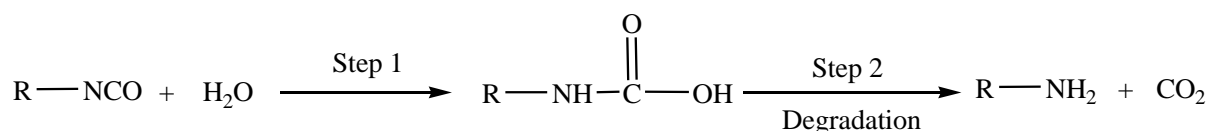
296 dimensional networks with high molecular weight. In some aspects, polyurethane can be a
297 macromolecule, a giant molecule (Petrovic 2008).

298



299 **Figure 3.** FTIR spectrums of several important peaks between polyurethane, PKO-p and MDI

300 However, the reaction between MDI and PEG as a chain extender where oxygen on the
 301 nucleophile PEG attacks the NCO group in the MDI to form two intermediate complexes A
 302 and B can occur. Nevertheless, nucleophilic substitution reactions have a greater tendency to
 303 occur in PKOp compared to PEG because the presence of nitrogen atoms is more
 304 electropositive than oxygen atoms in PEG. Amine has a higher probability of reacting
 305 compared to hydroxyl (Herrington & Hock 1997). Amine with high alkalinity reacts with
 306 carbon atoms on MDI as proposed by Wong and Badri (2012). PKOp contains long carbon
 307 chains that can easily stabilize alkyl ions when intermediate complexes are formed. Therefore,
 308 the polyol is more reactive than PEG to react with MDI. However, the addition of PEG will
 309 increase the length of the polyurethane chain and prevent side effects such as the formation of
 310 urea by-products of the NCO group reaction in urethane pre-polymer and water molecules from
 311 the environment. If the NCO group reacts with the excess water in the environment, the
 312 formation of urea and carbon dioxide gas will also occur excessively (**Figure 4**). This reaction
 313 can cause a polyurethane foam, not polyurethane film as we studied the film.



314
 315 **Figure 4.** The reaction between NCO group and water producing carbon dioxide
 316

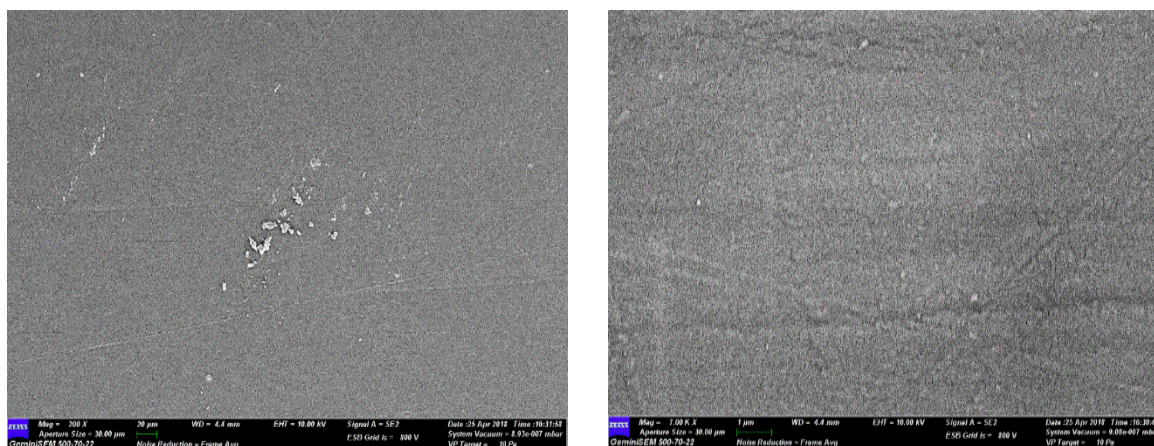
317 Furthermore, the application of PEG can influence the conductivity of PU where
 318 Porcarelli et al. (2017) have reported the application of PEG using several molecular weights.
 319 PEG 1500 decreased the conductivity of PU in consequence of the semicrystalline phase of
 320 PEG 1500 that acted as a poor ion conducting phase for PU. It is also well known that PEG
 321 with a molecular weight of more than 1000 g·mol⁻¹ tends to crystallize with deleterious effects
 322 on room temperature ionic conductivity (Porcarelli et al. 2017).

323

324 b. Morphological analysis

325 The Field Emission Scanning Electron Microscope (FESEM) micrograph in **Figure 5** shows
326 the formation of a uniform polymer film contributed by the polymerization method applied.
327 The magnification used for this surface analysis ranged from 200 to 5000 \times . The
328 polymerization method can also avoid the failure of the reaction in PU polymerization.
329 Furthermore, no trace of separation was detected by FESEM. This has also been justified by
330 the wavelengths obtained by the FTIR spectrums above.

331



332 **Figure 5.** The micrograph of polyurethane films analysed by FESEM at (a) 200 \times and (b)
333 5000 \times magnifications.

334 c. The crosslinking analysis

336 Soxhlet analysis was applied to determine the degree of crosslinking between the hard
337 segments and the soft segments in the polyurethane. The urethane group on the hard segment
338 along the polyurethane chain is polar (Cuve & Pascault 1991). Therefore, during the testing, it
339 was very difficult to dissolve in toluene, as the testing reagent. The degree of crosslinking is
340 determined by the percentage of the gel content. The analysis result obtained from the Soxhlet
341 testing indicating a 99.3 % gel content. This is significant in getting a stable polymer at higher
342 working temperature (Rogulska et al. 2007).

343

$$\text{Gel content (\%)} = \frac{(0.6 - 0.301) \text{ g}}{0.301 \text{ g}} \times 100\% = 99.33\%$$

344

345

346 d. The thermal analysis

347 Thermogravimetric analysis (TGA) can be used to observe the material mass based on

348 temperature shift. It can also examine and estimate the thermal stability and materials

349 properties such as the alteration weight owing to absorption or desorption, decomposition,

350 reduction and oxidation. The material composition of polymer is specified by analysing the

351 temperatures and the heights of the individual mass steps (Alamawi et al. 2019). **Figure 6**

352 shows the TGA and DTG thermograms of polyurethane. The percentage weight loss (%) is

353 listed in **Table 2**. Generally, only a small amount of weight was observed. It is shown in **Figure**

354 **6** in the region of 45 – 180°C. This is due to the presence of condensation on moisture and

355 solvent residues.

356

357 **Table2** Weight loss percentage of (wt%) polyurethane film

| Sample | % Weight loss (wt%) | | | | Total of weight loss (%) | Residue after 550°C (%) |
|--------------|-----------------------|-------------------------------|-------------------------------|-------------------------------|--------------------------|-------------------------|
| | T _{max} , °C | T _{d1} , 200 – 290°C | T _{d2} , 350 – 500°C | T _{d3} , 500 – 550°C | | |
| Polyurethane | 240 | 8.04 | 39.29 | 34.37 | 81.7 | 18.3 |

358

359 The bio polyurethane is thermally stable up to 240 °C before it has undergone thermal

360 degradation (Agrawal et al. 2017). The first stage of thermal degradation (T_{d1}) on polyurethane

361 films was shown in the region of 200 – 290 °C as shown in **Figure 6**. The T_{d1} is associated with

362 degradation of the hard segments of the urethane bond, forming alcohol or degradation of the

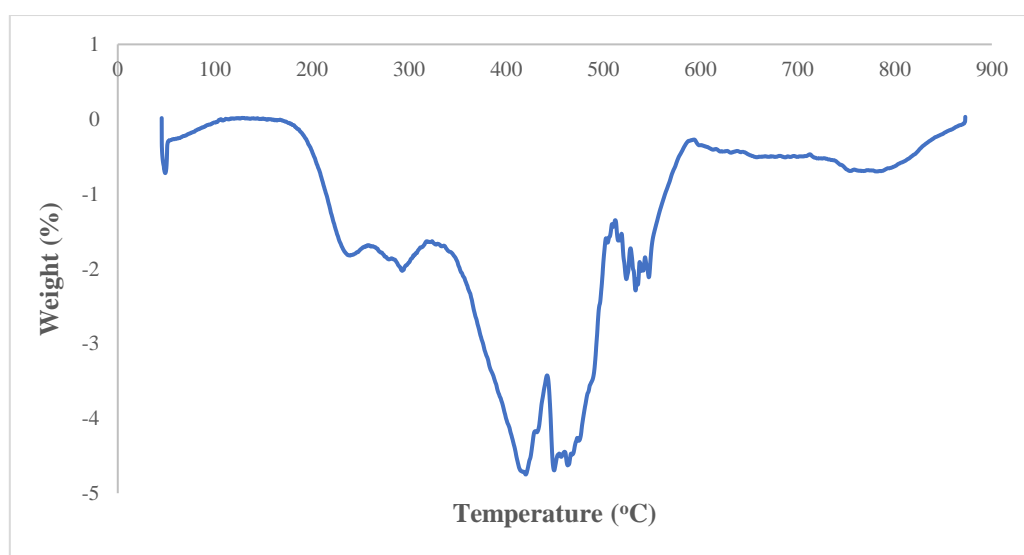
363 polyol chains and releasing of isocyanates (Berta et al. 2006), primary and secondary amines

364 as well as carbon dioxide (Corcuera et al. 2011; Pan & Webster 2012). Meanwhile, the second

365 thermal degradation stage (T_{d2}) of polyurethane films experienced a weight loss of 39.29 %.
366 This endotherm of T_{d2} is related to the dimerization of isocyanates to form carbodiimides and
367 release CO_2 . The formed carbodiimide reacts with alcohol to form urea. The third stage of
368 thermal degradation (T_{d3}) is related to the degradation of urea (Berta et al. 2006) and the soft
369 segment on polyurethane.

370

371 Generally, DSC analysis exhibited thermal transitions as well as the initial
372 crystallisation and melting temperatures of the polyurethane (Khairuddin et al. 2018). It serves
373 to analyse changes in thermal behavior due to changes occurring in the chemical chain structure
374 based on the glass transition temperature (T_g) of the sample obtained from the DSC thermogram
375 (Figure 7). DSC analysis on polyurethane film was performed in the temperature at the range
376 100 °C to 200 °C using nitrogen gas as a blanket as proposed by Furtwengler et al. (2017). The
377 glass transition temperature (T_g) on polyurethane was above room temperature, at 78.1 °C
378 indicated the state of glass on polyurethane. The presence of MDI contributes to the formation
379 of hard segments in polyurethanes. Porcarelli et al. (2017) stated that possess a low glass
380 transition (T_g) may contribute to PU conductivity.

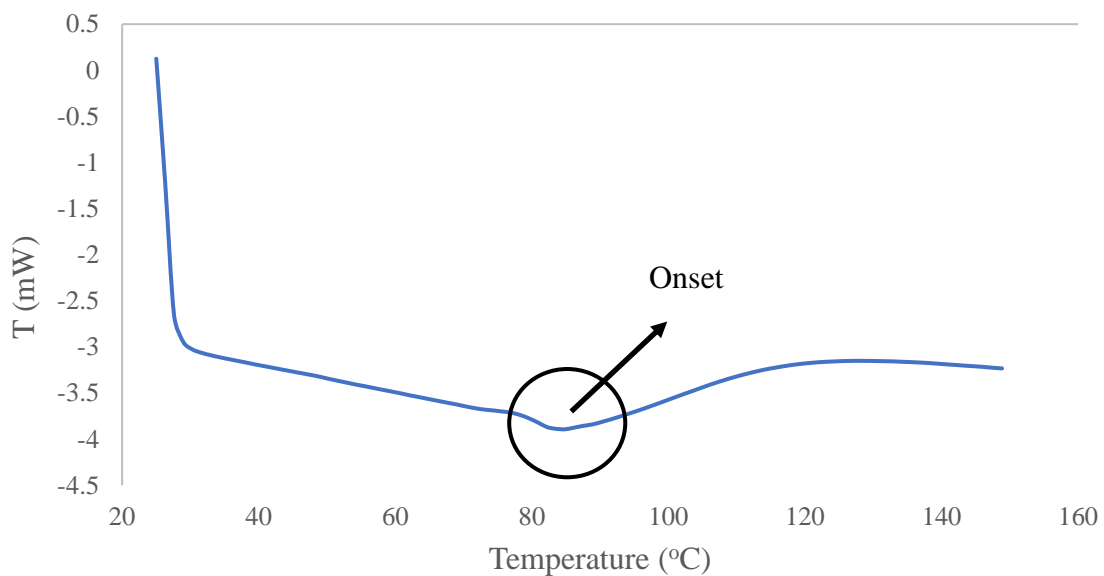


381

382

Figure 6. DTG thermogram of polyurethane film

383 During polymerization, this hard segment restricts the mobility of the polymer chain
384 (Ren et al. 2013) owing to the steric effect on the benzene ring in the hard segment. The
385 endothermic peak of acetone used as the solvent in this study was supposedly at 56°C.
386 However, it was detected in the DSC thermogram nor the TGA thermogram, which indicates
387 that acetone was removed from the polyurethane during the synthesis process, owing to its
388 volatility nature. The presence of acetone in the synthesis was to lower the reaction kinetics.



389 **Figure 7.** DSC thermogram of polyurethane film

390
391
392
393 e. The solubility and mechanical properties of the polyurethane film

394 The chemical resistivity of a polymer will be the determinant in performing as a conductor.
395 Thus, its solubility in various solvents was determined by dissolving the polymer in selected
396 solvents such as hexane, benzene, acetone, tetrahydrofuran (THF), dimethylformamide (DMF)
397 and dimethylformamide (DMSO). On the other hand, the mechanical properties of of
398 polyurethane were determined based on the standard testing following ASTM D 638 (Standard
399 Test Method for Tensile Properties of Plastics). The results from the polyurethane film
400 solubility and tensile test are shown in **Table 3**. Polyurethane films were insoluble with

401 benzene, hexane and acetone and are only slightly soluble in tetrahydrofuran (THF),
 402 dimethylformamide (DMF) and dimethylformamide (DMSO) solutions. While the tensile
 403 strength of a PU film indicated how much elongation load the film was capable of withstanding
 404 the material before breaking.

405

406 **Table 3** The solubility and mechanical properties of the polyurethane film

407

| Parameters | Polyurethane film |
|----------------------------|----------------------|
| Solubility | Benzene Insoluble |
| | Hexane Insoluble |
| | Acetone Insoluble |
| | THF Less soluble |
| | DMF Less soluble |
| | DMSO Less soluble |
| Stress (MPa) | 8.53 |
| Elongation percentage (%) | 43.34 |
| Strain modulus (100) (MPa) | 222.10 |

408

409 The tensile stress, strain and modulus of polyurethane film also indicated that polyurethane has
 410 good mechanical properties that are capable of being a supporting substrate for the next stage
 411 of study. In the production of polyurethane, the properties of a polyurethane are easily
 412 influenced by the content of MDI and polyol used. The length of the chain and its flexibility
 413 are contributed by the polyol which makes it elastic. High crosslinking content can also produce
 414 hard and rigid polymers. MDI is a major component in the formation of hard segments in
 415 polyurethane. It is this hard segment that determines the rigidity of the PU. Therefore, high

416 isocyanate content results in higher rigidity on PU (Petrovic et al. 2002). Thus, the polymer has
417 a higher resistance to deformation and more stress can be applied to the PU.

418

419 f. The conductivity of the polyurethane as a polymeric film on SPE

420 Polyurethane film deposited onto the screen-printed electrode by casting method as shown in

421 **Figure 1**. After that, the modified electrode was analysed using cyclic voltammetry (CV) and

422 differential pulse voltammetry (DPV) in order to study the behaviour of modified electrode.

423 The modified electrode was tested in a 0.1 mmol/L KCl solution containing 5 mmol/L (K_3Fe

424 $(CN)_6$). The use of potassium ferricyanide is intended to increase the sensitivity of the KCl

425 solution. The conductivity of the modified electrode was studied. The electrode was analyzed

426 by cyclic voltammetry method with a potential range of -1.00 to +1.00 with a scan rate of 0.05

427 V/s. The voltammograms at electrode have shown a specific redox reaction. Furthermore, the

428 conductivity of the modified electrode is lower due to the use of polyurethane. This occurs due

429 to PU is a natural polymer produced from the polyol of palm kernel oil. The electrochemical

430 signal at the electrode is low if there is a decrease in electrochemical conductivity (El - Raheem

431 et al. 2020). It can be concluded that polyurethane is a bio-polymer with a low conductivity

432 value. The current of the modified electrode was found at 5.3×10^{-5} A or 53 μ A. Nevertheless,

433 the electroconductivity of PU in this study shows better conductivity several times compared

434 to Bahrami et al. (2019) that reported the conductivity of PU as 1.26×10^{-6} A, whereas Li et al.

435 (2019) reported the PU conductivity in their study was even very low, namely 10^{-14} A. The

436 conductivity of PU owing to the benzene ring in the hard segment (MDI) could exhibit the

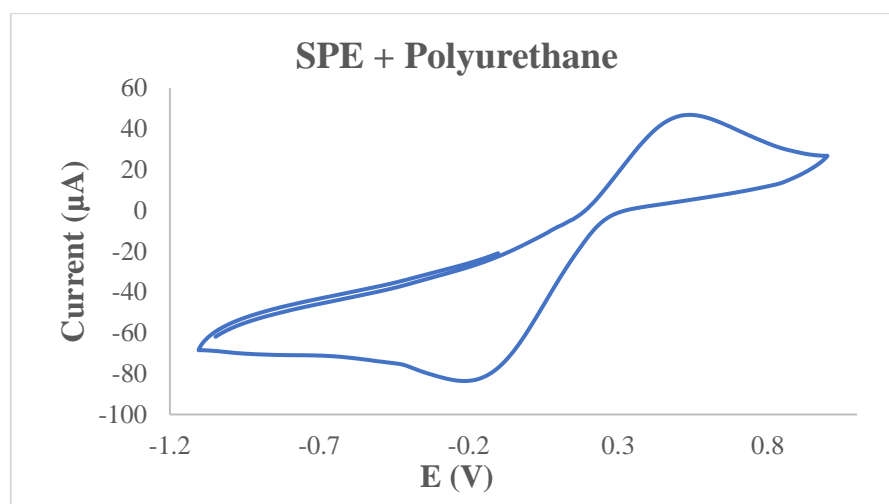
437 conductivity by inducing electron delocalization along the polyurethane chain (Wong et al.

438 2014). The conductivity of PU can also be caused by PEG. The application of PEG as polyol

439 has been studied by Porcarelli et al. (2017), that reported that the conductivity of PU based on

440 PEG – polyol was 9.2×10^{-8} .

441 According to **Figure 8**, it can be concluded that the anodic peak present in the modified
442 electrode was at +0.5 V, it also represented the oxidation process of the modified electrode.
443 The first oxidation scan on both electrodes ranged from -0.2 to +1.0 V, which showed a
444 significant anodic peak at a potential of +0.5 V.
445



446
447 **Figure 8.** The voltammogram of SPE – PU modified electrode after analysed using cyclic
448 voltammetry (CV) technique

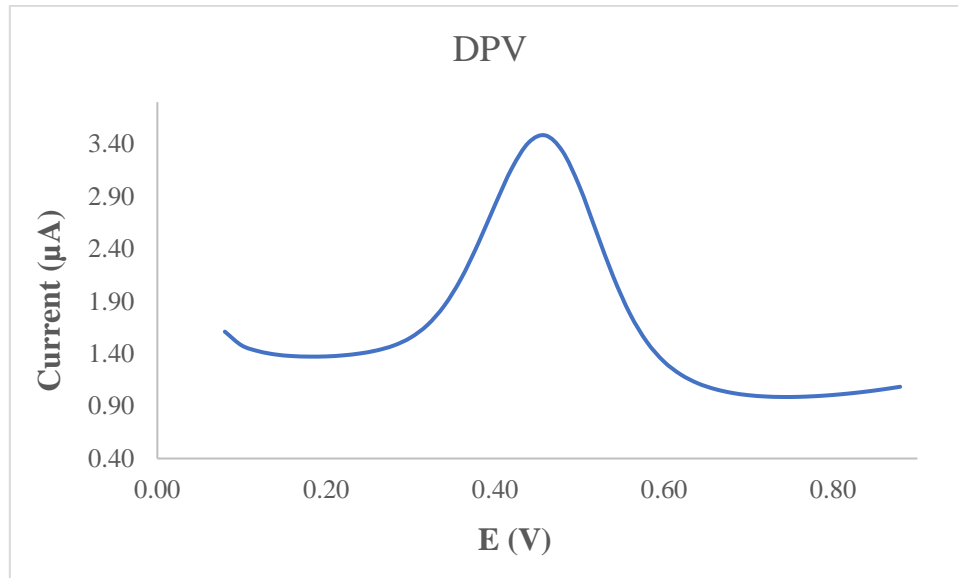
449
450 **Figure 9** also presents the DPV voltammogram of modified electrode. DPV is a measurement
451 based on the difference in potential pulses that produce an electric current. Scanning the
452 capability pulses to the working electrode will produce different currents. Optimal peak
453 currents will be produced to the reduction capacity of the redox material. The peak current
454 produced is proportional to the concentration of the redox substance and can be detected up to
455 concentration below 10^{-8} M. DPV was conducted to obtain the current value that more accurate
456 than CV (Lee et al. 2018).

457
458 This study used a redox pair ($K_3Fe(CN)_6$) as a test device (probe). The currents generated by
459 SPE-PU and proved by CV and DPV have shown conductivity on polyurethane films. This
460 suggests that polyurethane films can conduct electron transfer. The electrochemical area on the

461 modified electrode can be calculated using the formula from Randles-Sevcik (Butwong et al.
 462 2019), where the electrochemical area for SPE-PU is considered to be A, using Equation 2:

463
$$\text{Current of SPE-PU, } I_p = 2.65 \times 10^5 n^{3/2} A v^{1/2} C D^{1/2} \quad (2)$$

464



465

466 **Figure 9.** The voltammogram of SPE – PU modified electrode after analyzed using
 467 differential pulse voltammetry (DPV) technique

468

469 Where, $n - 1$ is the amount of electron transfer involved, while C is the solvent concentration
 470 used (mmol/L) and the value of D is the diffusion constant of 5 mmol/L at $(K_3Fe(CN)_6)$
 471 dissolved using 0.1 mmol/L KCl. The estimated surface area of the electrode (**Figure 1**) was
 472 0.2 cm^2 where the length and width of the electrode used during the study was $0.44 \text{ cm} \times 0.44$
 473 cm while the surface area of the modified electrode was 0.25 cm^2 with the length and width of
 474 the electrode estimated at $0.5 \text{ cm} \times 0.5 \text{ cm}$, and causing the modified electrode has a larger
 475 surface. The corresponding surface concentration (τ) (mol/cm^2) is calculated using Equation 3.

476
$$I_p = (n^2 F^2 / 4RT) A \tau v \quad (3)$$

477 I_p is the peak current (A), while A is the surface area of the electrode (cm^2), the value of v is
 478 the applied scan rate (mV/s) and F is the Faraday constant (96,584 C/mol), R is the constant
 479 ideal gas (8.314 J/mol K) and T is the temperature used during the experiment being conducted

480 (298 K) (Koita et al. 2014). The development of conducting polymer from palm oil-based
481 biomaterials seems to be one of the potential future applications of palm oil products, as this
482 novel material has the potential to contribute positively to the analytical industry. Likewise,
483 other palm oil-based products, such as refined-bleached-deodorised (RBD) palm oil, palm oil,
484 and palm stearin are abundantly available in Malaysia. They are known to be economical,
485 sustainable, and environmentally biodegradable. These palm oil-based products are promising
486 prospects for manufacturing biomaterials that become alternative products to other polymers
487 from synthetic/chemical-based (Tajao et al. 2021). Several studies have been reported the
488 application of PU to produce elastic conductive fibres and films owing to it is highly elastic,
489 scratch resistant and adhesive (Tadese et al. 2019), thus it is easy for PU to adhere on the
490 screen-printed electrode in order to modify the electrode. PU is also being used as a composite
491 material to make elastic conducting composite films (Khatoon & Ahmad 2017).

492

493 **4. Conclusion**

494 Polyurethane film was prepared by pre-polymerization between palm kernel oil-based polyol
495 (PKO-p) with MDI. The presence of PEG 400 as the chain extender formed freestanding
496 flexible film. Acetone was used as the solvent to lower the reaction kinetics since the pre-
497 polymerization was carried out at room temperature. The formation of urethane links (NHCO
498 – backbone) after polymerization was confirmed by the absence of N=C=O peak at 2241 cm^{-1}
499 and the presence of N-H peak at 3300 cm^{-1} , carbonyl (C=O) at 1710 cm^{-1} , carbamate (C-N) at
500 1600 cm^{-1} , ether (C-O-C) at 1065 cm^{-1} , benzene ring (C = C) at 1535 cm^{-1} in the bio
501 polyurethane chain structure. Soxhlet analysis for the determination of crosslinking on
502 polyurethane films has yielded a high percentage of 99.33 %. This is contributed by the hard
503 segments formed from the reaction between isocyanates and hydroxyl groups causing
504 elongation of polymer chains. FESEM analysis exhibited an absence of phase separation and

505 smooth surface. Meanwhile, the current of modified electrode was found at 5.2×10^{-5} A. This
506 bio polyurethane film can be used as a conducting bio-polymer and it is very useful for other
507 studies such as electrochemical sensor purposes. Furthermore, advanced technologies are
508 promising and the future of bio-based polyol looks very bright.

509

510 **5. Acknowledgment**

511 The authors would like to thank Universitas Alma Ata for the sponsorship given to the first
512 author. We would like to also, thank The Department of Chemical Sciences, Universiti
513 Kebangsaan Malaysia for the laboratory facilities and CRIM, UKM for the analysis
514 infrastructure.

515

516 **6. Conflict of Interest**

517 The authors declare no conflict of interest.

518

519 **7. References**

- 520 Agrawal, A., Kaur, R., Walia, R. S. (2017). PU foam derived from renewable sources:
521 Perspective on properties enhancement: An overview. *European Polymer Journal*. 95:
522 255 – 274.
- 523 Akindoyo, J. O., Beg, M.D.H., Ghazali, S., Islam, M.R., Jeyaratnam, N. & Yuvaraj, A.R.
524 (2016). Polyurethane types, synthesis and applications – a review. *RSC Advances*. 6:
525 114453 – 114482.
- 526 Alamawi, M. Y., Khairuddin, F. H., Yusoff, N. I. M., Badri, K., Ceylan, H. (2019).
527 Investigation on physical, thermal and chemical properties of palm kernel oil polyol bio
528 – based binder as a replacement for bituminous binder. *Construction and Building*
529 *Materials*. 204: 122 – 131.

530 Alqarni, S. A., Hussein, M. A., Ganash, A. A. & Khan, A. (2020). Composite material – based
531 conducting polymers for electrochemical sensor applications: a mini review.
532 *BioNanoScience*. **10**: 351 – 364.

533 Badan, A., Majka, T. M. (2017). The influence of vegetable – oil based polyols on physico –
534 mechanical and thermal properties of polyurethane foams. *Proceedings*. 1 – 7.

535 Badri, K.H. (2012) Biobased polyurethane from palm kernel oil-based polyol. In Polyurethane;
536 Zafar, F., Sharmin, E., Eds. InTechOpen: Rijeka, Croatia. pp. 447–470.

537 Badri, K.H., Ahmad, S.H. & Zakaria, S. 2000. Production of a high-functionality RBD palm
538 kernel oil – based polyester polyol. *Journal of Applied Polymer Science* 81(2): 384 –
539 389.

540 Baig, N., Sajid, M. and Saleh, T. A. 2019. Recent trends in nanomaterial – modified electrodes
541 for electroanalytical applications. *Trends in Analytical Chemistry*. 111: 47 – 61.

542 Berta, M., Lindsay, C., Pans, G., & Camino, G. (2006). Effect of chemical structure on
543 combustion and thermal behaviour of polyurethane elastomer layered silicate
544 nanocomposites. *Polymer Degradation and Stability*. **91**: 1179-1191.

545 Borowicz, M., Sadowska, J. P., Lubczak, J. & Czuprynski, B. (2019). Biodegradable, flame –
546 retardant, and bio – based rigid polyurethane/polyisocyanurate foams for thermal
547 insulation application. *Polymers*. 11: 1816 – 1839.

548 Butwong, N., Khajonklin, J., Thongbor, A. & Luong, J.H.T. (2019). Electrochemical sensing
549 of histamine using a glassy carbon electrode modified with multiwalled carbon nanotubes
550 decorated with Ag – Ag₂O nanoparticles. *Microchimica Acta*. **186** (11): 1 – 10.

551 Chokkareddy, R., Thondavada, N., Kabane, B. & Redhi, G. G. (2020). A novel ionic liquid
552 based electrochemical sensor for detection of pyrazinamide. *Journal of the Iranian*
553 *Chemical Society*. 18: 621 – 629.

554 Chokkareddy, R., Kanchi, S. & Inamuddin (2020). Simultaneous detection of ethambutol and
555 pyrazinamide with IL@CoFe₂O₄NPs@MWCNTs fabricated glassy carbon electrode.
556 *Scientific Reports*. 10: 13563.

557 Clemitson, I. (2008). Castable Polyurethane Elastomers. Taylor & Francis Group, New York.
558 doi:10.1201/9781420065770.

559 Corcuera, M.A., Rueda, L., Saralegui, A., Martin, M.D., Fernandez-d'Arlas, B., Mondragon,
560 I. & Eceiza, A. (2011). Effect of diisocyanate structure on the properties and
561 microstructure of polyurethanes based on polyols derived from renewable resources.
562 *Journal of Applied Polymer Science*. **122**: 3677-3685.

563 Cuve, L. & Pascault, J.P. (1991). Synthesis and properties of polyurethanes based on
564 polyolefine: Rigid polyurethanes and amorphous segmented polyurethanes prepared in
565 polar solvents under homogeneous conditions. *Polymer*. **32** (2): 343- 352.

566 Degefu, H., Amare, M., Tessema, M. & Admassie, S. (2014). Lignin modified glassy carbon
567 electrode for the electrochemical determination of histamine in human urine and wine
568 samples. *Electrochimica Acta*. 121: 307 – 314.

569 Dzulkipli, M. Z., Karim, J., Ahmad, A., Dzulkurnain, N. A., Su'ait, M S., Fujita, M. Y., Khoon,
570 L. T. & Hassan, N. H. (2021). The influences of 1-butyl-3-methylimidazolium
571 tetrafluoroborate on electrochemical, thermal and structural studies as ionic liquid gel
572 polymer electrolyte. *Polymers*. 13 (8): 1277 – 1294.

573 El-Raheem, H.A., Hassan, R.Y.A., Khaled, R., Farghali, A. & El-Sherbiny, I.M. (2020).
574 Polyurethane – doped platinum nanoparticles modified carbon paste electrode for the
575 sensitive and selective voltammetric determination of free copper ions in biological
576 samples. *Microchemical Journal*. **155**: 104765.

577 Fei, T., Li, Y., Liu, B. & Xia, C. (2019). Flexible polyurethane/boron nitride composites with
578 enhanced thermal conductivity. *High Performance Polymers*. **32** (3): 1 – 10.

579 Furtwengler, P., Perrin R., Redl, A. & Averous, L. (2017). Synthesis and characterization of
580 polyurethane foams derived of fully renewable polyesters polyols from sorbitol.
581 *European Polymer Journal*. **97**: 319 – 327.

582 Ghosh, S., Ganguly, S., Remanan, S., Mondal, S., Jana, S., Maji, P. K., Singha, N., Das, N. C.
583 (2018). Ultra – light weight, water durable and flexible highly electrical conductive
584 polyurethane foam for superior electromagnetic interference shielding materials. *Journal*
585 *of Materials Science: Materials in Electronics*. 29: 10177 – 10189.

586 Guo, S., Zhang, C., Yang, M., Zhou, Y., Bi, C., Lv, Q. & Ma, N. (2020). A facile and sensitive
587 electrochemical sensor for non – enzymatic glucose detection based on three –
588 dimensional flexible polyurethane sponge decorated with nickel hydroxide. *Analytica*
589 *Chimica Acta*. **1109**: 130 – 139.

590 Hamuzan, H.A. & Badri, K.H. (2016). The role of isocyanates in determining the viscoelastic
591 properties of polyurethane. AIP Conference Proceedings. 1784, Issue 1.

592 Herrington, R. & Hock, K. (1997). Flexible polyurethane foams. 2nd Edition. Dow Chemical
593 Company. Midlan.

594 Janpoung, P., Pattanauwat, P. & Potiyaraj, P. (2020). Improvement of electrical conductivity
595 of polyurethane/polypyrrole blends by graphene. *Key Engineering Materials*. **831**: 122 –
596 126.

597 Khairuddin, F.H., Yusof, N. I. M., Badri, K., Ceylan, H., Tawil, S. N. M. (2018). Thermal,
598 chemical and imaging analysis of polyurethane/cecabase modified bitumen. *IOP Conf.*
599 *Series: Materials Science and Engineering*. 512: 012032.

600 Khatoon, H., Ahmad, S. (2017). A review on conducting polymer reinforced polyurethane
601 composites. *Journal of Industrial and Engineering Chemistry*. 53: 1 – 22.

602 Kilele, J. C., Chokkareddy, R., Rono, N. & Redhi, G. G. (2020). A novel electrochemical
603 sensor for selective determination of theophylline in pharmaceutical formulations.
604 *Journal of the Taiwan Institute of Chemical Engineers*. 1 – 11.

605 Kilele, J. C., Chokkareddy, R. & Redhi, G. G. (2021). Ultra – sensitive electrochemical sensor
606 for fenitrothion pesticide residues in fruit samples using IL@CoFe₂ONPs@MWCNTs
607 nanocomposite. *Microchemical Journal*. 164: 106012.

608 Koita, D., Tzedakis, T., Kane, C., Diaw, M., Sock, O. & Lavedan, P. (2014). Study of the
609 histamine electrochemical oxidation catalyzed by nickel sulfate. *Electroanalysis*. **26 (10)**:
610 2224 – 2236.

611 Kotal, M., Srivastava, S.K. & Paramanik, B. (2011). Enhancements in conductivity and thermal
612 stabilities of polyurethane/polypyrrole nanoblends. *The Journal of Physical Chemistry*
613 *C*. **115 (5)**: 1496 – 1505.

614 Ladan, M., Basirun, W.J., Kazi, S.N., Rahman, F.A. (2017). Corrosion protection of AISI 1018
615 steel using Co – doped TiO₂/polypyrrole nanocomposites in 3.5% NaCl solution.
616 *Materials Chemistry and Physics*. **192**: 361 – 373.

617 Lampman, G.M., Pavia, D.L., Kriz, G.S. & Vyvyan, J.R. (2010). Spectroscopy. 4th Edition.
618 Brooks/Cole Cengage Learning, Belmont, USA.

619 Lee, K.J., Elgrishi, N., Kandemir, B. & Dempsey, J.L. 2018. Electrochemical and spectroscopic
620 methods for evaluating molecular electrocatalysts. *Nature Reviews Chemistry* 1(5): 1 -
621 14.

622 Leykin, A., Shapovalov, L. & Figovsky, O. (2016). Non – isocyanate polyurethanes –
623 Yesterday, today and tomorrow. *Alternative Energy and Ecology*. **191 (3 – 4)**: 95 – 108.

624 Li, H., Yuan, D., Li, P., He, C. (2019). High conductive and mechanical robust carbon
625 nanotubes/waterborne polyurethane composite films for efficient electromagnetic
626 interference shielding. *Composites Part A*. 121: 411 – 417.

- 627 Nakthong, P., Kondo, T., Chailapakul, O., Siangproh, W. (2020). Development of an
628 unmodified screen – printed graphene electrode for nonenzymatic histamine detection.
629 *Analytical Methods*. 12: 5407 – 5414.
- 630 Mishra, K., Narayan, R., Raju, K.V.S.N. & Aminabhavi, T.M. (2012). Hyperbranched
631 polyurethane (HBPU)-urea and HBPU-imide coatings: Effect of chain extender and
632 NCO/OH ratio on their properties. *Progress in Organic Coatings*. 74: 134 – 141.
- 633 Mohd Noor, M. A., Tuan Ismail, T. N. M., Ghazali, R. (2020). Bio – based content of oligomers
634 derived from palm oil: Sample combustion and liquid scintillation counting technique.
635 *Malaysia Journal of Analytical Science*. 24: 906 – 917.
- 636 Mutsuhisa F., Ken, K. & Shohei, N. (2007). Microphase separated structure and mechanical
637 properties of norbornane diisocyanate – based polyurethane. *Polymer*. 48 (4): 997 – 1004.
- 638 Mustapha, R., Rahmat, A. R., Abdul Majid, R., Mustapha, S. N. H. (2019). Vegetable oil –
639 based epoxy resins and their composites with bio – based hardener: A short review.
640 *Polymer- Plastic Technology and Materials*. 58: 1311 – 1326.
- 641 Nohra, B., Candy, L., Blancos, J.F., Guerin, C., Raoul, Y. & Mouloungui, Z. (2013). From
642 petrochemical polyurethanes to biobased polyhydroxyurethanes. *Macromolecules*. 46
643 (10): 3771 – 3792.
- 644 Pan, T. & Yu, Q. (2016). Anti – corrosion methods and materials comprehensive evaluation of
645 anti – corrosion capacity of electroactive polyaniline for steels. *Anti – Corrosion Methods
646 and Materials*. 63: 360 – 368.
- 647 Pan, X. & Webster, D.C. (2012). New biobased high functionality polyols and their use in
648 polyurethane coatings. *ChemSusChem*. 5: 419-429.
- 649 Petrovic, Z.S. (2008). Polyurethanes from vegetable oils. *Polymer Reviews*. 48 (1): 109 – 155.

650 Porcarelli, L., Manojkumar, K., Sardon, H., Llorente, O., Shaplov, A. S., Vijayakrishna, K.,
651 Gerbaldi, C., Mecerreyes, D. (2017). Single ion conducting polymer electrolytes based
652 on versatile polyurethanes. *Electrochimica Acta*. 241: 526 – 534.

653 Priya, S. S., Karthika, M., Selvasekarapandian, S. & Manjuladevi, R. (2018). Preparation and
654 characterization of polymer electrolyte based on biopolymer I-carrageenan with
655 magnesium nitrate. *Solid State Ionics*. **327**: 136 – 149.

656 Ren, D. & Frazier, C.E. (2013). Structure–property behaviour of moisture-cure polyurethane
657 wood adhesives: Influence of hard segment content. *Adhesion and Adhesives*. **45**: 118-
658 124.

659 Rogulska, S.K., Kultys, A. & Podkoscielny, W. (2007). Studies on thermoplastic polyurethanes
660 based on new diphenylethane – derivative diols. II. Synthesis and characterization of
661 segmented polyurethanes from HDI and MDI. *European Polymer Journal*. **43**: 1402 –
662 1414.

663 Romaskevicius, T., Budriene, S., Pielichowski, K. & Pielichowski, J. (2006). Application of
664 polyurethane – based materials for immobilization of enzymes and cells: a review.
665 *Chemija*. **17**: 74 – 89.

666 Sengodu, P. & Deshmukh, A. D. (2015). Conducting polymers and their inorganic composites
667 for advanced Li-ion batteries: a review. *RSC Advances*. **5**: 42109 – 42130.

668 Septevani, A. A., Evans, D. A. C., Chaleat, C., Martin, D. J., Annamalai, P. K. (2015). A
669 systematic study substituting polyether polyol with palm kernel oil based polyester
670 polyol in rigid polyurethane foam. *Industrial Corps and Products*. 66: 16 – 26.

671 Su'ait, M. S., Ahmad, A., Badri, K. H., Mohamed, N. S., Rahman, M. Y. A., Ricardi, C. L. A.
672 & Scardi, P. The potential of polyurethane bio – based solid polymer electrolyte for
673 photoelectrochemical cell application. *International Journal of Hydrogen Energy*. 39 (6):
674 3005 – 3017.

675 Tadesse, M. G., Mengistie, D. A., Chen, Y., Wang, L., Loghin, C., Nierstrasz, V. (2019).
676 Electrically conductive highly elastic polyamide/lycra fabric treated with PEDOT: PSS
677 and polyurethane. *Journal of Materials Science*. 54: 9591 – 9602.

678 Tajau, R., R, Rosiah, Alias, M. S., Mudri, N. H., Halim, K. A. A., Harun, M. H., Isa, N. M.,
679 Ismail, R. C., Faisal, S. M., Talib, M., Zin, M. R. M., Yusoff, I. I., Zaman, N. K., Illias,
680 I. A. (2021). Emergence of polymeric material utilising sustainable radiation curable
681 palm oil – based products for advanced technology applications. *Polymers*. 13: 1865 –
682 1886.

683 Tran, V.H., Kim, J.D., Kim, J.H., Kim, S.K., Lee, J.M. (2020). Influence of cellulose
684 nanocrystal on the cryogenic mechanical behaviour and thermal conductivity of
685 polyurethane composite. *Journal of Polymers and The Environment*. **28**: 1169 – 1179.

686 Viera, I.R.S., Costa, L.D.F.D.O., Miranda, G.D.S., Nardehcia, S., Monteiro, M.S.D. S.D.B.,
687 Junior, E.R. & Delpech, M.C. (2020). Waterborne poly (urethane – urea)s
688 nanocomposites reinforced with clay, reduced graphene oxide and respective hybrids:
689 Synthesis, stability and structural characterization. *Journal of Polymers and The
690 Environment*. **28**: 74 – 90.

691 Wang, B., Wang, L., Li, X., Liu, Y., Zhang, Z., Hedrick, E., Safe, S., Qiu, J., Lu, G. & Wang,
692 S. (2018). Template – free fabrication of vertically – aligned polymer nanowire array on
693 the flat – end tip for quantifying the single living cancer cells and nanosurface interaction.
694 *a Manufacturing Letters*. **16**: 27 – 31.

695 Wang, J., Xiao, L., Du, X., Wang, J. & Ma, H. (2017). Polypyrrole composites with carbon
696 materials for supercapacitors. *Chemical Papers*. **71** (2): 293 – 316.

697 Wong, C.S. & Badri, K.H. (2012). Chemical analyses of palm kernel oil – based polyurethane
698 prepolymer. *Materials Sciences and Applications*. **3**: 78 – 86.

- 699 Wong, C. S., Badri, K., Ataollahi, N., Law, K., Su'ait, M. S., Hassan, N. I. (2014). Synthesis
700 of new bio – based solid polymer electrolyte polyurethane – LiClO₄ via
701 prepolymerization method: Effect of NCO/OH ratio on their chemical, thermal properties
702 and ionic conductivity. *World Academy of Science, Engineering and Technology,*
703 *International Journal of Chemical, Molecular, Nuclear, Materials and Metallurgical*
704 *Engineering.* 8: 1243 – 1250.
- 705 Yong, Z., Bo, Z.M., Bo, W., Lin, J.Z. & Jun, N. (2009). Synthesis and properties of novel
706 polyurethane acrylate containing 3-(2-Hydroxyethyl) isocyanurate segment. *Progress in*
707 *Organic Coatings.* **67**: 264 – 268
- 708 Zia, K. M., Anjum, S., Zuber, M., Mujahid, M. & Jamil, T. (2014). Synthesis and molecular
709 characterization of chitosan based polyurethane elastomers using aromatic diisocyanate.
710 *International of Journal of Biological Macromolecules.* **66**: 26 – 32.

Hasil Reviu 4 dan Submit Revisi: 2 Desember 2021

Hindawi

Joanna Rydz

Decision

Major Revision Requested

Message for Author

Dear Authors,

The reviewers have raised points that were not fully taken into consideration and revision of the manuscript before it is suitable for publication is still required.

The journal should follow certain standards, such as compliance with general recommendations (IUPAC, SI, manual for authors), so please review and correct manuscript again.

Comments have been entered into the manuscript as a track changes with comments and will be sent additionally.

We look forward to receiving your revised manuscript.

— Response to Revision Request

Muhammad Abdurrahman Munir

02.12.2021

Your Reply

Greetings, Dear Dr. Peter Foot, Thank you so much for your suggestions to the manuscript. For your information, we have followed your suggestion and ensured the manuscript has been followed the journal regulation. The file contains the revised manuscript and the answer for the reviewer. Please check the manuscript and inform us if there is any revision that should be made. We hope this study can be published in this journal. Best Regards.

File

Manuscript - Munir.docx 873 kB



1 **Design and Synthesis of Conducting Polymer Based on Polyurethane**
2 **produced from Palm Kernel Oil**

3
4 Muhammad Abdurrahman Munir^{1*}, Khairiah Haji Badri^{2,3}, Lee Yook Heng², Ahlam
5 Inayatullah⁴, Ari Susiana Wulandari¹, Emelda¹, Eliza Dwinta¹, Rachmad Bagus Yahya
6 Supriyono¹

7
8 ¹Department of Pharmacy, Faculty of Health Science, Universitas Alma Ata, Daerah
9 Istimewa Yogyakarta, 55183, Indonesia

10 ²Department of Chemical Sciences, Faculty of Science and Technology, Universiti
11 Kebangsaan Malaysia, Bangi, 43600, Malaysia

12 ³Polymer Research Center, Universiti Kebangsaan Malaysia, Bangi, 43600, Malaysia

13 ⁴Faculty of Science and Technology, Universiti Sains Islam Malaysia, Nilai, 71800, Malaysia

14 *Email: muhammad@almaata.ac.id

15
16 **Abstract**

17 Polyurethane (PU) is a unique polymer that has versatile processing methods and mechanical
18 properties upon inclusion of selected additives. In this study, a freestanding bio-polyurethane
19 film on screen-printed electrode (SPE) was prepared by the solution casting technique, using
20 acetone as solvent. It was a one-pot synthesis between major reactants namely, palm kernel oil-
21 based polyol (PKOp) and 4,4-methylene diisocyanate. The PU has strong adhesion on SPE
22 surface. The synthesized polyurethane was characterized using thermogravimetry analysis
23 (TGA), differential scanning calorimetry (DSC), Fourier – transform infrared spectroscopy
24 (FTIR), surface area analysis by field emission scanning electron microscope (FESEM) and

25 cyclic voltammetry (CV). Cyclic voltammetry was employed to study electro-catalytic
26 properties of SPE-Polyurethane towards oxidation of PU. Remarkably, SPE-PU exhibited
27 improved anodic peak current as compared to SPE itself using the differential pulse
28 voltammetry (DPV) method. Furthermore, the formation of urethane linkages (NHCO
29 backbone) after polymerization was analysed using FTIR and confirmed by the absence of
30 N=C=O peak at 2241 cm^{-1} . The glass transition temperature (T_g) of the polyurethane was
31 detected at 78.1°C .

32

33 **Keywords:** Polyurethane, polymerization, screen-printed electrode, voltammetry

34

35

36 1. Introduction

37 Polymers are molecules composed of many repeated sub-units referred to as monomers
38 (Sengodu & Deshmukh 2015). Conducting polymers (CPs) are polymers that exhibit electrical
39 behavior (Alqarni et al. 2020). The conductivity of CPs was first observed in polyacetylene,
40 nevertheless owing to its instability led to the discovery of other forms of CPs such as
41 polyaniline (PANI), poly (o-toluidine) (PoT), polythiophene (PTh), polyfluorene (PF) and
42 polyurethane (PU). Furthermore, natural CPs have low conductivity and are often semi-
43 conductive. Therefore, it is essential to increase their conductivity mainly for use in
44 electrochemical sensor programs (Dzulkipli et al. 2021; Wang et al. 2018). Conducting
45 polymers (CPs) represent a sizeable range of useful organic substances. Their unique electrical,
46 chemical and physical properties; reasonable price; simple preparation; small dimensions and
47 large surface area have enabled researchers to discover a wide variety of uses such as sensors,
48 biochemical applications, solar cells and electrochromic devices (Alqarni et al. 2020; Ghosh et
49 al. 2018). There are scientific documentation on the use of conductive polymers in various

50 studies such as polyaniline (Pan & Yu 2016), polypyrrole (Ladan et al. 2017) and polyurethane
51 (Tran et al. 2020; Vieira et al. 2020; Guo et al. 2020; Fei et al. 2020).

52

53 The application of petroleum as polyol in order to produce polyurethane has been applied. Coal
54 and crude oil were used as raw materials to produce it. Nevertheless, these materials have
55 become very rare to find and the price is very expensive at the same time required a
56 sophisticated system to produce it. These reasons have been considered and finding utilizing
57 plants that can be used as alternative polyols should be done immediately (Badri 2012).
58 Furthermore, in order to avoid the application of petroleum as raw material for a polyol,
59 vegetable oils become a better choice as polyol in order to obtain a biodegradable polyol.
60 Vegetable oils that are generally used for synthesis polyurethane are soybean oil, corn oil,
61 sunflower seed oil, coconut oil, nuts oil, rapeseed, olive oil and palm oil (Badri 2012; Borowicz
62 et al. 2019).

63

64 It is very straightforward for vegetable oils to react with a specific group in order to form PU
65 such as epoxy, hydroxyl, carboxyl and acrylate owing to the existence of (-C=C-) in vegetable
66 oils. Thus, it has provided appealing profits to vegetable oils compared to petroleum considered
67 the toxicity, price and harm to the environment (Mustapha et al. 2019; Mohd Noor et al. 2020).
68 Palm oil becomes the chosen in this study to produce PU owing to it is largely cultivated in
69 South Asia particularly in Malaysia and Indonesia. It has several profits compared to other
70 vegetable oils such as the easiest materials obtained, the lowest cost of all the common
71 vegetable oils and recognized as the plantation that has a low environmental impact and
72 removing CO₂ from the atmosphere as net sequester (Tajau et al. 2021; Septevani et al. 2015).
73 Biopolymer, a natural biodegradable polymer has attracted much attention in recent years.
74 Global environmental awareness and fossil fuel depletion urged researchers to work in the

75 biopolymer field (Priya et al. 2018). Polyurethane is one of the most common, versatile and
76 researched materials in the world. These materials combine the durability and toughness of
77 metals with the elasticity of rubber, making them suitable to replace metals, plastics and rubber
78 in several engineered products. They have been widely applied in biomedical applications,
79 building and construction applications, automotive, textiles and in several other industries due
80 to their superior properties in terms of hardness, elongation, strength and modulus (Zia et al.
81 2014; Romaskevicius et al. 2006). Polyurethanes are also considered to be one of the most useful
82 materials with many profits such as, possess low conductivity, low density, absorption
83 capability and dimensional stability. They are clearly a great research subject owing to their
84 mechanical, physical and chemical properties (Badan & Majka 2017).

85

86 The urethane group is the major repeating unit in PUs and is produced from the reaction
87 between alcohol (-OH) and isocyanate (NCO); albeit polyurethanes also contain other groups
88 such as ethers, esters, urea and some aromatic compounds. Due to the wide variety of sources
89 from which PUs can be synthesized, thus a wide range of specific applications can be generated.
90 They are grouped into several different classes based on the desired properties: rigid, flexible,
91 thermoplastic, waterborne, binders, coating, adhesives, sealants and elastomers (Akindoyo et
92 al. 2016).

93

94 Although, PU has low conductivity, it is lighter than other materials such as metals. The
95 hardness of PU also relies on the number of the aromatic rings in the polymer structure
96 (Janpoung et al, 2020; Su'ait et al. 2014), majorly contributed by the isocyanate derivatives.
97 PU has also a conjugate structure where electrons can move in the main chain that causing
98 electricity produced even the conductivity is low. The electrical conductivity of conjugated
99 linear (π) can be explained by the distance between the highest energy level containing

100 electrons (HOMO) called valence band and the lowest energy level not containing electrons
101 (LUMO) called the conduction band (Wang et al. 2017; Kotal et al. 2011).

102

103 In the recent past, several conventional methods have been developed such as capillary
104 electrophoresis, liquid and gas chromatography coupled with several detectors. Nevertheless,
105 although chromatographic and spectrometric approaches are well developed for qualitative and
106 quantitative analyses of analytes, several limitations emerged such as complicated
107 instrumentation, expensive, tedious sample preparations and requiring large amounts of
108 expensive solvents that will harm the users and environment (Kilele et al. 2020). Therefore, is
109 is imperative to obtain and develop an alternative material that can be used to analyse a specific
110 analyte. Electrochemical methods are extremely promising methods in the determination of an
111 analyte in samples owing to the high selectivities, sensitivities, inexpensive, requirements of
112 small amounts of solvents and can be operated by people who have no background in analytical
113 chemistry. In addition, the sample preparation such as separation and extraction steps are not
114 needed owing to the selectivity of this instrument where no obvious interference on the current
115 response recorded (Chokkareddy et al. 2020). Few works have been reported on the
116 electrochemical methods for the determination of analyte using electrode combined with
117 several electrode modifiers such as carbon nanotube, gold and graphene (Chokkareddy et al.
118 2020; Kilele et al. 2021). Nevertheless, the materials are costly and the modification procedures
119 are not straightforward. Thus, an electrochemical approach using inexpensive and easily
120 available materials as electrode modifiers should be developed (Degefu et al. 2014).

121

122 Nowadays, screen-printed electrodes (SPEs) modified with conducting polymer have been
123 developed for various electrochemical sensing. SPE becomes the best solution owing to its
124 frugal manufacture, tiny size, able to produce on large-scale and can be applied for on-site

125 detection (Nakthong et al. 2020). Conducting polymers (CPs) become an alternative to
126 modifying the screen-printed electrodes due to their electrical conductivity, able to capture
127 analyte by chemical/physical adsorption, large surface area and making CPs are very appealing
128 materials from electrochemical perspectives (Baig et al. 2019). Such advantages of SPE
129 encourage us to construct a new electrode for electrochemical sensing, and no research reported
130 on the direct electrochemical oxidation of histamine using screen-printed electrode modified
131 by polyurethane. Therefore, this research is the first to develop a new electrode using (screen
132 printed polyurethane electrode) SPPE without any conducting materials.

133

134 The purpose of this work was to synthesize, characterize and study the conductivity of
135 polyurethane using cyclic voltammetry (CV) and differential pulse voltammetry (DPV)
136 attached to screen-printed electrode (SPE). To the best of our knowledge, this is the first
137 attempt to use a modified polyurethane electrode. The electrochemistry of polyurethane
138 mounted onto screen-printed electrode (SPE) is discussed in detail. Polyurethane is possible to
139 become an advanced frontier material is chemically modified electrodes for bio/chemical
140 sensing application.

141

142 **2. Experimental**

143 **2.1 Chemicals**

144 ***Synthesis of polyurethane film:*** Palm kernel oil (PKOp) supplied by UKM Technology Sdn
145 Bhd through MPOB/UKM station plant, Pekan Bangi Lama, Selangor and prepared using
146 Badri et al. (2000) method. 4, 4-diphenylmethane diisocyanate (MDI) was acquired from
147 Cosmopolyurethane (M) Sdn. Bhd., Klang, Malaysia. Solvents and analytical reagents were
148 benzene ($\geq 99.8\%$), toluene ($\geq 99.8\%$), hexane ($\geq 99\%$), acetone ($\geq 99\%$), tetrahydrofuran
149 (THF), dimethylformamide (DMF) ($\geq 99.8\%$), dimethylsulfoxide (DMSO) ($\geq 99.9\%$) and

150 polyethylene glycol (PED) with a molecular weight of 400 Da obtained from Sigma Aldrich
151 Sdn Bhd, Shah Alam.

152

153 **2.2 Apparatus**

154 Tensile testing was performed using a universal testing machine model Instron 5566 following
155 ASTM 638 (Standard Test Method for Tensile Properties of Plastics). The tensile properties of
156 the polyurethane film were measured at a velocity of 10 mm/min with a cell load of 5 kN.

157 The thermal properties were performed using thermogravimetry analysis (TGA) and
158 differential scanning calorimetry (DSC) analysis. TGA was performed using a thermal analyzer
159 of Perkin Elmer Pyris model with a heating rate of 10 °C/minute at a temperature range of 30
160 to 800 °C under a nitrogen gas atmosphere. The DSC analysis was performed using a thermal
161 analyzer of Perkin Elmer Pyris model with a heating rate of 10 °C /minute at a temperature
162 range of -100 to 200 °C under a nitrogen gas atmosphere. Approximately, 5-10 mg of PU was
163 weighed. The sample was heated from 25 to 150 °C for one minute, then cooled immediately
164 from 150 -100 °C for another one minute and finally, reheated to 200 °C at a rate of 10 °C /min.
165 At this point, the polyurethane encounters changes from elastic properties to brittle due to
166 changes in the movement of the polymer chains. Therefore, the temperature in the middle of
167 the inclined regions is taken as the glass transition temperature (T_g). The melting temperature
168 (T_m) is identified as the maximum endothermic peak by taking the area below the peak as the
169 enthalpy point (ΔH_m).

170

171 The morphological analysis of PU film was performed by Field Emission Scanning Electron
172 Microscope (FESEM) model Gemini SEM microscope model 500-70-22. Before the analysis
173 was carried out, the polyurethane film was coated with a thin layer of gold to increase the
174 conductivity of the film. The coating method was carried out using a sputter-coater. The

175 observations were conducted at a magnification of 200× and 5000 × with 10.00 kV (Electron
176 high tension - EHT).

177

178 The crosslinking of PU was determined using the soxhlet extraction method. About 0.60 g of
179 PU sample was weighed and put in an extractor tube containing 250 ml of toluene, used as a
180 solvent. This flow of toluene was let running for 24 hours. Mass of the PU was weighed before
181 and after the reflux process was carried out. Then, the sample was dried in the conventional
182 oven at 100 °C for 24 hours in order to get a constant mass. The percentage of crosslinking
183 content known as the gel content can be calculated using Equation (1).

$$184 \quad \text{Gel content (\%)} = \frac{W_0 - W}{W} \times 100 \% \quad (1)$$

185 W_0 is the mass of PU before the reflux process (g) and W is the mass of PU after the reflux
186 process (g).

187

188 FTIR spectroscopic analysis was performed using a Perkin-Elmer Spectrum BX instrument
189 using the Diamond Attenuation Total Reflectance (DATR) method to confirm the
190 polyurethane, PKOp and MDI functional group. FTIR spectroscopic analysis was performed
191 at a wave number of 4000 to 600 cm^{-1} to identify the peaks of the major functional groups in
192 the formation of the polymer such as amide group (-NH), urethane carbonyl group (-C = O)
193 and carbamate group (-CN).

194

195 **2.3 Synthesis of Polyurethane**

196 Palm kernel oil (PKO)p and polyethylene glycol (PEG) 400 (100:40 g/g) were combined and
197 dissolved by acetone 30% in order to form a polyol prepolymer solution. The mixture was
198 mixed using centrifuge with 100 rpm for 5 min to acquire a homogenized solution. Whereas,
199 diisocyanate prepolymer was obtained by mixing 4,4'-diphenyl-methane diisocyanate (MDI)
200 (100 g) to acetone 30%, afterward the mixture was mixed using centrifuge for 1 min to obtain

201 a homogenized solution. Then, 10 g of diisocyanate solution was poured into a container that
202 containing 10 g of a polyol prepolymer solution slowly in order to avoid an exothermic reaction
203 occur. The mixture was mixed for 30 sec until a homogenized solution acquired. Lastly, the
204 polyurethane solution was poured on the electrode surface by using casting method and dried
205 at ambient temperature for 12 hours.

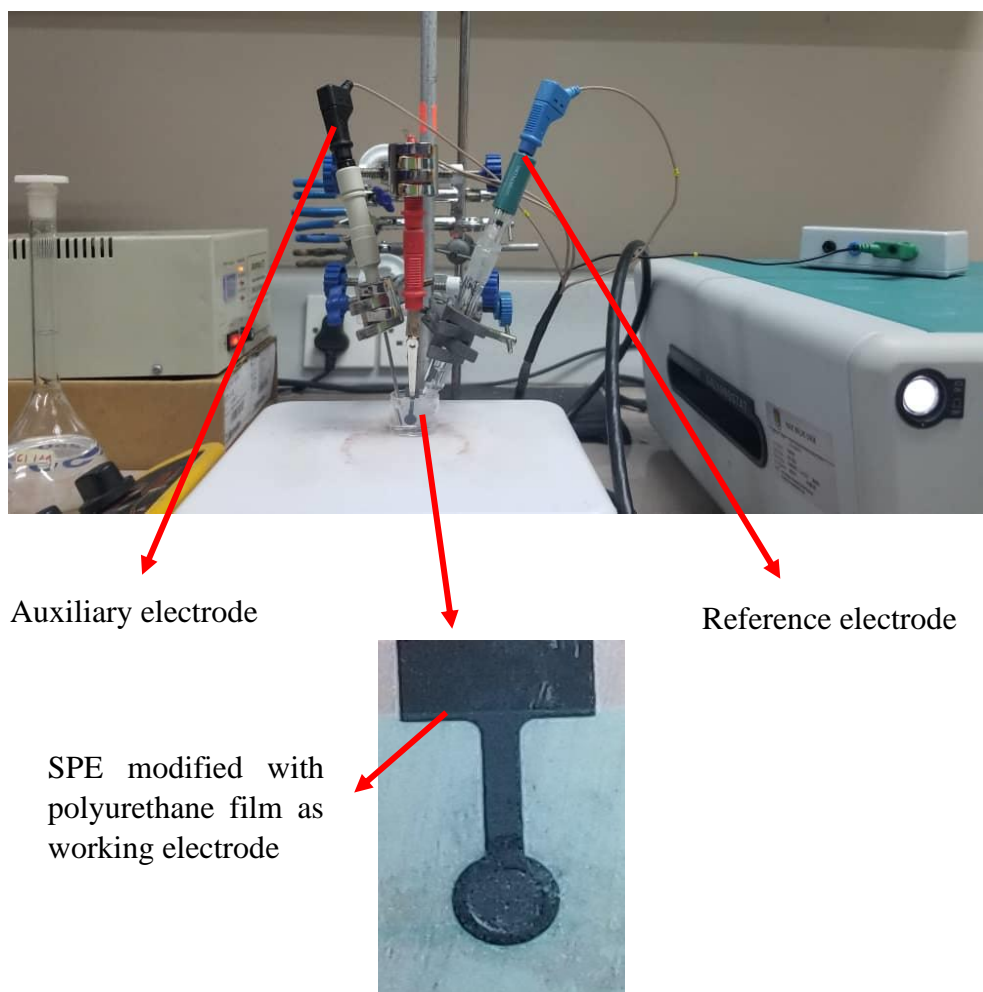
206

207 **2.4 Modification of Electrode**

208 Voltammetric tests were performed using Metrohm Autolab Software (**Figure 1**) analyzer
209 using cyclic voltammetry (CV) method or known as amperometric mode and differential pulse
210 voltammetry (DPV). All electrochemical experiments were carried out using screen-printed
211 electrode (diameter 3 mm) modified using polyurethane film as working electrode, platinum
212 wire as auxiliary electrode and Ag/AgCl electrode as a reference electrode. All experiments
213 were conducted at a temperature of $20 \pm 2^\circ\text{C}$.

214

215 The PU was cast onto the screen – printed electrode (SPE + PU) and analyzed using a single
216 voltammetric cycle between -1200 and +1500 mV (vs Ag/AgCl) of ten cycles at a scanning
217 rate of 100 mV/s in 5 ml of KCl in order to study the activity of SPE and polyurethane film.
218 Approximately (0.1, 0.3 & 0.5) mg of palm-based prepolyurethane was dropped separately
219 onto the surface of the SPE and dried at room temperature. The modified palm-based
220 polyurethane electrodes were then rinsed with deionized water to remove physically adsorbed
221 impurities and residues of unreacted material on the electrode surface. All electrochemical
222 materials and calibration measurements were carried out in a 5 mL glass beaker with a
223 configuration of three electrodes inside it. Platinum wire and silver/silver chloride (Ag/AgCl)
224 electrodes were used as auxiliary and reference electrodes, while screen-printed electrode that
225 had been modified with polyurethane was applied as a working electrode.



226 **Figure 1.** Potentiostat instrument to study the conductivity of SPE modified with
 227 polyurethane film using cyclic voltammetry (CV) and differential pulse voltammetry (DPV)

228

229 3. Results and Discussion

230 The synthesis of PU films was carried out using pre-polymerization method which involves
 231 the formation of urethane polymer at an early stage. The reaction took place between palm
 232 kernel oil-based polyol (PKOp) and diisocyanate (MDI). **Table 1** presents the PKO-p
 233 properties used in this study. The structural chain was extended with the aid of polyethylene
 234 glycol (PEG) to form flexible and elastic polyurethane film. In order to form the urethane
 235 prepolymer, one of the isocyanate groups (NCO) reacts with one hydroxyl group (OH) of
 236 polyol while the other isocyanate group attacks another hydroxyl group in the polyol (Wong &
 237 Badri 2012) as shown in **Figure 2**.

238 **Table 1** The specification of PKO-p (Badri et al. (2000)).

| Property | Values |
|------------------------------|-----------|
| Viscosity at 25°C (cps) | 1313.3 |
| Specific gravity (g/mL) | 1.114 |
| Moisture content (%) | 0.09 |
| pH value | 10 – 11 |
| The hydroxyl number mg KOH/g | 450 - 470 |

239

240

241 a. FTIR analysis

242 **Figure 3** shows the FTIR spectrum for polyurethane, exhibiting the important functional group
 243 peaks. According to a study researched by Wong & Badri 2012, PKO-p reacts with MDI to
 244 form urethane prepolymers. The NCO group on MDI reacts with the OH group on polyol
 245 whether PKOp or PEG. It can be seen there are no important peaks of MDI in the FTIR
 246 spectrums. This is further verified by the absence of peak at the 2400 cm⁻¹ belongs to MDI (-
 247 NCO groups). This could also confirm that the NCO group on MDI had completely reacted
 248 with PKO-p to form the urethane –NHC (O) backbone. The presence of amides (-NH),
 249 carbonyl urethane group (-C = O), carbamate group (C-NH) and -C-O-C confirmed the
 250 formation of urethane chains. In this study, the peak of carbonyl urethane (C = O) detected at
 251 1727 cm⁻¹ indicated that the carbonyl urethane group was bonded without hydrogen owing to
 252 the hydrogen reacted with the carbonyl urethane group.

253

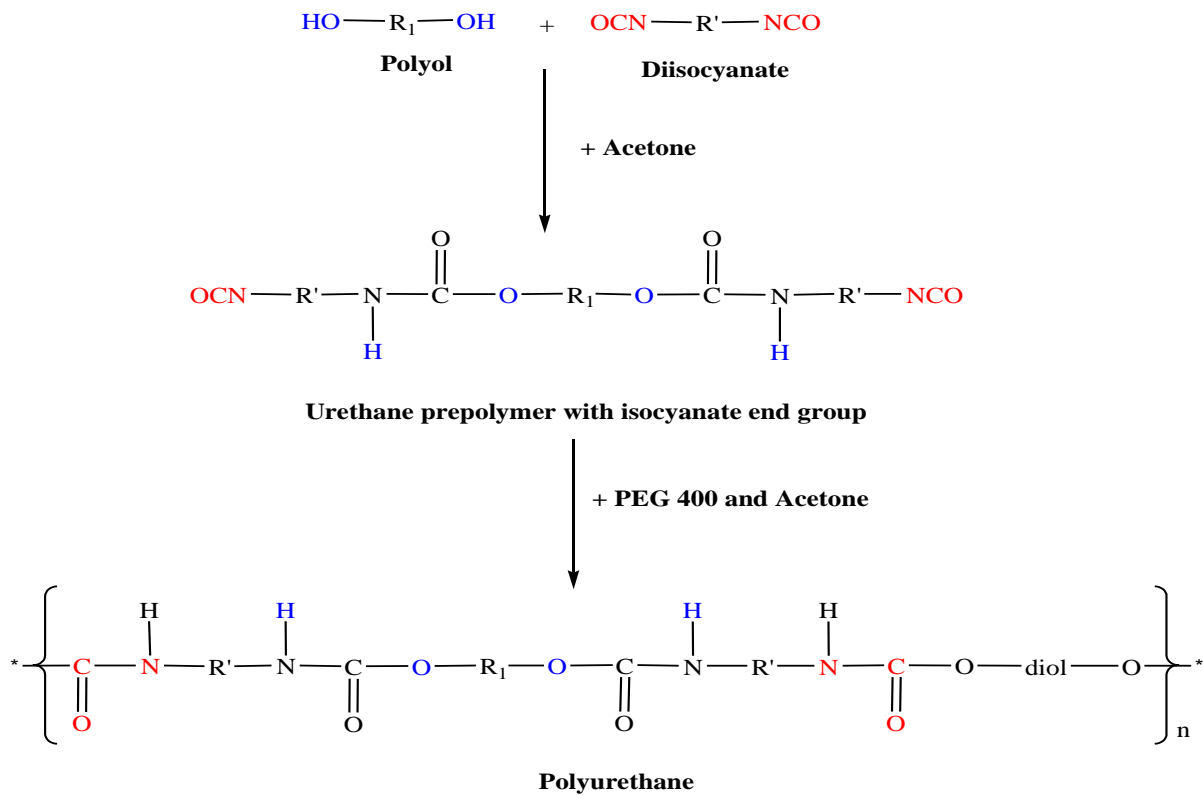
254 The reaction of polyurethane has been studied by Hamuzan & Badri (2016) where the urethane
 255 carbonyl group was detected at 1730 – 1735 cm⁻¹ while the MDI carbonyl was detected at 2400
 256 cm⁻¹. The absence of peaks at 2250 – 2270 cm⁻¹ indicates the absence of NCO groups. It shows

257 that the polymerization reaction occurs entirely between NCO groups in MDI with hydroxyl
258 groups on polyols and PEG (Mishra et al. 2012). The absence of peaks at 1690 cm^{-1}
259 representing urea ($\text{C} = \text{O}$) in this study indicated, there is no urea formation as a byproduct
260 (Clemitson 2008) of the polymerization reaction that possibly occurs due to the excessive
261 water. For the amine (NH) group, hydrogen-bond to NH and oxygen to form ether and
262 hydrogen bond to NH and oxygen to form carbonyl on urethane can be detected at the peak of
263 3301 cm^{-1} and in the wavenumber at range $3326 - 3428\text{ cm}^{-1}$. This has also been studied and
264 detected by Lampman et. al. (2010) and Mutsuhisa et al. (2007). In this study, the hydrogen
265 bond formed by $\text{C} = \text{O}$ acts as a proton acceptor whereas NH acts as a proton donor. The
266 urethane group in the hard segment (MDI) has electrostatic forces on the oxygen, hydrogen
267 and nitrogen atoms and these charged atoms form dipoles that attract other opposite atoms.
268 These properties make isocyanates are highly reactive and having different properties (Leykin
269 et al. 2016).

270

271 MDI was one of the isocyanates used in this study, has an aromatic group and is more
272 reactive compared to aliphatic group isocyanates such as hexamethylene diisocyanate (HDI)
273 or isophorone diisocyanate (IPDI). Isocyanates have two groups of isocyanates on each
274 molecule. Diphenylmethane diisocyanate is an exception owing to its structure consists of two,
275 three, four or more isocyanate groups (Nohra et al. 2013). The use of PEG 400 in this study as
276 a chain extender for polyurethane increases the chain mobility of polyurethane at an optimal
277 amount. The properties of a polyurethane are contributed by hard and soft copolymer segments
278 of both polyol monomers and MDI. This makes the hard segment of urethane serves as a
279 crosslinking site between the soft segments of the polyol (Leykin et al. 2016).

280



281

282 **Figure 2.** The chemical route of producing polyurethane via pre-polymerization method

283

(Wong & Badri 2012).

284

285 The mechanism of the pre-polymerization in urethane chains formation is a

286 nucleophilic substitution reaction as studied by Yong et al. (2009). However, this study found

287 amines as nucleophiles. Amine attacks carbonyl on isocyanate in MDI in order to form two

288 resonance structures of intermediate complexes A and B. Intermediate complex B has a greater

289 tendency to react with polyols due to stronger carbonyl (C = O) bonds than C = N bonds on

290 intermediate complexes A. Thus, intermediate complex B is more stable than intermediate

291 complex A, as suggested by previous researchers who have conducted by Wong and Badri

292 (2012). Moreover, nitrogen was more electropositive than oxygen, therefore, -CN bonds were

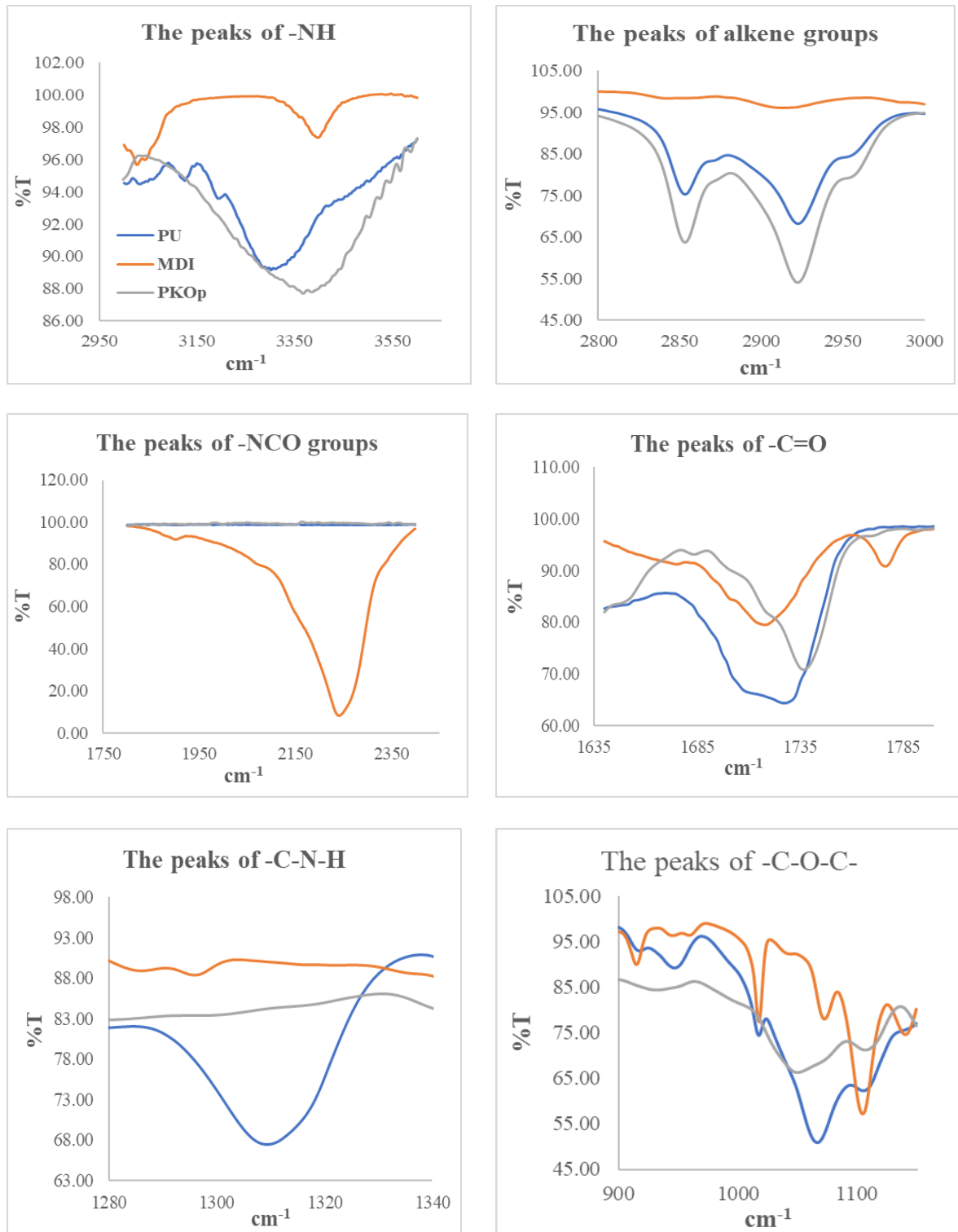
293 more attracted to cations (H⁺) than -CO. The combination between long polymer chain and

294 low cross-linking content gives the polymer elastic properties whereas short chain and high

295 cross linking producing hard and rigid polymers. Cross-linking in polymers consists of three-

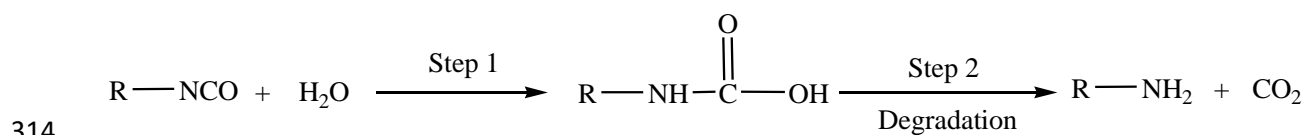
296 dimensional networks with high molecular weight. In some aspects, polyurethane can be a
297 macromolecule, a giant molecule (Petrovic 2008).

298



299 **Figure 3.** FTIR spectrums of several important peaks between polyurethane, PKO-p and MDI

300 However, the reaction between MDI and PEG as a chain extender where oxygen on the
 301 nucleophile PEG attacks the NCO group in the MDI to form two intermediate complexes A
 302 and B can occur. Nevertheless, nucleophilic substitution reactions have a greater tendency to
 303 occur in PKOp compared to PEG because the presence of nitrogen atoms is more
 304 electropositive than oxygen atoms in PEG. Amine has a higher probability of reacting
 305 compared to hydroxyl (Herrington & Hock 1997). Amine with high alkalinity reacts with
 306 carbon atoms on MDI as proposed by Wong and Badri (2012). PKOp contains long carbon
 307 chains that can easily stabilize alkyl ions when intermediate complexes are formed. Therefore,
 308 the polyol is more reactive than PEG to react with MDI. However, the addition of PEG will
 309 increase the length of the polyurethane chain and prevent side effects such as the formation of
 310 urea by-products of the NCO group reaction in urethane pre-polymer and water molecules from
 311 the environment. If the NCO group reacts with the excess water in the environment, the
 312 formation of urea and carbon dioxide gas will also occur excessively (**Figure 4**). This reaction
 313 can cause a polyurethane foam, not polyurethane film as we studied the film.



315 **Figure 4.** The reaction between NCO group and water producing carbon dioxide

316

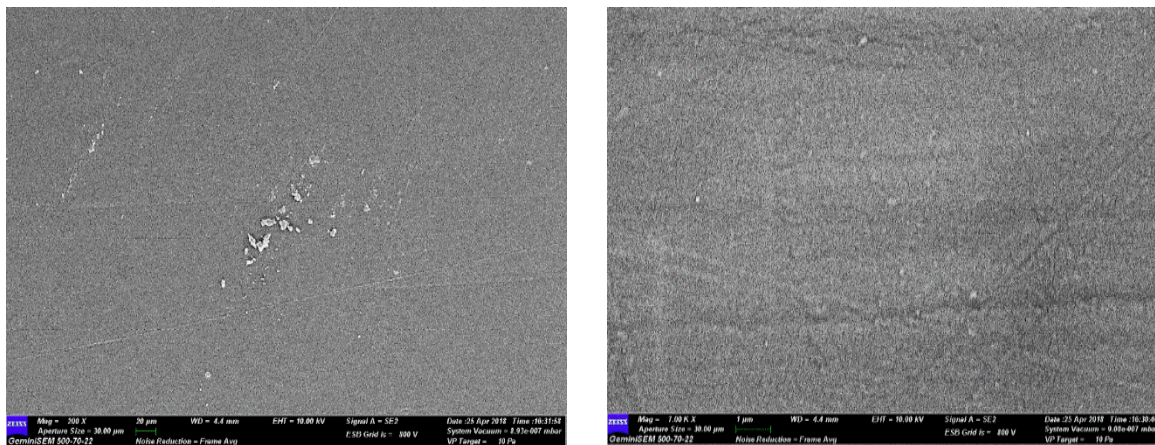
317 Furthermore, the application of PEG can influence the conductivity of PU where
 318 Porcarelli et al. (2017) have reported the application of PEG using several molecular weights.
 319 PEG 1500 decreased the conductivity of PU in consequence of the semicrystalline phase of
 320 PEG 1500 that acted as a poor ion conducting phase for PU. It is also well known that PEG
 321 with a molecular weight of more than 1000 g·mol⁻¹ tends to crystallize with deleterious effects
 322 on room temperature ionic conductivity (Porcarelli et al. 2017).

323

324 b. Morphological analysis

325 The Field Emission Scanning Electron Microscope (FESEM) micrograph in **Figure 5** shows
326 the formation of a uniform polymer film contributed by the polymerization method applied.
327 The magnification used for this surface analysis ranged from 200 to 5000 \times . The
328 polymerization method can also avoid the failure of the reaction in PU polymerization.
329 Furthermore, no trace of separation was detected by FESEM. This has also been justified by
330 the wavelengths obtained by the FTIR spectrums above.

331



332 **Figure 5.** The micrograph of polyurethane films analysed by FESEM at (a) 200 \times and (b)
333 5000 \times magnifications.

334 c. The crosslinking analysis

336 Soxhlet analysis was applied to determine the degree of crosslinking between the hard
337 segments and the soft segments in the polyurethane. The urethane group on the hard segment
338 along the polyurethane chain is polar (Cuve & Pascault 1991). Therefore, during the testing, it
339 was very difficult to dissolve in toluene, as the testing reagent. The degree of crosslinking is
340 determined by the percentage of the gel content. The analysis result obtained from the Soxhlet
341 testing indicating a 99.3 % gel content. This is significant in getting a stable polymer at higher
342 working temperature (Rogulska et al. 2007).

343

$$\text{Gel content (\%)} = \frac{(0.6 - 0.301) \text{ g}}{0.301 \text{ g}} \times 100\% = 99.33\%$$

344

345

346 d. The thermal analysis

347 Thermogravimetric analysis (TGA) can be used to observe the material mass based on

348 temperature shift. It can also examine and estimate the thermal stability and materials

349 properties such as the alteration weight owing to absorption or desorption, decomposition,

350 reduction and oxidation. The material composition of polymer is specified by analysing the

351 temperatures and the heights of the individual mass steps (Alamawi et al. 2019). **Figure 6**

352 shows the TGA and DTG thermograms of polyurethane. The percentage weight loss (%) is

353 listed in **Table 2**. Generally, only a small amount of weight was observed. It is shown in **Figure**

354 **6** in the region of 45 – 180°C. This is due to the presence of condensation on moisture and

355 solvent residues.

356

357 **Table2** Weight loss percentage of (wt%) polyurethane film

| Sample | % Weight loss (wt%) | | | | Total of weight loss (%) | Residue after 550°C (%) |
|--------------|--------------------------|----------------------------------|----------------------------------|----------------------------------|--------------------------------|----------------------------|
| | T _{max} , °C | T _{d1} , 200 – 290°C | T _{d2} , 350 – 500°C | T _{d3} , 500 – 550°C | | |
| Polyurethane | 240 | 8.04 | 39.29 | 34.37 | 81.7 | 18.3 |

358

359 The bio polyurethane is thermally stable up to 240 °C before it has undergone thermal

360 degradation (Agrawal et al. 2017). The first stage of thermal degradation (T_{d1}) on polyurethane

361 films was shown in the region of 200 – 290 °C as shown in **Figure 6**. The T_{d1} is associated with

362 degradation of the hard segments of the urethane bond, forming alcohol or degradation of the

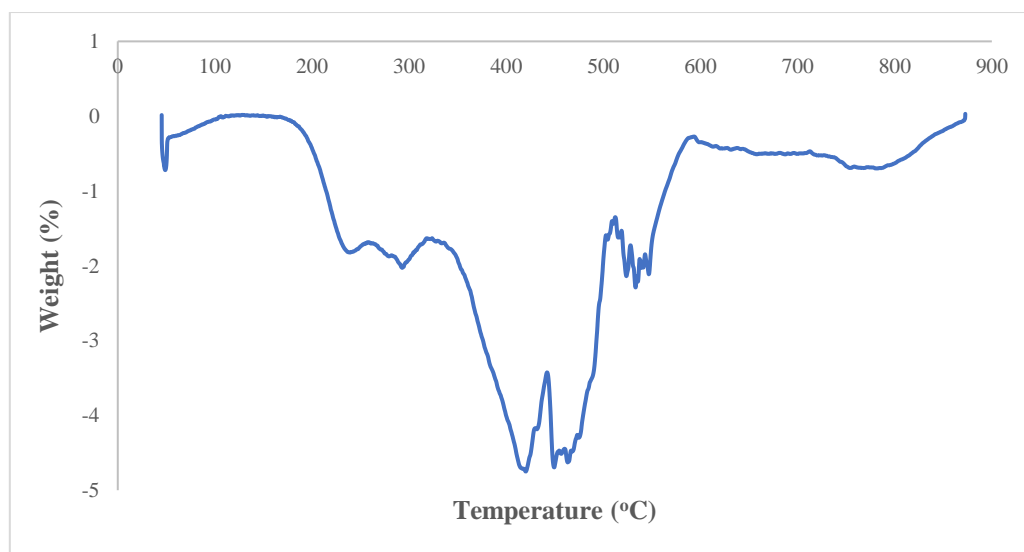
363 polyol chains and releasing of isocyanates (Berta et al. 2006), primary and secondary amines

364 as well as carbon dioxide (Corcuera et al. 2011; Pan & Webster 2012). Meanwhile, the second

365 thermal degradation stage (T_{d2}) of polyurethane films experienced a weight loss of 39.29 %.
366 This endotherm of T_{d2} is related to the dimerization of isocyanates to form carbodiimides and
367 release CO_2 . The formed carbodiimide reacts with alcohol to form urea. The third stage of
368 thermal degradation (T_{d3}) is related to the degradation of urea (Berta et al. 2006) and the soft
369 segment on polyurethane.

370

371 Generally, DSC analysis exhibited thermal transitions as well as the initial
372 crystallisation and melting temperatures of the polyurethane (Khairuddin et al. 2018). It serves
373 to analyse changes in thermal behavior due to changes occurring in the chemical chain structure
374 based on the glass transition temperature (T_g) of the sample obtained from the DSC thermogram
375 (**Figure 7**). DSC analysis on polyurethane film was performed in the temperature at the range
376 100 °C to 200 °C using nitrogen gas as a blanket as proposed by Furtwengler et al. (2017). The
377 glass transition temperature (T_g) on polyurethane was above room temperature, at 78.1 °C
378 indicated the state of glass on polyurethane. The presence of MDI contributes to the formation
379 of hard segments in polyurethanes. Porcarelli et al. (2017) stated that possess a low glass
380 transition (T_g) may contribute to PU conductivity.

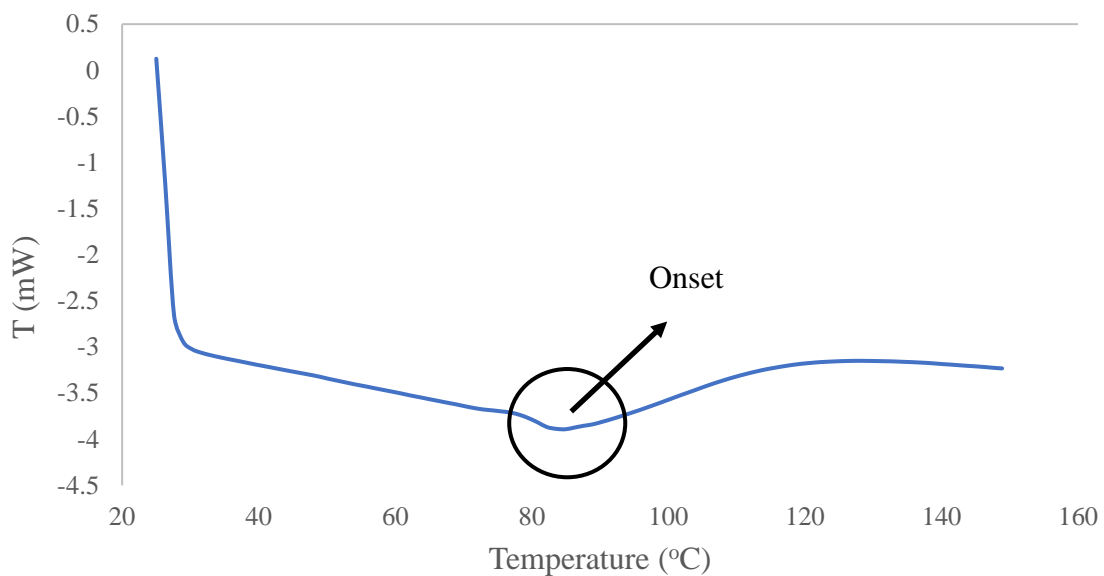


381

382

Figure 6. DTG thermogram of polyurethane film

383 During polymerization, this hard segment restricts the mobility of the polymer chain
384 (Ren et al. 2013) owing to the steric effect on the benzene ring in the hard segment. The
385 endothermic peak of acetone used as the solvent in this study was supposedly at 56°C.
386 However, it was detected in the DSC thermogram nor the TGA thermogram, which indicates
387 that acetone was removed from the polyurethane during the synthesis process, owing to its
388 volatility nature. The presence of acetone in the synthesis was to lower the reaction kinetics.



389 **Figure 7.** DSC thermogram of polyurethane film

390
391
392
393 e. The solubility and mechanical properties of the polyurethane film

394 The chemical resistivity of a polymer will be the determinant in performing as a conductor.
395 Thus, its solubility in various solvents was determined by dissolving the polymer in selected
396 solvents such as hexane, benzene, acetone, tetrahydrofuran (THF), dimethylformamide (DMF)
397 and dimethylformamide (DMSO). On the other hand, the mechanical properties of of
398 polyurethane were determined based on the standard testing following ASTM D 638 (Standard
399 Test Method for Tensile Properties of Plastics). The results from the polyurethane film
400 solubility and tensile test are shown in **Table 3**. Polyurethane films were insoluble with

401 benzene, hexane and acetone and are only slightly soluble in tetrahydrofuran (THF),
 402 dimethylformamide (DMF) and dimethylformamide (DMSO) solutions. While the tensile
 403 strength of a PU film indicated how much elongation load the film was capable of withstanding
 404 the material before breaking.

405

406 **Table 3** The solubility and mechanical properties of the polyurethane film

407

| Parameters | Polyurethane film | |
|----------------------------|-------------------|--------------|
| Solubility | Benzene | Insoluble |
| | Hexane | Insoluble |
| | Acetone | Insoluble |
| | THF | Less soluble |
| | DMF | Less soluble |
| | DMSO | Less soluble |
| Stress (MPa) | 8.53 | |
| Elongation percentage (%) | 43.34 | |
| Strain modulus (100) (MPa) | 222.10 | |

408

409 The tensile stress, strain and modulus of polyurethane film also indicated that polyurethane has
 410 good mechanical properties that are capable of being a supporting substrate for the next stage
 411 of study. In the production of polyurethane, the properties of a polyurethane are easily
 412 influenced by the content of MDI and polyol used. The length of the chain and its flexibility
 413 are contributed by the polyol which makes it elastic. High crosslinking content can also produce
 414 hard and rigid polymers. MDI is a major component in the formation of hard segments in
 415 polyurethane. It is this hard segment that determines the rigidity of the PU. Therefore, high

416 isocyanate content results in higher rigidity on PU (Petrovic et al. 2002). Thus, the polymer has
417 a higher resistance to deformation and more stress can be applied to the PU.

418

419 f. The conductivity of the polyurethane as a polymeric film on SPE

420 Polyurethane film deposited onto the screen-printed electrode by casting method as shown in

421 **Figure 1**. After that, the modified electrode was analysed using cyclic voltammetry (CV) and

422 differential pulse voltammetry (DPV) in order to study the behaviour of modified electrode.

423 The modified electrode was tested in a 0.1 mmol/L KCl solution containing 5 mmol/L (K_3Fe

424 $(CN)_6$). The use of potassium ferricyanide is intended to increase the sensitivity of the KCl

425 solution. The conductivity of the modified electrode was studied. The electrode was analyzed

426 by cyclic voltammetry method with a potential range of -1.00 to +1.00 with a scan rate of 0.05

427 V/s. The voltammograms at electrode have shown a specific redox reaction. Furthermore, the

428 conductivity of the modified electrode is lower due to the use of polyurethane. This occurs due

429 to PU is a natural polymer produced from the polyol of palm kernel oil. The electrochemical

430 signal at the electrode is low if there is a decrease in electrochemical conductivity (El - Raheem

431 et al. 2020). It can be concluded that polyurethane is a bio-polymer with a low conductivity

432 value. The current of the modified electrode was found at 5.3×10^{-5} A or 53 μ A. Nevertheless,

433 the electroconductivity of PU in this study shows better conductivity several times compared

434 to Bahrami et al. (2019) that reported the conductivity of PU as 1.26×10^{-6} A, whereas Li et al.

435 (2019) reported the PU conductivity in their study was even very low, namely 10^{-14} A. The

436 conductivity of PU owing to the benzene ring in the hard segment (MDI) could exhibit the

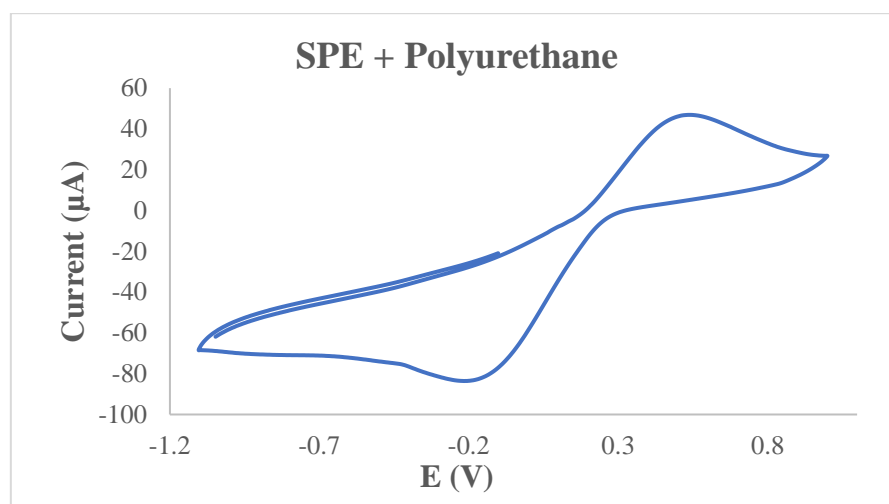
437 conductivity by inducing electron delocalization along the polyurethane chain (Wong et al.

438 2014). The conductivity of PU can also be caused by PEG. The application of PEG as polyol

439 has been studied by Porcarelli et al. (2017), that reported that the conductivity of PU based on

440 PEG – polyol was 9.2×10^{-8} .

441 According to **Figure 8**, it can be concluded that the anodic peak present in the modified
442 electrode was at +0.5 V, it also represented the oxidation process of the modified electrode.
443 The first oxidation scan on both electrodes ranged from -0.2 to +1.0 V, which showed a
444 significant anodic peak at a potential of +0.5 V.
445



446
447 **Figure 8.** The voltammogram of SPE – PU modified electrode after analysed using cyclic
448 voltammetry (CV) technique

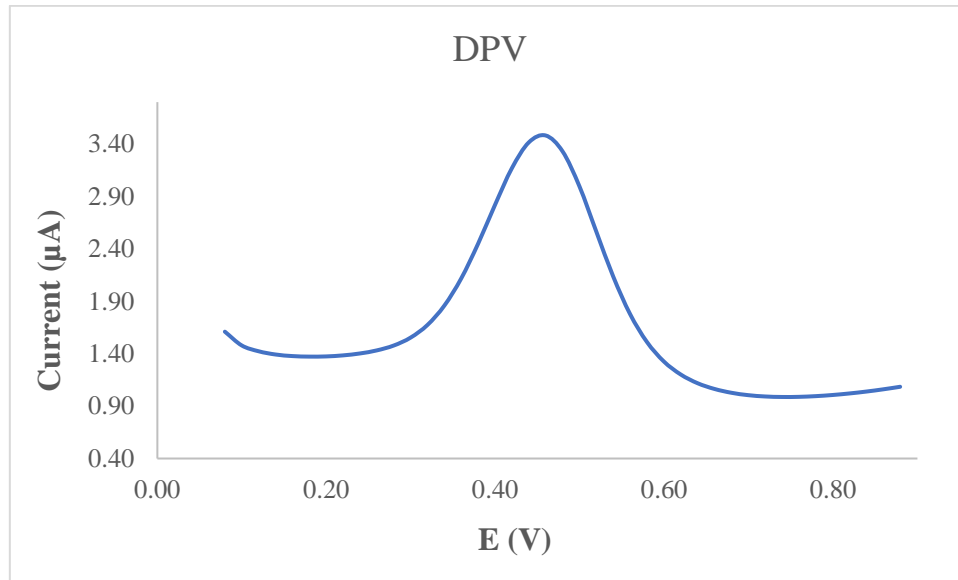
449
450 **Figure 9** also presents the DPV voltammogram of modified electrode. DPV is a measurement
451 based on the difference in potential pulses that produce an electric current. Scanning the
452 capability pulses to the working electrode will produce different currents. Optimal peak
453 currents will be produced to the reduction capacity of the redox material. The peak current
454 produced is proportional to the concentration of the redox substance and can be detected up to
455 concentration below 10^{-8} M. DPV was conducted to obtain the current value that more accurate
456 than CV (Lee et al. 2018).

457
458 This study used a redox pair ($K_3Fe(CN)_6$) as a test device (probe). The currents generated by
459 SPE-PU and proved by CV and DPV have shown conductivity on polyurethane films. This
460 suggests that polyurethane films can conduct electron transfer. The electrochemical area on the

461 modified electrode can be calculated using the formula from Randles-Sevcik (Butwong et al.
 462 2019), where the electrochemical area for SPE-PU is considered to be A, using Equation 2:

463 **Current of SPE-PU , $I_p = 2.65 \times 10^5 n^{3/2} A v^{1/2} C D^{1/2}$** (2)

464



465

466 **Figure 9.** The voltammogram of SPE – PU modified electrode after analyzed using
 467 differential pulse voltammetry (DPV) technique

468

469 Where, $n - 1$ is the amount of electron transfer involved, while C is the solvent concentration
 470 used (mmol/L) and the value of D is the diffusion constant of 5 mmol/L at $(K_3Fe(CN)_6)$
 471 dissolved using 0.1 mmol/L KCl. The estimated surface area of the electrode (**Figure 1**) was
 472 0.2 cm^2 where the length and width of the electrode used during the study was $0.44 \text{ cm} \times 0.44$
 473 cm while the surface area of the modified electrode was 0.25 cm^2 with the length and width of
 474 the electrode estimated at $0.5 \text{ cm} \times 0.5 \text{ cm}$, and causing the modified electrode has a larger
 475 surface. The corresponding surface concentration (τ) (mol/cm^2) is calculated using Equation 3.

476

$$I_p = (n^2 F^2 / 4RT) A \tau v \quad (3)$$

477

478 I_p is the peak current (A), while A is the surface area of the electrode (cm^2), the value of v is
 479 the applied scan rate (mV/s) and F is the Faraday constant (96,584 C/mol), R is the constant
 ideal gas (8.314 J/mol K) and T is the temperature used during the experiment being conducted

480 (298 K) (Koita et al. 2014). The development of conducting polymer from palm oil-based
481 biomaterials seems to be one of the potential future applications of palm oil products, as this
482 novel material has the potential to contribute positively to the analytical industry. Likewise,
483 other palm oil-based products, such as refined-bleached-deodorised (RBD) palm oil, palm oil,
484 and palm stearin are abundantly available in Malaysia. They are known to be economical,
485 sustainable, and environmentally biodegradable. These palm oil-based products are promising
486 prospects for manufacturing biomaterials that become alternative products to other polymers
487 from synthetic/chemical-based (Tajao et al. 2021). Several studies have been reported the
488 application of PU to produce elastic conductive fibres and films owing to it is highly elastic,
489 scratch resistant and adhesive (Tadese et al. 2019), thus it is easy for PU to adhere on the
490 screen-printed electrode in order to modify the electrode. PU is also being used as a composite
491 material to make elastic conducting composite films (Khatoon & Ahmad 2017).

492

493 **4. Conclusion**

494 Polyurethane film was prepared by pre-polymerization between palm kernel oil-based polyol
495 (PKO-p) with MDI. The presence of PEG 400 as the chain extender formed freestanding
496 flexible film. Acetone was used as the solvent to lower the reaction kinetics since the pre-
497 polymerization was carried out at room temperature. The formation of urethane links (NHCO
498 – backbone) after polymerization was confirmed by the absence of N=C=O peak at 2241 cm^{-1}
499 and the presence of N-H peak at 3300 cm^{-1} , carbonyl (C=O) at 1710 cm^{-1} , carbamate (C-N) at
500 1600 cm^{-1} , ether (C-O-C) at 1065 cm^{-1} , benzene ring (C = C) at 1535 cm^{-1} in the bio
501 polyurethane chain structure. Soxhlet analysis for the determination of crosslinking on
502 polyurethane films has yielded a high percentage of 99.33 %. This is contributed by the hard
503 segments formed from the reaction between isocyanates and hydroxyl groups causing
504 elongation of polymer chains. FESEM analysis exhibited an absence of phase separation and

505 smooth surface. Meanwhile, the current of modified electrode was found at 5.2×10^{-5} A. This
506 bio polyurethane film can be used as a conducting bio-polymer and it is very useful for other
507 studies such as electrochemical sensor purposes. Furthermore, advanced technologies are
508 promising and the future of bio-based polyol looks very bright.

509

510 **5. Acknowledgment**

511 The authors would like to thank Universitas Alma Ata for the sponsorship given to the first
512 author. We would like to also, thank The Department of Chemical Sciences, Universiti
513 Kebangsaan Malaysia for the laboratory facilities and CRIM, UKM for the analysis
514 infrastructure.

515

516 **6. Conflict of Interest**

517 The authors declare no conflict of interest.

518

519 **7. References**

- 520 Agrawal, A., Kaur, R., Walia, R. S. (2017). PU foam derived from renewable sources:
521 Perspective on properties enhancement: An overview. *European Polymer Journal*. 95:
522 255 – 274.
- 523 Akindoyo, J. O., Beg, M.D.H., Ghazali, S., Islam, M.R., Jeyaratnam, N. & Yuvaraj, A.R.
524 (2016). Polyurethane types, synthesis and applications – a review. *RSC Advances*. 6:
525 114453 – 114482.
- 526 Alamawi, M. Y., Khairuddin, F. H., Yusoff, N. I. M., Badri, K., Ceylan, H. (2019).
527 Investigation on physical, thermal and chemical properties of palm kernel oil polyol bio
528 – based binder as a replacement for bituminous binder. *Construction and Building*
529 *Materials*. 204: 122 – 131.

530 Alqarni, S. A., Hussein, M. A., Ganash, A. A. & Khan, A. (2020). Composite material – based
531 conducting polymers for electrochemical sensor applications: a mini review.
532 *BioNanoScience*. **10**: 351 – 364.

533 Badan, A., Majka, T. M. (2017). The influence of vegetable – oil based polyols on physico –
534 mechanical and thermal properties of polyurethane foams. *Proceedings*. 1 – 7.

535 Badri, K.H. (2012) Biobased polyurethane from palm kernel oil-based polyol. In Polyurethane;
536 Zafar, F., Sharmin, E., Eds. InTechOpen: Rijeka, Croatia. pp. 447–470.

537 Badri, K.H., Ahmad, S.H. & Zakaria, S. 2000. Production of a high-functionality RBD palm
538 kernel oil – based polyester polyol. *Journal of Applied Polymer Science* 81(2): 384 –
539 389.

540 Baig, N., Sajid, M. and Saleh, T. A. 2019. Recent trends in nanomaterial – modified electrodes
541 for electroanalytical applications. *Trends in Analytical Chemistry*. 111: 47 – 61.

542 Berta, M., Lindsay, C., Pans, G., & Camino, G. (2006). Effect of chemical structure on
543 combustion and thermal behaviour of polyurethane elastomer layered silicate
544 nanocomposites. *Polymer Degradation and Stability*. **91**: 1179-1191.

545 Borowicz, M., Sadowska, J. P., Lubczak, J. & Czuprynski, B. (2019). Biodegradable, flame –
546 retardant, and bio – based rigid polyurethane/polyisocyanurate foams for thermal
547 insulation application. *Polymers*. 11: 1816 – 1839.

548 Butwong, N., Khajonklin, J., Thongbor, A. & Luong, J.H.T. (2019). Electrochemical sensing
549 of histamine using a glassy carbon electrode modified with multiwalled carbon nanotubes
550 decorated with Ag – Ag₂O nanoparticles. *Microchimica Acta*. **186** (11): 1 – 10.

551 Chokkareddy, R., Thondavada, N., Kabane, B. & Redhi, G. G. (2020). A novel ionic liquid
552 based electrochemical sensor for detection of pyrazinamide. *Journal of the Iranian*
553 *Chemical Society*. 18: 621 – 629.

554 Chokkareddy, R., Kanchi, S. & Inamuddin (2020). Simultaneous detection of ethambutol and
555 pyrazinamide with IL@CoFe₂O₄NPs@MWCNTs fabricated glassy carbon electrode.
556 *Scientific Reports*. 10: 13563.

557 Clemitson, I. (2008). Castable Polyurethane Elastomers. Taylor & Francis Group, New York.
558 doi:10.1201/9781420065770.

559 Corcuera, M.A., Rueda, L., Saralegui, A., Martin, M.D., Fernandez-d'Arlas, B., Mondragon,
560 I. & Eceiza, A. (2011). Effect of diisocyanate structure on the properties and
561 microstructure of polyurethanes based on polyols derived from renewable resources.
562 *Journal of Applied Polymer Science*. **122**: 3677-3685.

563 Cuve, L. & Pascault, J.P. (1991). Synthesis and properties of polyurethanes based on
564 polyolefine: Rigid polyurethanes and amorphous segmented polyurethanes prepared in
565 polar solvents under homogeneous conditions. *Polymer*. **32** (2): 343- 352.

566 Degefu, H., Amare, M., Tessema, M. & Admassie, S. (2014). Lignin modified glassy carbon
567 electrode for the electrochemical determination of histamine in human urine and wine
568 samples. *Electrochimica Acta*. 121: 307 – 314.

569 Dzulkipli, M. Z., Karim, J., Ahmad, A., Dzulkurnain, N. A., Su'ait, M S., Fujita, M. Y., Khoon,
570 L. T. & Hassan, N. H. (2021). The influences of 1-butyl-3-methylimidazolium
571 tetrafluoroborate on electrochemical, thermal and structural studies as ionic liquid gel
572 polymer electrolyte. *Polymers*. 13 (8): 1277 – 1294.

573 El-Raheem, H.A., Hassan, R.Y.A., Khaled, R., Farghali, A. & El-Sherbiny, I.M. (2020).
574 Polyurethane – doped platinum nanoparticles modified carbon paste electrode for the
575 sensitive and selective voltammetric determination of free copper ions in biological
576 samples. *Microchemical Journal*. **155**: 104765.

577 Fei, T., Li, Y., Liu, B. & Xia, C. (2019). Flexible polyurethane/boron nitride composites with
578 enhanced thermal conductivity. *High Performance Polymers*. **32** (3): 1 – 10.

579 Furtwengler, P., Perrin R., Redl, A. & Averous, L. (2017). Synthesis and characterization of
580 polyurethane foams derived of fully renewable polyesters polyols from sorbitol.
581 *European Polymer Journal*. **97**: 319 – 327.

582 Ghosh, S., Ganguly, S., Remanan, S., Mondal, S., Jana, S., Maji, P. K., Singha, N., Das, N. C.
583 (2018). Ultra – light weight, water durable and flexible highly electrical conductive
584 polyurethane foam for superior electromagnetic interference shielding materials. *Journal*
585 *of Materials Science: Materials in Electronics*. 29: 10177 – 10189.

586 Guo, S., Zhang, C., Yang, M., Zhou, Y., Bi, C., Lv, Q. & Ma, N. (2020). A facile and sensitive
587 electrochemical sensor for non – enzymatic glucose detection based on three –
588 dimensional flexible polyurethane sponge decorated with nickel hydroxide. *Analytica*
589 *Chimica Acta*. **1109**: 130 – 139.

590 Hamuzan, H.A. & Badri, K.H. (2016). The role of isocyanates in determining the viscoelastic
591 properties of polyurethane. AIP Conference Proceedings. 1784, Issue 1.

592 Herrington, R. & Hock, K. (1997). Flexible polyurethane foams. 2nd Edition. Dow Chemical
593 Company. Midlan.

594 Janpoung, P., Pattanauwat, P. & Potiyaraj, P. (2020). Improvement of electrical conductivity
595 of polyurethane/polypyrrole blends by graphene. *Key Engineering Materials*. **831**: 122 –
596 126.

597 Khairuddin, F.H., Yusof, N. I. M., Badri, K., Ceylan, H., Tawil, S. N. M. (2018). Thermal,
598 chemical and imaging analysis of polyurethane/cecabase modified bitumen. *IOP Conf.*
599 *Series: Materials Science and Engineering*. 512: 012032.

600 Khatoon, H., Ahmad, S. (2017). A review on conducting polymer reinforced polyurethane
601 composites. *Journal of Industrial and Engineering Chemistry*. 53: 1 – 22.

602 Kilele, J. C., Chokkareddy, R., Rono, N. & Redhi, G. G. (2020). A novel electrochemical
603 sensor for selective determination of theophylline in pharmaceutical formulations.
604 *Journal of the Taiwan Institute of Chemical Engineers*. 1 – 11.

605 Kilele, J. C., Chokkareddy, R. & Redhi, G. G. (2021). Ultra – sensitive electrochemical sensor
606 for fenitrothion pesticide residues in fruit samples using IL@CoFe₂ONPs@MWCNTs
607 nanocomposite. *Microchemical Journal*. 164: 106012.

608 Koita, D., Tzedakis, T., Kane, C., Diaw, M., Sock, O. & Lavedan, P. (2014). Study of the
609 histamine electrochemical oxidation catalyzed by nickel sulfate. *Electroanalysis*. **26 (10)**:
610 2224 – 2236.

611 Kotal, M., Srivastava, S.K. & Paramanik, B. (2011). Enhancements in conductivity and thermal
612 stabilities of polyurethane/polypyrrole nanoblends. *The Journal of Physical Chemistry*
613 *C*. **115 (5)**: 1496 – 1505.

614 Ladan, M., Basirun, W.J., Kazi, S.N., Rahman, F.A. (2017). Corrosion protection of AISI 1018
615 steel using Co – doped TiO₂/polypyrrole nanocomposites in 3.5% NaCl solution.
616 *Materials Chemistry and Physics*. **192**: 361 – 373.

617 Lampman, G.M., Pavia, D.L., Kriz, G.S. & Vyvyan, J.R. (2010). Spectroscopy. 4th Edition.
618 Brooks/Cole Cengage Learning, Belmont, USA.

619 Lee, K.J., Elgrishi, N., Kandemir, B. & Dempsey, J.L. 2018. Electrochemical and spectroscopic
620 methods for evaluating molecular electrocatalysts. *Nature Reviews Chemistry* 1(5): 1 -
621 14.

622 Leykin, A., Shapovalov, L. & Figovsky, O. (2016). Non – isocyanate polyurethanes –
623 Yesterday, today and tomorrow. *Alternative Energy and Ecology*. **191 (3 – 4)**: 95 – 108.

624 Li, H., Yuan, D., Li, P., He, C. (2019). High conductive and mechanical robust carbon
625 nanotubes/waterborne polyurethane composite films for efficient electromagnetic
626 interference shielding. *Composites Part A*. 121: 411 – 417.

- 627 Nakthong, P., Kondo, T., Chailapakul, O., Siangproh, W. (2020). Development of an
628 unmodified screen – printed graphene electrode for nonenzymatic histamine detection.
629 *Analytical Methods*. 12: 5407 – 5414.
- 630 Mishra, K., Narayan, R., Raju, K.V.S.N. & Aminabhavi, T.M. (2012). Hyperbranched
631 polyurethane (HBPU)-urea and HBPU-imide coatings: Effect of chain extender and
632 NCO/OH ratio on their properties. *Progress in Organic Coatings*. 74: 134 – 141.
- 633 Mohd Noor, M. A., Tuan Ismail, T. N. M., Ghazali, R. (2020). Bio – based content of oligomers
634 derived from palm oil: Sample combustion and liquid scintillation counting technique.
635 *Malaysia Journal of Analytical Science*. 24: 906 – 917.
- 636 Mutsuhisa F., Ken, K. & Shohei, N. (2007). Microphase separated structure and mechanical
637 properties of norbornane diisocyanate – based polyurethane. *Polymer*. 48 (4): 997 – 1004.
- 638 Mustapha, R., Rahmat, A. R., Abdul Majid, R., Mustapha, S. N. H. (2019). Vegetable oil –
639 based epoxy resins and their composites with bio – based hardener: A short review.
640 *Polymer- Plastic Technology and Materials*. 58: 1311 – 1326.
- 641 Nohra, B., Candy, L., Blancos, J.F., Guerin, C., Raoul, Y. & Mouloungui, Z. (2013). From
642 petrochemical polyurethanes to biobased polyhydroxyurethanes. *Macromolecules*. 46
643 (10): 3771 – 3792.
- 644 Pan, T. & Yu, Q. (2016). Anti – corrosion methods and materials comprehensive evaluation of
645 anti – corrosion capacity of electroactive polyaniline for steels. *Anti – Corrosion Methods
646 and Materials*. 63: 360 – 368.
- 647 Pan, X. & Webster, D.C. (2012). New biobased high functionality polyols and their use in
648 polyurethane coatings. *ChemSusChem*. 5: 419-429.
- 649 Petrovic, Z.S. (2008). Polyurethanes from vegetable oils. *Polymer Reviews*. 48 (1): 109 – 155.

650 Porcarelli, L., Manojkumar, K., Sardon, H., Llorente, O., Shaplov, A. S., Vijayakrishna, K.,
651 Gerbaldi, C., Mecerreyes, D. (2017). Single ion conducting polymer electrolytes based
652 on versatile polyurethanes. *Electrochimica Acta*. 241: 526 – 534.

653 Priya, S. S., Karthika, M., Selvasekarapandian, S. & Manjuladevi, R. (2018). Preparation and
654 characterization of polymer electrolyte based on biopolymer I-carrageenan with
655 magnesium nitrate. *Solid State Ionics*. **327**: 136 – 149.

656 Ren, D. & Frazier, C.E. (2013). Structure–property behaviour of moisture-cure polyurethane
657 wood adhesives: Influence of hard segment content. *Adhesion and Adhesives*. **45**: 118-
658 124.

659 Rogulska, S.K., Kultys, A. & Podkoscielny, W. (2007). Studies on thermoplastic polyurethanes
660 based on new diphenylethane – derivative diols. II. Synthesis and characterization of
661 segmented polyurethanes from HDI and MDI. *European Polymer Journal*. **43**: 1402 –
662 1414.

663 Romaskevicius, T., Budriene, S., Pielichowski, K. & Pielichowski, J. (2006). Application of
664 polyurethane – based materials for immobilization of enzymes and cells: a review.
665 *Chemija*. **17**: 74 – 89.

666 Sengodu, P. & Deshmukh, A. D. (2015). Conducting polymers and their inorganic composites
667 for advanced Li-ion batteries: a review. *RSC Advances*. **5**: 42109 – 42130.

668 Septevani, A. A., Evans, D. A. C., Chaleat, C., Martin, D. J., Annamalai, P. K. (2015). A
669 systematic study substituting polyether polyol with palm kernel oil based polyester
670 polyol in rigid polyurethane foam. *Industrial Corps and Products*. 66: 16 – 26.

671 Su'ait, M. S., Ahmad, A., Badri, K. H., Mohamed, N. S., Rahman, M. Y. A., Ricardi, C. L. A.
672 & Scardi, P. The potential of polyurethane bio – based solid polymer electrolyte for
673 photoelectrochemical cell application. *International Journal of Hydrogen Energy*. 39 (6):
674 3005 – 3017.

675 Tadesse, M. G., Mengistie, D. A., Chen, Y., Wang, L., Loghin, C., Nierstrasz, V. (2019).
676 Electrically conductive highly elastic polyamide/lycra fabric treated with PEDOT: PSS
677 and polyurethane. *Journal of Materials Science*. 54: 9591 – 9602.

678 Tajau, R., R, Rosiah, Alias, M. S., Mudri, N. H., Halim, K. A. A., Harun, M. H., Isa, N. M.,
679 Ismail, R. C., Faisal, S. M., Talib, M., Zin, M. R. M., Yusoff, I. I., Zaman, N. K., Illias,
680 I. A. (2021). Emergence of polymeric material utilising sustainable radiation curable
681 palm oil – based products for advanced technology applications. *Polymers*. 13: 1865 –
682 1886.

683 Tran, V.H., Kim, J.D., Kim, J.H., Kim, S.K., Lee, J.M. (2020). Influence of cellulose
684 nanocrystal on the cryogenic mechanical behaviour and thermal conductivity of
685 polyurethane composite. *Journal of Polymers and The Environment*. **28**: 1169 – 1179.

686 Viera, I.R.S., Costa, L.D.F.D.O., Miranda, G.D.S., Nardehcia, S., Monteiro, M.S.D. S.D.B.,
687 Junior, E.R. & Delpech, M.C. (2020). Waterborne poly (urethane – urea)s
688 nanocomposites reinforced with clay, reduced graphene oxide and respective hybrids:
689 Synthesis, stability and structural characterization. *Journal of Polymers and The
690 Environment*. **28**: 74 – 90.

691 Wang, B., Wang, L., Li, X., Liu, Y., Zhang, Z., Hedrick, E., Safe, S., Qiu, J., Lu, G. & Wang,
692 S. (2018). Template – free fabrication of vertically – aligned polymer nanowire array on
693 the flat – end tip for quantifying the single living cancer cells and nanosurface interaction.
694 *a Manufacturing Letters*. **16**: 27 – 31.

695 Wang, J., Xiao, L., Du, X., Wang, J. & Ma, H. (2017). Polypyrrole composites with carbon
696 materials for supercapacitors. *Chemical Papers*. **71** (2): 293 – 316.

697 Wong, C.S. & Badri, K.H. (2012). Chemical analyses of palm kernel oil – based polyurethane
698 prepolymer. *Materials Sciences and Applications*. **3**: 78 – 86.

- 699 Wong, C. S., Badri, K., Ataollahi, N., Law, K., Su'ait, M. S., Hassan, N. I. (2014). Synthesis
700 of new bio – based solid polymer electrolyte polyurethane – LiClO₄ via
701 prepolymerization method: Effect of NCO/OH ratio on their chemical, thermal properties
702 and ionic conductivity. *World Academy of Science, Engineering and Technology,*
703 *International Journal of Chemical, Molecular, Nuclear, Materials and Metallurgical*
704 *Engineering.* 8: 1243 – 1250.
- 705 Yong, Z., Bo, Z.M., Bo, W., Lin, J.Z. & Jun, N. (2009). Synthesis and properties of novel
706 polyurethane acrylate containing 3-(2-Hydroxyethyl) isocyanurate segment. *Progress in*
707 *Organic Coatings.* **67**: 264 – 268
- 708 Zia, K. M., Anjum, S., Zuber, M., Mujahid, M. & Jamil, T. (2014). Synthesis and molecular
709 characterization of chitosan based polyurethane elastomers using aromatic diisocyanate.
710 *International of Journal of Biological Macromolecules.* **66**: 26 – 32.

Hasil Reviu 5 dan Submit Revisi: 2 Februari 2022

Hindawi

Joanna Rydz

10.02.2022

Decision

Minor Revision Requested

Message for Author

Dear authors,

The text still needs to be improved.

1. Please properly describe the results from FTIR throughout the text also in Conclusion.

"N=C=O is not a peak. Functional groups give characteristic signals in a spectrum. Please use scientific language throughout your text and please describe the FTIR spectra properly"

"Thank you for your suggestion. Nevertheless, the reading of this spectrum based on Spectroscopy book 4th Edition by Lampman et al. It is written on Page 29, 77 and 78 (Figure 2.64) about the spectrum of N=C=O. According to their research, the isocyanates have sp-hybridized carbon atoms similar to the C=C bond. The absorption occurs in 2100-2270 cm⁻¹"

Exactly, then why do you write "N=C=O peak"? It is a scientific work and that is the language it should use.

"and confirmed by the absence of peak at 2241 cm⁻¹ attributed to the sp-hybridized carbon atoms of"/or "absorption bands at 2241 cm⁻¹ associated with N=C=O bond stretching...." Please correct.

2. "bio based" is one word and should be spelled the same way throughout the text, see lines 21 and 75 (correct). Please correct throughout the text (It is best to use the find options throughout the text).

3. Line 150-152: The reagent purity record was perfectly correct and please restore it. The note was about DMSO, which was 2 times.

4. Line 220: the parenthesis is missing.

5. Line 369, 507, 513: "bio polyurethane". Should be bio-based polyurethane. A single comment applies to the entire text!

6. Table 2: Please explain variables such as T_{max}, etc. under the table.

The table has not been corrected and is still incomprehensible. It not only shows the "weight loss percentage" as its caption suggests, but also other parameters. Please properly title it. Right now, the table shows that the weight loss percentage of sample T_{max} has changed by 240!

The first row should be discarded. The table shows the TGA parameters of one sample, so there is no need to put it in the table. Please correct.

— Response to Revision Request

Muhammad Abdurrahman Munir

10.02.2022

Your Reply

Greetings, Dear Dr. Joanna Rydz We would like to inform you that the manuscript has been revised according to the reviewer's comments. Journal: International

Hindawi

Journal of Polymer Science Manuscript ID: 6815187 Title: "Design and Synthesis of Conducting Polymer Based on Polyurethane produced from Palm Kernel Oil"
Comments and track changes are attached. We look forward to receiving your revision if any. Best Regards.

File

Manuscript - Munir.docx 916 kB



1 **Design and Synthesis of Conducting Polymer Based on Polyurethane**
2 **produced from Palm Kernel Oil**

3
4 Muhammad Abdurrahman Munir^{1*}, Khairiah Haji Badri^{2,3}, Lee Yook Heng², Ahlam
5 Inayatullah⁴, Ari Susiana Wulandari¹, Emelda¹, Eliza Dwinta¹, Veriani Aprillia⁵, Rachmad
6 Bagas Yahya Supriyono¹

7
8 ¹Department of Pharmacy, Faculty of Health Science, Alma Ata University, Daerah Istimewa
9 Yogyakarta, 55183, Indonesia

10 ²Department of Chemical Sciences, Faculty of Science and Technology, Universiti
11 Kebangsaan Malaysia, Bangi, 43600, Malaysia

12 ³Polymer Research Center, Universiti Kebangsaan Malaysia, Bangi, 43600, Malaysia

13 ⁴Faculty of Science and Technology, Universiti Sains Islam Malaysia, Nilai, 71800, Malaysia

14 ⁵Department of Nutrition Science, Alma Ata School of Health Sciences, Alma Ata
15 University, Daerah Istimewa Yogyakarta, 55183, Indonesia

16
17 *Email: muhammad@almaata.ac.id

18
19 **Abstract**

20 Polyurethane (PU) is a unique polymer that has versatile processing methods and mechanical
21 properties upon the inclusion of selected additives. In this study, a freestanding bio-
22 polyurethane film the screen-printed electrode (SPE) was prepared by the solution casting
23 technique, using acetone as solvent. It was a one-pot synthesis between major reactants namely,
24 palm kernel oil-based polyol (PKOp) and 4,4-methylene diisocyanate. The PU has strong

25 adhesion on the SPE surface. The synthesized polyurethane was characterized using
26 thermogravimetry analysis (TGA), differential scanning calorimetry (DSC), Fourier –
27 transform infrared spectroscopy (FTIR), surface area analysis by field emission scanning
28 electron microscope (FESEM), and cyclic voltammetry (CV). Cyclic voltammetry was
29 employed to study electro-catalytic properties of SPE-Polyurethane towards oxidation of PU.
30 Remarkably, SPE-PU exhibited improved anodic peak current as compared to SPE itself using
31 the differential pulse voltammetry (DPV) method. Furthermore, the formation of urethane
32 linkages (NHCO backbone) after polymerization was analyzed using FTIR and confirmed by
33 the absence of N=C=O peak at 2241 cm^{-1} . The glass transition temperature (T_g) of the
34 polyurethane was detected at 78.1°C .

35

36 **Keywords:** Polyurethane, polymerization, screen-printed electrode, voltammetry

37

38

39 **1. Introduction**

40 Conducting polymers (CPs) are polymers that can release a current (Alqarni et al. 2020). The
41 conductivity of CPs was first observed in polyacetylene, nevertheless owing to its instability,
42 the invention of various CPs have been studied and reported such as polyaniline (PANI), poly
43 (o-toluidine) (PoT), polythiophene (PTH), polyfluorene (PF), and polyurethane (PU).
44 Furthermore, natural CPs have low conductivity and are often semi-conductive. Therefore, it
45 is imperative to improve their conductivity for electrochemical sensor purposes (Sengodu &
46 Deshmukh 2015; Dzulkipli et al. 2021; Wang et al. 2018). The CPs can be produced from many
47 organic materials and they have several advantages such as having an electrical current,
48 inexpensive materials, massive surface area, small dimensions, and the production is
49 straightforward. Furthermore, according to these properties, many studies have been reported

50 by researchers to study and report the variety of CPs applications such as sensors, biochemical
51 applications, electrochromic devices, and solar cells (Alqarni et al. 2020; Ghosh et al. 2018).
52 There is scientific documentation on the use of conductive polymers in various studies such as
53 polyaniline (Pan & Yu 2016), polypyrrole (Ladan et al. 2017), and polyurethane (Tran et al.
54 2020; Vieira et al. 2020; Guo et al. 2020; Fei et al. 2020).

55

56 Polyurethane productions can be obtained by using several materials as polyols such as
57 petroleum, coal, and crude oils. Nevertheless, these materials have become very rare to find
58 and the price is very expensive at the same time required a sophisticated system to produce it.
59 The reasons such as price and time consuming to produce polyols have been considered by
60 many researchers, furthermore, finding utilizing plants that can be used as alternative polyols
61 should be done immediately (Badri 2012). Thus, to avoid the use of petroleum, coal, and crude
62 oils as raw materials for a polyol, vegetable oils become a better choice to produce polyol in
63 order to obtain a biodegradable polymer. Vegetable oils that are generally used for
64 polyurethane synthesis are soybean oil, corn oil, sunflower seed oil, coconut oil, nuts oil,
65 rapeseed, olive oil, and palm oil (Badri 2012; Borowicz et al. 2019).

66

67 It is very straightforward for vegetable oils to react with a specific group to produce a PU such
68 as epoxy, hydroxyl, carboxyl, and acrylate owing to the existence of (-C=C-) in vegetable oils.
69 Thus, it provides appealing profits to vegetable oils compared to petroleum considering the
70 toxicity, price, and harm to the environment (Mustapha et al. 2019; Mohd Noor et al. 2020).
71 Palm oil becomes the chosen in this study to produce PU owing to it being largely cultivated
72 in South Asia particularly in Malaysia and Indonesia. It has several profits compared to other
73 vegetable oils such as the easiest materials obtained, the lowest cost of all the common

74 vegetable oils, and recognized as the plantation that has a low environmental impact and
75 removing CO₂ from the atmosphere as a net sequester (Tajau et al. 2021; Septevani et al. 2015).

76

77 The application of biopolymer has appealed much attention until now. Global environmental
78 activists have forced researchers to discover another material producing biopolymers (Priya et
79 al. 2018). PUs have many advantages that have been used by many researchers, they are not
80 merely versatile materials but also have the durability of metal and the flexibility of rubber.
81 Furthermore, they can be promoted to replace rubber, metals, and plastics in several aspects.
82 Several applications of Pus have been reported and studied such as textiles, automotive,
83 building and construction applications, and biomedical applications (Zia et al. 2014;
84 Romaskevic et al. 2006). Polyurethanes are also considered to be one of the most useful
85 materials with many profits such as; possessing low conductivity, low density, absorption
86 capability, and dimensional stability. They are a great research subject due to their mechanical,
87 physical, and chemical properties (Badan & Majka 2017; Munir et al. 2021).

88

89 PU structure contains the urethane group that can be formed from the reaction between
90 isocyanate groups (-NCO) and hydroxyl group (-OH). Nevertheless, several groups can be
91 found in PU structure such as urea, esters, ethers, and several aromatic groups. Furthermore,
92 PUs can be produced from different sources as long as they contain specific materials (polyol
93 & MDI) and making them very useful for specific applications. Thus, according to the desired
94 properties, PUs can be divided into several types such as waterborne, flexible, rigid, coating,
95 binding, sealants, adhesives, and elastomers (Akindoyo et al. 2016).

96

97 PUs have low conductivity and are lighter than other materials such as metals, gold, and
98 platinum. The hardness of PU also relies on the number of the aromatic rings in the polymer

99 structure (Janpoung et al, 2020; Su'ait et al. 2014), majorly contributed by the isocyanate
100 derivatives. PUs have also a conjugate structure where electrons can move in the main chain
101 that causes electricity produced even the current is low. The current of conjugated linear (π)
102 can be elaborated by the gap between the valence band and the conduction band, or called high
103 energy level containing electrons (HOMO) and lowest energy level not containing electrons
104 (LUMO), respectively (Wang et al. 2017; Kotal et al. 2011).

105

106 In the recent past, several conventional methods have been developed such as capillary
107 electrophoresis, liquid, and gas chromatography coupled with several detectors. Nevertheless,
108 although chromatographic and spectrometric approaches are well developed for qualitative and
109 quantitative analyses of analytes, several limitations emerged such as complicated
110 instrumentation, expensive, tedious sample preparations, and requiring large amounts of
111 expensive solvents that will harm the users and environment (Kilele et al. 2020; Inayatullah et
112 al. 2021; Munir et al. 2021; Harmayani et al. 2014; Nurwanti et al. 2018). Therefore, it is
113 imperative to obtain and develop an alternative material that can be used to analyze a specific
114 analyte. Electrochemical methods are extremely promising methods in the determination of an
115 analyte in samples owing to the high selectivities, sensitivities, inexpensive, requirements of
116 small amounts of solvents, and can be operated by people who have no background in analytical
117 chemistry. In addition, sample preparation such as separation and extraction steps are not
118 needed owing to the selectivity of this instrument where no obvious interference on the current
119 response is recorded (Chokkareddy et al. 2020). Few works have been reported on the
120 electrochemical methods for the determination of analyte using electrodes combined with
121 several electrode modifiers such as carbon nanotube, gold, and graphene (Chokkareddy et al.
122 2020; Kilele et al. 2021). Nevertheless, the materials are expensive and the production is

123 difficult. Thus, an electrochemical approach using inexpensive and easily available materials
124 as electrode modifiers should be developed (Degefu et al. 2014).

125

126 Nowadays, screen-printed electrodes (SPEs) modified with conducting polymer have been
127 developed for various electrochemical sensing. SPE becomes the best solution owing to the
128 electrode having several advantages such as frugal manufacture, tiny size, being able to
129 produce on a large scale, and can be applied for on-site detection (Nakthong et al. 2020).
130 Conducting polymers (CPs) become an alternative to modifying the screen-printed electrodes
131 due to their electrical conductivity, able to capture analyte by chemical/physical adsorption,
132 large surface area, and making CPs are very appealing materials from electrochemical
133 perspectives (Baig et al. 2019). Such advantages of SPE encourage us to construct a new
134 electrode for electrochemical sensing, and no research reported on the direct electrochemical
135 oxidation of histamine using a screen-printed electrode modified by polyurethane. Therefore,
136 this research is the first to develop a new electrode using (screen printed polyurethane
137 electrode) SPPE without any conducting materials.

138

139 The purpose of this work was to synthesize, characterize and study the electro behavior of
140 polyurethane using cyclic voltammetry (CV) and differential pulse voltammetry (DPV)
141 attached to the screen-printed electrode (SPE). To the best of our knowledge, this is the first
142 attempt to use a modified polyurethane electrode. The electrochemistry of polyurethane
143 mounted onto screen-printed electrode (SPE) is discussed in detail. PUs are possible to become
144 an advanced frontier material that has been chemically modified the specific electrodes for
145 bio/chemical sensing application.

146

147

148 **2. Experimental**

149 **2.1 Chemicals**

150 *Synthesis of polyurethane film:* Palm kernel oil (PKOp) supplied by UKM Technology Sdn
151 Bhd through MPOB/UKM station plant, Pekan Bangi Lama, Selangor and prepared using
152 Badri et al. (2000) method. 4, 4-diphenylmethane diisocyanate (MDI) was acquired from
153 Cosmopolyurethane (M) Sdn. Bhd., Klang, Malaysia. Solvents and analytical reagents were
154 benzene ($\geq 99.8\%$), toluene ($\geq 99.8\%$), hexane ($\geq 99\%$), acetone ($\geq 99\%$), dimethylsulfoxide
155 (DMSO) ($\geq 99.9\%$), dimethylformamide (DMF) ($\geq 99.8\%$), tetrahydrofuran (THF) ($\geq 99.8\%$),
156 dimethylsulfoxide (DMSO) ($\geq 99.9\%$), and polyethylene glycol (PEG) with a molecular weight
157 of 400 Da obtained from Sigma Aldrich Sdn Bhd, Shah Alam.

158

159 **2.2 Apparatus**

160 Tensile testing was performed using a universal testing machine model Instron 5566 following
161 ASTM 638 (Standard Test Method for Tensile Properties of Plastics). The tensile properties of
162 the polyurethane film were measured at a velocity of 10 mm/min with a cell load of 5 kN.

163 The thermal properties were performed using thermogravimetry analysis (TGA) and
164 differential scanning calorimetry (DSC) analysis. TGA was performed using a thermal analyzer
165 of the Perkin Elmer Pyris model with a heating rate of 10 °C/min at a temperature range of 30
166 to 800 °C under a nitrogen gas atmosphere. The DSC analysis was performed using a thermal
167 analyzer of the Perkin Elmer Pyris model with a heating rate of 10 °C /minute at a temperature
168 range of -100 to 200 °C under a nitrogen gas atmosphere. Approximately, 5-10 mg of PU was
169 weighed. The sample was heated from 25 to 150 °C for one minute, then cooled immediately
170 from 150 -100 °C for another one minute and finally, reheated to 200 °C at a rate of 10 °C /min.
171 At this point, the polyurethane encounters changes from elastic properties to brittle due to
172 changes in the movement of the polymer chains. Therefore, the temperature in the middle of

173 the inclined regions is taken as the glass transition temperature (T_g). The melting temperature
174 (T_m) is identified as the maximum endothermic peak by taking the area below the peak as the
175 enthalpy point (ΔH_m).

176

177 The morphological analysis of PU film was performed by Field Emission Scanning Electron
178 Microscope (FESEM) model Gemini SEM microscope model 500-70-22. Before the analysis
179 was carried out, the polyurethane film was coated with a thin layer of gold to increase the
180 conductivity of the film. The coating method was carried out using a sputter-coater. The
181 observations were conducted at a magnification of 200 \times and 5000 \times with 10.00 kV (Electron
182 high tension - EHT).

183

184 The crosslinking of PU was determined using the soxhlet extraction method. About 0.60 g of
185 PU sample was weighed and put in an extractor tube containing 250 ml of toluene, used as a
186 solvent. This flow of toluene was let running for 24 hours. Mass of the PU was weighed before
187 and after the reflux process was carried out. Then, the sample was dried in the conventional
188 oven at 100 °C for 24 hours in order to get a constant mass. The percentage of crosslinking
189 content known as the gel content can be calculated using Equation (1).

$$190 \quad \text{Gel content (\%)} = \frac{W_0 - W}{W} \times 100 \% \quad (1)$$

191 W_0 is the mass of PU before the reflux process (g) and W is the mass of PU after the reflux
192 process (g).

193

194 FTIR spectroscopic analysis was performed using a Perkin-Elmer Spectrum BX instrument
195 using the Diamond Attenuation Total Reflectance (DATR) method to confirm the
196 polyurethane, PKOp, and MDI functional group. FTIR spectroscopic analysis was performed
197 at a wavenumber of 4000 to 600 cm^{-1} to identify the peaks of the major functional groups in

198 the formation of the polymer such as amide group (-NH), urethane carbonyl group (-C = O),
199 and carbamate group (-CN).

200

201 **2.3 Synthesis of Polyurethane**

202 Firstly, the polyol prepolymer solution was produced by combining palm kernel oil (PKO)p
203 and polyethylene glycol (PEG) 400 (100:40 g/g), acetone 30% was used as a solution. The
204 compound was homogenized using a centrifuge (100 rpm) for 5 min. Whereas diisocyanate
205 prepolymer was obtained by mixing 4,4'-diphenylmethane diisocyanate (MDI) (100 g) to
206 acetone 30%, afterward the mixture was mixed using a centrifuge for 1 min to obtain a
207 homogenized solution. Afterward, diisocyanate solution (10 g) was poured into a container that
208 contains polyol prepolymer solution (10 g) slowly to avoid an exothermic reaction occurring.
209 The mixture was mixed for 30 sec until a homogenized solution was acquired. Lastly, the
210 polyurethane solution was poured on the electrode surface by using the casting method and
211 dried at ambient temperature for 12 hours.

212

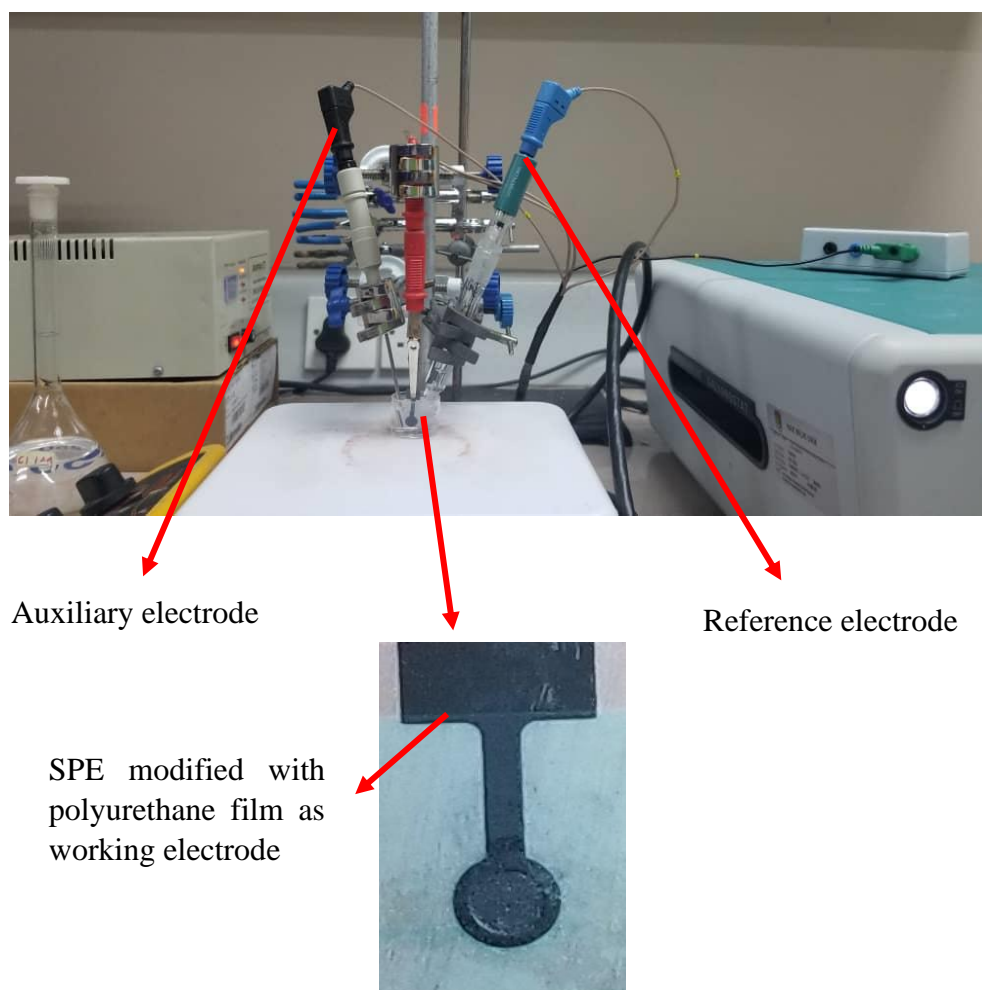
213 **2.4 Modification of Electrode**

214 Voltammetric tests were performed using Metrohm Autolab Software (**Figure 1**) analyzer
215 using cyclic voltammetry (CV) method or known as amperometric mode and differential pulse
216 voltammetry (DPV). All electrochemical experiments were carried out using screen-printed
217 electrode (diameter 3 mm) modified using polyurethane film as working electrode, platinum
218 wire as the auxiliary electrode, and Ag/AgCl electrode as a reference electrode. All experiments
219 were conducted at a temperature of $20 \pm 2^\circ\text{C}$.

220

221 The PU was cast onto the screen-printed electrode (SPE + PU) and analyzed using a single
222 voltammetric cycle between -1200 and +1500 mV (vs Ag/AgCl) of ten cycles at a scanning

223 rate of 100 mV/s in 5 ml of KCl in order to study the activity of SPE and polyurethane film.
224 Approximately (0.1, 0.3 & 0.5) mg of palm-based pre-polyurethane was dropped separately
225 onto the surface of the SPE and dried at room temperature. The modified palm-based
226 polyurethane electrodes were then rinsed with deionized water to remove physically adsorbed
227 impurities and residues of unreacted material on the electrode surface. All electrochemical
228 materials and calibration measurements were carried out in a 5 mL glass beaker with a
229 configuration of three electrodes inside it. Platinum wire and silver/silver chloride (Ag/AgCl)
230 electrodes were used as auxiliary and reference electrodes, while a screen-printed electrode
231 that had been modified with polyurethane was applied as a working electrode.



232 **Figure 1.** Potentiostat instrument to study the conductivity of SPE modified with
233 polyurethane film using voltammetric approach: CV and DPV

234

235 **3. Results and Discussion**

236 The synthesis of PU films was carried out using a pre-polymerization method which involves
237 the formation of urethane polymer at an early stage. The reaction took place between
238 diisocyanate (MDI) and palm kernel oil-based polyol (PKOp). **Table 1** presents the PKO-p
239 properties used in this study. The structural chain was extended with the aid of polyethylene
240 glycol (PEG) to form flexible and elastic polyurethane film. In order to produce the urethane
241 prepolymer, the isocyanate group (NCO) attacks with the hydroxyl group (OH) of polyol
242 (PKOp) while the other hydroxyl group of the polyol is attacked by the other isocyanate group
243 (Wong & Badri 2012) as shown in **Figure 2**.

244 **Table 1** The specification of PKO-p (Badri et al. (2000)).

| Property | Values |
|------------------------------|-----------|
| Viscosity at 25°C (cps) | 1313.3 |
| Specific gravity (g/mL) | 1.114 |
| Moisture content (%) | 0.09 |
| pH value | 10 – 11 |
| The hydroxyl number mg KOH/g | 450 - 470 |

245

246

247 a. FTIR analysis

248 **Figure 3** shows the FTIR spectra for polyurethane, exhibiting the important functional group
249 peaks. According to a study researched by Wong & Badri 2012, PKO-p reacts with MDI to
250 form urethane prepolymers. The NCO group on MDI reacts with the OH group on polyol
251 whether PKOp or PEG. It can be seen there are no important peaks of MDI in the FTIR spectra.
252 This is further verified by the absence of a peak at the 2400 cm⁻¹ belonging to MDI (-NCO
253 groups). This could also confirm that the NCO group on MDI had completely reacted with

254 PKO-p to form the urethane –NHC (O) backbone. The presence of amides (-NH), carbonyl
255 urethane group (-C = O), carbamate group (C-NH), and -C-O-C confirmed the formation of
256 urethane chains. In this study, the peak of carbonyl urethane (C = O) detected at 1727 cm⁻¹
257 indicated that the carbonyl urethane group was bonded without hydrogen owing to the
258 hydrogen reacts with the carbonyl urethane group.

259

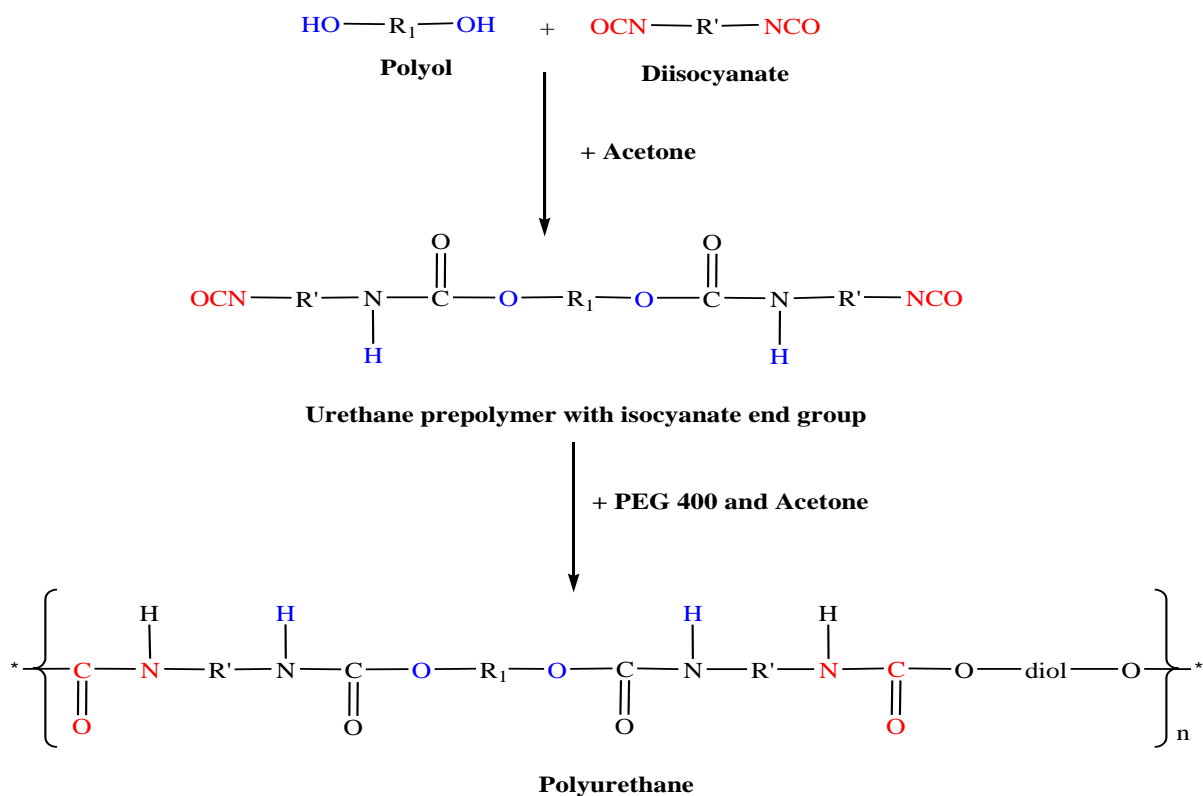
260 The reaction of polyurethane has been studied by Hamuzan & Badri (2016) where the urethane
261 carbonyl group was detected at 1730 – 1735 cm⁻¹ while the MDI carbonyl was detected at 2400
262 cm⁻¹. The absence of peaks at 2250 – 2270 cm⁻¹ indicates the absence of NCO groups. It shows
263 that the polymerization reaction occurs entirely between NCO groups in MDI with hydroxyl
264 groups on polyols and PEG (Mishra et al. 2012). The absence of peaks at 1690 cm⁻¹
265 representing urea (C = O) in this study indicated, there is no urea formation as a byproduct
266 (Clemitson 2008) of the polymerization reaction that possibly occurs due to the excessive
267 water. For the amine (NH) group, hydrogen-bond to NH and oxygen to form ether and
268 hydrogen bond to NH and oxygen to form carbonyl on urethane can be detected at the peak of
269 3301 cm⁻¹ and in the wavenumber at range 3326 – 3428 cm⁻¹. This has also been studied and
270 detected by Mutsuhisa et al. (2007) and Lampman et. al. (2010). In this research, the proton
271 acceptor is carbonyl (-C=O) while the proton donor is an amine (-NH) to form a hydrogen
272 bond. The MDI chemical structure has the electrostatic capability that produces dipoles from
273 several atoms such as hydrogen, oxygen, and nitrogen atoms. These properties make
274 isocyanates are highly reactive, and have different properties (Leykin et al. 2016).

275

276 MDI was one of the isocyanates used in this study, has an aromatic group, and is more
277 reactive compared to aliphatic group isocyanates such as hexamethylene diisocyanate (HDI)
278 or isophorone diisocyanate (IPDI). Isocyanates have two groups of isocyanates on each

279 molecule. Diphenylmethane diisocyanate is an exception owing to its structure consisting of
 280 two, three, four, or more isocyanate groups (Nohra et al. 2013). The use of PEG 400 in this
 281 study as a chain extender for polyurethane increases the chain mobility of polyurethane at an
 282 optimal amount. The properties of polyurethane are contributed by hard and soft copolymer
 283 segments of both polyol monomers and MDI. This makes the hard segment of urethane serves
 284 as a crosslinking site between the soft segments of the polyol (Leykin et al. 2016).

285



286

287 **Figure 2.** PU production via the pre-polymerization method (Wong & Badri 2012).

288

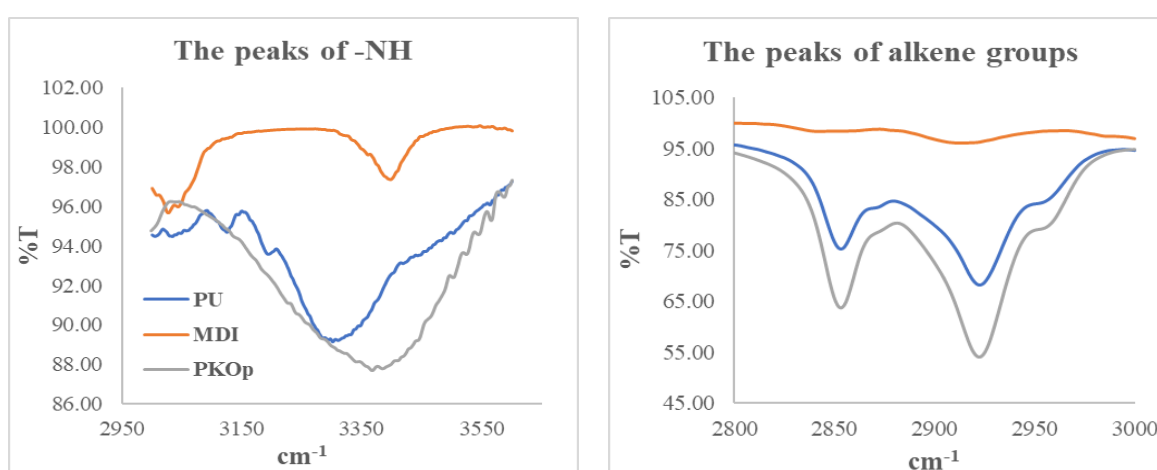
289 The mechanism of the pre-polymerization in urethane chains formation is a
 290 nucleophilic substitution reaction as studied by Yong et al. (2009). However, this study found
 291 amines as nucleophiles. Amine attacks carbonyl on isocyanate in MDI in order to form two
 292 resonance structures of intermediate complexes A and B. Intermediate complex B has a greater
 293 tendency to react with polyols due to stronger carbonyl (C = O) bonds than C = N bonds on

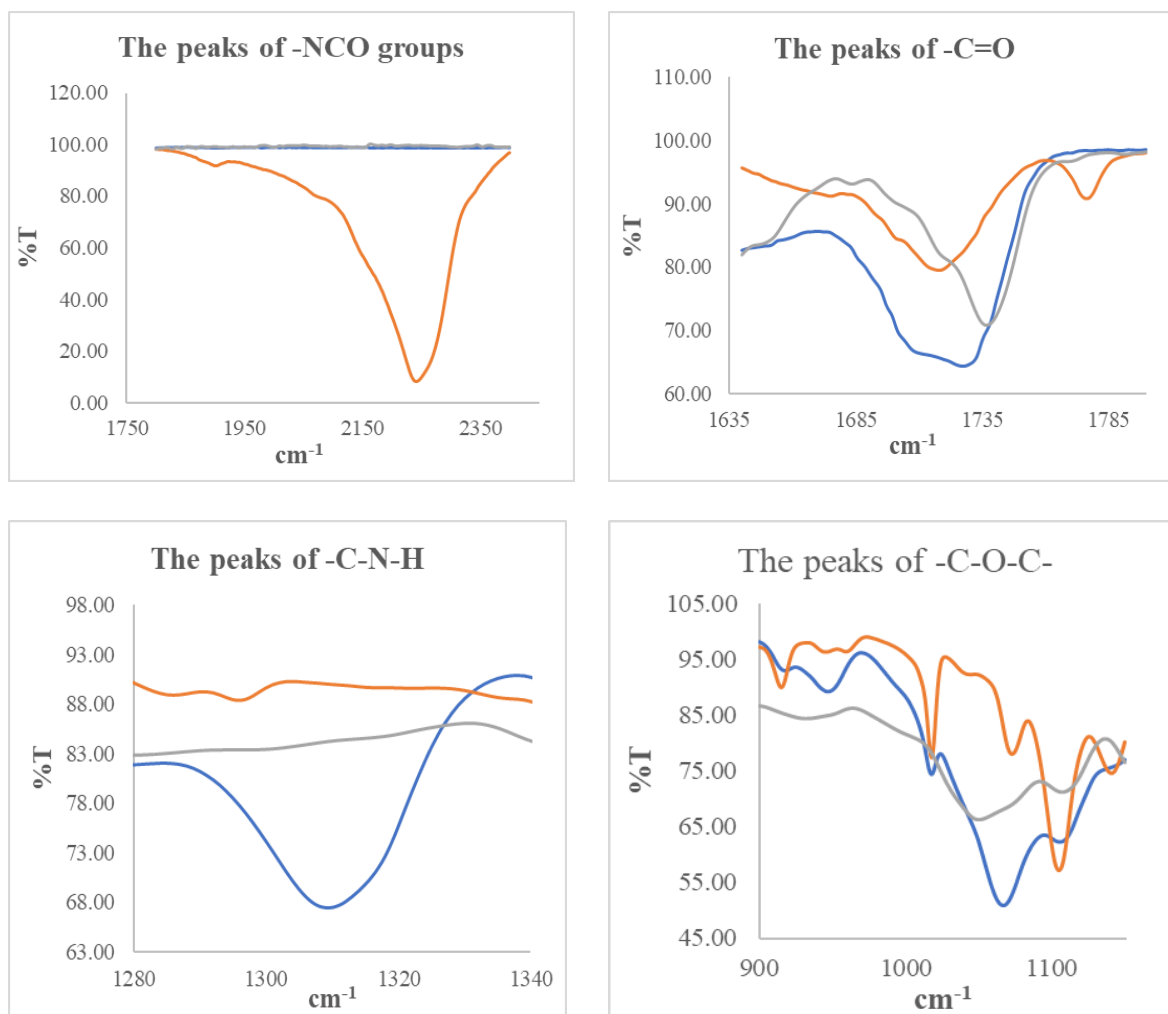
294 intermediate complexes A. Thus, intermediate complex B is more stable than intermediate
295 complex A, as suggested by previous researchers who have conducted by Wong and Badri
296 (2012). Moreover, oxygen is more electronegative than nitrogen causing cations (H^+) to tend
297 to attack $-CN$ bonds compared to $-CO$. The combination between long polymer chain and low
298 cross-linking content gives the polymer elastic properties whereas short-chain and high cross-
299 linking produce hard and rigid polymers. Cross-linking in polymers consists of three-
300 dimensional networks with high molecular weight. In some aspects, polyurethane can be a
301 macromolecule, a giant molecule (Petrovic 2008).

302

303 However, complexes A and B intermediate were produced after the nucleophile of PEG
304 attacking the isocyanate group in the MDI. However, PEG contains oxygen atoms that are more
305 electronegative than nitrogen atoms inside the PKOp chemical structure causing the reaction
306 of nucleophilic substitution that occurs in PKOp. Furthermore, amine has a higher probability
307 of reacting compared to hydroxyl (Herrington & Hock 1997). Amine with high alkalinity reacts
308 with carbon atoms on MDI as proposed by Wong and Badri (2012).

309





310 **Figure 3.** FTIR spectra of several important peaks between polyurethane, PKO-p, and MDI

311

312

313

314 The production of intermediate complexes unstabilizes the alkyl ions, nevertheless, the

315 long carbon chains of PKOp ensure the stability of alkyl ions. The addition of PEG in this study

316 is imperative, not merely to increase the chain length of PU but also to avoid the production of

317 urea as a by-product after the NCO group reacts with H_2O from the environment. If the NCO

318 group reacts with the excess water in the environment, the formation of urea and carbon dioxide

319 gas will also occur excessively (**Figure 4**). This reaction can cause a polyurethane foam, not

320 polyurethane film as we studied the film.

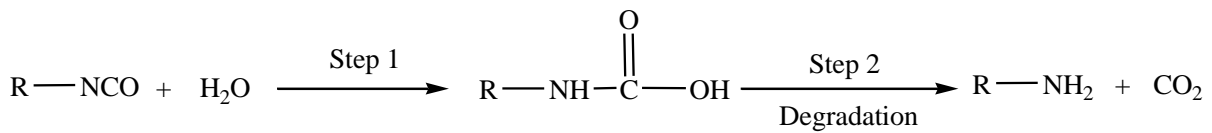
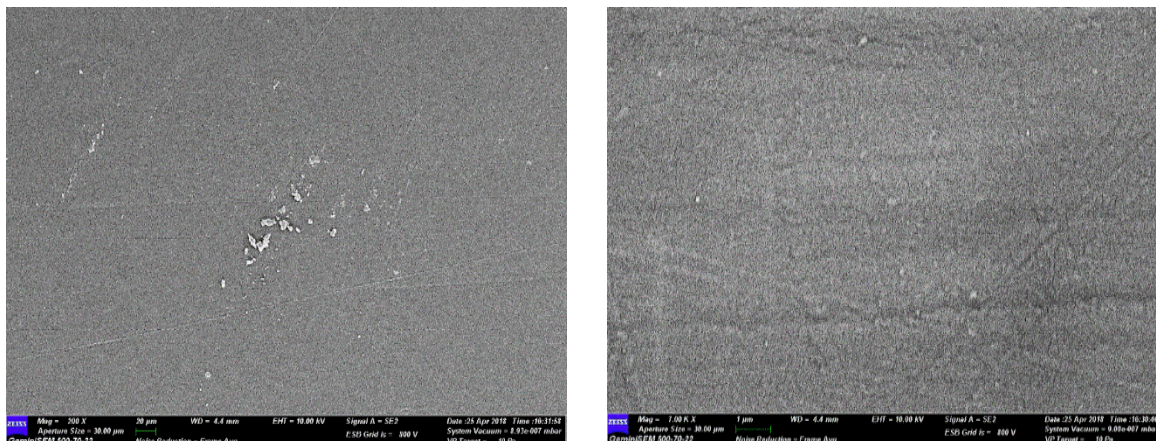


Figure 4. The reaction between the NCO group and water producing carbon dioxide

Furthermore, the application of PEG can influence the conductivity of PU whereby Porcarelli et al. (2017) have reported the application of PEG using several molecular weights. PEG 1500 decreased the conductivity of PU in consequence of the semicrystalline phase of PEG 1500 that acted as a poor ion-conducting phase for PU. It is also well known that PEG with a molecular weight of more than 1000 g·mol⁻¹ tends to crystallize with deleterious effects on room temperature ionic conductivity (Porcarelli et al. 2017).

b. Morphological analysis

The Field Emission Scanning Electron Microscope (FESEM) micrograph in **Figure 5** shows the formation of a uniform polymer film contributed by the polymerization method applied. The magnification used for this surface analysis ranged from 200 to 5000 ×. The polymerization method can also avoid the failure of the reaction in PU polymerization. Furthermore, no trace of separation was detected by FESEM. This has also been justified by the wavelengths obtained by the FTIR spectra above.



339 **Figure 5.** The micrograph of polyurethane films was analyzed by FESEM at (a) 200 × and
340 (b) 5000× magnifications.

341
342 c. The crosslinking analysis

343 Soxhlet analysis was applied to determine the degree of crosslinking between the hard
344 segments and the soft segments in the polyurethane. The urethane group on the hard segment
345 along the polyurethane chain is polar (Cuve & Pascault 1991). Therefore, during the testing, it
346 was very difficult to dissolve in toluene, as the testing reagent. The degree of crosslinking is
347 determined by the percentage of the gel content. The analysis result obtained from the Soxhlet
348 testing indicated a 99.3 % gel content. This is significant in getting a stable polymer at a higher
349 working temperature (Rogulska et al. 2007).

350

$$\text{Gel content (\%)} = \frac{(0.6 - 0.301) \text{ g}}{0.301 \text{ g}} \times 100\% = 99.33\%$$

351

352

353

354

355

356

357 d. The thermal analysis

358 Thermogravimetric analysis (TGA) can be used to observe the material mass based on
359 temperature shift. It can also examine and estimate the thermal stability and materials
360 properties such as the alteration weight owing to absorption or desorption, decomposition,
361 reduction, and oxidation. The material composition of polymer is specified by analyzing the
362 temperatures and the heights of the individual mass steps (Alamawi et al. 2019). **Figure 6**
363 shows the TGA and DTG thermograms of polyurethane. The percentage weight loss (%) is

364 listed in **Table 2**. Generally, only a small amount of weight was observed. It is shown in **Figure**
 365 **6** in the region of 45 – 180°C. This is due to the presence of condensation on moisture and
 366 solvent residues.

367

368

Table2 Weight loss percentage of (wt%) polyurethane film

| Sample | % Weight loss (wt%) | | | | Total of weight loss (%) | Residue after 550°C (%) |
|--------------|---------------------|-------------------|-------------------|-------------------|--------------------------------|----------------------------|
| | T _{max} , | T _{d1} , | T _{d2} , | T _{d3} , | | |
| | °C | 200 – 290°C | 350 – 500°C | 500 – 550°C | | |
| Polyurethane | 240 | 8.04 | 39.29 | 34.37 | 81.7 | 18.3 |

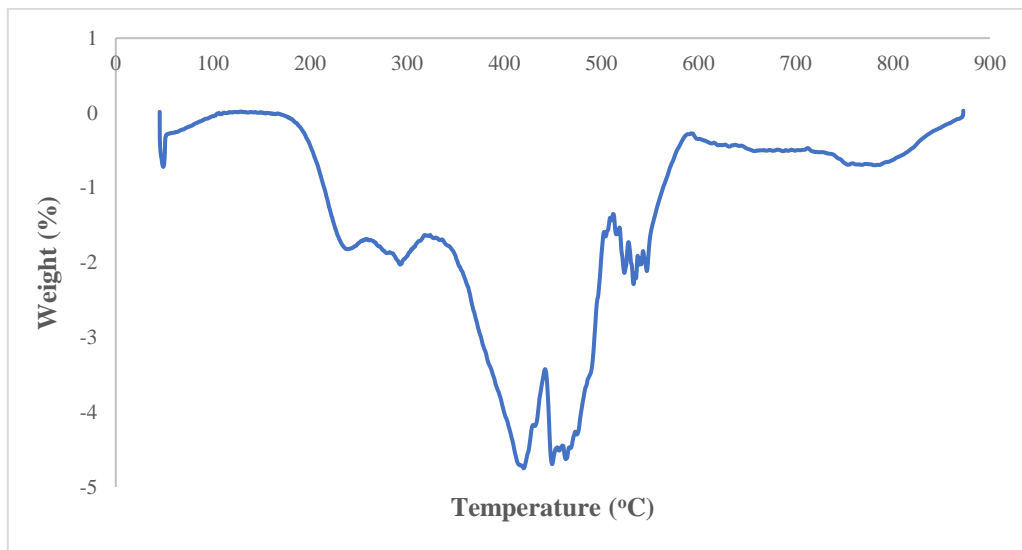
369

370 The bio polyurethane is thermally stable up to 240 °C before it has undergone thermal
 371 degradation (Agrawal et al. 2017). The first stage of thermal degradation (T_{d1}) on polyurethane
 372 films was shown in the region of 200 – 290 °C as shown in **Figure 6**. The T_{d1} is associated with
 373 degradation of the hard segments of the urethane bond, forming alcohol or degradation of the
 374 polyol chains and releasing of isocyanates (Berta et al. 2006), primary and secondary amines
 375 as well as carbon dioxide (Corcuera et al. 2011; Pan & Webster 2012). Meanwhile, the second
 376 thermal degradation stage (T_{d2}) of polyurethane films experienced a weight loss of 39.29 %.
 377 This endotherm of T_{d2} is related to the dimerization of isocyanates to form carbodiimides and
 378 release CO₂. The formed carbodiimide reacts with alcohol to form urea. The third stage of
 379 thermal degradation (T_{d3}) is related to the degradation of urea (Berta et al. 2006) and the soft
 380 segment on polyurethane.

381

382 Generally, DSC analysis exhibited thermal transitions as well as the initial
 383 crystallization and melting temperatures of the polyurethane (Khairuddin et al. 2018). It serves
 384 to analyze changes in thermal behavior due to changes occurring in the chemical chain structure
 385 based on the glass transition temperature (T_g) of the sample obtained from the DSC thermogram

386 (Figure 7). DSC analysis on polyurethane film was performed in the temperature at the range
387 100 °C to 200 °C of using nitrogen gas as a blanket as proposed by Furtwengler et al. (2017).
388 The glass transition temperature (T_g) on polyurethane was above room temperature, at 78.1 °C
389 indicated the state of glass on polyurethane. The presence of MDI contributes to the formation
390 of hard segments in polyurethanes. Porcarelli et al. (2017) stated that possessing a low glass
391 transition (T_g) may contribute to PU conductivity.



392
393
394

Figure 6. DTG thermogram of polyurethane film

395 During polymerization, this hard segment restricts the mobility of the polymer chain
396 (Ren et al. 2013) owing to the steric effect on the benzene ring in the hard segment. The
397 endothermic peak of acetone used as the solvent in this study was supposedly at 56°C.
398 However, it was detected in the DSC thermogram nor the TGA thermogram, which indicates
399 that acetone was removed from the polyurethane during the synthesis process, owing to its
400 volatile nature. The presence of acetone in the synthesis was to lower the reaction kinetics.

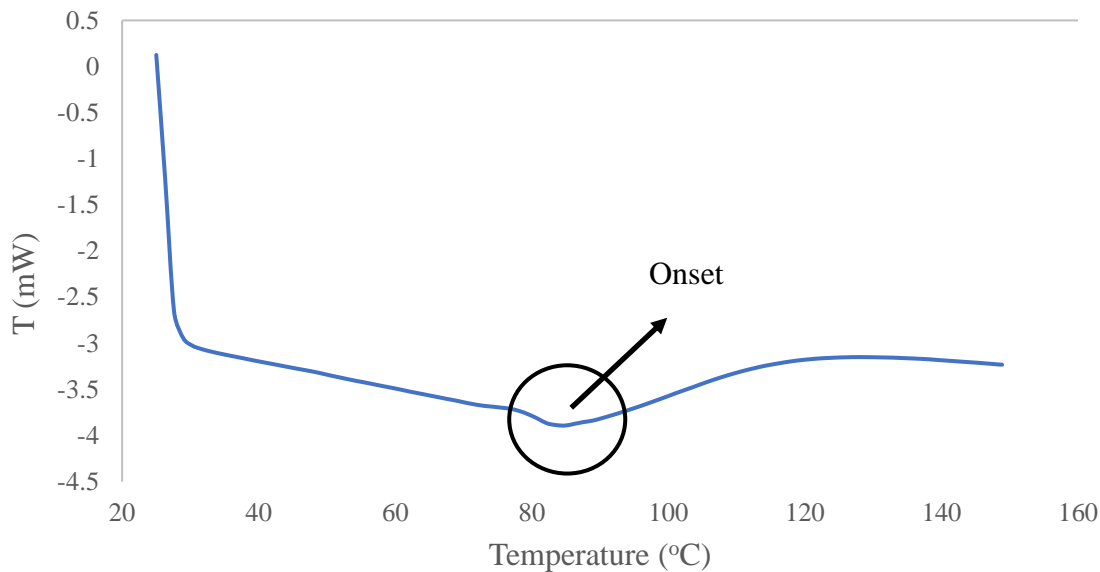


Figure 7. DSC thermogram of polyurethane film

e. The solubility and mechanical properties of the polyurethane film

The chemical resistivity of a polymer will be the determinant in performing as a conductor. Thus, its solubility in various solvents was determined by dissolving the polymer in selected solvents such as hexane, benzene, acetone, tetrahydrofuran (THF), dimethylformamide (DMF), and dimethyl sulfoxide (DMSO). On the other hand, the mechanical properties of polyurethane were determined based on the standard testing following ASTM D 638 (Standard Test Method for Tensile Properties of Plastics). The results from the polyurethane film solubility and tensile test are shown in **Table 3**. Polyurethane films were insoluble with acetone, hexane, and benzene and are only slightly soluble in tetrahydrofuran (THF), dimethylformamide (DMF), and dimethyl sulfoxide (DMSO) solutions. While the tensile strength of a PU film indicated how much elongation load the film was capable of withstanding the material before breaking.

Table 3 The solubility and mechanical properties of the polyurethane film

| Parameters | Polyurethane film |
|------------|-------------------|
|------------|-------------------|

| | | |
|----------------------------|---------|--------------|
| | Benzene | Insoluble |
| | Hexane | Insoluble |
| | Acetone | Insoluble |
| Solubility | THF | Less soluble |
| | DMF | Less soluble |
| | DMSO | Less soluble |
| Stress (MPa) | | 8.53 |
| Elongation percentage (%) | | 43.34 |
| Strain modulus (100) (MPa) | | 222.10 |

418

419 The tensile stress, strain, and modulus of polyurethane film also indicated that polyurethane
420 has good mechanical properties that are capable of being a supporting substrate for the next
421 stage of the study. In the production of polyurethane, the properties of polyurethane are easily
422 influenced by the content of MDI and polyol used. The length of the chain and its flexibility
423 are contributed by the polyol which makes it elastic. High crosslinking content can also produce
424 hard and rigid polymers. MDI is a major component in the formation of hard segments in
425 polyurethane. It is this hard segment that determines the rigidity of the PU. Therefore, high
426 isocyanate content results in higher rigidity on PU (Petrovic et al. 2002). Thus, the polymer has
427 a higher resistance to deformation and more stress can be applied to the PU.

428

429

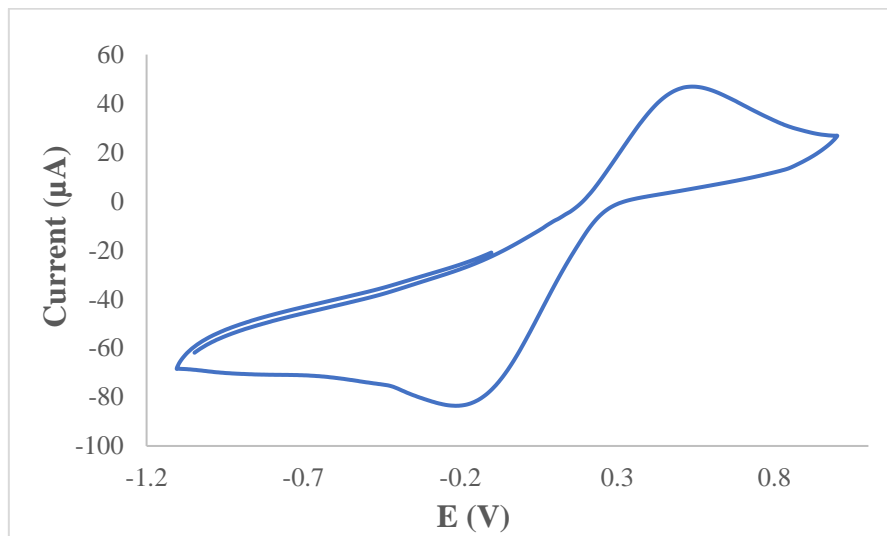
430

431

432 f. The conductivity of the polyurethane as a polymeric film on SPE

433 Polyurethane film was deposited onto the screen-printed electrode by casting method as shown
434 in **Figure 1**. After that, the modified electrode was analyzed using cyclic voltammetry (CV)
435 and differential pulse voltammetry (DPV) in order to study the behavior of the modified
436 electrode. The modified electrode was tested in a $0.1 \text{ mmol}\cdot\text{L}^{-1}$ KCl solution containing 5
437 $\text{mmol}\cdot\text{L}^{-1}$ ($\text{K}_3\text{Fe}(\text{CN})_6$). The use of potassium ferricyanide is intended to increase the sensitivity
438 of the KCl solution. The conductivity of the modified electrode was studied. The electrode was
439 analyzed by cyclic voltammetry method with a potential range of -1.00 to $+1.00$ with a scan
440 rate of $0.05 \text{ V}\cdot\text{s}^{-1}$. The voltammograms at the electrode have shown a specific redox reaction.
441 Furthermore, the conductivity of the modified electrode is lower due to the use of polyurethane.
442 This occurs due to PU being a natural polymer produced from the polyol of palm kernel oil.
443 The electrochemical signal at the electrode is low if there is a decrease in electrochemical
444 conductivity (El - Raheem et al. 2020). It can be concluded that polyurethane is a bio-polymer
445 with a low current value. The current of the modified electrode was found at $5.3 \times 10^{-5} \text{ A}$ or 53
446 μA . Nevertheless, the current of PU in this study showed better results compared to Bahrami
447 et al. (2019) that reported the current of PU as $1.26 \times 10^{-6} \text{ A}$, whereas Li et al. (2019) reported
448 the PU current in their study was even very low, namely 10^{-14} A . The PU can obtain a current
449 owing to the benzene ring in the hard segment (MDI) could exhibit the current by inducing
450 electron delocalization along the polyurethane chain (Wong et al. 2014). The PU can also
451 release a current caused by PEG. The application of PEG as polyol has been studied by
452 Porcarelli et al. (2017), that reported that the current of PU based on PEG – polyol was $9.2 \times$
453 10^{-8} A .

454 According to **Figure 8**, it can be concluded that the anodic peak present in the modified
455 electrode was at $+0.5 \text{ V}$, it also represented the anodic peak of the SPE-PU. The first oxidation
456 signal on both electrodes ranged from -0.2 to $+1.0 \text{ V}$, which revealed a particular oxidative
457 peak at a potential of $+0.5 \text{ V}$.



459

460 **Figure 8.** The voltammogram of SPE – PU modified electrode after analyzed using cyclic
 461 voltammetry (CV) technique

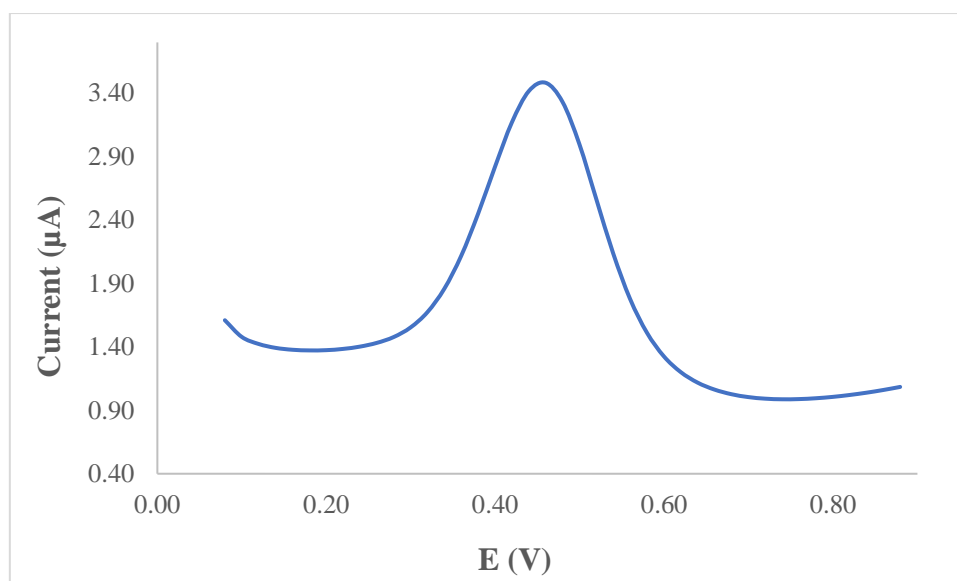
462

463 **Figure 9** also presents the DPV voltammogram of the modified electrode. DPV is a
 464 measurement based on the difference in potential pulses that produce an electric current.
 465 Scanning the capability pulses to the working electrode will produce different currents. Optimal
 466 peak currents will be produced to the reduction capacity of the redox material. The peak current
 467 produced is proportional to the concentration of the redox substance and can be detected up to
 468 a concentration below 10^{-8} M. DPV was conducted to obtain the current value that is more
 469 accurate than CV (Lee et al. 2018).

470 This study used a redox pair ($K_3Fe(CN)_6$) as a test device (probe). The currents generated by
 471 SPE-PU and proved by CV and DPV have shown conductivity on polyurethane films. This
 472 suggests that polyurethane films can conduct electron transfer. The electrochemical area on the
 473 modified electrode can be calculated using the formula from Randles-Sevcik (Butwong et al.
 474 2019), where the electrochemical area for SPE-PU is considered to be A, using Equation 2:

475

$$\text{Current of SPE-PU, } I_p = 2.65 \times 10^5 A C n^{3/2} \nu^{1/2} D^{1/2} \quad (2)$$



476
477 **Figure 9.** The voltammogram of SPE – PU modified electrode after analyzed using
478 differential pulse voltammetry (DPV) technique
479

480 Where, $n - 1$ is the amount of electron transfer involved, while C is the solvent concentration
481 used ($\text{mmol}\cdot\text{L}^{-1}$) and the value of D is the diffusion constant of $5 \text{ mmol}\cdot\text{L}^{-1}$ at $(\text{K}_3\text{Fe}(\text{CN})_6)$
482 dissolved using $0.1 \text{ mmol}\cdot\text{L}^{-1}$ KCl. The estimated surface area of the electrode (**Figure 1**) was
483 0.2 cm^2 where the length and width of the electrode used during the study was $0.44 \text{ cm} \times 0.44$
484 cm while the surface area of the SPE-PU was 0.25 cm^2 with the length and width of the
485 electrode estimated at $0.5 \text{ cm} \times 0.5 \text{ cm}$, and causing the SPE-PU has a larger surface. The
486 corresponding surface concentration (τ) (mol/cm^2) is measured using Equation 3.

$$487 \quad I_p = (n^2 F^2 / 4RT) A \tau v \quad (3)$$

488 I_p is the peak current (A), while A is the surface area of the electrode (cm^2), the value of v is
489 the applied scan rate (mV/s) and F is the Faraday constant ($96,584 \text{ C}/\text{mol}$), R is the constant
490 ideal gas ($8.314 \text{ J}/\text{mol K}$) and T is the temperature used during the experiment being conducted
491 (298 K) (Koita et al. 2014). The application of PKOp to produce a conducting polymer will be
492 a great prospect as this material can be employed in the analytical industry in order to modify
493 electrodes for electrochemical purposes.

494 Furthermore, number of palm oils is abundant in Malaysia and Indonesia such as palm stearin
495 and refined-bleached-deodorized (RBD) palm oil. They have several benefits such as being
496 sustainable, cheap, and environmentally biodegradable. These palms are the potential to
497 produce biomaterials that can be used to replace other polymers that are chemical-based (Tajao
498 et al. 2021). Several studies have been reported the application of PU to produce elastic
499 conductive fibres and films owing to it being highly elastic, scratch-resistant, and adhesive
500 (Tadese et al. 2019), thus it is easy for PU to adhere to the screen-printed electrode to modify
501 the electrode. PU is also being used as a composite material to make elastic conducting
502 composite films (Khatoon & Ahmad 2017).

503

504 **4. Conclusion**

505 Polyurethane film was prepared by pre-polymerization between palm kernel oil-based polyol
506 (PKO-p) with MDI. The presence of PEG 400 as the chain extender formed freestanding
507 flexible film. Acetone was used as the solvent to lower the reaction kinetics since the pre-
508 polymerization was carried out at room temperature. The formation of urethane links (NHCO
509 – backbone) after polymerization was confirmed by the absence of N=C=O peak at 2241 cm^{-1}
510 and the presence of N-H peak at 3300 cm^{-1} , carbonyl (C=O) at 1710 cm^{-1} , carbamate (C-N) at
511 1600 cm^{-1} , ether (C-O-C) at 1065 cm^{-1} , benzene ring (C = C) at 1535 cm^{-1} in the bio
512 polyurethane chain structure. Soxhlet analysis for the determination of crosslinking on
513 polyurethane films has yielded a high percentage of 99.33 %. This is contributed by the hard
514 segments formed from the reaction between isocyanates and hydroxyl groups causing
515 elongation of polymer chains. FESEM analysis exhibited an absence of phase separation and
516 smooth surface. Meanwhile, the current of the modified electrode was found at $5.2 \times 10^{-5}\text{ A}$.
517 This bio polyurethane film can be used as a conducting bio-polymer and it is very useful for

518 other studies such as electrochemical sensor purposes. Furthermore, advanced technologies are
519 promising and the future of bio-based polyol looks very bright.

520 **5. Acknowledgment**

521 The authors would like to thank Alma Ata University for the sponsorship given to the first
522 author. We would like to also, thank The Department of Chemical Sciences, Universiti
523 Kebangsaan Malaysia for the laboratory facilities and CRIM, UKM for the analysis
524 infrastructure.

525

526 **6. Conflict of Interest**

527 The authors declare no conflict of interest.

528

529 **7. References**

530 Agrawal, A., Kaur, R., Walia, R. S. (2017). PU foam derived from renewable sources:
531 Perspective on properties enhancement: An overview. *European Polymer Journal*. **95**:
532 255 – 274.

533 Akindoyo, J. O., Beg, M.D.H., Ghazali, S., Islam, M.R., Jeyaratnam, N. & Yuvaraj, A.R.
534 (2016). Polyurethane types, synthesis, and applications – a review. *RSC Advances*. **6**:
535 114453 – 114482.

536 Alamawi, M. Y., Khairuddin, F. H., Yusoff, N. I. M., Badri, K., Ceylan, H. (2019).
537 Investigation on physical, thermal, and chemical properties of palm kernel oil polyobio-
538 based binder as a replacement for bituminous binder. *Construction and Building*
539 *Materials*. **204**: 122 – 131.

540 Alqarni, S. A., Hussein, M. A., Ganash, A. A. & Khan, A. (2020). Composite material-based
541 conducting polymers for electrochemical sensor applications: a mini-review.
542 *BioNanoScience*. **10**: 351 – 364.

543 Badan, A., Majka, T. M. (2017). The influence of vegetable – oil based polyols on physico –
544 mechanical and thermal properties of polyurethane foams. *Proceedings*. 1 – 7.

545 Badri, K.H. (2012) Biobased polyurethane from palm kernel oil-based polyol. In Polyurethane;
546 Zafar, F., Sharmin, E., Eds. InTechOpen: Rijeka, Croatia. pp. 447–470.

547 Badri, K.H., Ahmad, S.H. & Zakaria, S. 2000. Production of a high-functionality RBD palm
548 kernel oil-based polyester polyol. *Journal of Applied Polymer Science*. **81**(2): 384 – 389.

549 Baig, N., Sajid, M. and Saleh, T. A. 2019. Recent trends in nanomaterial–modified electrodes
550 for electroanalytical applications. *Trends in Analytical Chemistry*. **111**: 47 – 61.

551 Berta, M., Lindsay, C., Pans, G., & Camino, G. (2006). Effect of chemical structure on
552 combustion and thermal behaviour of polyurethane elastomer layered silicate
553 nanocomposites. *Polymer Degradation and Stability*. **91**: 1179-1191.

554 Borowicz, M., Sadowska, J. P., Lubczak, J. & Czuprynski, B. (2019). Biodegradable, flame–
555 retardant, and bio-based rigid polyurethane/polyisocyanurate foams for thermal
556 insulation application. *Polymers*. **11**: 1816 – 1839.

557 Butwong, N., Khajonklin, J., Thongbor, A. & Luong, J.H.T. (2019). Electrochemical sensing
558 of histamine using a glassy carbon electrode modified with multiwalled carbon nanotubes
559 decorated with Ag – Ag₂O nanoparticles. *Microchimica Acta*. **186** (11): 1 – 10.

560 Chokkareddy, R., Thondavada, N., Kabane, B. & Redhi, G. G. (2020). A novel ionic liquid
561 based electrochemical sensor for detection of pyrazinamide. *Journal of the Iranian*
562 *Chemical Society*. **18**: 621 – 629.

563 Chokkareddy, R., Kanchi, S. & Inamuddin (2020). Simultaneous detection of ethambutol and
564 pyrazinamide with IL@CoFe₂O₄NPs@MWCNTs fabricated glassy carbon electrode.
565 *Scientific Reports*. **10**: 13563.

566 Clemitson, I. (2008). Castable Polyurethane Elastomers. Taylor & Francis Group, New York.
567 doi:10.1201/9781420065770.

568 Corcuera, M.A., Rueda, L., Saralegui, A., Martin, M.D., Fernandez-d'Arlas, B., Mondragon,
569 I. & Eceiza, A. (2011). Effect of diisocyanate structure on the properties and
570 microstructure of polyurethanes based on polyols derived from renewable resources.
571 *Journal of Applied Polymer Science*. **122**: 3677-3685.

572 Cuve, L. & Pascault, J.P. (1991). Synthesis and properties of polyurethanes based on
573 polyolefine: Rigid polyurethanes and amorphous segmented polyurethanes prepared in
574 polar solvents under homogeneous conditions. *Polymer*. **32** (2): 343- 352.

575 Degefu, H., Amare, M., Tessema, M. & Admassie, S. (2014). Lignin modified glassy carbon
576 electrode for the electrochemical determination of histamine in human urine and wine
577 samples. *Electrochimica Acta*. **121**: 307 – 314.

578 Dzulkipli, M. Z., Karim, J., Ahmad, A., Dzulkurnain, N. A., Su'ait, M S., Fujita, M. Y., Khoon,
579 L. T. & Hassan, N. H. (2021). The influences of 1-butyl-3-methylimidazolium
580 tetrafluoroborate on electrochemical, thermal and structural studies as ionic liquid gel
581 polymer electrolyte. *Polymers*. **13** (8): 1277 – 1294.

582 El-Raheem, H.A., Hassan, R.Y.A., Khaled, R., Farghali, A. & El-Sherbiny, I.M. (2020).
583 Polyurethane-doped platinum nanoparticles modified carbon paste electrode for the
584 sensitive and selective voltammetric determination of free copper ions in biological
585 samples. *Microchemical Journal*. **155**: 104765.

586 Fei, T., Li, Y., Liu, B. & Xia, C. (2019). Flexible polyurethane/boron nitride composites with
587 enhanced thermal conductivity. *High Performance Polymers*. **32** (3): 1 – 10.

588 Furtwengler, P., Perrin R., Redl, A. & Averous, L. (2017). Synthesis and characterization of
589 polyurethane foams derived of fully renewable polyesters polyols from sorbitol.
590 *European Polymer Journal*. **97**: 319 – 327.

591 Ghosh, S., Ganguly, S., Remanan, S., Mondal, S., Jana, S., Maji, P. K., Singha, N., Das, N. C.
592 (2018). Ultra-light weight, water durable and flexible highly electrical conductive

593 polyurethane foam for superior electromagnetic interference shielding materials. *Journal*
594 *of Materials Science: Materials in Electronics*. **29**: 10177 – 10189.

595 Guo, S., Zhang, C., Yang, M., Zhou, Y., Bi, C., Lv, Q. & Ma, N. (2020). A facile and sensitive
596 electrochemical sensor for non – enzymatic glucose detection based on three –
597 dimensional flexible polyurethane sponge decorated with nickel hydroxide. *Analytica*
598 *Chimica Acta*. **1109**: 130 – 139.

599 Hamuzan, H.A. & Badri, K.H. (2016). The role of isocyanates in determining the viscoelastic
600 properties of polyurethane. *AIP Conference Proceedings*. 1784, Issue 1.

601 Harmayani, E., Aprilia, V. & Marsono, Y. (2014). Characterization of glucomannan from
602 *Amorphophallus oncophyllus* and its prebiotic activity in vivo. *Carbohydrate Polymers*.
603 **112**: 475-79.

604 Herrington, R. & Hock, K. (1997). Flexible polyurethane foams. 2nd Edition. Dow Chemical
605 Company. Midlan.

606 Inayatullah, A., Badrul, H.A., Munir, M.A. (2021). Fish analysis containing biogenic amines
607 using gas chromatography flame ionization detector. *Science and Technology Indonesia*.
608 **6** (1): 1-7.

609 Janpoung, P., Pattanauwat, P. & Potiyaraj, P. (2020). Improvement of electrical conductivity
610 of polyurethane/polypyrrole blends by graphene. *Key Engineering Materials*. **831**: 122 –
611 126.

612 Khairuddin, F.H., Yusof, N. I. M., Badri, K., Ceylan, H., Tawil, S. N. M. (2018). Thermal,
613 chemical and imaging analysis of polyurethane/cecabase modified bitumen. *IOP Conf.*
614 *Series: Materials Science and Engineering*. **512**: 012032.

615 Khatoun, H., Ahmad, S. (2017). A review on conducting polymer reinforced polyurethane
616 composites. *Journal of Industrial and Engineering Chemistry*. **53**: 1 – 22.

617 Kilele, J. C., Chokkareddy, R., Rono, N. & Redhi, G. G. (2020). A novel electrochemical
618 sensor for selective determination of theophylline in pharmaceutical formulations.
619 *Journal of the Taiwan Institute of Chemical Engineers*. 111: 228-238.

620 Kilele, J. C., Chokkareddy, R. & Redhi, G. G. (2021). Ultra-sensitive electrochemical sensor
621 for fenitrothion pesticide residues in fruit samples using IL@CoFe₂ONPs@MWCNTs
622 nanocomposite. *Microchemical Journal*. **164**: 106012.

623 Koita, D., Tzedakis, T., Kane, C., Diaw, M., Sock, O. & Lavedan, P. (2014). Study of the
624 histamine electrochemical oxidation catalyzed by nickel sulfate. *Electroanalysis*. **26 (10)**:
625 2224 – 2236.

626 Kotal, M., Srivastava, S.K. & Paramanik, B. (2011). Enhancements in conductivity and thermal
627 stabilities of polyurethane/polypyrrole nanoblends. *The Journal of Physical Chemistry*
628 *C*. **115 (5)**: 1496 – 1505.

629 Ladan, M., Basirun, W.J., Kazi, S.N., Rahman, F.A. (2017). Corrosion protection of AISI 1018
630 steel using Co-doped TiO₂/polypyrrole nanocomposites in 3.5% NaCl solution.
631 *Materials Chemistry and Physics*. **192**: 361 – 373.

632 Lampman, G.M., Pavia, D.L., Kriz, G.S. & Vyvyan, J.R. (2010). Spectroscopy. 4th Edition.
633 Brooks/Cole Cengage Learning, Belmont, USA.

634 Lee, K.J., Elgrishi, N., Kandemir, B. & Dempsey, J.L. 2018. Electrochemical and spectroscopic
635 methods for evaluating molecular electrocatalysts. *Nature Reviews Chemistry*. **1(5)**: 1 -
636 14.

637 Leykin, A., Shapovalov, L. & Figovsky, O. (2016). Non – isocyanate polyurethanes –
638 Yesterday, today and tomorrow. *Alternative Energy and Ecology*. **191 (3 – 4)**: 95 – 108.

639 Li, H., Yuan, D., Li, P., He, C. (2019). High conductive and mechanical robust carbon
640 nanotubes/waterborne polyurethane composite films for efficient electromagnetic
641 interference shielding. *Composites Part A*. **121**: 411 – 417.

642 Nakthong, P., Kondo, T., Chailapakul, O., Siangproh, W. (2020). Development of an
643 unmodified screen-printed electrode for nonenzymatic histamine detection. *Analytical*
644 *Methods*. **12**: 5407 – 5414.

645 Mishra, K., Narayan, R., Raju, K.V.S.N. & Aminabhavi, T.M. (2012). Hyperbranched
646 polyurethane (HBPU)-urea and HBPU-imide coatings: Effect of chain extender and
647 NCO/OH ratio on their properties. *Progress in Organic Coatings*. **74**: 134 – 141.

648 Mohd Noor, M. A., Tuan Ismail, T. N. M., Ghazali, R. (2020). Bio-based content of oligomers
649 derived from palm oil: Sample combustion and liquid scintillation counting technique.
650 *Malaysia Journal of Analytical Science*. **24**: 906 – 917.

651 Munir, M. A., Heng, L. Y., Badri, K. H. (2021). Polyurethane modified screen-printed
652 electrode for the electrochemical detection of histamine in fish. *IOP Conference Series:*
653 *Earth and Environmental Science*. **880**: 012032.

654 Munir, M.A., Mackeen, M.M.M., Heng, L.Y. Badri, K.H. (2021). Study of histamine detection
655 using liquid chromatography and gas chromatography. *ASM Science Journal*. **16**: 1-9.

656 Mutsuhisa F., Ken, K. & Shohei, N. (2007). Microphase separated structure and mechanical
657 properties of norbornane diisocyanate-based polyurethane. *Polymer*. **48 (4)**: 997 – 1004.

658 Mustapha, R., Rahmat, A. R., Abdul Majid, R., Mustapha, S. N. H. (2019). Vegetable oil-based
659 epoxy resins and their composites with bio-based hardener: A short review. *Polymer-*
660 *Plastic Technology and Materials*. **58**: 1311 – 1326.

661 Nohra, B., Candy, L., Blancos, J.F., Guerin, C., Raoul, Y. & Mouloungui, Z. (2013). From
662 petrochemical polyurethanes to bio-based polyhydroxyurethanes. *Macromolecules*. **46**
663 **(10)**: 3771 – 3792.

664 Nurwanti, E., Uddin, M., Chang, J.S., Hadi, H., Abdul, S.S., Su, E.C.Y., Nursetyo, A.A.,
665 Masud, J.H.B. & Bai, C.H. (2018). Roles of sedentary behaviors and unhealthy foods in

666 increasing the obesity risk in adult men and women: A cross-sectional national study.
667 *Nutrients*. **10** (6): 704-715.

668 Pan, T. & Yu, Q. (2016). Anti-corrosion methods and materials comprehensive evaluation of
669 anti-corrosion capacity of electroactive polyaniline for steels. *Anti – Corrosion Methods
670 and Materials*. **63**: 360 – 368.

671 Pan, X. & Webster, D.C. (2012). New biobased high functionality polyols and their use in
672 polyurethane coatings. *ChemSusChem*. **5**: 419-429.

673 Petrovic, Z.S. (2008). Polyurethanes from vegetable oils. *Polymer Reviews*. **48** (1): 109 – 155.

674 Porcarelli, L., Manojkumar, K., Sardon, H., Llorente, O., Shaplov, A. S., Vijayakrishna, K.,
675 Gerbaldi, C., Mecerreyes, D. (2017). Single ion conducting polymer electrolytes based
676 on versatile polyurethanes. *Electrochimica Acta*. **241**: 526 – 534.

677 Priya, S. S., Karthika, M., Selvasekarapandian, S. & Manjuladevi, R. (2018). Preparation and
678 characterization of polymer electrolyte based on biopolymer I-carrageenan with
679 magnesium nitrate. *Solid State Ionics*. **327**: 136 – 149.

680 Ren, D. & Frazier, C.E. (2013). Structure–property behaviour of moisture-cure polyurethane
681 wood adhesives: Influence of hard segment content. *Adhesion and Adhesives*. **45**: 118-
682 124.

683 Rogulska, S.K., Kultys, A. & Podkoscielny, W. (2007). Studies on thermoplastic polyurethanes
684 based on newdiphe – derivative diols. II. Synthesis and characterization of segmented
685 polyurethanes from HDI and MDI. *European Polymer Journal*. **43**: 1402 – 1414.

686 Romaskevicius, T., Budriene, S., Pielichowski, K. & Pielichowski, J. (2006). Application of
687 polyurethane-based materials for immobilization of enzymes and cells: a review.
688 *Chemija*. **17**: 74 – 89.

689 Sengodu, P. & Deshmukh, A. D. (2015). Conducting polymers and their inorganic composites
690 for advanced Li-ion battery electrolytes: a review. *RSC Advances*. **5**: 42109 – 42130.

691 Septevani, A. A., Evans, D. A. C., Chaleat, C., Martin, D. J., Annamalai, P. K. (2015). A
692 systematic study substituting polyether polyol with palm kernel oil based polyester
693 polyol in rigid polyurethane foam. *Industrial Crops and Products*. **66**: 16 – 26.

694 Su'ait, M. S., Ahmad, A., Badri, K. H., Mohamed, N. S., Rahman, M. Y. A., Ricardi, C. L. A.
695 & Scardi, P. The potential of polyurethane bio-based solid polymer electrolyte for
696 photoelectrochemical cell application. *International Journal of Hydrogen Energy*. **39** (6):
697 3005 – 3017.

698 Tadesse, M. G., Mengistie, D. A., Chen, Y., Wang, L., Loghin, C., Nierstrasz, V. (2019).
699 Electrically conductive highly elastic polyamide/lycra fabric treated with PEDOT: PSS
700 and polyurethane. *Journal of Materials Science*. **54**: 9591 – 9602.

701 Tajau, R., R, Rosiah, Alias, M. S., Mudri, N. H., Halim, K. A. A., Harun, M. H., Isa, N. M.,
702 Ismail, R. C., Faisal, S. M., Talib, M., Zin, M. R. M., Yusoff, I. I., Zaman, N. K., Illias,
703 I. A. (2021). Emergence of polymeric material utilising sustainable radiation curable
704 palm oil-based products for advanced technology applications. *Polymers*. **13**: 1865 –
705 1886.

706 Tran, V.H., Kim, J.D., Kim, J.H., Kim, S.K., Lee, J.M. (2020). Influence of cellulose
707 nanocrystal on the cryogenic mechanical behaviour and thermal conductivity of
708 polyurethane composite. *Journal of Polymers and The Environment*. **28**: 1169 – 1179.

709 Viera, I.R.S., Costa, L.D.F.D.O., Miranda, G.D.S., Nardehhcia, S., Monteiro, M.S.D. S.D.B.,
710 Junior, E.R. & Delpech, M.C. (2020). Waterborne poly (urethane – urea)s
711 nanocomposites reinforced with clay, reduced graphene oxide and respective hybrids:
712 Synthesis, stability and structural characterization. *Journal of Polymers and The
713 Environment*. **28**: 74 – 90.

714 Wang, B., Wang, L., Li, X., Liu, Y., Zhang, Z., Hedrick, E., Safe, S., Qiu, J., Lu, G. & Wang,
715 S. (2018). Template-free fabrication of vertically–aligned polymer nanowire array on the

716 flat–end tip for quantifying the single living cancer cells and nanosurface interaction. a
717 *Manufacturing Letters*. **16**: 27 – 31.

718 Wang, J., Xiao, L., Du, X., Wang, J. & Ma, H. (2017). Polypyrrole composites with carbon
719 materials for supercapacitors. *Chemical Papers*. **71** (2): 293 – 316.

720 Wong, C.S. & Badri, K.H. (2012). Chemical analyses of palm kernel oil-based polyurethane
721 prepolymer. *Materials Sciences and Applications*. **3**: 78 – 86.

722 Wong, C. S., Badri, K., Ataollahi, N., Law, K., Su'ait, M. S., Hassan, N. I. (2014). Synthesis
723 of new bio–based solid polymer electrolyte polyurethane – LiClO₄ via prepolymerization
724 method: Effect of NCO/OH ratio on their chemical, thermal properties and ionic
725 conductivity. *World Academy of Science, Engineering and Technology, International*
726 *Journal of Chemical, Molecular, Nuclear, Materials and Metallurgical Engineering*. **8**:
727 1243 – 1250.

728 Yong, Z., Bo, Z.M., Bo, W., Lin, J.Z. & Jun, N. (2009). Synthesis and properties of novel
729 polyurethane acrylate containing 3-(2-Hydroxyethyl) isocyanurate segment. *Progress in*
730 *Organic Coatings*. **67**: 264 – 268

731 Zia, K. M., Anjum, S., Zuber, M., Mujahid, M. & Jamil, T. (2014). Synthesis and molecular
732 characterization of chitosan based polyurethane elastomers using aromatic diisocyanate.
733 *International of Journal of Biological Macromolecules*. **66**: 26 – 32.

734

735

736

737

738

739

740

Hasil Reviu 6 dan Submit Revisi: 13 Februari 2022

Decision

Minor Revision Requested

Message for Author

1. "bio based" is one word and should be spelled the same way throughout the text. Please correct throughout the text.

"Please correct throughout the text" means using the search option to find "bio based" throughout the text. The reviewer only has to point out what is wrong. Please correct in lines 77 and 518.

2. Conclusion: "and the presence of N-H peak at 3300 cm⁻¹"

N-H is also not a peak. Neither linkage is a peak.

Please correct on: "and the presence of absorption bands associated with N-H at 3300 cm⁻¹"

Please also correct throughout the text!

3. Table 2.

The table shows the "Thermal degradation parameters determined by TGA".

Please remove "% Weight loss (wt%) and thermal degradation (Td)" from the table and leave only two rows with variables (first) and data (second).

Thermogravimetric analysis is measurement of thermal stability of materials. In this method, changes in the weight of a specimen are measured while its temperature is increased. It does not need to be written in the row of table.

In this section (d. The thermal analysis), the authors write both mass and weight.

Please change everything to mass.

Line 369 "Tmax: The temperature of polyurethane started to degrade"

Tmax represents the temperature at the maximum mass-loss rate. "The temperature of material started to degrade" is onset temperature usually given for 5% (T5%) because it is difficult to accurately determine the beginning (Tonset). What temperature did the authors mean?

The authors rightly speak of "individual mass steps"

Td1 is probably temperature at the first onset or at the first Tmax (at the first mass loss step).

Please use the IUPAC nomenclature and correctly present and describe the TGA variables (<https://www.degruyter.com/database/iupac/html>).

— Response to Revision Request

Muhammad Abdurrahman Munir

13.02.2022

Your Reply

Dear Dr. Joanna, Thank you for your comments and we have done revisions based on your comments above. Nevertheless, for the comment no. 6, we want to elaborate about the Tmax, where according to Figure 7. DTG thermogram of PU film, Page 19. The temperature was started to degrade at 240 C, that's why we called it as Tmax. So, the Td1, Td2 and Td3 in this manuscript are the thermal degradation

that we have plotted based on the specific region. However, if the revisions we have made are not sufficient, please guide us to improve this manuscript so it can be published to this Journal. We are looking forward to hear from you. Best Regards.

File

Manuscript - Munir.docx 902 kB



1 **Design and Synthesis of Conducting Polymer Based on Polyurethane**
2 **Produced from Palm Kernel Oil**

3
4 Muhammad Abdurrahman Munir^{1*}, Khairiah Haji Badri^{2,3}, Lee Yook Heng², Ahlam
5 Inayatullah⁴, Ari Susiana Wulandari¹, Emelda¹, Eliza Dwinta¹, Veriani Aprillia⁵, Rachmad
6 Bagas Yahya Supriyono¹

7
8 ¹Department of Pharmacy, Faculty of Health Science, Alma Ata University, Daerah Istimewa
9 Yogyakarta, 55183, Indonesia

10 ²Department of Chemical Sciences, Faculty of Science and Technology, Universiti
11 Kebangsaan Malaysia, Bangi, 43600, Malaysia

12 ³Polymer Research Center, Universiti Kebangsaan Malaysia, Bangi, 43600, Malaysia

13 ⁴Faculty of Science and Technology, Universiti Sains Islam Malaysia, Nilai, 71800, Malaysia

14 ⁵Department of Nutrition Science, Alma Ata School of Health Sciences, Alma Ata
15 University, Daerah Istimewa Yogyakarta, 55183, Indonesia

16
17 *Email: muhammad@almaata.ac.id

18
19 **Abstract**

20 Polyurethane (PU) is a unique polymer that has versatile processing methods and mechanical
21 properties upon the inclusion of selected additives. In this study, a freestanding **bio based**
22 **polyurethane** film the screen-printed electrode (SPE) was prepared by the solution casting
23 technique, using acetone as solvent. It was a one-pot synthesis between major reactants namely,
24 palm kernel oil-based polyol and 4,4-methylene diisocyanate. The PU has strong adhesion on

Commented [j1]: What the authors mean by "bio-polyurethane"? Bio-based or for medical purpose? The title given should be bio-based. Please correct.

Commented [MAM2R1]: The use of bio in this statement owing to the application of palm kernel oil acts as a polyol.

25 the SPE surface. The synthesized polyurethane was characterized using thermogravimetry
26 analysis, differential scanning calorimetry, Fourier-transform infrared spectroscopy (FTIR),
27 surface area analysis by field emission scanning electron microscope, and cyclic voltammetry.
28 Cyclic voltammetry was employed to study electro-catalytic properties of SPE-polyurethane
29 towards oxidation of PU. Remarkably, SPE-PU exhibited improved anodic peak current as
30 compared to SPE itself using the differential pulse voltammetry method. Furthermore, the
31 formation of urethane linkages ($-\text{NHC}(\text{O})$ backbone) after polymerization was analyzed using
32 FTIR and confirmed by the absence of $\text{N}=\text{C}=\text{O}$ peak at 2241 cm^{-1} . The glass transition
33 temperature of the polyurethane was detected at $78.1\text{ }^{\circ}\text{C}$.

35 **Keywords:** polyurethane, polymerization, screen-printed electrode, voltammetry

38 1. Introduction

39 Conducting polymers (CPs) are polymers that can release a current (Alqarni et al. 2020). The
40 conductivity of CPs was first observed in polyacetylene, nevertheless owing to its instability,
41 the invention of various CPs have been studied and reported such as polyaniline (PANI),
42 poly(*o*-toluidine) (PoT), polythiophene (PTH), polyfluorene (PF), and polyurethane (PU).
43 Furthermore, natural CPs have low conductivity and are often semi-conductive. Therefore, it
44 is imperative to improve their conductivity for electrochemical sensor purposes (Sengodu &
45 Deshmukh 2015; Dzulkipli et al. 2021; Wang et al. 2018). The CPs can be produced from many
46 organic materials and they have several advantages such as having an electrical current,
47 inexpensive materials, massive surface area, small dimensions, and the production is
48 straightforward. Furthermore, according to these properties, many studies have been reported
49 by researchers to study and report the variety of CPs applications such as sensors, biochemical

Commented [j3]: Please clean up the groups and backbones that are presented differently each time. For example -NHC(O)

Commented [MAM4R3]: Done

Commented [j5]: $\text{N}=\text{C}=\text{O}$ is not a peak. Functional groups give characteristic signals in a spectrum. Please use scientific language throughout your text and please describe the FTIR spectra properly.

Commented [MAM6R5]: Thank you for your suggestion. Nevertheless, the reading of this spectrum based on Spectroscopy book 4th Edition by Lampman et al. It is written on Page 29, 77 and 78 (Figure 2.64) about the spectrum of $\text{N}=\text{C}=\text{O}$. According to their research, the isocyanates have *sp*-hybridized carbon atoms similar to the $\text{C}\equiv\text{C}$ bond. The absorption occurs in $2100\text{-}2270\text{ cm}^{-1}$.

Commented [j7]: What do "natural CPs" mean? Natural polymers occurring in nature?

Commented [MAM8R7]: This statement about natural polymers, we acquired from the manuscript that studied by Bharadwaz & Jayasuriya 2020 (doi.org/10.1016/j.msec.2020.110698).

This paper has studied about the natural polymer and the synthetic polymer.

50 applications, electrochromic devices, and solar cells (Alqarni et al. 2020; Ghosh et al. 2018).
51 There is scientific documentation on the use of conductive polymers in various studies such as
52 polyaniline (Pan & Yu 2016), polypyrrole (Ladan et al. 2017), and polyurethane (Tran et al.
53 2020; Vieira et al. 2020; Guo et al. 2020; Fei et al. 2020).

54
55 Polyurethane productions can be obtained by using several materials as polyols such as
56 petroleum, coal, and crude oils. Nevertheless, these materials have become very rare to find
57 and the price is very expensive at the same time required a sophisticated system to produce it.

58 The reasons such as price and time consuming to produce polyols have been considered by
59 many researchers, furthermore, finding utilizing plants that can be used as alternative polyols
60 should be done immediately (Badri 2012). Thus, to avoid the use of petroleum, coal, and crude
61 oils as raw materials for a polyol, vegetable oils become a better choice to produce polyol in
62 order to obtain a biodegradable polymer. Vegetable oils that are generally used for
63 polyurethane synthesis are soybean oil, corn oil, sunflower seed oil, coconut oil, nuts oil,
64 rapeseed, olive oil, and palm oil (Badri 2012; Borowicz et al. 2019).

65
66 It is very straightforward for vegetable oils to react with a specific group to produce a PU such
67 as epoxy, hydroxyl, carboxyl, and acrylate owing to the existence of (-C=C-) in vegetable oils.
68 Thus, it provides appealing profits to vegetable oils compared to petroleum considering the
69 toxicity, price, and harm to the environment (Mustapha et al. 2019; Mohd Noor et al. 2020).

70 Palm oil becomes the chosen in this study to produce PU owing to it being largely cultivated
71 in South Asia particularly in Malaysia and Indonesia. It has several profits compared to other
72 vegetable oils such as the easiest materials obtained, the lowest cost of all the common
73 vegetable oils, and recognized as the plantation that has a low environmental impact and
74 removing CO₂ from the atmosphere as a net sequester (Tajau et al. 2021; Septevani et al. 2015).

75
76 The application of bio-based polymer has appealed much attention until now. Global
77 environmental activists have forced researchers to discover another material producing
78 polymers (Priya et al. 2018). PUs have many advantages that have been used by many
79 researchers, they are not merely versatile materials but also have the durability of metal and
80 the flexibility of rubber. Furthermore, they can be promoted to replace rubber, metals, and
81 plastics in several aspects. Several applications of PUs have been reported and studied such as
82 textiles, automotive, building and construction applications, and biomedical applications (Zia
83 et al. 2014; Romaskevicius et al. 2006). Polyurethanes are also considered to be one of the most
84 useful materials with many profits such as; possessing low conductivity, low density,
85 absorption capability, and dimensional stability. They are a great research subject due to their
86 mechanical, physical, and chemical properties (Badan & Majka 2017; Munir et al. 2021).

87
88 PU structure contains the urethane group that can be formed from the reaction between
89 isocyanate groups (-NCO) and hydroxyl group (-OH). Nevertheless, several groups can be
90 found in PU structure such as urea, esters, ethers, and several aromatic groups. Furthermore,
91 PUs can be produced from different sources as long as they contain specific materials (polyol
92 and methylene diphenyl diisocyanate (MDI) and making them very useful for specific
93 applications. Thus, according to the desired properties, PUs can be divided into several types
94 such as waterborne, flexible, rigid, coating, binding, sealants, adhesives, and elastomers
95 (Akindoyo et al. 2016).

96
97 PUs are lighter than other materials such as metals, gold, and platinum. The hardness of PU
98 also relies on the number of the aromatic rings in the polymer structure (Janpoung et al, 2020;
99 Su'ait et al. 2014), majorly contributed by the isocyanate derivatives. PUs have also a conjugate

Commented [j9]: Authors should be careful when using the prefix "bio", as it gives words a strictly defined meaning (biopolymers, bioplastics, biomaterials). According IUPAC biopolymers are macromolecules formed by living organisms (including proteins, nucleic acids and polysaccharides). The authors, however, probably mean something else. Please correct.

Commented [MAM10R9]: Done. The authors want to stated the biopolymer owing to the bio polyol was applied in this study, namely palm kernel oil

Commented [j11]: Reviewer's note 5 was not taken into account. Please correct.

Commented [MAM12R11]: Done

Commented [j13]: The abbreviation should be explained where it is first used.

Commented [MAM14R13]: Done

100 structure where electrons can move in the main chain that causes electricity produced even the
101 current is low. The current of conjugated linear (π) can be elaborated by the gap between the
102 valence band and the conduction band, or called high energy level containing electrons
103 (HOMO) and lowest energy level not containing electrons (LUMO), respectively (Wang et al.
104 2017; Kotal et al. 2011).

105
106 In the recent past, several conventional methods have been developed such as capillary
107 electrophoresis, liquid, and gas chromatography coupled with several detectors. Nevertheless,
108 although chromatographic and spectrometric approaches are well developed for qualitative and
109 quantitative analyses of analytes, several limitations emerged such as complicated
110 instrumentation, expensive, tedious sample preparations, and requiring large amounts of
111 expensive solvents that will harm the users and environment (Kilele et al. 2020; Inayatullah et
112 al. 2021; Munir et al. 2021; Harmayani et al. 2014; Nurwanti et al. 2018). Therefore, it is
113 imperative to obtain and develop an alternative material that can be used to analyze a specific
114 analyte. Electrochemical methods are extremely promising methods in the determination of an
115 analyte in samples owing to the high selectivities, sensitivities, inexpensive, requirements of
116 small amounts of solvents, and can be operated by people who have no background in analytical
117 chemistry. In addition, sample preparation such as separation and extraction steps are not
118 needed owing to the selectivity of this instrument where no obvious interference on the current
119 response is recorded (Chokkareddy et al. 2020). Few works have been reported on the
120 electrochemical methods for the determination of analyte using electrodes combined with
121 several electrode modifiers such as carbon nanotube, gold, and graphene (Chokkareddy et al.
122 2020; Kilele et al. 2021). Nevertheless, the materials are expensive and the production is
123 difficult. Thus, an electrochemical approach using inexpensive and easily available materials
124 as electrode modifiers should be developed (Degefu et al. 2014; Munir et al. 2022).

125 Nowadays, screen-printed electrodes (SPEs) modified with conducting polymer have been
126 developed for various electrochemical sensing. SPE becomes the best solution owing to the
127 electrode having several advantages such as frugal manufacture, tiny size, being able to
128 produce on a large scale, and can be applied for on-site detection (Nakthong et al. 2020).
129 Conducting polymers (CPs) become an alternative to modifying the screen-printed electrodes
130 due to their electrical conductivity, able to capture analyte by chemical/physical adsorption,
131 large surface area, and making CPs are very appealing materials from electrochemical
132 perspectives (Baig et al. 2019). Such advantages of SPE encourage us to construct a new
133 electrode for electrochemical sensing, and no research reported on the direct electrochemical
134 oxidation of histamine using a screen-printed electrode modified by polyurethane. Therefore,
135 this research is the first to develop a new electrode using (screen printed polyurethane
136 electrode) SPPE without any conducting materials.

137

138 The purpose of this work was to synthesise, characterize and study the electro behavior of
139 polyurethane using cyclic voltammetry (CV) and differential pulse voltammetry (DPV)
140 attached to the screen-printed electrode. To the best of our knowledge, this is the first attempt
141 to use a modified polyurethane electrode. The electrochemistry of polyurethane mounted onto
142 SPE is discussed in detail. PUs are possible to become an advanced frontier material that has
143 been chemically modified the specific electrodes for bio/chemical sensing application.

144

145 2. Experimental

146 2.1 Chemicals

147 *Synthesis of polyurethane film:* Palm kernel oil (PKOp) based polyol supplied by UKM
148 Technology Sdn Bhd through MPOB/UKM station plant, Pekan Bangi Lama, Selangor and
149 prepared using Badri et al. (2000) method. 4, 4-diphenylmethane diisocyanate (MDI) was

Commented [j15]: Is this palm kernel oil-based polyol? Please select one writing option also for the abbreviation. There are 3 types in the text. And please explain the abbreviation only once. This applies to all abbreviations. Please correct it throughout.

Commented [MAM16R15]: Yes, the Palm Kernel Oil acts as polyol for this study. The revisions have been followed.

150 acquired from Cosmopolyurethane (M) Sdn. Bhd., Klang, Malaysia. Solvents and analytical
151 reagents were benzene, toluene, hexane, acetone, dimethylsulfoxide (DMSO),
152 dimethylformamide (DMF), tetrahydrofuran (THF), (the purity of solvents is $\geq 99.8\%$), and
153 polyethylene glycol (PEG) with a molecular weight of 400 Da obtained from Sigma Aldrich
154 Sdn Bhd, Shah Alam.

155

156 2.2 Apparatus

157 Tensile testing was performed using a universal testing machine model Instron 5566 following
158 ASTM D638 (Standard Test Method for Tensile Properties of Plastics). The tensile properties
159 of the polyurethane film were measured at a velocity of 10 mm/min with a cell load of 5 kN.

160 The thermal properties were performed using thermogravimetry analysis (TGA) and
161 differential scanning calorimetry (DSC) analysis. TGA was performed using a thermal analyzer
162 of the Perkin Elmer Pyris model with a heating rate of 10 °C/min at a temperature range of 30
163 to 800 °C under a nitrogen gas atmosphere. The DSC analysis was performed using a thermal
164 analyzer of the Perkin Elmer Pyris model with a heating rate of 10 °C /minute at a temperature
165 range of -100 to 200 °C under a nitrogen gas atmosphere. Approximately, 5–10 mg of PU was
166 weighed. The sample was heated from 25 to 150 °C for one minute, then cooled immediately
167 from 150 to 100 °C for another one minute and finally, reheated to 200 °C at a rate of 10 °C
168 /min. At this point, the polyurethane encounters changing from elastic properties to brittle due
169 to changes in the movement of the polymer chains. Therefore, the temperature in the middle of
170 the inclined regions is taken as the glass transition temperature (T_g). The melting temperature
171 (T_m) is identified as the maximum endothermic peak by taking the area below the peak as the
172 enthalpy point (ΔH_m).

173

Commented [j17]: Different purity?

Commented [MAM18R17]: Similar purity, yet different solvents. that's why the authors write all of solvents purity.

174 The morphological analysis of PU film was performed by field emission scanning electron
175 microscope (FESEM) model Gemini SEM microscope model 500-70-22. Before the analysis
176 was carried out, the polyurethane film was coated with a thin layer of gold to increase the
177 conductivity of the film. The coating method was carried out using a sputter-coater. The
178 observations were conducted at a magnification of 200× and 5000× with 10.00 kV (Electron
179 high tension – EHT).

Commented [j19]: The notation should be the same.
Please correct through the text

Commented [MAM20R19]: Done.

180
181 The crosslinking of PU was determined using the soxhlet extraction method. About 0.60 g of
182 PU sample was weighed and put in an extractor tube containing 250 ml of toluene, used as a
183 solvent. This flow of toluene was let running for 24 h. Mass of the PU was weighed before and
184 after the reflux process was carried out. Then, the sample was dried in the conventional oven
185 at 100 °C for 24 h in order to get a constant mass. The percentage of crosslinking content
186 known as the gel content can be calculated using Equation (1).

$$187 \quad \text{Gel content (\%)} = \frac{W_0 - W}{W} \times 100 \% \quad (1)$$

188 W_0 is the mass of PU before the reflux process (g) and W is the mass of PU after the reflux
189 process (g).

190
191 FTIR spectroscopic analysis was performed using a Perkin-Elmer Spectrum BX instrument
192 using the diamond attenuation total reflectance (DATR) method to confirm the polyurethane,
193 PKOp, and MDI functional group. FTIR spectroscopic analysis was performed at a
194 wavenumber of 4000 to 600 cm^{-1} to identify the peaks of the major functional groups in the
195 formation of the polymer such as amide group (-NH), urethane carbonyl group (-C=O),
196 isocyanate group (-O=C=N-), and carbamate group (-CN).

197

198

199

200 2.3 Synthesis of Polyurethane

201 Firstly, the polyol prepolymer solution was produced by combining palm kernel oil-based
202 polyol and poly(ethylene glycol) (PEG) 400 (100:40 g/g), acetone 30% was used as a solution.

203 The compound was homogenized using a centrifuge (100 rpm) for 5 min. Whereas diisocyanate
204 prepolymer was obtained by mixing 4,4'-diphenylmethane diisocyanate (100 g) to acetone
205 30%, afterward the mixture was mixed using a centrifuge for 1 min to obtain a homogenized
206 solution. Afterward, diisocyanate solution (10 g) was poured into a container that contains
207 polyol prepolymer solution (10 g) slowly to avoid an exothermic reaction occurring. The
208 mixture was mixed for 30 sec until a homogenized solution was acquired. Lastly, the
209 polyurethane solution was poured on the electrode surface by using the casting method and
210 dried at ambient temperature for 12 h.

211

212 2.4 Modification of Electrode

213 Voltammetric tests were performed using Metrohm Autolab Software (**Figure 1**) analyzer
214 using cyclic voltammetry method or known as amperometric mode and differential pulse
215 voltammetry. All electrochemical experiments were carried out using screen-printed electrode
216 (diameter 3 mm) modified using polyurethane film as working electrode, platinum wire as the
217 auxiliary electrode, and Ag/AgCl electrode as a reference electrode. All experiments were
218 conducted at a temperature of 20 ± 2 °C.

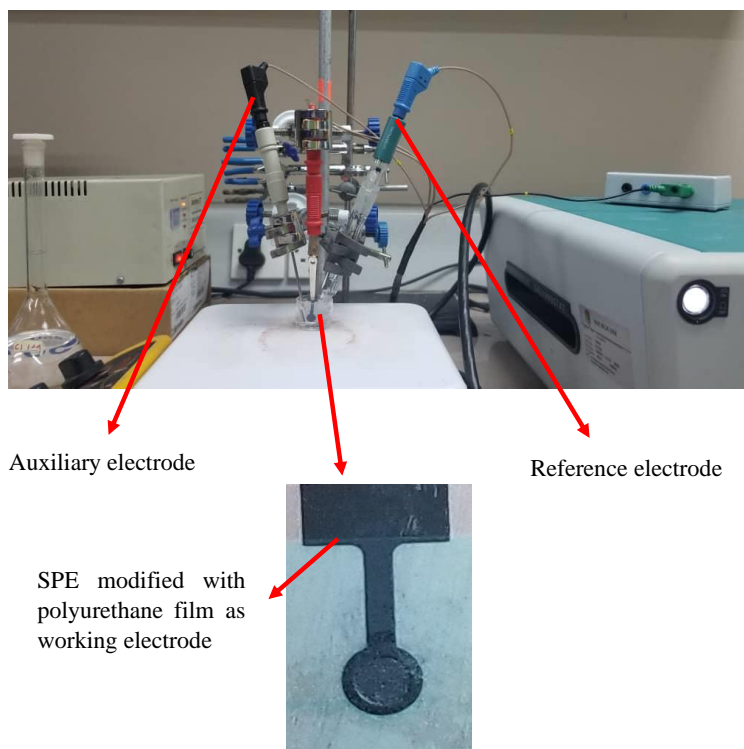
219

220 The PU was cast onto the screen-printed electrode (SPE) and analyzed using a single
221 voltammetric cycle between -1200 and +1500 mV (vs Ag/AgCl) of ten cycles at a scanning
222 rate of 100 mV/s in 5 ml of KCl in order to study the activity of SPE and polyurethane film.

223 Approximately (0.1, 0.3 and 0.5) mg of palm-based pre-polyurethane was dropped separately
224 onto the surface of the SPE and dried at room temperature. The modified palm-based

Commented [j21]: According IUPAC nomenclature names of polymers whose monomers consist of two words or more are written with parentheses

225 polyurethane electrodes were then rinsed with deionized water to remove physically adsorbed
226 impurities and residues of unreacted material on the electrode surface. All electrochemical
227 materials and calibration measurements were carried out in a 5 mL glass beaker with a
228 configuration of three electrodes inside it. Platinum wire and silver/silver chloride (Ag/AgCl)
229 electrodes were used as auxiliary and reference electrodes, while a screen-printed electrode
230 that had been modified with polyurethane was applied as a working electrode.



231 **Figure 1.** Potentiostat instrument to study the conductivity of SPE modified with
232 polyurethane film using voltammetric approach: CV and DPV

233

234 3. Results and Discussion

235 The synthesis of PU films was carried out using a pre-polymerization method which involves
236 the formation of urethane polymer at an early stage. The reaction took place between

237 diisocyanate (MDI) and palm kernel oil-based polyol. **Table 1** presents the PKO-p properties
238 used in this study.

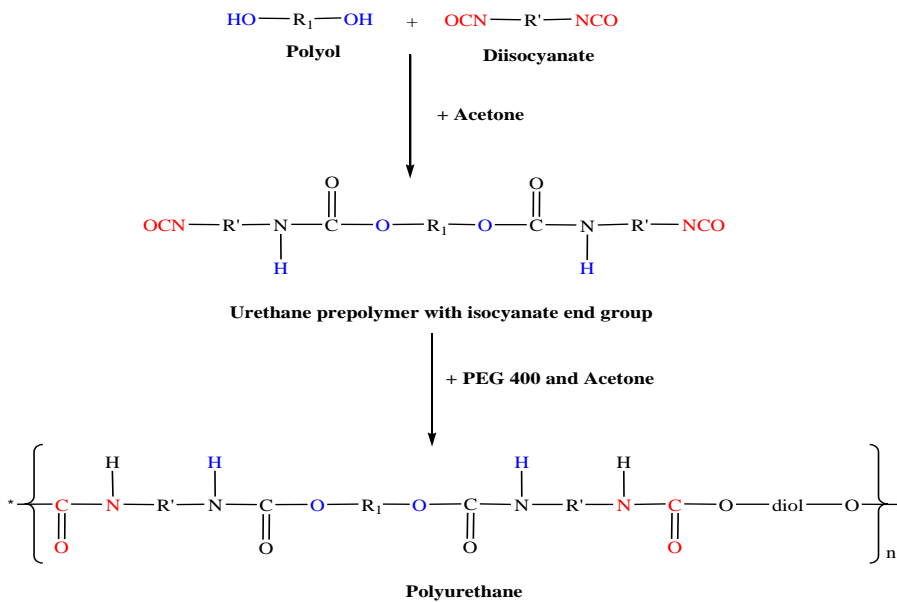
239 **Table 1** The specification of PKO-p (Badri et al. (2000)).

| Property | Values |
|------------------------------|---------|
| Viscosity at 25 °C (cps) | 1313.3 |
| Specific gravity (g/mL) | 1.114 |
| Moisture content (%) | 0.09 |
| pH value | 10–11 |
| The hydroxyl number mg KOH/g | 450–470 |

240

241 The structural chain was extended with the aid of poly(ethylene glycol) to form flexible and
242 elastic polyurethane film. In order to produce the urethane prepolymer, the isocyanate group (-
243 NCO) attacks with the hydroxyl group (-OH) of polyol (PKOp) while the other hydroxyl group
244 of the polyol is attacked by the other isocyanate group (Wong & Badri 2012) as shown in
245 **Figure 2**.

246



247

248

Figure 2. PU production via the pre-polymerization method (Wong & Badri 2012).

249

250

a. FTIR analysis

251

252

253

254

255

256

257

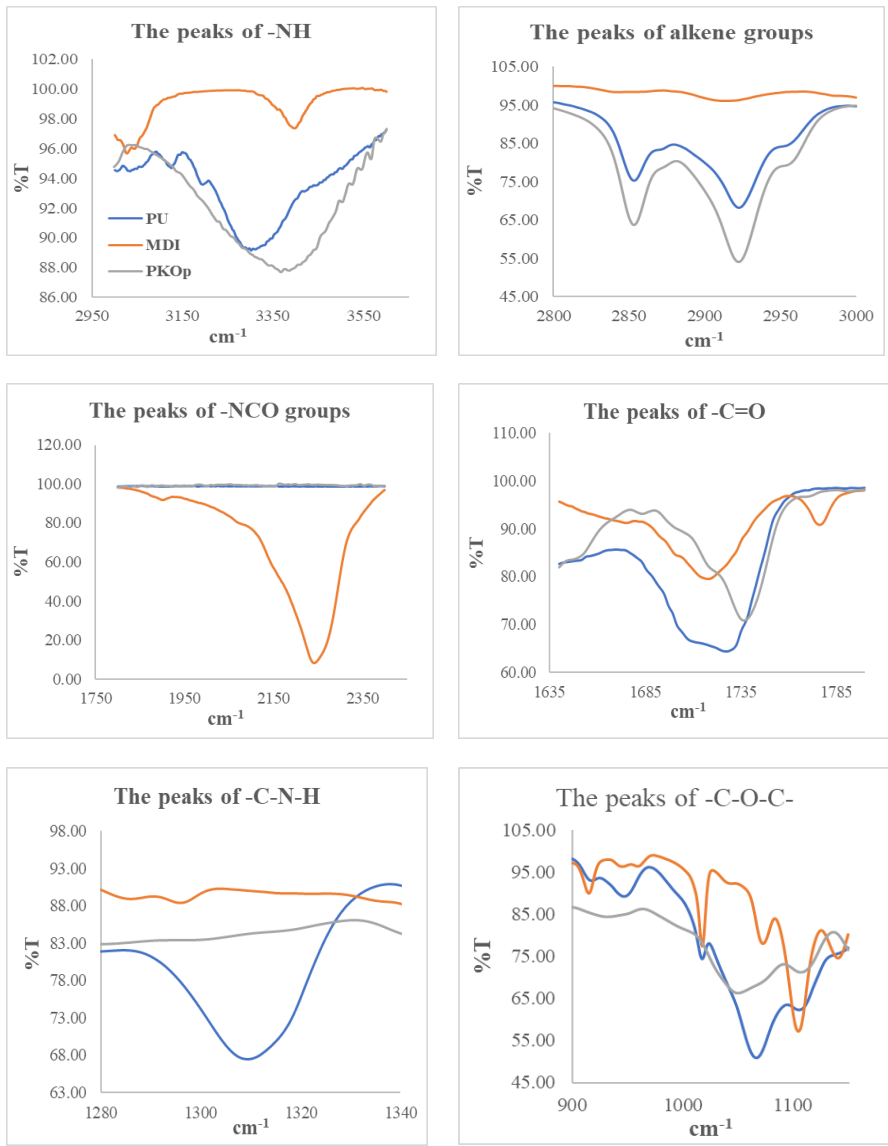
258

259

260

261

Figure 3 shows the FTIR spectra for polyurethane, exhibiting the important functional group peaks. According to a study researched by Wong & Badri 2012, PKO-p reacts with MDI to form urethane prepolymers. The NCO group on MDI reacts with the OH group on polyol whether PKOp or PEG. It can be seen there are no important peaks of MDI in the FTIR spectra. This is further verified by the absence of a peak at the 2400 cm^{-1} belonging to MDI (-NCO groups). This could also confirm that the -NCO group on MDI had completely reacted with PKO-p to form the urethane -NHC(O) backbone. The presence of amides (-NH), carbonyl urethane group (-C=O), carbamate group (C-NH), and -C-O-C confirmed the formation of urethane chains. In this study, the peak of carbonyl urethane (-C=O) detected at 1727 cm^{-1} indicated that the carbonyl urethane group was bonded without hydrogen owing to the hydrogen reacts with the carbonyl urethane group.



262 **Figure 3.** FTIR spectra of several important peaks between polyurethane, PKO-p, and MDI
 263
 264 The reaction of polyurethane has been studied by Hamuzan & Badri (2016) where the urethane
 265 carbonyl group was detected at 1730–1735 cm^{-1} while the MDI carbonyl was detected at 2400

266 cm^{-1} . The absence of peaks at 2250–2270 cm^{-1} indicates the absence of NCO groups. It shows
267 that the polymerization reaction occurs entirely between NCO groups in MDI with hydroxyl
268 groups on polyols and PEG (Mishra et al. 2012). The absence of peaks at 1690 cm^{-1}
269 representing urea (C=O) in this study indicated, there is no urea formation as a byproduct
270 (Clemitsen 2008) of the polymerization reaction that possibly occurs due to the excessive
271 water. For the amine (-NH) group, hydrogen-bond to -NH and oxygen to form ether and
272 hydrogen bond to NH and oxygen to form carbonyl on urethane can be detected at the peak of
273 3301 cm^{-1} and in the wavenumber at range 3326–3428 cm^{-1} . This has also been studied and
274 detected by Mutsuhisa et al. (2007) and Lampman et. al. (2010). In this research, the proton
275 acceptor is carbonyl (-C=O) while the proton donor is an amine (-NH) to form a hydrogen
276 bond. The MDI chemical structure has the electrostatic capability that produces dipoles from
277 several atoms such as hydrogen, oxygen, and nitrogen atoms. These properties make
278 isocyanates are highly reactive, and have different properties (Leykin et al. 2016).

279
280 MDI was one of the isocyanates used in this study, has an aromatic group, and is more
281 reactive compared to aliphatic group isocyanates such as hexamethylene diisocyanate (HDI)
282 or isophorone diisocyanate (IPDI). Isocyanates have two groups of isocyanates on each
283 molecule. Diphenylmethane diisocyanate is an exception owing to its structure consisting of
284 two, three, four, or more isocyanate groups (Nohra et al. 2013). The use of PEG 400 in this
285 study as a chain extender for polyurethane increases the chain mobility of polyurethane at an
286 optimal amount. The properties of polyurethane are contributed by hard and soft copolymer
287 segments of both polyol monomers and MDI. This makes the hard segment of urethane serves
288 as a crosslinking site between the soft segments of the polyol (Leykin et al. 2016).

289

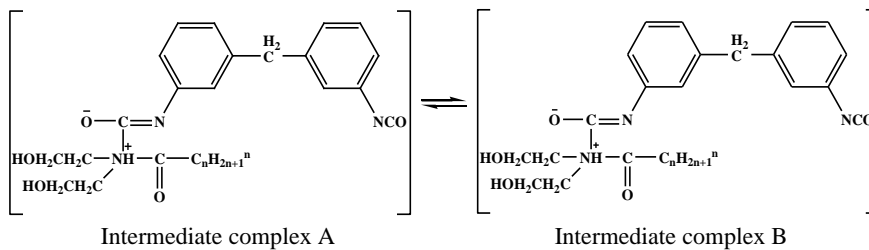
290

291 The mechanism of the pre-polymerization in urethane chains formation is a
 292 nucleophilic substitution reaction as studied by Yong et al. (2009). However, this study found
 293 amines as nucleophiles. Amine attacks carbonyl on isocyanate in MDI in order to form two
 294 resonance structures of intermediate complexes A and B (Figure 4). Intermediate complex B
 295 has a greater tendency to react with polyols due to stronger carbonyl (C=O) bonds than C=N
 296 bonds on intermediate complexes A. Thus, intermediate complex B is more stable than
 297 intermediate complex A, as suggested by previous researchers who have conducted by Wong
 298 and Badri (2012).

Commented [jj22]: There is no A and B in the Figure. Is this about something else?

Commented [MAM23R22]: Done.

299



300

Figure 4. The formation of intermediate complexes

301 Moreover, oxygen is more electronegative than nitrogen causing cations (H+) to tend
 302 to attack -CN bonds compared to -CO. The combination between long polymer chain and low
 303 cross-linking content gives the polymer elastic properties whereas short-chain and high cross-
 304 linking produce hard and rigid polymers. Cross-linking in polymers consists of three-
 305 dimensional networks with high molecular weight. In some aspects, polyurethane can be a
 306 macromolecule, a giant molecule (Petrovic 2008).

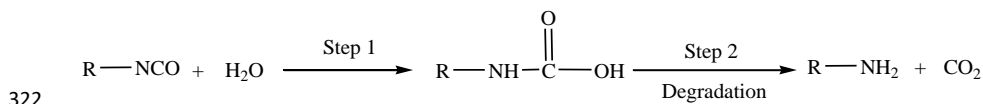
307

308 However, complexes A and B intermediate were produced after the nucleophile of PEG
 309 attacking the isocyanate group in the MDI. However, PEG contains oxygen atoms that are more
 310 electronegative than nitrogen atoms inside the PKOp chemical structure causing the reaction
 311 of nucleophilic substitution that occurs in PKOp. Furthermore, amine has a higher probability

312 of reacting compared to hydroxyl (Herrington & Hock 1997). Amine with high alkalinity reacts
313 with carbon atoms on MDI as proposed by Wong and Badri (2012).

314

315 The production of intermediate complexes unstabilizes the alkyl ions, nevertheless, the
316 long carbon chains of PKOp ensure the stability of alkyl ions. The addition of PEG in this study
317 is imperative, not merely to increase the chain length of PU but also to avoid the production of
318 urea as a by-product after the NCO group reacts with H₂O from the environment. If the NCO
319 group reacts with the excess water in the environment, the formation of urea and carbon dioxide
320 gas will also occur excessively (**Figure 5**). This reaction can cause a polyurethane foam, not
321 polyurethane film as we studied the film.



323 **Figure 5.** The reaction between the NCO group and water producing carbon dioxide

324

325 Furthermore, the application of PEG can influence the conductivity of PU whereby
326 Porcarelli et al. (2017) have reported the application of PEG using several molecular weights.
327 PEG 1500 decreased the conductivity of PU in consequence of the semicrystalline phase of
328 PEG 1500 that acted as a poor ion-conducting phase for PU. It is also well known that PEG
329 with a molecular weight of more than 1000 g·mol⁻¹ tends to crystallize with deleterious effects
330 on room temperature ionic conductivity (Porcarelli et al. 2017).

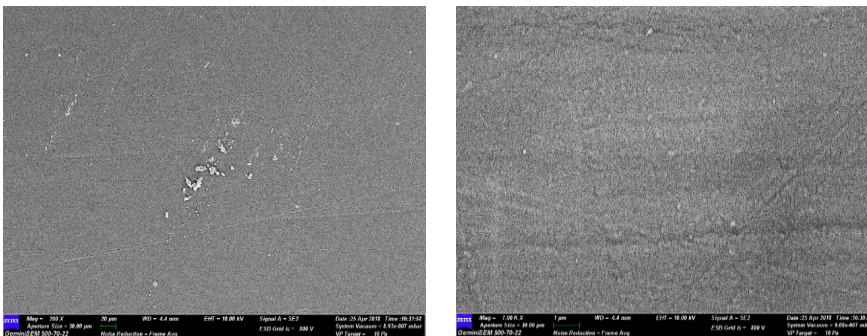
331

332 b. Morphological analysis

333 The field emission scanning electron microscope micrograph in **Figure 6** shows the formation
334 of a uniform polymer film contributed by the polymerization method applied. The
335 magnification used for this surface analysis ranged from 200 to 5000×. The polymerization

336 method can also avoid the failure of the reaction in PU polymerization. Furthermore, no trace
337 of separation was detected by FESEM. This has also been justified by the wavelengths obtained
338 by the FTIR spectra above.

339



340 **Figure 6.** The micrograph of polyurethane films was analyzed by FESEM at (a) 200× and (b)
341 5000× magnifications.

342

343 c. The crosslinking analysis

344 Soxhlet analysis was applied to determine the degree of crosslinking between the hard
345 segments and the soft segments in the polyurethane. The urethane group on the hard segment
346 along the polyurethane chain is polar (Cuve & Pascault 1991). Therefore, during the testing, it
347 was very difficult to dissolve in toluene, as the testing reagent. The degree of crosslinking is
348 determined by the percentage of the gel content. The analysis result obtained from the Soxhlet
349 testing indicated a 99.3% gel content. This is significant in getting a stable polymer at a higher
350 working temperature (Rogulska et al. 2007).

351

$$\text{Gel content (\%)} = \frac{(0.6 - 0.301) \text{ g}}{0.301 \text{ g}} \times 100\% = 99.33\%$$

352

353

354

355 d. The thermal analysis

356 Thermogravimetric analysis can be used to observe the material mass based on temperature
 357 shift. It can also examine and estimate the thermal stability and materials properties such as the
 358 alteration weight owing to absorption or desorption, decomposition, reduction, and oxidation.
 359 The material composition of polymer is specified by analyzing the temperatures and the heights
 360 of the individual mass steps (Alamawi et al. 2019). **Figure 7** shows the TGA and derivative
 361 thermogravimetry (DTG) thermograms of polyurethane. The percentage weight loss (%) is
 362 listed in **Table 2**. Generally, only a small amount of weight was observed. It is shown in **Figure**
 363 **7** in the region of 45–180 °C. This is due to the presence of condensation on moisture and
 364 solvent residues.

366 **Table2** Weight loss percentage of (wt%) polyurethane film

| Sample | % Weight loss (wt%) | | | | Total of weight loss (%) | Residue after 550 °C (%) |
|--------------|---------------------|----------------------|-----------------------|-----------------------|--------------------------|--------------------------|
| | T_{max} , (°C) | T_{d1} , 200–90 °C | T_{d2} , 350–500 °C | T_{d3} , 500–550 °C | | |
| Polyurethane | 240 | 8.04 | 39.29 | 34.37 | 81.7 | 18.3 |

367 The bio polyurethane is thermally stable up to 240 °C before it has undergone thermal
 368 degradation (Agrawal et al. 2017). The first stage of thermal degradation (T_{d1}) on polyurethane
 369 films was shown in the region of 200–290 °C as shown in **Figure 7**. The T_{d1} is associated with
 370 degradation of the hard segments of the urethane bond, forming alcohol or degradation of the
 371 polyol chains and releasing of isocyanates (Berta et al. 2006), primary and secondary amines
 372 as well as carbon dioxide (Corcuera et al. 2011; Pan & Webster 2012). Meanwhile, the second
 373 thermal degradation stage (T_{d2}) of polyurethane films experienced a weight loss of 39.29%.
 374 This endotherm of T_{d2} is related to the dimerization of isocyanates to form carbodiimides and
 375 release CO₂. The formed carbodiimide reacts with alcohol to form urea. The third stage of
 376

Commented [j24]: please explain

Commented [MAM25R24]: Done

Commented [j26]: These are different samples?

Commented [j27]: Please use the correct sign for the grades

Commented [MAM28R27]: Done

Commented [j29]: Is this the % Weight loss. The table is illegible, please rewrite it. Variables should be explained and written in italic.

Commented [MAM30R29]: Yes, this is the weight loss.

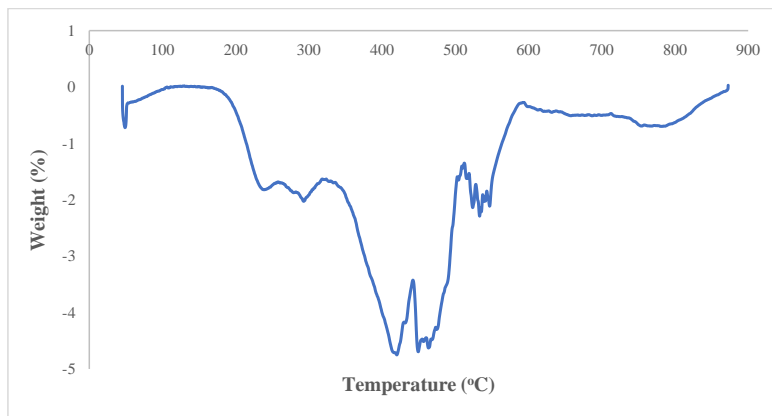
Commented [j31]: Before % was without a gap. Please standardize.

Commented [MAM32R31]: Done.

377 thermal degradation (T_{d3}) is related to the degradation of urea (Berta et al. 2006) and the soft
378 segment on polyurethane.

379

380 Generally, DSC analysis exhibited thermal transitions as well as the initial
381 crystallization and melting temperatures of the polyurethane (Khairuddin et al. 2018). It serves
382 to analyze changes in thermal behavior due to changes occurring in the chemical chain structure
383 based on the T_g of the sample obtained from the DSC thermogram (**Figure 8**). DSC analysis
384 on polyurethane film was performed in the temperature at the range 100 °C to 200 °C of using
385 nitrogen gas as a blanket as proposed by Furtwengler et al. (2017). The glass transition
386 temperature on polyurethane was above room temperature, at 78.1 °C indicated the state of
387 glass on polyurethane. The presence of MDI contributes to the formation of hard segments in
388 polyurethanes. Porcarelli et al. (2017) stated that possessing a low T_g may contribute to PU
389 conductivity.



390

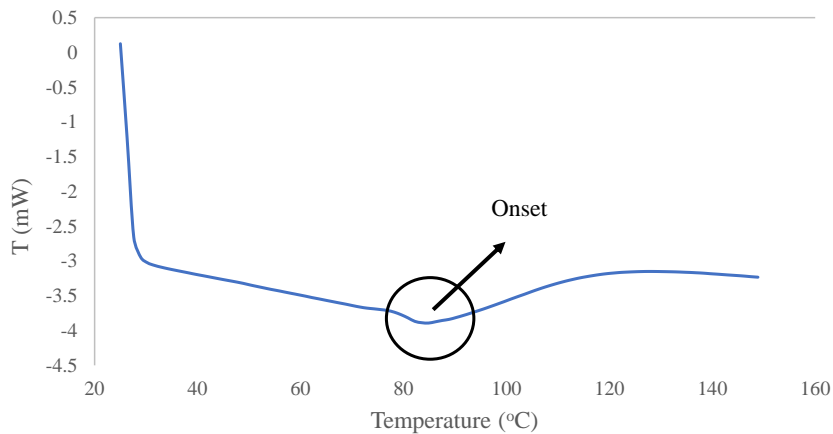
Figure 7. DTG thermogram of polyurethane film

391

392

393 During polymerization, this hard segment restricts the mobility of the polymer chain
394 (Ren et al. 2013) owing to the steric effect on the benzene ring in the hard segment. The
395 endothermic peak of acetone used as the solvent in this study was supposedly at 56 °C.

396 However, it was detected in the DSC thermogram nor the TGA thermogram, which indicates
397 that acetone was removed from the polyurethane during the synthesis process, owing to its
398 volatile nature. The presence of acetone in the synthesis was to lower the reaction kinetics.



399 **Figure 8.** DSC thermogram of polyurethane film

401
402
403 e. The solubility and mechanical properties of the polyurethane film

404 The chemical resistivity of a polymer will be the determinant in performing as a conductor.
405 Thus, its solubility in various solvents was determined by dissolving the polymer in selected
406 solvents such as hexane, benzene, acetone, THF, DMF, and DMSO. On the other hand, the
407 mechanical properties of polyurethane were determined based on the standard testing following
408 ASTM D638. The results from the polyurethane film solubility and tensile test are shown in
409 **Table 3.** Polyurethane films were insoluble with acetone, hexane, and benzene and are only
410 slightly soluble in THF, DMF, and DMSO solutions. While the tensile strength of a PU film
411 indicated how much elongation load the film was capable of withstanding the material before
412 breaking.

413

414 **Table 3** The solubility and mechanical properties of the polyurethane film

415

| Parameters | Polyurethane film | |
|----------------------------|-------------------|--------------|
| Solubility | Benzene | Insoluble |
| | Hexane | Insoluble |
| | Acetone | Insoluble |
| | THF | Less soluble |
| | DMF | Less soluble |
| | DMSO | Less soluble |
| | Stress (MPa) | 8.53 |
| Elongation percentage (%) | 43.34 | |
| Strain modulus (100) (MPa) | 222.10 | |

416

417 The tensile stress, strain, and modulus of polyurethane film also indicated that polyurethane

418 has good mechanical properties that are capable of being a supporting substrate for the next

419 stage of the study. In the production of polyurethane, the properties of polyurethane are easily

420 influenced by the content of MDI and polyol used. The length of the chain and its flexibility

421 are contributed by the polyol which makes it elastic. High crosslinking content can also produce

422 hard and rigid polymers. MDI is a major component in the formation of hard segments in

423 polyurethane. It is this hard segment that determines the rigidity of the PU. Therefore, high

424 isocyanate content results in higher rigidity on PU (Petrovic et al. 2002). Thus, the polymer has

425 a higher resistance to deformation and more stress can be applied to the PU.

426

427 f. The conductivity of the polyurethane as a polymeric film on SPE

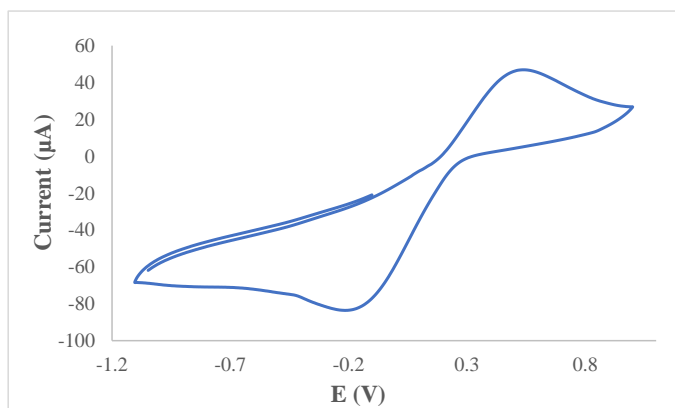
428 Polyurethane film was deposited onto the screen-printed electrode by casting method as shown

429 in **Figure 1**. After that, the modified electrode was analyzed using cyclic voltammetry and

430 differential pulse voltammetry in order to study the behavior of the modified electrode. The
431 modified electrode was tested in a 0.1 mmol·L⁻¹ KCl solution containing 5 mmol·L⁻¹
432 (K₃Fe(CN)₆). The use of potassium ferricyanide is intended to increase the sensitivity of the
433 KCl solution. The conductivity of the modified electrode was studied. The electrode was
434 analyzed by cyclic voltammetry method with a potential range of -1.00 to +1.00 with a scan
435 rate of 0.05 V·s⁻¹. The voltammograms at the electrode have shown a specific redox reaction.
436 Furthermore, the conductivity of the modified electrode is lower due to the use of polyurethane.
437 This occurs due to PU being a natural polymer produced from the polyol of palm kernel oil-
438 based polyol. The electrochemical signal at the electrode is low if there is a decrease in
439 electrochemical conductivity (El - Raheem et al. 2020). It can be concluded that polyurethane
440 is a bio-polymer with a low current value. The current of the modified electrode was found at
441 5.3 x 10⁻⁵ A or 53 μA. Nevertheless, the current of PU in this study showed better results
442 compared to Bahrami et al. (2019) that reported the current of PU as 1.26 x 10⁻⁶ A, whereas Li
443 et al. (2019) reported the PU current in their study was even very low, namely 10⁻¹⁴ A. The PU
444 can obtain a current owing to the benzene ring in the hard segment (MDI) could exhibit the
445 current by inducing electron delocalization along the polyurethane chain (Wong et al. 2014).
446 The PU can also release a current caused by PEG. The application of PEG as polyol has been
447 studied by Porcarelli et al. (2017), that reported that the current of PU based on PEG – polyol
448 was 9.2 x 10⁻⁸ A.

449 According to **Figure 9**, it can be concluded that the anodic peak present in the modified
450 electrode was at +0.5 V, it also represented the anodic peak of the SPE-PU. The first oxidation
451 signal on both electrodes ranged from -0.2 to +1.0 V, which revealed a particular oxidative
452 peak at a potential of +0.5 V.

453

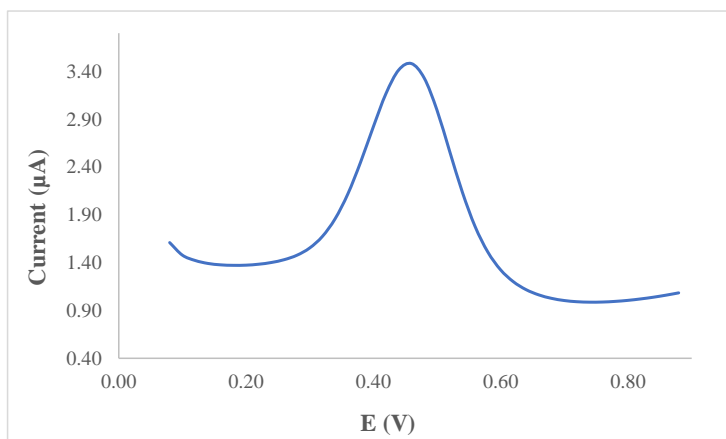


454 **Figure 9.** The voltammogram of SPE-PU modified electrode after analyzed using cyclic
 455 voltammetry technique
 456

457 **Figure 10** also presents the DPV voltammogram of the modified electrode. DPV is a
 458 measurement based on the difference in potential pulses that produce an electric current.
 459 Scanning the capability pulses to the working electrode will produce different currents. Optimal
 460 peak currents will be produced to the reduction capacity of the redox material. The peak current
 461 produced is proportional to the concentration of the redox substance and can be detected up to
 462 a concentration below 10^{-8} M. DPV was conducted to obtain the current value that is more
 463 accurate than CV (Lee et al. 2018).
 464

465 This study used a redox pair ($K_3Fe(CN)_6$) as a test device (probe). The currents generated by
 466 SPE-PU and proved by CV and DPV have shown conductivity on polyurethane films. This
 467 suggests that polyurethane films can conduct electron transfer. The electrochemical area on the
 468 modified electrode can be calculated using the formula from Randles-Sevcik (Butwong et al.
 469 2019), where the electrochemical area for SPE-PU is considered to be A, using Equation 2:

470 **Current of SPE-PU, $I_p = 2.65 \times 10^5 A C n^{3/2} \nu^{1/2} D^{1/2}$** (2)



471 **Figure 10.** The voltammogram of SPE – PU modified electrode after analyzed using
 472 differential pulse voltammetry technique
 473

474
 475 Where, $n - 1$ is the amount of electron transfer involved, while C is the solvent concentration
 476 used ($\text{mmol}\cdot\text{L}^{-1}$) and the value of D is the diffusion constant of $5 \text{ mmol}\cdot\text{L}^{-1}$ at $(\text{K}_3\text{Fe}(\text{CN})_6)$
 477 dissolved using $0.1 \text{ mmol}\cdot\text{L}^{-1}$ KCl. The estimated surface area of the electrode (**Figure 1**) was
 478 0.2 cm^2 where the length and width of the electrode used during the study was $0.44 \text{ cm} \times 0.44$
 479 cm while the surface area of the SPE-PU was 0.25 cm^2 with the length and width of the
 480 electrode estimated at $0.5 \text{ cm} \times 0.5 \text{ cm}$, and causing the SPE-PU has a larger surface. The
 481 corresponding surface concentration (τ) (mol/cm^2) is measured using Equation 3.

$$482 \quad I_p = \frac{n^2 F^2}{4RT} A \tau v \quad (3)$$

483 I_p is the peak current (A), while A is the surface area of the electrode (cm^2), the value of v is
 484 the applied scan rate (mV/s) and F is the Faraday constant ($96,584 \text{ C}/\text{mol}$), R is the constant
 485 ideal gas ($8.314 \text{ J}/\text{mol K}$) and T is the temperature used during the experiment being conducted
 486 (298 K) (Koita et al. 2014). The application of PKOp to produce a conducting polymer will be
 487 a great prospect as this material can be employed in the analytical industry in order to modify
 488 electrodes for electrochemical purposes.

489 Furthermore, number of palm oils is abundant in Malaysia and Indonesia such as palm stearin
490 and refined-bleached-deodorized (RBD) palm oil. They have several benefits such as being
491 sustainable, cheap, and environmentally biodegradable. These palms are the potential to
492 produce biomaterials that can be used to replace other polymers that are chemical-based (Tajao
493 et al. 2021). Several studies have been reported the application of PU to produce elastic
494 conductive fibres and films owing to it being highly elastic, scratch-resistant, and adhesive
495 (Tadese et al. 2019), thus it is easy for PU to adhere to the screen-printed electrode to modify
496 the electrode. PU is also being used as a composite material to make elastic conducting
497 composite films (Khatoon & Ahmad 2017).

498

499 **4. Conclusion**

500 Polyurethane film was prepared by pre-polymerization between palm kernel oil-based polyol
501 (PKO-p) with MDI. The presence of PEG 400 as the chain extender formed freestanding
502 flexible film. Acetone was used as the solvent to lower the reaction kinetics since the pre-
503 polymerization was carried out at room temperature. The formation of urethane links (-
504 NHC(O) backbone) after polymerization was confirmed by the absence of N=C=O peak at
505 2241 cm^{-1} and the presence of N-H peak at 3300 cm^{-1} , carbonyl (C=O) at 1710 cm^{-1} , carbamate
506 (C-N) at 1600 cm^{-1} , ether (C-O-C) at 1065 cm^{-1} , benzene ring (C=C) at 1535 cm^{-1} in the bio
507 polyurethane chain structure. Soxhlet analysis for the determination of crosslinking on
508 polyurethane films has yielded a high percentage of 99.33%. This is contributed by the hard
509 segments formed from the reaction between isocyanates and hydroxyl groups causing
510 elongation of polymer chains. FESEM analysis exhibited an absence of phase separation and
511 smooth surface. Meanwhile, the current of the modified electrode was found at $5.2 \times 10^{-5}\text{ A}$.
512 This bio polyurethane film can be used as a conducting bio-polymer and it is very useful for

513 other studies such as electrochemical sensor purposes. Furthermore, advanced technologies are
514 promising and the future of bio-based polyol looks very bright.

515

516 **5. Acknowledgment**

517 The authors would like to thank Alma Ata University for the sponsorship given to the first
518 author. We would like to also, thank The Department of Chemical Sciences, Universiti
519 Kebangsaan Malaysia for the laboratory facilities and CRIM, UKM for the analysis
520 infrastructure.

521

522 **6. Conflict of Interest**

523 The authors declare no conflict of interest.

524

525 **7. References**

526 Agrawal, A., Kaur, R., Walia, R. S. (2017). PU foam derived from renewable sources:
527 Perspective on properties enhancement: An overview. *European Polymer Journal*. **95**:
528 255 – 274.

529 Akindoyo, J. O., Beg, M.D.H., Ghazali, S., Islam, M.R., Jeyaratnam, N. & Yuvaraj, A.R.
530 (2016). Polyurethane types, synthesis, and applications – a review. *RSC Advances*. **6**:
531 114453 – 114482.

532 Alamawi, M. Y., Khairuddin, F. H., Yusoff, N. I. M., Badri, K., Ceylan, H. (2019).
533 Investigation on physical, thermal, and chemical properties of palm kernel oil polybio-
534 based binder as a replacement for bituminous binder. *Construction and Building*
535 *Materials*. **204**: 122 – 131.

536 Alqarni, S. A., Hussein, M. A., Ganash, A. A. & Khan, A. (2020). Composite material-based
537 conducting polymers for electrochemical sensor applications: a mini-review.
538 *BioNanoScience*. **10**: 351 – 364.

539 Badan, A., Majka, T. M. (2017). The influence of vegetable – oil based polyols on physico –
540 mechanical and thermal properties of polyurethane foams. *Proceedings*. 1 – 7.

541 Badri, K.H. (2012) Biobased polyurethane from palm kernel oil-based polyol. In Polyurethane;
542 Zafar, F., Sharmin, E., Eds. InTechOpen: Rijeka, Croatia. pp. 447–470.

543 Badri, K.H., Ahmad, S.H. & Zakaria, S. 2000. Production of a high-functionality RBD palm
544 kernel oil-based polyester polyol. *Journal of Applied Polymer Science*. **81**(2): 384 – 389.

545 Baig, N., Sajid, M. and Saleh, T. A. 2019. Recent trends in nanomaterial–modified electrodes
546 for electroanalytical applications. *Trends in Analytical Chemistry*. **111**: 47 – 61.

547 Berta, M., Lindsay, C., Pans, G., & Camino, G. (2006). Effect of chemical structure on
548 combustion and thermal behaviour of polyurethane elastomer layered silicate
549 nanocomposites. *Polymer Degradation and Stability*. **91**: 1179-1191.

550 Borowicz, M., Sadowska, J. P., Lubczak, J. & Czuprynski, B. (2019). Biodegradable, flame–
551 retardant, and bio-based rigid polyurethane/polyisocyanurate foams for thermal
552 insulation application. *Polymers*. **11**: 1816 – 1839.

553 Butwong, N., Khajonklin, J., Thongbor, A. & Luong, J.H.T. (2019). Electrochemical sensing
554 of histamine using a glassy carbon electrode modified with multiwalled carbon nanotubes
555 decorated with Ag – Ag₂O nanoparticles. *Microchimica Acta*. **186** (11): 1 – 10.

556 Chokkareddy, R., Thondavada, N., Kabane, B. & Redhi, G. G. (2020). A novel ionic liquid
557 based electrochemical sensor for detection of pyrazinamide. *Journal of the Iranian*
558 *Chemical Society*. **18**: 621 – 629.

559 Chokkareddy, R., Kanchi, S. & Inamuddin (2020). Simultaneous detection of ethambutol and
560 pyrazinamide with IL@CoFe₂O₄NPs@MWCNTs fabricated glassy carbon electrode.
561 *Scientific Reports*. **10**: 13563.

562 Clemitson, I. (2008). Castable Polyurethane Elastomers. Taylor & Francis Group, New York.
563 doi:10.1201/9781420065770.

564 Corcuera, M.A., Rueda, L., Saralegui, A., Martin, M.D., Fernandez-d'Arlas, B., Mondragon,
565 I. & Eceiza, A. (2011). Effect of diisocyanate structure on the properties and
566 microstructure of polyurethanes based on polyols derived from renewable resources.
567 *Journal of Applied Polymer Science*. **122**: 3677-3685.

568 Cuve, L. & Pascault, J.P. (1991). Synthesis and properties of polyurethanes based on
569 polyolefine: Rigid polyurethanes and amorphous segmented polyurethanes prepared in
570 polar solvents under homogeneous conditions. *Polymer*. **32** (2): 343- 352.

571 Degefu, H., Amare, M., Tessema, M. & Admassie, S. (2014). Lignin modified glassy carbon
572 electrode for the electrochemical determination of histamine in human urine and wine
573 samples. *Electrochimica Acta*. **121**: 307 – 314.

574 Dzulkipli, M. Z., Karim, J., Ahmad, A., Dzulkurnain, N. A., Su'ait, M S., Fujita, M. Y., Khoon,
575 L. T. & Hassan, N. H. (2021). The influences of 1-butyl-3-methylimidazolium
576 tetrafluoroborate on electrochemical, thermal and structural studies as ionic liquid gel
577 polymer electrolyte. *Polymers*. **13** (8): 1277 – 1294.

578 El-Raheem, H.A., Hassan, R.Y.A., Khaled, R., Farghali, A. & El-Sherbiny, I.M. (2020).
579 Polyurethane-doped platinum nanoparticles modified carbon paste electrode for the
580 sensitive and selective voltammetric determination of free copper ions in biological
581 samples. *Microchemical Journal*. **155**: 104765.

582 Fei, T., Li, Y., Liu, B. & Xia, C. (2019). Flexible polyurethane/boron nitride composites with
583 enhanced thermal conductivity. *High Performance Polymers*. **32** (3): 1 – 10.

584 Furtwengler, P., Perrin R., Redl, A. & Averous, L. (2017). Synthesis and characterization of
585 polyurethane foams derived of fully renewable polyesters polyols from sorbitol.
586 *European Polymer Journal*. **97**: 319 – 327.

587 Ghosh, S., Ganguly, S., Remanan, S., Mondal, S., Jana, S., Maji, P. K., Singha, N., Das, N. C.
588 (2018). Ultra-light weight, water durable and flexible highly electrical conductive
589 polyurethane foam for superior electromagnetic interference shielding materials. *Journal*
590 *of Materials Science: Materials in Electronics*. **29**: 10177 – 10189.

591 Guo, S., Zhang, C., Yang, M., Zhou, Y., Bi, C., Lv, Q. & Ma, N. (2020). A facile and sensitive
592 electrochemical sensor for non – enzymatic glucose detection based on three –
593 dimensional flexible polyurethane sponge decorated with nickel hydroxide. *Analytica*
594 *Chimica Acta*. **1109**: 130 – 139.

595 Hamuzan, H.A. & Badri, K.H. (2016). The role of isocyanates in determining the viscoelastic
596 properties of polyurethane. *AIP Conference Proceedings*. 1784, Issue 1.

597 Harmayani, E., Aprilia, V. & Marsono, Y. (2014). Characterization of glucomannan from
598 *Amorphophallus oncophyllus* and its prebiotic activity in vivo. *Carbohydrate Polymers*.
599 **112**: 475-79.

600 Herrington, R. & Hock, K. (1997). Flexible polyurethane foams. 2nd Edition. Dow Chemical
601 Company. Midlan.

602 Inayatullah, A., Badrul, H.A., Munir, M.A. (2021). Fish analysis containing biogenic amines
603 using gas chromatography flame ionization detector. *Science and Technology Indonesia*.
604 **6** (1): 1-7.

605 Janpoung, P., Pattanauwat, P. & Potiyaraj, P. (2020). Improvement of electrical conductivity
606 of polyurethane/polypyrrole blends by graphene. *Key Engineering Materials*. **831**: 122 –
607 126.

608 Khairuddin, F.H., Yusof, N. I. M., Badri, K., Ceylan, H., Tawil, S. N. M. (2018). Thermal,
609 chemical and imaging analysis of polyurethane/cecabase modified bitumen. *IOP Conf.*
610 *Series: Materials Science and Engineering*. **512**: 012032.

611 Khatoon, H., Ahmad, S. (2017). A review on conducting polymer reinforced polyurethane
612 composites. *Journal of Industrial and Engineering Chemistry*. **53**: 1 – 22.

613 Kilele, J. C., Chokkareddy, R., Rono, N. & Redhi, G. G. (2020). A novel electrochemical
614 sensor for selective determination of theophylline in pharmaceutical formulations.
615 *Journal of the Taiwan Institute of Chemical Engineers*. 111: 228-238.

616 Kilele, J. C., Chokkareddy, R. & Redhi, G. G. (2021). Ultra-sensitive electrochemical sensor
617 for fenitrothion pesticide residues in fruit samples using IL@CoFe₂ONPs@MWCNTs
618 nanocomposite. *Microchemical Journal*. **164**: 106012.

619 Koita, D., Tzedakis, T., Kane, C., Diaw, M., Sock, O. & Lavedan, P. (2014). Study of the
620 histamine electrochemical oxidation catalyzed by nickel sulfate. *Electroanalysis*. **26 (10)**:
621 2224 – 2236.

622 Kotal, M., Srivastava, S.K. & Paramanik, B. (2011). Enhancements in conductivity and thermal
623 stabilities of polyurethane/polypyrrole nanoblends. *The Journal of Physical Chemistry*
624 *C*. **115 (5)**: 1496 – 1505.

625 Ladan, M., Basirun, W.J., Kazi, S.N., Rahman, F.A. (2017). Corrosion protection of AISI 1018
626 steel using Co-doped TiO₂/polypyrrole nanocomposites in 3.5% NaCl solution.
627 *Materials Chemistry and Physics*. **192**: 361 – 373.

628 Lampman, G.M., Pavia, D.L., Kriz, G.S. & Vyvyan, J.R. (2010). Spectroscopy. 4th Edition.
629 Brooks/Cole Cengage Learning, Belmont, USA.

630 Lee, K.J., Elgrishi, N., Kandemir, B. & Dempsey, J.L. 2018. Electrochemical and spectroscopic
631 methods for evaluating molecular electrocatalysts. *Nature Reviews Chemistry*. **1(5)**: 1 -
632 14.

633 Leykin, A., Shapovalov, L. & Figovsky, O. (2016). Non – isocyanate polyurethanes –
634 Yesterday, today and tomorrow. *Alternative Energy and Ecology*. **191** (3 – 4): 95 – 108.

635 Li, H., Yuan, D., Li, P., He, C. (2019). High conductive and mechanical robust carbon
636 nanotubes/waterborne polyurethane composite films for efficient electromagnetic
637 interference shielding. *Composites Part A*. **121**: 411 – 417.

638 Nakthong, P., Kondo, T., Chailapakul, O., Siangproh, W. (2020). Development of an
639 unmodified screen-printed electrode for nonenzymatic histamine detection. *Analytical*
640 *Methods*. **12**: 5407 – 5414.

641 Mishra, K., Narayan, R., Raju, K.V.S.N. & Aminabhavi, T.M. (2012). Hyperbranched
642 polyurethane (HBPU)-urea and HBPU-imide coatings: Effect of chain extender and
643 NCO/OH ratio on their properties. *Progress in Organic Coatings*. **74**: 134 – 141.

644 Mohd Noor, M. A., Tuan Ismail, T. N. M., Ghazali, R. (2020). Bio-based content of oligomers
645 derived from palm oil: Sample combustion and liquid scintillation counting technique.
646 *Malaysia Journal of Analytical Science*. **24**: 906 – 917.

647 Munir, M. A., Badri, K. H., Heng, L. Y., Inayatullah, A., Nurinda, E., Estiningsih, D.,
648 Fatmawati, A., Aprilia, V., Syafitri, N. (2022). The application of polyurethane-LiClO₄
649 to modify screen-printed electrodes analyzing histamine in mackerel using a
650 voltammetric approach. *ACS Omega*. Doi.org/10.1021/acsomega.1c06295.

651 Munir, M. A., Heng, L. Y., Sage, E. E., Mackeen, M. M. M., Badri, K. H. (2021). Histaine
652 detection in mackerel (*Scomberomorus* Sp.) and its products derivatized with 9-
653 fluorenilmethylchloroformate. *Pakistan Journal of Analytical and Environmental*
654 *Chemistry*. **22** (2): 243-251.

655 Munir, M. A., Heng, L. Y., Badri, K. H. (2021). Polyurethane modified screen-printed
656 electrode for the electrochemical detection of histamine in fish. *IOP Conference Series:*
657 *Earth and Environmental Science*. **880**: 012032.

658 Munir, M.A., Mackeen, M.M.M., Heng, L.Y. Badri, K.H. (2021). Study of histamine detection
659 using liquid chromatography and gas chromatography. *ASM Science Journal*. **16**: 1-9.

660 Mutsuhisa F., Ken, K. & Shohei, N. (2007). Microphase separated structure and mechanical
661 properties of norbornane diisocyanate-based polyurethane. *Polymer*. **48** (4): 997 – 1004.

662 Mustapha, R., Rahmat, A. R., Abdul Majid, R., Mustapha, S. N. H. (2019). Vegetable oil-based
663 epoxy resins and their composites with bio-based hardener: A short review. *Polymer-*
664 *Plastic Technology and Materials*. **58**: 1311 – 1326.

665 Nohra, B., Candy, L., Blancos, J.F., Guerin, C., Raoul, Y. & Mouloungui, Z. (2013). From
666 petrochemical polyurethanes to bio-based polyhydroxyurethanes. *Macromolecules*. **46**
667 (10): 3771 – 3792.

668 Nurwanti, E., Uddin, M., Chang, J.S., Hadi, H., Abdul, S.S., Su, E.C.Y., Nursetyo, A.A.,
669 Masud, J.H.B. & Bai, C.H. (2018). Roles of sedentary behaviors and unhealthy foods in
670 increasing the obesity risk in adult men and women: A cross-sectional national study.
671 *Nutrients*. **10** (6): 704-715.

672 Pan, T. & Yu, Q. (2016). Anti-corrosion methods and materials comprehensive evaluation of
673 anti-corrosion capacity of electroactive polyaniline for steels. *Anti – Corrosion Methods*
674 *and Materials*. **63**: 360 – 368.

675 Pan, X. & Webster, D.C. (2012). New biobased high functionality polyols and their use in
676 polyurethane coatings. *ChemSusChem*. **5**: 419-429.

677 Petrovic, Z.S. (2008). Polyurethanes from vegetable oils. *Polymer Reviews*. **48** (1): 109 – 155.

678 Porcarelli, L., Manojkumar, K., Sardon, H., Llorente, O., Shaplov, A. S., Vijayakrishna, K.,
679 Gerbaldi, C., Mecerreyes, D. (2017). Single ion conducting polymer electrolytes based
680 on versatile polyurethanes. *Electrochimica Acta*. **241**: 526 – 534.

681 Priya, S. S., Karthika, M., Selvasekarapandian, S. & Manjuladevi, R. (2018). Preparation and
682 characterization of polymer electrolyte based on biopolymer I-carrageenan with
683 magnesium nitrate. *Solid State Ionics*. **327**: 136 – 149.

684 Ren, D. & Frazier, C.E. (2013). Structure–property behaviour of moisture-cure polyurethane
685 wood adhesives: Influence of hard segment content. *Adhesion and Adhesives*. **45**: 118-
686 124.

687 Rogulska, S.K., Kultys, A. & Podkoscielny, W. (2007). Studies on thermoplastic polyurethanes
688 based on newdiphe – derivative diols. II. Synthesis and characterization of segmented
689 polyurethanes from HDI and MDI. *European Polymer Journal*. **43**: 1402 – 1414.

690 Romaskevicius, T., Budriene, S., Pielichowski, K. & Pielichowski, J. (2006). Application of
691 polyurethane-based materials for immobilization of enzymes and cells: a review.
692 *Chemija*. **17**: 74 – 89.

693 Sengodu, P. & Deshmukh, A. D. (2015). Conducting polymers and their inorganic composites
694 for advanced Li-ion battery electrolytes: a review. *RSC Advances*. **5**: 42109 – 42130.

695 Septevani, A. A., Evans, D. A. C., Chaleat, C., Martin, D. J., Annamalai, P. K. (2015). A
696 systematic study substituting polyether polyol with palm kernel oil based polyester
697 polyol in rigid polyurethane foam. *Industrial Crops and Products*. **66**: 16 – 26.

698 Su'ait, M. S., Ahmad, A., Badri, K. H., Mohamed, N. S., Rahman, M. Y. A., Ricardi, C. L. A.
699 & Scardi, P. The potential of polyurethane bio-based solid polymer electrolyte for
700 photoelectrochemical cell application. *International Journal of Hydrogen Energy*. **39** (6):
701 3005 – 3017.

702 Tadesse, M. G., Mengistie, D. A., Chen, Y., Wang, L., Loghin, C., Nierstrasz, V. (2019).
703 Electrically conductive highly elastic polyamide/lycra fabric treated with PEDOT: PSS
704 and polyurethane. *Journal of Materials Science*. **54**: 9591 – 9602.

705 Tajau, R., R. Rosiah, Alias, M. S., Mudri, N. H., Halim, K. A. A., Harun, M. H., Isa, N. M.,
706 Ismail, R. C., Faisal, S. M., Talib, M., Zin, M. R. M., Yusoff, I. I., Zaman, N. K., Ilias,
707 I. A. (2021). Emergence of polymeric material utilising sustainable radiation curable
708 palm oil-based products for advanced technology applications. *Polymers*. **13**: 1865 –
709 1886.

710 Tran, V.H., Kim, J.D., Kim, J.H., Kim, S.K., Lee, J.M. (2020). Influence of cellulose
711 nanocrystal on the cryogenic mechanical behaviour and thermal conductivity of
712 polyurethane composite. *Journal of Polymers and The Environment*. **28**: 1169 – 1179.

713 Viera, I.R.S., Costa, L.D.F.D.O., Miranda, G.D.S., Nardehcia, S., Monteiro, M.S.D. S.D.B.,
714 Junior, E.R. & Delpech, M.C. (2020). Waterborne poly (urethane – urea)s
715 nanocomposites reinforced with clay, reduced graphene oxide and respective hybrids:
716 Synthesis, stability and structural characterization. *Journal of Polymers and The
717 Environment*. **28**: 74 – 90.

718 Wang, B., Wang, L., Li, X., Liu, Y., Zhang, Z., Hedrick, E., Safe, S., Qiu, J., Lu, G. & Wang,
719 S. (2018). Template-free fabrication of vertically–aligned polymer nanowire array on the
720 flat–end tip for quantifying the single living cancer cells and nanosurface interaction. a
721 *Manufacturing Letters*. **16**: 27 – 31.

722 Wang, J., Xiao, L., Du, X., Wang, J. & Ma, H. (2017). Polypyrrole composites with carbon
723 materials for supercapacitors. *Chemical Papers*. **71** (2): 293 – 316.

724 Wong, C.S. & Badri, K.H. (2012). Chemical analyses of palm kernel oil-based polyurethane
725 prepolymer. *Materials Sciences and Applications*. **3**: 78 – 86.

726 Wong, C. S., Badri, K., Ataollahi, N., Law, K., Su'ait, M. S., Hassan, N. I. (2014). Synthesis
727 of new bio–based solid polymer electrolyte polyurethane – LiClO₄ via prepolymerization
728 method: Effect of NCO/OH ratio on their chemical, thermal properties and ionic
729 conductivity. *World Academy of Science, Engineering and Technology, International*

- 730 *Journal of Chemical, Molecular, Nuclear, Materials and Metallurgical Engineering*. **8**:
731 1243 – 1250.
- 732 Yong, Z., Bo, Z.M., Bo, W., Lin, J.Z. & Jun, N. (2009). Synthesis and properties of novel
733 polyurethane acrylate containing 3-(2-Hydroxyethyl) isocyanurate segment. *Progress in*
734 *Organic Coatings*. **67**: 264 – 268.
- 735 Zia, K. M., Anjum, S., Zuber, M., Mujahid, M. & Jamil, T. (2014). Synthesis and molecular
736 characterization of chitosan based polyurethane elastomers using aromatic diisocyanate.
737 *International of Journal of Biological Macromolecules*. **66**: 26 – 32.

Pemberitahuan Diterima: 22 Maret 2022

— Editorial Comments

| | |
|-------------|------------|
| Joanna Rydz | 22.03.2022 |
| Decision | |
| Publish | |

— Response to Revision Request


<https://review.hindawi.com/details/144f98bd-c59b-46ba-8cd2-e5f205db16df/59621baf-c257-4a21-ac40-c08205551978>

Muhammad Abdurrahman Munir

Your Reply

Dear Dr. Joanna, We are thank you so much for you suggestion to this manuscript. We have followed your revisions and looking forward to hear from you. We apologize for the inconvenience during the revision process. Please check the revision and inform us if there is any revision. Best Regards.

File

| | | |
|-------------------------|--------|---|
| Manuscript - Munir.docx | 902 kB |  |
|-------------------------|--------|---|

+ Reviewer Reports

1 **Design and Synthesis of Conducting Polymer Bio-Based Polyurethane**
2 **Produced from Palm Kernel Oil**

3
4 Muhammad Abdurrahman Munir^{1*}, Khairiah Haji Badri^{2,3}, Lee Yook Heng², Ahlam
5 Inayatullah⁴, Ari Susiana Wulandari¹, Emelda¹, Eliza Dwinta¹, Veriani Aprillia⁵, Rachmad
6 Bagas Yahya Supriyono¹

7
8 ¹Department of Pharmacy, Faculty of Health Science, Alma Ata University, Daerah Istimewa
9 Yogyakarta, 55183, Indonesia

10 ²Department of Chemical Sciences, Faculty of Science and Technology, Universiti
11 Kebangsaan Malaysia, Bangi, 43600, Malaysia

12 ³Polymer Research Center, Universiti Kebangsaan Malaysia, Bangi, 43600, Malaysia

13 ⁴Faculty of Science and Technology, Universiti Sains Islam Malaysia, Nilai, 71800, Malaysia

14 ⁵Department of Nutrition Science, Alma Ata School of Health Sciences, Alma Ata
15 University, Daerah Istimewa Yogyakarta, 55183, Indonesia

16
17 *Email: muhammad@almaata.ac.id
18

19 **Abstract**

20 Polyurethane (PU) is a unique polymer that has versatile processing methods and mechanical
21 properties upon the inclusion of selected additives. In this study, a freestanding bio-based
22 polyurethane film the screen-printed electrode (SPE) was prepared by the solution casting
23 technique, using acetone as solvent. It was a one-pot synthesis between major reactants namely,
24 palm kernel oil-based polyol and 4,4-methylene diisocyanate. The PU has strong adhesion on

25 the SPE surface. The synthesized bio-based polyurethane was characterized using
26 thermogravimetry analysis, differential scanning calorimetry, Fourier-transform infrared
27 spectroscopy (FTIR), surface area analysis by field emission scanning electron microscope,
28 and cyclic voltammetry. Cyclic voltammetry was employed to study electro-catalytic
29 properties of SPE-polyurethane towards oxidation of PU. Remarkably, SPE-PU exhibited
30 improved anodic peak current as compared to SPE itself using the differential pulse
31 voltammetry method. Furthermore, the formation of urethane linkages (-NHC(O) backbone)
32 after polymerization was analyzed using FTIR and confirmed by the absence of peak at 2241
33 cm^{-1} attributed to the sp-hybridized carbons atoms of $\text{C}\equiv\text{C}$ bonds . The glass transition
34 temperature of the polyurethane was detected at 78.1 °C.

35

36 **Keywords:** polyurethane, polymerization, screen-printed electrode, voltammetry

37

38

39 **1. Introduction**

40 Conducting polymers (CPs) are polymers that can release a current (Alqarni et al. 2020). The
41 conductivity of CPs was first observed in polyacetylene, nevertheless owing to its instability,
42 the invention of various CPs have been studied and reported such as polyaniline (PANI),
43 poly(*o*-toluidine) (PoT), polythiophene (PTH), polyfluorene (PF), and polyurethane (PU).
44 Furthermore, natural CPs have low conductivity and are often semi-conductive. Therefore, it
45 is imperative to improve their conductivity for electrochemical sensor purposes (Sengodu &
46 Deshmukh 2015; Dzulkipli et al. 2021; Wang et al. 2018). The CPs can be produced from many
47 organic materials and they have several advantages such as having an electrical current,
48 inexpensive materials, massive surface area, small dimensions, and the production is
49 straightforward. Furthermore, according to these properties, many studies have been reported

50 by researchers to study and report the variety of CPs applications such as sensors, biochemical
51 applications, electrochromic devices, and solar cells (Alqarni et al. 2020; Ghosh et al. 2018).
52 There is scientific documentation on the use of conductive polymers in various studies such as
53 polyaniline (Pan & Yu 2016), polypyrrole (Ladan et al. 2017), and polyurethane (Tran et al.
54 2020; Vieira et al. 2020; Guo et al. 2020; Fei et al. 2020).

55

56 Polyurethane productions can be obtained by using several materials as polyols such as
57 petroleum, coal, and crude oils. Nevertheless, these materials have become very rare to find
58 and the price is very expensive at the same time required a sophisticated system to produce it.
59 The reasons such as price and time consuming to produce polyols have been considered by
60 many researchers, furthermore, finding utilizing plants that can be used as alternative polyols
61 should be done immediately (Badri 2012). Thus, to avoid the use of petroleum, coal, and crude
62 oils as raw materials for a polyol, vegetable oils become a better choice to produce polyol in
63 order to obtain a biodegradable polymer. Vegetable oils that are generally used for
64 polyurethane synthesis are soybean oil, corn oil, sunflower seed oil, coconut oil, nuts oil,
65 rapeseed, olive oil, and palm oil (Badri 2012; Borowicz et al. 2019).

66

67 It is very straightforward for vegetable oils to react with a specific group to produce a PU such
68 as epoxy, hydroxyl, carboxyl, and acrylate owing to the existence of (-C=C-) in vegetable oils.
69 Thus, it provides appealing profits to vegetable oils compared to petroleum considering the
70 toxicity, price, and harm to the environment (Mustapha et al. 2019; Mohd Noor et al. 2020).
71 Palm oil becomes the chosen in this study to produce PU owing to it being largely cultivated
72 in South Asia particularly in Malaysia and Indonesia. It has several profits compared to other
73 vegetable oils such as the easiest materials obtained, the lowest cost of all the common

74 vegetable oils, and recognized as the plantation that has a low environmental impact and
75 removing CO₂ from the atmosphere as a net sequester (Tajau et al. 2021; Septevani et al. 2015).

76

77 The application of bio based polymer has appealed much attention until now. Global
78 environmental activists have forced researchers to discover another material producing
79 polymers (Priya et al. 2018). PUs have many advantages that have been used by many
80 researchers, they are not merely versatile materials but also have the durability of metal and
81 the flexibility of rubber. Furthermore, they can be promoted to replace rubber, metals, and
82 plastics in several aspects. Several applications of PUs have been reported and studied such as
83 textiles, automotive, building and construction applications, and biomedical applications (Zia
84 et al. 2014; Romaskevicius et al. 2006). Polyurethanes are also considered to be one of the most
85 useful materials with many profits such as; possessing low conductivity, low density,
86 absorption capability, and dimensional stability. They are a great research subject due to their
87 mechanical, physical, and chemical properties (Badan & Majka 2017; Munir et al. 2021).

88

89 PU structure contains the urethane group that can be formed from the reaction between
90 isocyanate groups (-NCO) and hydroxyl group (-OH). Nevertheless, several groups can be
91 found in PU structure such as urea, esters, ethers, and several aromatic groups. Furthermore,
92 PUs can be produced from different sources as long as they contain specific materials (polyol
93 and methylene diphenyl diisocyanate (MDI) and making them very useful for specific
94 applications. Thus, according to the desired properties, PUs can be divided into several types
95 such as waterborne, flexible, rigid, coating, binding, sealants, adhesives, and elastomers
96 (Akindoyo et al. 2016).

97

98 PUs are lighter than other materials such as metals, gold, and platinum. The hardness of PU
99 also relies on the number of the aromatic rings in the polymer structure (Janpoung et al, 2020;
100 Su'ait et al. 2014), majorly contributed by the isocyanate derivatives. PUs have also a conjugate
101 structure where electrons can move in the main chain that causes electricity produced even the
102 current is low. The current of conjugated linear (π) can be elaborated by the gap between the
103 valence band and the conduction band, or called high energy level containing electrons
104 (HOMO) and lowest energy level not containing electrons (LUMO), respectively (Wang et al.
105 2017; Kotal et al. 2011).

106

107 In the recent past, several conventional methods have been developed such as capillary
108 electrophoresis, liquid, and gas chromatography coupled with several detectors. Nevertheless,
109 although chromatographic and spectrometric approaches are well developed for qualitative and
110 quantitative analyses of analytes, several limitations emerged such as complicated
111 instrumentation, expensive, tedious sample preparations, and requiring large amounts of
112 expensive solvents that will harm the users and environment (Kilele et al. 2020; Inayatullah et
113 al. 2021; Munir et al. 2021; Harmayani et al. 2014; Nurwanti et al. 2018). Therefore, it is
114 imperative to obtain and develop an alternative material that can be used to analyze a specific
115 analyte. Electrochemical methods are extremely promising methods in the determination of an
116 analyte in samples owing to the high selectivities, sensitivities, inexpensive, requirements of
117 small amounts of solvents, and can be operated by people who have no background in analytical
118 chemistry. In addition, sample preparation such as separation and extraction steps are not
119 needed owing to the selectivity of this instrument where no obvious interference on the current
120 response is recorded (Chokkareddy et al. 2020). Few works have been reported on the
121 electrochemical methods for the determination of analyte using electrodes combined with
122 several electrode modifiers such as carbon nanotube, gold, and graphene (Chokkareddy et al.

123 2020; Kilele et al. 2021). Nevertheless, the materials are expensive and the production is
124 difficult. Thus, an electrochemical approach using inexpensive and easily available materials
125 as electrode modifiers should be developed (Degefu et al. 2014; Munir et al. 2022).

126

127 Nowadays, screen-printed electrodes (SPEs) modified with conducting polymer have been
128 developed for various electrochemical sensing. SPE becomes the best solution owing to the
129 electrode having several advantages such as frugal manufacture, tiny size, being able to
130 produce on a large scale, and can be applied for on-site detection (Nakthong et al. 2020).

131 Conducting polymers (CPs) become an alternative to modifying the screen-printed electrodes
132 due to their electrical conductivity, able to capture analyte by chemical/physical adsorption,
133 large surface area, and making CPs are very appealing materials from electrochemical
134 perspectives (Baig et al. 2019). Such advantages of SPE encourage us to construct a new
135 electrode for electrochemical sensing, and no research reported on the direct electrochemical
136 oxidation of histamine using a screen-printed electrode modified by bio-based polyurethane.
137 Therefore, this research is the first to develop a new electrode using (screen printed
138 polyurethane electrode) SPPE without any conducting materials.

139

140 The purpose of this work was to synthesize, characterize and study the electro behavior of
141 polyurethane using cyclic voltammetry (CV) and differential pulse voltammetry (DPV)
142 attached to the screen-printed electrode. To the best of our knowledge, this is the first attempt
143 to use a modified polyurethane electrode. The electrochemistry of polyurethane mounted onto
144 SPE is discussed in detail. PUs are possible to become an advanced frontier material that has
145 been chemically modified the specific electrodes for bio/chemical sensing application.

146

147

148 **2. Experimental**

149 **2.1 Chemicals**

150 *Synthesis of bio-based polyurethane film:* Palm kernel oil (PKOp) based polyol supplied by
151 UKM Technology Sdn Bhd through MPOB/UKM station plant, Pekan Bangi Lama, Selangor
152 and prepared using Badri et al. (2000) method. 4, 4-diphenylmethane diisocyanate (MDI) was
153 acquired from Cosmopolyurethane (M) Sdn. Bhd., Klang, Malaysia. Solvents and analytical
154 reagents were benzene ($\geq 99.8\%$), toluene ($\geq 99.8\%$), hexane ($\geq 99\%$), acetone ($\geq 99\%$),
155 dimethylsulfoxide (DMSO) ($\geq 99.9\%$), dimethylformamide (DMF) ($\geq 99.8\%$), tetrahydrofuran
156 (THF) ($\geq 99.8\%$), and polyethylene glycol (PEG) with a molecular weight of 400 Da obtained
157 from Sigma Aldrich Sdn Bhd, Shah Alam.

158

159 **2.2 Apparatus**

160 Tensile testing was performed using a universal testing machine model Instron 5566 following
161 ASTM D638 (Standard Test Method for Tensile Properties of Plastics). The tensile properties
162 of the polyurethane film were measured at a velocity of 10 mm/min with a cell load of 5 kN.
163 The thermal properties were performed using thermogravimetry analysis (TGA) and
164 differential scanning calorimetry (DSC) analysis. TGA was performed using a thermal analyzer
165 of the Perkin Elmer Pyris model with a heating rate of 10 °C/min at a temperature range of 30
166 to 800 °C under a nitrogen gas atmosphere. The DSC analysis was performed using a thermal
167 analyzer of the Perkin Elmer Pyris model with a heating rate of 10 °C /minute at a temperature
168 range of -100 to 200 °C under a nitrogen gas atmosphere. Approximately, 5–10 mg of PU was
169 weighed. The sample was heated from 25 to 150 °C for one minute, then cooled immediately
170 from 150 to 100 °C for another one minute and finally, reheated to 200 °C at a rate of 10 °C
171 /min. At this point, the polyurethane encounters changing from elastic properties to brittle due
172 to changes in the movement of the polymer chains. Therefore, the temperature in the middle of

173 the inclined regions is taken as the glass transition temperature (T_g). The melting temperature
174 (T_m) is identified as the maximum endothermic peak by taking the area below the peak as the
175 enthalpy point (ΔH_m).

176

177 The morphological analysis of PU film was performed by field emission scanning electron
178 microscope (FESEM) model Gemini SEM microscope model 500-70-22. Before the analysis
179 was carried out, the polyurethane film was coated with a thin layer of gold to increase the
180 conductivity of the film. The coating method was carried out using a sputter-coater. The
181 observations were conducted at a magnification of 200 \times and 5000 \times with 10.00 kV (Electron
182 high tension – EHT).

183

184 The crosslinking of PU was determined using the soxhlet extraction method. About 0.60 g of
185 PU sample was weighed and put in an extractor tube containing 250 ml of toluene, used as a
186 solvent. This flow of toluene was let running for 24 h. Mass of the PU was weighed before and
187 after the reflux process was carried out. Then, the sample was dried in the conventional oven
188 at 100 °C for 24 h in order to get a constant mass. The percentage of crosslinking content
189 known as the gel content can be calculated using Equation (1).

$$190 \quad \text{Gel content (\%)} = \frac{W_0 - W}{W} \times 100 \% \quad (1)$$

191 W_0 is the mass of PU before the reflux process (g) and W is the mass of PU after the reflux
192 process (g).

193

194 FTIR spectroscopic analysis was performed using a Perkin-Elmer Spectrum BX instrument
195 using the diamond attenuation total reflectance (DATR) method to confirm the polyurethane,
196 PKOp, and MDI functional group. FTIR spectroscopic analysis was performed at a
197 wavenumber of 4000 to 600 cm^{-1} to identify the peaks of the major functional groups in the

198 formation of the polymer such as amide group (-NH), urethane carbonyl group (-C=O),
199 isocyanate group (-O=C=N-), and carbamate group (-CN).

200

201 **2.3 Synthesis of Polyurethane**

202 Firstly, the polyol prepolymer solution was produced by combining palm kernel oil-based
203 polyol and poly(ethylene glycol) (PEG) 400 (100:40 g/g), acetone 30% was used as a solution.

204 The compound was homogenized using a centrifuge (100 rpm) for 5 min. Whereas diisocyanate
205 prepolymer was obtained by mixing 4,4'-diphenylmethane diisocyanate (100 g) to acetone

206 30%, afterward the mixture was mixed using a centrifuge for 1 min to obtain a homogenized

207 solution. Afterward, diisocyanate solution (10 g) was poured into a container that contains

208 polyol prepolymer solution (10 g) slowly to avoid an exothermic reaction occurring. The

209 mixture was mixed for 30 sec until a homogenized solution was acquired. Lastly, the

210 polyurethane solution was poured on the electrode surface by using the casting method and

211 dried at ambient temperature for 12 h.

212

213 **2.4 Modification of Electrode**

214 Voltammetric tests were performed using Metrohm Autolab Software (**Figure 1**) analyzer

215 using cyclic voltammetry method or known as amperometric mode and differential pulse

216 voltammetry. All electrochemical experiments were carried out using screen-printed electrode

217 (diameter 3 mm) modified using polyurethane film as working electrode, platinum wire as the

218 auxiliary electrode, and Ag/AgCl electrode as a reference electrode. All experiments were

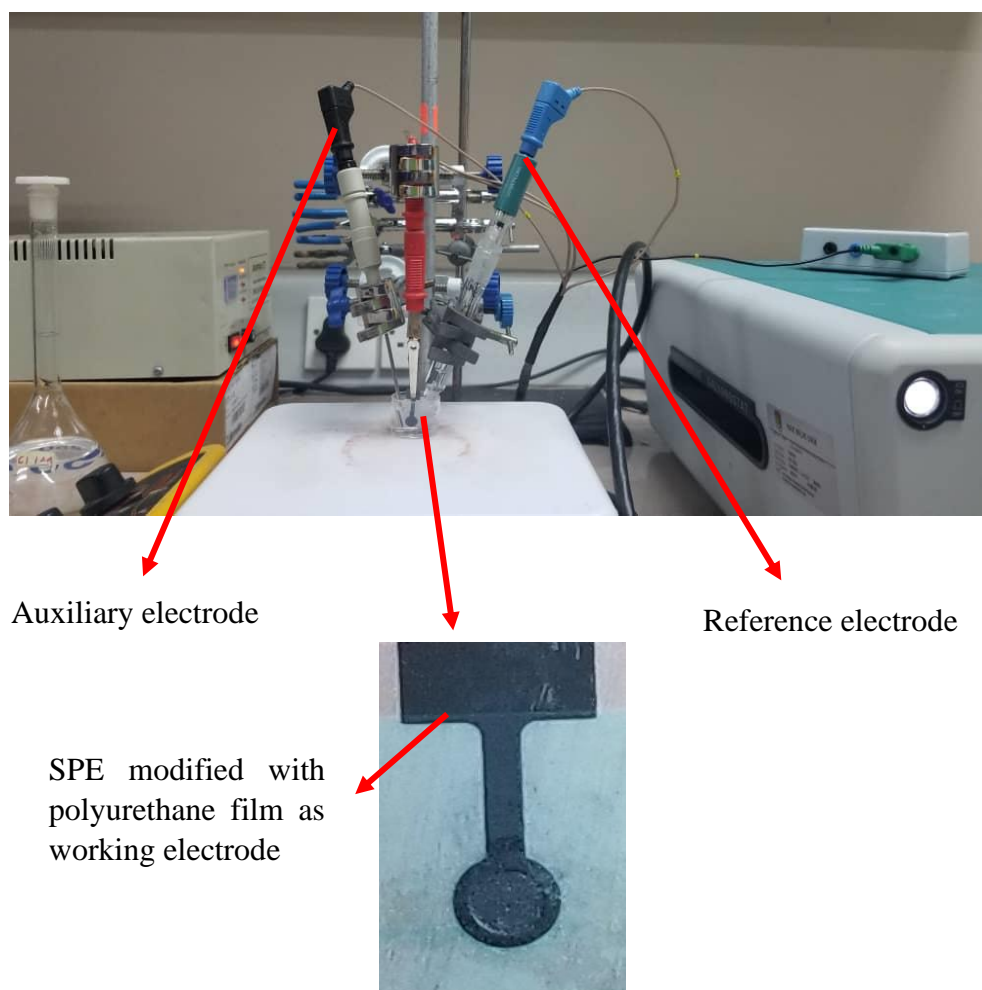
219 conducted at a temperature of 20 ± 2 °C.

220

221 The PU was cast onto the screen-printed electrode (SPE) and analyzed using a single

222 voltammetric cycle between -1200 and +1500 mV (vs Ag/AgCl) of ten cycles at a scanning

223 rate of 100 mV/s in 5 ml of KCl in order to study the activity of SPE and polyurethane film.
224 Approximately (0.1, 0.3 and 0.5) mg of bio-based polyurethane was dropped separately onto
225 the surface of the SPE and dried at room temperature. The modified palm-based polyurethane
226 electrodes were then rinsed with deionized water to remove physically adsorbed impurities and
227 residues of unreacted material on the electrode surface. All electrochemical materials and
228 calibration measurements were carried out in a 5 mL glass beaker with a configuration of three
229 electrodes inside it. Platinum wire and silver/silver chloride (Ag/AgCl) electrodes were used
230 as auxiliary and reference electrodes, while a screen-printed electrode that had been modified
231 with polyurethane was applied as a working electrode.



232 **Figure 1.** Potentiostat instrument to study the conductivity of SPE modified with
233 polyurethane film using voltammetric approach: CV and DPV

234

235 **3. Results and Discussion**

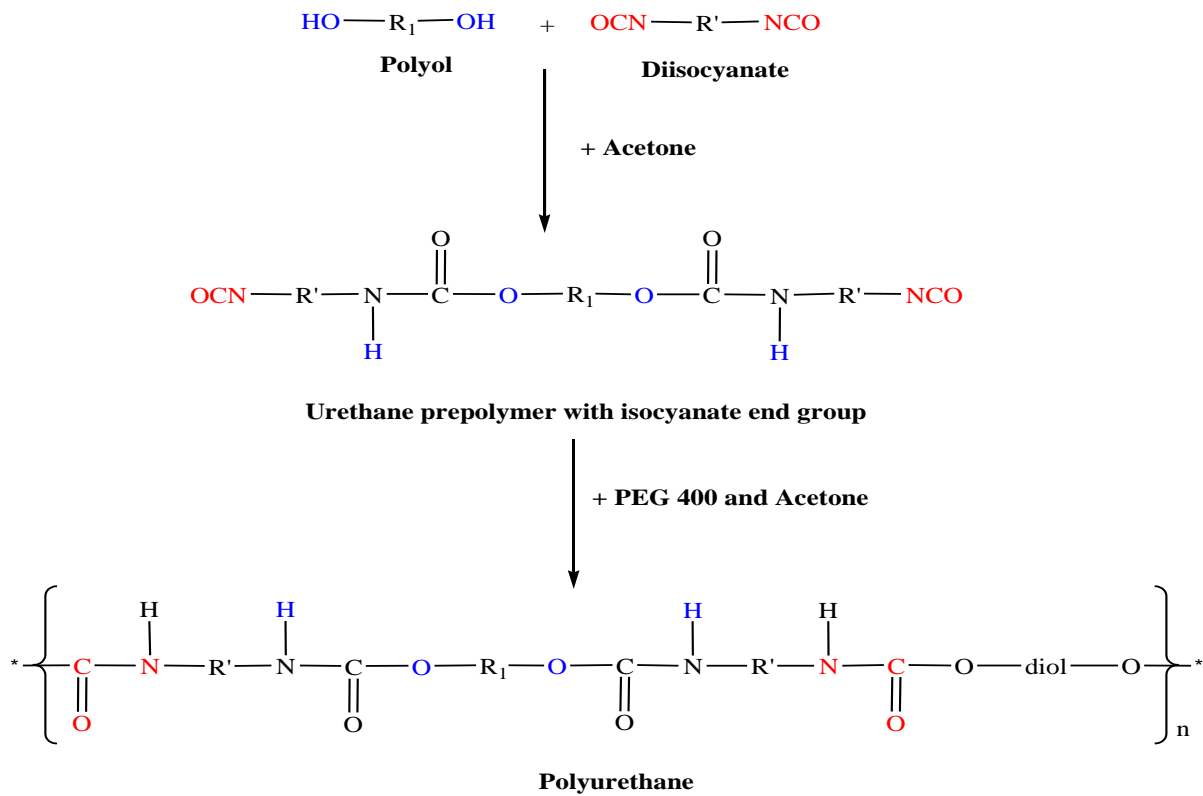
236 The synthesis of PU films was carried out using a pre-polymerization method which involves
237 the formation of urethane polymer at an early stage. The reaction took place between
238 diisocyanate (MDI) and palm kernel oil-based polyol. **Table 1** presents the PKO-p properties
239 used in this study.

240 **Table 1** The specification of PKO-p (Badri et al. (2000)).

| Property | Values |
|------------------------------|---------|
| Viscosity at 25 °C (cps) | 1313.3 |
| Specific gravity (g/mL) | 1.114 |
| Moisture content (%) | 0.09 |
| pH value | 10–11 |
| The hydroxyl number mg KOH/g | 450–470 |

241
242 The structural chain was extended with the aid of poly(ethylene glycol) to form flexible and
243 elastic polyurethane film. In order to produce the urethane prepolymer, the isocyanate group (-
244 NCO) attacks with the hydroxyl group (-OH) of polyol (PKOp) while the other hydroxyl group
245 of the polyol is attacked by the other isocyanate group (Wong & Badri 2012) as shown in
246 **Figure 2.**

247



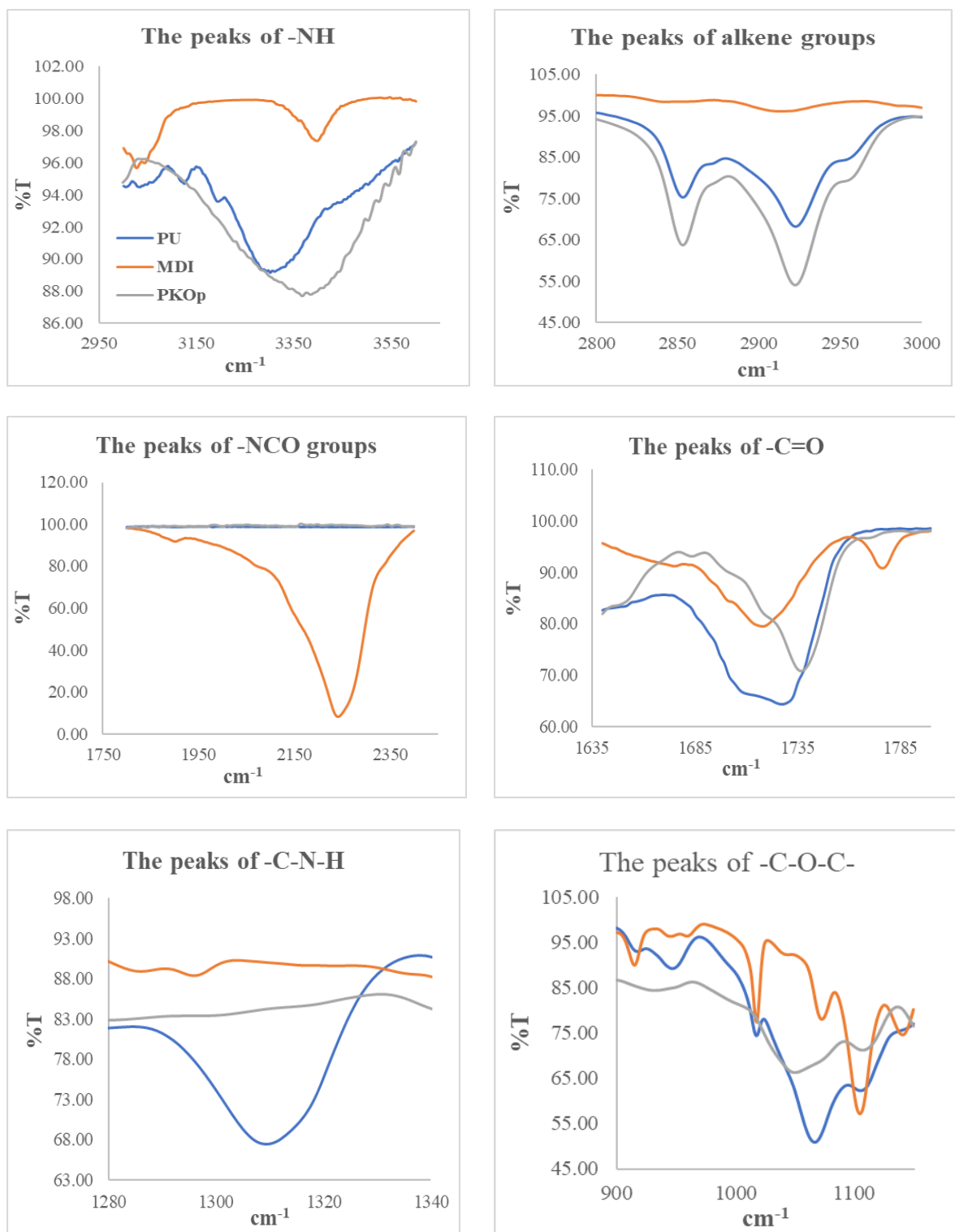
248

249 **Figure 2.** PU production via the pre-polymerization method (Wong & Badri 2012).

250

251 a. FTIR analysis

252 **Figure 3** shows the FTIR spectra for polyurethane, exhibiting the important functional group
 253 peaks. According to a study researched by Wong & Badri 2012, PKO-p reacts with MDI to
 254 form urethane prepolymers. The NCO group on MDI reacts with the OH group on polyol
 255 whether PKOp or PEG. It can be seen there are no important peaks of MDI in the FTIR spectra.
 256 This is further verified by the absence of an absorption bands at the 2400 cm^{-1} belonging to
 257 MDI (-NCO groups). This could also confirm that the -NCO group on MDI had completely
 258 reacted with PKO-p to form the urethane -NHC(O) backbone. The presence of amides (-NH),
 259 carbonyl urethane group (-C=O), carbamate group (C-NH), and -C-O-C confirmed the
 260 formation of urethane chains. In this study, the peak of carbonyl urethane (-C=O) detected at
 261 1727 cm^{-1} indicated that the carbonyl urethane group was bonded without hydrogen owing to
 262 the hydrogen reacts with the carbonyl urethane group.



263 **Figure 3.** FTIR spectra of several important peaks between polyurethane, PKO-p, and MDI
 264
 265 The reaction of polyurethane has been studied by Hamuzan & Badri (2016) where the urethane
 266 carbonyl group was detected at 1730–1735 cm^{-1} while the MDI carbonyl was detected at 2400

267 cm^{-1} . The absence of absorption bands at 2250–2270 cm^{-1} associated with $\text{N}=\text{C}=\text{O}$ bond
268 stretching indicates the absence of NCO groups. It shows that the polymerization reaction
269 occurs entirely between NCO groups in MDI with hydroxyl groups on polyols and PEG
270 (Mishra et al. 2012). The absence of peaks at 1690 cm^{-1} representing urea ($\text{C}=\text{O}$) in this study
271 indicated, there is no urea formation as a byproduct (Clemitson 2008) of the polymerization
272 reaction that possibly occurs due to the excessive water. For the amine ($-\text{NH}$) group, hydrogen-
273 bond to $-\text{NH}$ and oxygen to form ether and hydrogen bond to NH and oxygen to form carbonyl
274 on urethane can be detected at the peak of 3301 cm^{-1} and in the wavenumber at range 3326–
275 3428 cm^{-1} . This has also been studied and detected by Mutsuhisa et al. (2007) and Lampman
276 et. al. (2010). In this research, the proton acceptor is carbonyl ($-\text{C}=\text{O}$) while the proton donor
277 is an amine ($-\text{NH}$) to form a hydrogen bond. The MDI chemical structure has the electrostatic
278 capability that produces dipoles from several atoms such as hydrogen, oxygen, and nitrogen
279 atoms. These properties make isocyanates are highly reactive, and have different properties
280 (Leykin et al. 2016).

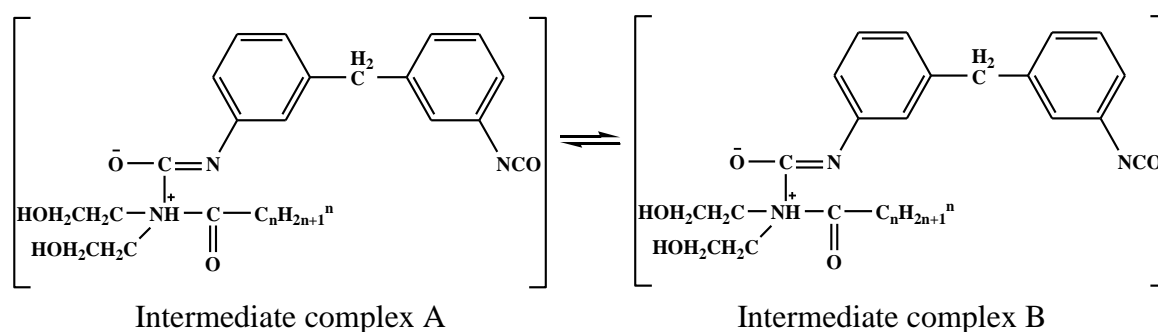
281

282 MDI was one of the isocyanates used in this study, has an aromatic group, and is more
283 reactive compared to aliphatic group isocyanates such as hexamethylene diisocyanate (HDI)
284 or isophorone diisocyanate (IPDI). Isocyanates have two groups of isocyanates on each
285 molecule. Diphenylmethane diisocyanate is an exception owing to its structure consisting of
286 two, three, four, or more isocyanate groups (Nohra et al. 2013). The use of PEG 400 in this
287 study as a chain extender for polyurethane increases the chain mobility of polyurethane at an
288 optimal amount. The properties of polyurethane are contributed by hard and soft copolymer
289 segments of both polyol monomers and MDI. This makes the hard segment of urethane serves
290 as a crosslinking site between the soft segments of the polyol (Leykin et al. 2016).

291

292 The mechanism of the pre-polymerization in urethane chains formation is a
 293 nucleophilic substitution reaction as studied by Yong et al. (2009). However, this study found
 294 amines as nucleophiles. Amine attacks carbonyl on isocyanate in MDI in order to form two
 295 resonance structures of intermediate complexes A and B (**Figure 4**). Intermediate complex B
 296 has a greater tendency to react with polyols due to stronger carbonyl (C=O) bonds than C=N
 297 bonds on intermediate complexes A. Thus, intermediate complex B is more stable than
 298 intermediate complex A, as suggested by previous researchers who have conducted by Wong
 299 and Badri (2012).

300



301

Figure 4. The formation of intermediate complexes

302

303 Moreover, oxygen is more electronegative than nitrogen causing cations (H⁺) to tend
 304 to attack -CN bonds compared to -CO. The combination between long polymer chain and low
 305 cross-linking content gives the polymer elastic properties whereas short-chain and high cross-
 306 linking produce hard and rigid polymers. Cross-linking in polymers consists of three-
 307 dimensional networks with high molecular weight. In some aspects, polyurethane can be a
 308 macromolecule, a giant molecule (Petrovic 2008).

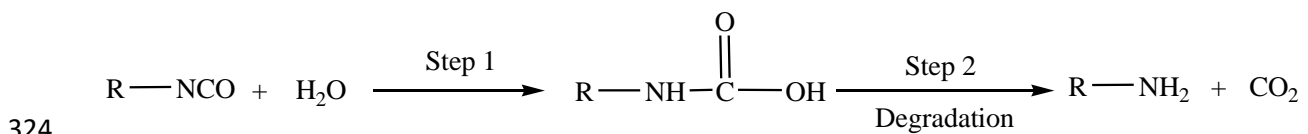
309

310 However, complexes A and B intermediate were produced after the nucleophile of PEG
 311 attacking the isocyanate group in the MDI. However, PEG contains oxygen atoms that are more
 312 electronegative than nitrogen atoms inside the PKOp chemical structure causing the reaction

313 of nucleophilic substitution that occurs in PKOp. Furthermore, amine has a higher probability
314 of reacting compared to hydroxyl (Herrington & Hock 1997). Amine with high alkalinity reacts
315 with carbon atoms on MDI as proposed by Wong and Badri (2012).

316

317 The production of intermediate complexes unstabilizes the alkyl ions, nevertheless, the
318 long carbon chains of PKOp ensure the stability of alkyl ions. The addition of PEG in this study
319 is imperative, not merely to increase the chain length of PU but also to avoid the production of
320 urea as a by-product after the NCO group reacts with H₂O from the environment. If the NCO
321 group reacts with the excess water in the environment, the formation of urea and carbon dioxide
322 gas will also occur excessively (**Figure 5**). This reaction can cause a polyurethane foam, not
323 polyurethane film as we studied the film.



325 **Figure 5.** The reaction between the NCO group and water producing carbon dioxide

326

327 Furthermore, the application of PEG can influence the conductivity of PU whereby
328 Porcarelli et al. (2017) have reported the application of PEG using several molecular weights.
329 PEG 1500 decreased the conductivity of PU in consequence of the semicrystalline phase of
330 PEG 1500 that acted as a poor ion-conducting phase for PU. It is also well known that PEG
331 with a molecular weight of more than 1000 g·mol⁻¹ tends to crystallize with deleterious effects
332 on room temperature ionic conductivity (Porcarelli et al. 2017).

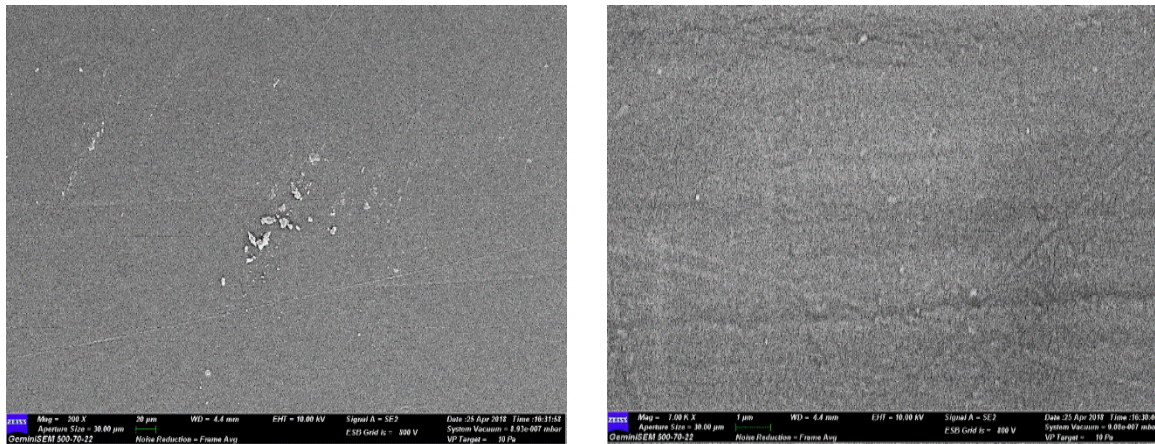
333

334 b. Morphological analysis

335 The field emission scanning electron microscope micrograph in **Figure 6** shows the formation
336 of a uniform polymer film contributed by the polymerization method applied. The

337 magnification used for this surface analysis ranged from 200 to 5000×. The polymerization
 338 method can also avoid the failure of the reaction in PU polymerization. Furthermore, no trace
 339 of separation was detected by FESEM. This has also been justified by the wavelengths obtained
 340 by the FTIR spectra above.

341



342 **Figure 6.** The micrograph of polyurethane films was analyzed by FESEM at (a) 200× and (b)
 343 5000× magnifications.

344

345 c. The crosslinking analysis

346 Soxhlet analysis was applied to determine the degree of crosslinking between the hard
 347 segments and the soft segments in the polyurethane. The urethane group on the hard segment
 348 along the polyurethane chain is polar (Cuve & Pascault 1991). Therefore, during the testing, it
 349 was very difficult to dissolve in toluene, as the testing reagent. The degree of crosslinking is
 350 determined by the percentage of the gel content. The analysis result obtained from the Soxhlet
 351 testing indicated a 99.3% gel content. This is significant in getting a stable polymer at a higher
 352 working temperature (Rogulska et al. 2007).

353

$$\text{Gel content (\%)} = \frac{(0.6 - 0.301) \text{ g}}{0.301 \text{ g}} \times 100\% = 99.33\%$$

354

355

356 d. The thermal analysis
 357 Thermogravimetric analysis can be used to observe the material mass based on temperature
 358 shift. It can also examine and estimate the thermal stability and materials properties such as the
 359 alteration weight owing to absorption or desorption, decomposition, reduction, and oxidation.
 360 The material composition of polymer is specified by analyzing the temperatures and the heights
 361 of the individual mass steps (Alamawi et al. 2019). **Figure 7** shows the TGA and derivative
 362 thermogravimetry (DTG) thermograms of polyurethane. The percentage weight loss (%) is
 363 listed in **Table 2**. Generally, only a small amount of weight was observed. It is shown in **Figure**
 364 **7** in the region of 45–180 °C. This is due to the presence of condensation on moisture and
 365 solvent residues.

366
 367 **Table 2** Weight loss percentage (wt%) and thermal degradation (T_d) of polyurethane film

| % Weight loss (wt%) and thermal degradation (T_d) | | | | | |
|---|--------------------------|--------------------------|--------------------------|--------------------------------|-----------------------------|
| T_{max} , (°C) | T_{d1} , 200–290 °C | T_{d2} , 350–500 °C | T_{d3} , 500–550 °C | Total of weight loss (%) | Residue after 550 °C (%) |
| 240 | 8.04 | 39.29 | 34.37 | 81.7 | 18.3 |

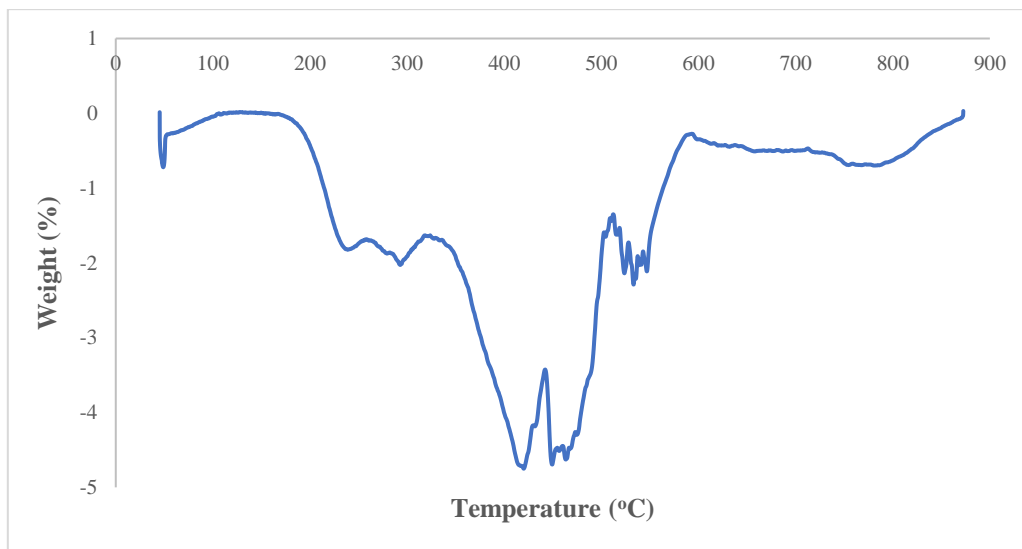
368 T_{max} : The temperature of polyurethane started to degrade; T_{d1} : Thermal degradation first; T_{d2} : Thermal degradation second;
 369 T_{d3} : Thermal degradation third

370
 371 The bio-based polyurethane is thermally stable up to 240 °C before it has undergone thermal
 372 degradation (Agrawal et al. 2017). The first stage of thermal degradation (T_{d1}) on polyurethane
 373 films was shown in the region of 200–290 °C as shown in **Figure 7**. The T_{d1} is associated with
 374 degradation of the hard segments of the urethane bond, forming alcohol or degradation of the
 375 polyol chains and releasing of isocyanates (Berta et al. 2006), primary and secondary amines
 376 as well as carbon dioxide (Corcuera et al. 2011; Pan & Webster 2012). Meanwhile, the second
 377 thermal degradation stage (T_{d2}) of polyurethane films experienced a weight loss of 39.29%.
 378 This endotherm of T_{d2} is related to the dimerization of isocyanates to form carbodiimides and
 379 release CO₂. The formed carbodiimide reacts with alcohol to form urea. The third stage of

380 thermal degradation (T_{d3}) is related to the degradation of urea (Berta et al. 2006) and the soft
381 segment on polyurethane.

382

383 Generally, DSC analysis exhibited thermal transitions as well as the initial
384 crystallization and melting temperatures of the polyurethane (Khairuddin et al. 2018). It serves
385 to analyze changes in thermal behavior due to changes occurring in the chemical chain structure
386 based on the T_g of the sample obtained from the DSC thermogram (**Figure 8**). DSC analysis
387 on polyurethane film was performed in the temperature at the range 100 °C to 200 °C of using
388 nitrogen gas as a blanket as proposed by Furtwengler et al. (2017). The glass transition
389 temperature on polyurethane was above room temperature, at 78.1 °C indicated the state of
390 glass on polyurethane. The presence of MDI contributes to the formation of hard segments in
391 polyurethanes. Porcarelli et al. (2017) stated that possessing a low T_g may contribute to PU
392 conductivity.



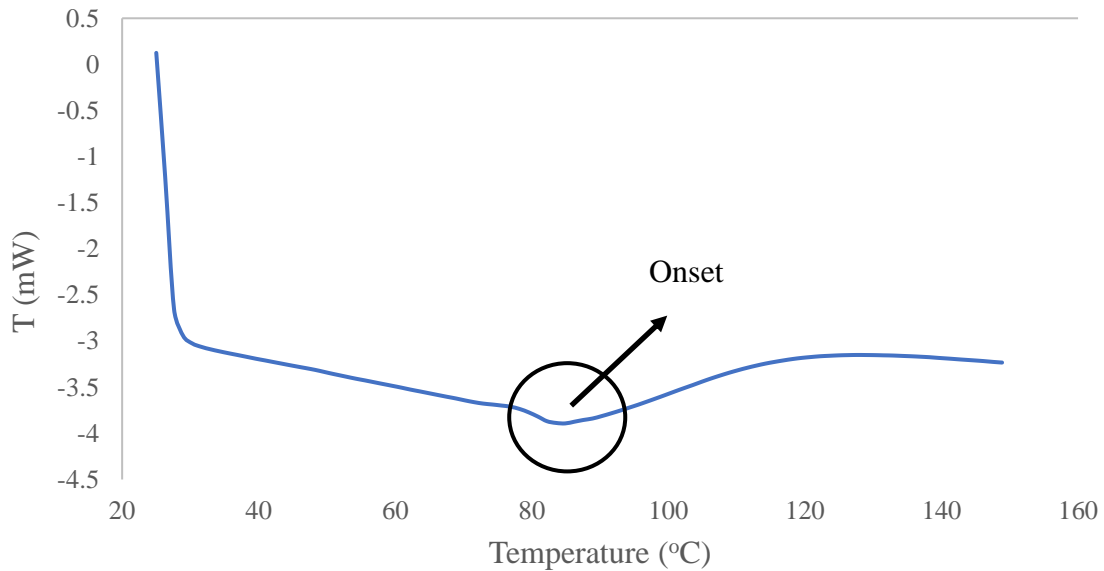
393

Figure 7. DTG thermogram of polyurethane film

394

395
396 During polymerization, this hard segment restricts the mobility of the polymer chain
397 (Ren et al. 2013) owing to the steric effect on the benzene ring in the hard segment. The
398 endothermic peak of acetone used as the solvent in this study was supposedly at 56 °C.

399 However, it was detected in the DSC thermogram nor the TGA thermogram, which indicates
400 that acetone was removed from the polyurethane during the synthesis process, owing to its
401 volatile nature. The presence of acetone in the synthesis was to lower the reaction kinetics.



402 **Figure 8.** DSC thermogram of polyurethane film

403
404
405
406 e. The solubility and mechanical properties of the polyurethane film

407 The chemical resistivity of a polymer will be the determinant in performing as a conductor.
408 Thus, its solubility in various solvents was determined by dissolving the polymer in selected
409 solvents such as hexane, benzene, acetone, THF, DMF, and DMSO. On the other hand, the
410 mechanical properties of polyurethane were determined based on the standard testing following
411 ASTM D638. The results from the polyurethane film solubility and tensile test are shown in
412 **Table 3.** Polyurethane films were insoluble with acetone, hexane, and benzene and are only
413 slightly soluble in THF, DMF, and DMSO solutions. While the tensile strength of a PU film
414 indicated how much elongation load the film was capable of withstanding the material before
415 breaking.

416

417 **Table 3** The solubility and mechanical properties of the polyurethane film

418

| Parameters | Polyurethane film | |
|----------------------------|-------------------|--------------|
| Solubility | Benzene | Insoluble |
| | Hexane | Insoluble |
| | Acetone | Insoluble |
| | THF | Less soluble |
| | DMF | Less soluble |
| | DMSO | Less soluble |
| Stress (MPa) | 8.53 | |
| Elongation percentage (%) | 43.34 | |
| Strain modulus (100) (MPa) | 222.10 | |

419

420 The tensile stress, strain, and modulus of polyurethane film also indicated that polyurethane

421 has good mechanical properties that are capable of being a supporting substrate for the next

422 stage of the study. In the production of polyurethane, the properties of polyurethane are easily

423 influenced by the content of MDI and polyol used. The length of the chain and its flexibility

424 are contributed by the polyol which makes it elastic. High crosslinking content can also produce

425 hard and rigid polymers. MDI is a major component in the formation of hard segments in

426 polyurethane. It is this hard segment that determines the rigidity of the PU. Therefore, high

427 isocyanate content results in higher rigidity on PU (Petrovic et al. 2002). Thus, the polymer has

428 a higher resistance to deformation and more stress can be applied to the PU.

429

430 f. The conductivity of the polyurethane as a polymeric film on SPE

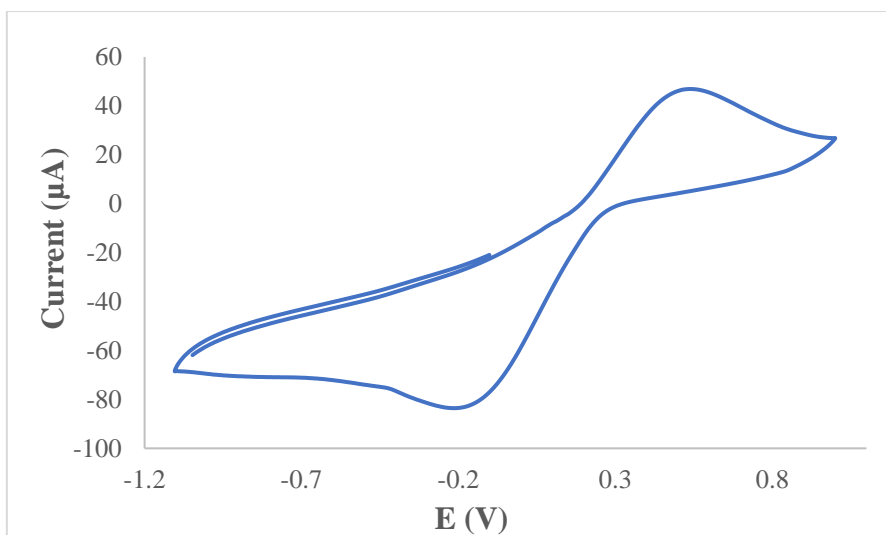
431 Polyurethane film was deposited onto the screen-printed electrode by casting method as shown

432 in **Figure 1**. After that, the modified electrode was analyzed using cyclic voltammetry and

433 differential pulse voltammetry in order to study the behavior of the modified electrode. The
434 modified electrode was tested in a $0.1 \text{ mmol}\cdot\text{L}^{-1}$ KCl solution containing $5 \text{ mmol}\cdot\text{L}^{-1}$
435 ($\text{K}_3\text{Fe}(\text{CN})_6$). The use of potassium ferricyanide is intended to increase the sensitivity of the
436 KCl solution. The conductivity of the modified electrode was studied. The electrode was
437 analyzed by cyclic voltammetry method with a potential range of -1.00 to $+1.00$ with a scan
438 rate of $0.05 \text{ V}\cdot\text{s}^{-1}$. The voltammograms at the electrode have shown a specific redox reaction.
439 Furthermore, the conductivity of the modified electrode is lower due to the use of polyurethane.
440 This occurs due to PU being a natural polymer produced from the polyol of palm kernel oil-
441 based polyol. The electrochemical signal at the electrode is low if there is a decrease in
442 electrochemical conductivity (El - Raheem et al. 2020). It can be concluded that polyurethane
443 is a bio-polymer with a low current value. The current of the modified electrode was found at
444 $5.3 \times 10^{-5} \text{ A}$ or $53 \text{ }\mu\text{A}$. Nevertheless, the current of PU in this study showed better results
445 compared to Bahrami et al. (2019) that reported the current of PU as $1.26 \times 10^{-6} \text{ A}$, whereas Li
446 et al. (2019) reported the PU current in their study was even very low, namely 10^{-14} A . The PU
447 can obtain a current owing to the benzene ring in the hard segment (MDI) could exhibit the
448 current by inducing electron delocalization along the polyurethane chain (Wong et al. 2014).
449 The PU can also release a current caused by PEG. The application of PEG as polyol has been
450 studied by Porcarelli et al. (2017), that reported that the current of PU based on PEG – polyol
451 was $9.2 \times 10^{-8} \text{ A}$.

452 According to **Figure 9**, it can be concluded that the anodic peak present in the modified
453 electrode was at $+0.5 \text{ V}$, it also represented the anodic peak of the SPE-PU. The first oxidation
454 signal on both electrodes ranged from -0.2 to $+1.0 \text{ V}$, which revealed a particular oxidative
455 peak at a potential of $+0.5 \text{ V}$.

456



457

458 **Figure 9.** The voltammogram of SPE-PU modified electrode after analyzed using cyclic
 459 voltammetry technique

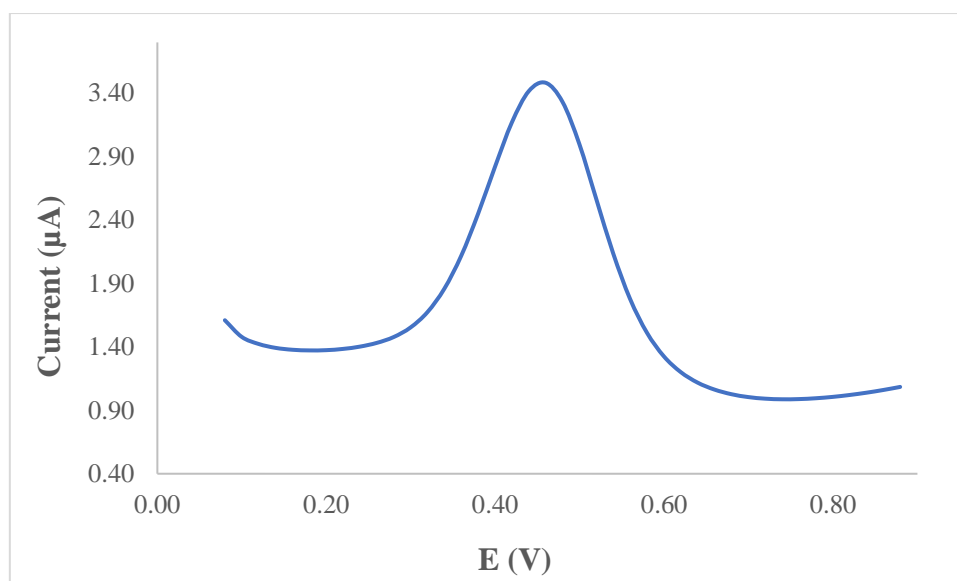
460

461 **Figure 10** also presents the DPV voltammogram of the modified electrode. DPV is a
 462 measurement based on the difference in potential pulses that produce an electric current.
 463 Scanning the capability pulses to the working electrode will produce different currents. Optimal
 464 peak currents will be produced to the reduction capacity of the redox material. The peak current
 465 produced is proportional to the concentration of the redox substance and can be detected up to
 466 a concentration below 10^{-8} M. DPV was conducted to obtain the current value that is more
 467 accurate than CV (Lee et al. 2018).

468 This study used a redox pair ($K_3Fe(CN)_6$) as a test device (probe). The currents generated by
 469 SPE-PU and proved by CV and DPV have shown conductivity on polyurethane films. This
 470 suggests that polyurethane films can conduct electron transfer. The electrochemical area on the
 471 modified electrode can be calculated using the formula from Randles-Sevcik (Butwong et al.
 472 2019), where the electrochemical area for SPE-PU is considered to be A, using Equation 2:

473

$$\text{Current of SPE-PU, } I_p = 2.65 \times 10^5 A C n^{3/2} \nu^{1/2} D^{1/2} \quad (2)$$



474
475 **Figure 10.** The voltammogram of SPE – PU modified electrode after analyzed using
476 differential pulse voltammetry technique

477

478 Where, $n - 1$ is the amount of electron transfer involved, while C is the solvent concentration
479 used ($\text{mmol}\cdot\text{L}^{-1}$) and the value of D is the diffusion constant of $5 \text{ mmol}\cdot\text{L}^{-1}$ at $(\text{K}_3\text{Fe}(\text{CN})_6)$
480 dissolved using $0.1 \text{ mmol}\cdot\text{L}^{-1}$ KCl. The estimated surface area of the electrode (**Figure 1**) was
481 0.2 cm^2 where the length and width of the electrode used during the study was $0.44 \text{ cm} \times 0.44$
482 cm while the surface area of the SPE-PU was 0.25 cm^2 with the length and width of the
483 electrode estimated at $0.5 \text{ cm} \times 0.5 \text{ cm}$, and causing the SPE-PU has a larger surface. The
484 corresponding surface concentration (τ) (mol/cm^2) is measured using Equation 3.

485

$$I_p = (n^2 F^2 / 4RT) A \tau v \quad (3)$$

486

487

488

489

490

491

I_p is the peak current (A), while A is the surface area of the electrode (cm^2), the value of v is
the applied scan rate (mV/s) and F is the Faraday constant ($96,584 \text{ C}/\text{mol}$), R is the constant
ideal gas ($8.314 \text{ J}/\text{mol K}$) and T is the temperature used during the experiment being conducted
(298 K) (Koita et al. 2014). The application of PKOp to produce a conducting polymer will be
a great prospect as this material can be employed in the analytical industry in order to modify
electrodes for electrochemical purposes.

492 Furthermore, number of palm oils is abundant in Malaysia and Indonesia such as palm stearin
493 and refined-bleached-deodorized (RBD) palm oil. They have several benefits such as being
494 sustainable, cheap, and environmentally biodegradable. These palms are the potential to
495 produce biomaterials that can be used to replace other polymers that are chemical-based (Tajao
496 et al. 2021). Several studies have been reported the application of PU to produce elastic
497 conductive fibres and films owing to it being highly elastic, scratch-resistant, and adhesive
498 (Tadese et al. 2019), thus it is easy for PU to adhere to the screen-printed electrode to modify
499 the electrode. PU is also being used as a composite material to make elastic conducting
500 composite films (Khatoon & Ahmad 2017).

501

502 **4. Conclusion**

503 Polyurethane film was prepared by pre-polymerization between palm kernel oil-based polyol
504 (PKO-p) with MDI. The presence of PEG 400 as the chain extender formed freestanding
505 flexible film. Acetone was used as the solvent to lower the reaction kinetics since the pre-
506 polymerization was carried out at room temperature. The formation of urethane links (-
507 NHC(O) backbone) after polymerization was confirmed by the absence of absorption bands at
508 2241 cm^{-1} associated with the N=C=O bond stretching, and the presence of N-H peak at 3300 cm^{-1} ,
509 carbonyl (C=O) at 1710 cm^{-1} , carbamate (C-N) at 1600 cm^{-1} , ether (C-O-C) at 1065 cm^{-1} ,
510 benzene ring (C=C) at 1535 cm^{-1} in the bio-based polyurethane chain structure. Soxhlet
511 analysis for the determination of crosslinking on polyurethane films has yielded a high
512 percentage of 99.33%. This is contributed by the hard segments formed from the reaction
513 between isocyanates and hydroxyl groups causing elongation of polymer chains. FESEM
514 analysis exhibited an absence of phase separation and smooth surface. Meanwhile, the current
515 of the modified electrode was found at $5.2 \times 10^{-5}\text{ A}$. This bio-based polyurethane film can be
516 used as a conducting bio-polymer and it is very useful for other studies such as electrochemical

517 sensor purposes. Furthermore, advanced technologies are promising and the future of bio based
518 polyol looks very bright.

519

520 **5. Acknowledgment**

521 The authors would like to thank Alma Ata University for the sponsorship given to the first
522 author. We would like to also, thank The Department of Chemical Sciences, Universiti
523 Kebangsaan Malaysia for the laboratory facilities and CRIM, UKM for the analysis
524 infrastructure.

525

526 **6. Conflict of Interest**

527 The authors declare no conflict of interest.

528

529 **7. References**

530 Agrawal, A., Kaur, R., Walia, R. S. (2017). PU foam derived from renewable sources:

531 Perspective on properties enhancement: An overview. *European Polymer Journal*. **95**:
532 255 – 274.

533 Akindoyo, J. O., Beg, M.D.H., Ghazali, S., Islam, M.R., Jeyaratnam, N. & Yuvaraj, A.R.

534 (2016). Polyurethane types, synthesis, and applications – a review. *RSC Advances*. **6**:
535 114453 – 114482.

536 Alamawi, M. Y., Khairuddin, F. H., Yusoff, N. I. M., Badri, K., Ceylan, H. (2019).

537 Investigation on physical, thermal, and chemical properties of palm kernel oil polyobio-
538 based binder as a replacement for bituminous binder. *Construction and Building*
539 *Materials*. **204**: 122 – 131.

540 Alqarni, S. A., Hussein, M. A., Ganash, A. A. & Khan, A. (2020). Composite material-based
541 conducting polymers for electrochemical sensor applications: a mini-review.
542 *BioNanoScience*. **10**: 351 – 364.

543 Badan, A., Majka, T. M. (2017). The influence of vegetable – oil based polyols on physico –
544 mechanical and thermal properties of polyurethane foams. *Proceedings*. 1 – 7.

545 Badri, K.H. (2012) Biobased polyurethane from palm kernel oil-based polyol. In Polyurethane;
546 Zafar, F., Sharmin, E., Eds. InTechOpen: Rijeka, Croatia. pp. 447–470.

547 Badri, K.H., Ahmad, S.H. & Zakaria, S. 2000. Production of a high-functionality RBD palm
548 kernel oil-based polyester polyol. *Journal of Applied Polymer Science*. **81**(2): 384 – 389.

549 Baig, N., Sajid, M. and Saleh, T. A. 2019. Recent trends in nanomaterial–modified electrodes
550 for electroanalytical applications. *Trends in Analytical Chemistry*. **111**: 47 – 61.

551 Berta, M., Lindsay, C., Pans, G., & Camino, G. (2006). Effect of chemical structure on
552 combustion and thermal behaviour of polyurethane elastomer layered silicate
553 nanocomposites. *Polymer Degradation and Stability*. **91**: 1179-1191.

554 Borowicz, M., Sadowska, J. P., Lubczak, J. & Czuprynski, B. (2019). Biodegradable, flame–
555 retardant, and bio-based rigid polyurethane/polyisocyanurate foams for thermal
556 insulation application. *Polymers*. **11**: 1816 – 1839.

557 Butwong, N., Khajonklin, J., Thongbor, A. & Luong, J.H.T. (2019). Electrochemical sensing
558 of histamine using a glassy carbon electrode modified with multiwalled carbon nanotubes
559 decorated with Ag – Ag₂O nanoparticles. *Microchimica Acta*. **186** (11): 1 – 10.

560 Chokkareddy, R., Thondavada, N., Kabane, B. & Redhi, G. G. (2020). A novel ionic liquid
561 based electrochemical sensor for detection of pyrazinamide. *Journal of the Iranian*
562 *Chemical Society*. **18**: 621 – 629.

563 Chokkareddy, R., Kanchi, S. & Inamuddin (2020). Simultaneous detection of ethambutol and
564 pyrazinamide with IL@CoFe₂O₄NPs@MWCNTs fabricated glassy carbon electrode.
565 *Scientific Reports*. **10**: 13563.

566 Clemitson, I. (2008). Castable Polyurethane Elastomers. Taylor & Francis Group, New York.
567 doi:10.1201/9781420065770.

568 Corcuera, M.A., Rueda, L., Saralegui, A., Martin, M.D., Fernandez-d'Arlas, B., Mondragon,
569 I. & Eceiza, A. (2011). Effect of diisocyanate structure on the properties and
570 microstructure of polyurethanes based on polyols derived from renewable resources.
571 *Journal of Applied Polymer Science*. **122**: 3677-3685.

572 Cuve, L. & Pascault, J.P. (1991). Synthesis and properties of polyurethanes based on
573 polyolefine: Rigid polyurethanes and amorphous segmented polyurethanes prepared in
574 polar solvents under homogeneous conditions. *Polymer*. **32** (2): 343- 352.

575 Degefu, H., Amare, M., Tessema, M. & Admassie, S. (2014). Lignin modified glassy carbon
576 electrode for the electrochemical determination of histamine in human urine and wine
577 samples. *Electrochimica Acta*. **121**: 307 – 314.

578 Dzulkipli, M. Z., Karim, J., Ahmad, A., Dzulkurnain, N. A., Su'ait, M S., Fujita, M. Y., Khoon,
579 L. T. & Hassan, N. H. (2021). The influences of 1-butyl-3-methylimidazolium
580 tetrafluoroborate on electrochemical, thermal and structural studies as ionic liquid gel
581 polymer electrolyte. *Polymers*. **13** (8): 1277 – 1294.

582 El-Raheem, H.A., Hassan, R.Y.A., Khaled, R., Farghali, A. & El-Sherbiny, I.M. (2020).
583 Polyurethane-doped platinum nanoparticles modified carbon paste electrode for the
584 sensitive and selective voltammetric determination of free copper ions in biological
585 samples. *Microchemical Journal*. **155**: 104765.

586 Fei, T., Li, Y., Liu, B. & Xia, C. (2019). Flexible polyurethane/boron nitride composites with
587 enhanced thermal conductivity. *High Performance Polymers*. **32** (3): 1 – 10.

588 Furtwengler, P., Perrin R., Redl, A. & Averous, L. (2017). Synthesis and characterization of
589 polyurethane foams derived of fully renewable polyesters polyols from sorbitol.
590 *European Polymer Journal*. **97**: 319 – 327.

591 Ghosh, S., Ganguly, S., Remanan, S., Mondal, S., Jana, S., Maji, P. K., Singha, N., Das, N. C.
592 (2018). Ultra-light weight, water durable and flexible highly electrical conductive
593 polyurethane foam for superior electromagnetic interference shielding materials. *Journal*
594 *of Materials Science: Materials in Electronics*. **29**: 10177 – 10189.

595 Guo, S., Zhang, C., Yang, M., Zhou, Y., Bi, C., Lv, Q. & Ma, N. (2020). A facile and sensitive
596 electrochemical sensor for non – enzymatic glucose detection based on three –
597 dimensional flexible polyurethane sponge decorated with nickel hydroxide. *Analytica*
598 *Chimica Acta*. **1109**: 130 – 139.

599 Hamuzan, H.A. & Badri, K.H. (2016). The role of isocyanates in determining the viscoelastic
600 properties of polyurethane. *AIP Conference Proceedings*. 1784, Issue 1.

601 Harmayani, E., Aprilia, V. & Marsono, Y. (2014). Characterization of glucomannan from
602 *Amorphophallus oncophyllus* and its prebiotic activity in vivo. *Carbohydrate Polymers*.
603 **112**: 475-79.

604 Herrington, R. & Hock, K. (1997). Flexible polyurethane foams. 2nd Edition. Dow Chemical
605 Company. Midlan.

606 Inayatullah, A., Badrul, H.A., Munir, M.A. (2021). Fish analysis containing biogenic amines
607 using gas chromatography flame ionization detector. *Science and Technology Indonesia*.
608 **6** (1): 1-7.

609 Janpoung, P., Pattanauwat, P. & Potiyaraj, P. (2020). Improvement of electrical conductivity
610 of polyurethane/polypyrrole blends by graphene. *Key Engineering Materials*. **831**: 122 –
611 126.

612 Khairuddin, F.H., Yusof, N. I. M., Badri, K., Ceylan, H., Tawil, S. N. M. (2018). Thermal,
613 chemical and imaging analysis of polyurethane/cecabase modified bitumen. *IOP Conf.*
614 *Series: Materials Science and Engineering*. **512**: 012032.

615 Khatoon, H., Ahmad, S. (2017). A review on conducting polymer reinforced polyurethane
616 composites. *Journal of Industrial and Engineering Chemistry*. **53**: 1 – 22.

617 Kilele, J. C., Chokkareddy, R., Rono, N. & Redhi, G. G. (2020). A novel electrochemical
618 sensor for selective determination of theophylline in pharmaceutical formulations.
619 *Journal of the Taiwan Institute of Chemical Engineers*. 111: 228-238.

620 Kilele, J. C., Chokkareddy, R. & Redhi, G. G. (2021). Ultra–sensitive electrochemical sensor
621 for fenitrothion pesticide residues in fruit samples using IL@CoFe₂ONPs@MWCNTs
622 nanocomposite. *Microchemical Journal*. **164**: 106012.

623 Koita, D., Tzedakis, T., Kane, C., Diaw, M., Sock, O. & Lavedan, P. (2014). Study of the
624 histamine electrochemical oxidation catalyzed by nickel sulfate. *Electroanalysis*. **26** (10):
625 2224 – 2236.

626 Kotal, M., Srivastava, S.K. & Paramanik, B. (2011). Enhancements in conductivity and thermal
627 stabilities of polyurethane/polypyrrole nanoblends. *The Journal of Physical Chemistry*
628 *C*. **115** (5): 1496 – 1505.

629 Ladan, M., Basirun, W.J., Kazi, S.N., Rahman, F.A. (2017). Corrosion protection of AISI 1018
630 steel using Co-doped TiO₂/polypyrrole nanocomposites in 3.5% NaCl solution.
631 *Materials Chemistry and Physics*. **192**: 361 – 373.

632 Lampman, G.M., Pavia, D.L., Kriz, G.S. & Vyvyan, J.R. (2010). Spectroscopy. 4th Edition.
633 Brooks/Cole Cengage Learning, Belmont, USA.

634 Lee, K.J., Elgrishi, N., Kandemir, B. & Dempsey, J.L. 2018. Electrochemical and spectroscopic
635 methods for evaluating molecular electrocatalysts. *Nature Reviews Chemistry*. **1**(5): 1 -
636 14.

637 Leykin, A., Shapovalov, L. & Figovsky, O. (2016). Non – isocyanate polyurethanes –
638 Yesterday, today and tomorrow. *Alternative Energy and Ecology*. **191** (3 – 4): 95 – 108.

639 Li, H., Yuan, D., Li, P., He, C. (2019). High conductive and mechanical robust carbon
640 nanotubes/waterborne polyurethane composite films for efficient electromagnetic
641 interference shielding. *Composites Part A*. **121**: 411 – 417.

642 Nakthong, P., Kondo, T., Chailapakul, O., Siangproh, W. (2020). Development of an
643 unmodified screen-printed electrode for nonenzymatic histamine detection. *Analytical
644 Methods*. **12**: 5407 – 5414.

645 Mishra, K., Narayan, R., Raju, K.V.S.N. & Aminabhavi, T.M. (2012). Hyperbranched
646 polyurethane (HBPU)-urea and HBPU-imide coatings: Effect of chain extender and
647 NCO/OH ratio on their properties. *Progress in Organic Coatings*. **74**: 134 – 141.

648 Mohd Noor, M. A., Tuan Ismail, T. N. M., Ghazali, R. (2020). Bio-based content of oligomers
649 derived from palm oil: Sample combustion and liquid scintillation counting technique.
650 *Malaysia Journal of Analytical Science*. **24**: 906 – 917.

651 Munir, M. A., Badri, K. H., Heng, L. Y., Inayatullah, A., Nurinda, E., Estiningsih, D.,
652 Fatmawati, A., Aprilia, V., Syafitri, N. (2022). The application of polyurethane-LiClO₄
653 to modify screen-printed electrodes analyzing histamine in mackerel using a
654 voltammetric approach. *ACS Omega*. doi.org/10.1021/acsomega.1c06295.

655 Munir, M. A., Heng, L. Y., Sage, E. E., Mackeen, M. M. M., Badri, K. H. (2021). Histamine
656 detection in mackerel (*Scomberomorus* Sp.) and its products derivatized with 9-
657 fluorenilmethylchloroformate. *Pakistan Journal of Analytical and Environmental
658 Chemistry*. **22** (2): 243-251.

659 Munir, M. A., Heng, L. Y., Badri, K. H. (2021). Polyurethane modified screen-printed
660 electrode for the electrochemical detection of histamine in fish. *IOP Conference Series:
661 Earth and Environmental Science*. **880**: 012032.

662 Munir, M.A., Mackeen, M.M.M., Heng, L.Y. Badri, K.H. (2021). Study of histamine detection
663 using liquid chromatography and gas chromatography. *ASM Science Journal*. **16**: 1-9.

664 Mutsuhisa F., Ken, K. & Shohei, N. (2007). Microphase separated structure and mechanical
665 properties of norbornane diisocyanate-based polyurethane. *Polymer*. **48** (4): 997 – 1004.

666 Mustapha, R., Rahmat, A. R., Abdul Majid, R., Mustapha, S. N. H. (2019). Vegetable oil-based
667 epoxy resins and their composites with bio-based hardener: A short review. *Polymer-*
668 *Plastic Technology and Materials*. **58**: 1311 – 1326.

669 Nohra, B., Candy, L., Blancos, J.F., Guerin, C., Raoul, Y. & Mouloungui, Z. (2013). From
670 petrochemical polyurethanes to bio-based polyhydroxyurethanes. *Macromolecules*. **46**
671 (10): 3771 – 3792.

672 Nurwanti, E., Uddin, M., Chang, J.S., Hadi, H., Abdul, S.S., Su, E.C.Y., Nursetyo, A.A.,
673 Masud, J.H.B. & Bai, C.H. (2018). Roles of sedentary behaviors and unhealthy foods in
674 increasing the obesity risk in adult men and women: A cross-sectional national study.
675 *Nutrients*. **10** (6): 704-715.

676 Pan, T. & Yu, Q. (2016). Anti-corrosion methods and materials comprehensive evaluation of
677 anti-corrosion capacity of electroactive polyaniline for steels. *Anti – Corrosion Methods*
678 *and Materials*. **63**: 360 – 368.

679 Pan, X. & Webster, D.C. (2012). New biobased high functionality polyols and their use in
680 polyurethane coatings. *ChemSusChem*. **5**: 419-429.

681 Petrovic, Z.S. (2008). Polyurethanes from vegetable oils. *Polymer Reviews*. **48** (1): 109 – 155.

682 Porcarelli, L., Manojkumar, K., Sardon, H., Llorente, O., Shaplov, A. S., Vijayakrishna, K.,
683 Gerbaldi, C., Mecerreyes, D. (2017). Single ion conducting polymer electrolytes based
684 on versatile polyurethanes. *Electrochimica Acta*. **241**: 526 – 534.

685 Priya, S. S., Karthika, M., Selvasekarapandian, S. & Manjuladevi, R. (2018). Preparation and
686 characterization of polymer electrolyte based on biopolymer I-carrageenan with
687 magnesium nitrate. *Solid State Ionics*. **327**: 136 – 149.

688 Ren, D. & Frazier, C.E. (2013). Structure–property behaviour of moisture-cure polyurethane
689 wood adhesives: Influence of hard segment content. *Adhesion and Adhesives*. **45**: 118-
690 124.

691 Rogulska, S.K., Kultys, A. & Podkoscielny, W. (2007). Studies on thermoplastic polyurethanes
692 based on newdiphe – derivative diols. II. Synthesis and characterization of segmented
693 polyurethanes from HDI and MDI. *European Polymer Journal*. **43**: 1402 – 1414.

694 Romaskevicius, T., Budriene, S., Pielichowski, K. & Pielichowski, J. (2006). Application of
695 polyurethane-based materials for immobilization of enzymes and cells: a review.
696 *Chemija*. **17**: 74 – 89.

697 Sengodu, P. & Deshmukh, A. D. (2015). Conducting polymers and their inorganic composites
698 for advanced Li-ion battery electrolytes: a review. *RSC Advances*. **5**: 42109 – 42130.

699 Septevani, A. A., Evans, D. A. C., Chaleat, C., Martin, D. J., Annamalai, P. K. (2015). A
700 systematic study substituting polyether polyol with palm kernel oil based polyester
701 polyol in rigid polyurethane foam. *Industrial Crops and Products*. **66**: 16 – 26.

702 Su'ait, M. S., Ahmad, A., Badri, K. H., Mohamed, N. S., Rahman, M. Y. A., Ricardi, C. L. A.
703 & Scardi, P. The potential of polyurethane bio-based solid polymer electrolyte for
704 photoelectrochemical cell application. *International Journal of Hydrogen Energy*. **39** (6):
705 3005 – 3017.

706 Tadesse, M. G., Mengistie, D. A., Chen, Y., Wang, L., Loghin, C., Nierstrasz, V. (2019).
707 Electrically conductive highly elastic polyamide/lycra fabric treated with PEDOT: PSS
708 and polyurethane. *Journal of Materials Science*. **54**: 9591 – 9602.

709 Tajau, R., R, Rosiah, Alias, M. S., Mudri, N. H., Halim, K. A. A., Harun, M. H., Isa, N. M.,
710 Ismail, R. C., Faisal, S. M., Talib, M., Zin, M. R. M., Yusoff, I. I., Zaman, N. K., Illias,
711 I. A. (2021). Emergence of polymeric material utilising sustainable radiation curable
712 palm oil-based products for advanced technology applications. *Polymers*. **13**: 1865 –
713 1886.

714 Tran, V.H., Kim, J.D., Kim, J.H., Kim, S.K., Lee, J.M. (2020). Influence of cellulose
715 nanocrystal on the cryogenic mechanical behaviour and thermal conductivity of
716 polyurethane composite. *Journal of Polymers and The Environment*. **28**: 1169 – 1179.

717 Viera, I.R.S., Costa, L.D.F.D.O., Miranda, G.D.S., Nardehcia, S., Monteiro, M.S.D. S.D.B.,
718 Junior, E.R. & Delpech, M.C. (2020). Waterborne poly (urethane – urea)s
719 nanocomposites reinforced with clay, reduced graphene oxide and respective hybrids:
720 Synthesis, stability and structural characterization. *Journal of Polymers and The
721 Environment*. **28**: 74 – 90.

722 Wang, B., Wang, L., Li, X., Liu, Y., Zhang, Z., Hedrick, E., Safe, S., Qiu, J., Lu, G. & Wang,
723 S. (2018). Template-free fabrication of vertically–aligned polymer nanowire array on the
724 flat–end tip for quantifying the single living cancer cells and nanosurface interaction. a
725 *Manufacturing Letters*. **16**: 27 – 31.

726 Wang, J., Xiao, L., Du, X., Wang, J. & Ma, H. (2017). Polypyrrole composites with carbon
727 materials for supercapacitors. *Chemical Papers*. **71 (2)**: 293 – 316.

728 Wong, C.S. & Badri, K.H. (2012). Chemical analyses of palm kernel oil-based polyurethane
729 prepolymer. *Materials Sciences and Applications*. **3**: 78 – 86.

730 Wong, C. S., Badri, K., Ataollahi, N., Law, K., Su’ait, M. S., Hassan, N. I. (2014). Synthesis
731 of new bio–based solid polymer electrolyte polyurethane – LiClO₄ via prepolymerization
732 method: Effect of NCO/OH ratio on their chemical, thermal properties and ionic
733 conductivity. *World Academy of Science, Engineering and Technology, International*

734 *Journal of Chemical, Molecular, Nuclear, Materials and Metallurgical Engineering*. **8**:
735 1243 – 1250.

736 Yong, Z., Bo, Z.M., Bo, W., Lin, J.Z. & Jun, N. (2009). Synthesis and properties of novel
737 polyurethane acrylate containing 3-(2-Hydroxyethyl) isocyanurate segment. *Progress in*
738 *Organic Coatings*. **67**: 264 – 268.

739 Zia, K. M., Anjum, S., Zuber, M., Mujahid, M. & Jamil, T. (2014). Synthesis and molecular
740 characterization of chitosan based polyurethane elastomers using aromatic diisocyanate.
741 *International of Journal of Biological Macromolecules*. **66**: 26 – 32.